



## AN ABSTRACT OF THE DISSERTATION OF

Fan Wu for the degree of Doctor of Philosophy in Environmental Engineering presented on May 8, 2017.

Title: Novel Approaches to Evaluate the Environmental Impacts of Nanomaterials

Abstract approved: \_\_\_\_\_

Stacey L. Harper

Numerous studies have shown that some nanomaterials are highly toxic to aquatic organisms and can potentially disrupt overall community health; however, current methods to evaluate the nanomaterials environmental impacts rarely consider the environmental realism or provide sufficient detail on the impact at the community level. Here we demonstrate three approaches that can effectively evaluate the environmental impacts of nanoparticle (NP) exposure: a chronic trophic food chain exposure, a rapid and cost-effective multi-species community exposure, and an end-of-life toxicity evaluation. The research comprising this dissertation primarily focuses on metal-based nanomaterials of varying size, surface functionalization, oxidation states, solubility, and aggregation behavior, and assesses the impacts of these variations on dissolution, uptake, and environmental toxicity. The chronic trophic food chain exposure demonstrates that NPs can transfer through the food chain and cause long-term toxicity to aquatic organisms, and additionally, elicits differential toxicity relative to direct

waterborne exposure. In the multi-species community exposure, dissolved metal ions contribute a large fraction of toxicity to the environment. However, NPs can also elicit particle-specific uptake and toxicity depending on the particle type, and surface functionalization can dramatically modify NP fate and toxicity. Finally, an end-of-life toxicity evaluation on monoalkyltin cluster coated thin film wafers was performed. The low toxicity suggests our synthesized tin clusters and the tin films can be environmentally benign materials suitable for large-scale use in the semiconductor industry. Most important, the multi-species community approach utilized in this dissertation demonstrates benefits, such as high repeatability, rapid execution and cost-effectiveness relative to other standardized methods. Due to these benefits, this assay could be established as a new standardized method to evaluate the environmental impacts of nanomaterials and enhance our ability to rapidly screen the toxicity of nanomaterials and understand their impacts at the community level. The comprehensive understanding gained throughout this dissertation provides the basis for nanomaterial environmental impact evaluation and risk management for sustainable nanotechnology development.

©Copyright by Fan Wu

May 8, 2017

All Rights Reserved

Novel Approaches to Evaluate the Environmental Impacts of Nanomaterials

by  
Fan Wu

A DISSERTATION

submitted to

Oregon State University

in partial fulfillment of  
the requirements for the  
degree of

Doctor of Philosophy

Presented May 8, 2017  
Commencement June 2017

Doctor of Philosophy dissertation of Fan Wu presented on May 8, 2017

APPROVED:

---

Major Professor, representing Environmental Engineering

---

Head of the School of Chemical, Biological, and Environmental Engineering

---

Dean of the Graduate School

I understand that my dissertation will become part of the permanent collection of Oregon State University libraries. My signature below authorizes release of my dissertation to any reader upon request.

---

Fan Wu, Author

## ACKNOWLEDGEMENTS

I would like to express sincere and immense appreciation to Dr. Stacey Harper; her constant stream of advice, guidance, and encouragement have been instrumental to the completion of this dissertation and to my personal development as a scientist and researcher. I also would like to thank Bryan Harper especially, his assistance in methods development and interpretation of results has been invaluable to me. My committee members, Dr. Tyler Radniecki, Dr. Jeffrey Nason, Dr. Lewis Semprini, and Dr. Perry Hystad, I cannot express how grateful I am of your genuine advice and commitment. I have benefitted from the knowledge and friendship of everyone in the Harper Lab group, especially Lauren Crandon, Amy Bortvedt, and Lindsay Denluck. I would love to thank my parents, Tangshun Wu and Shuhua Zhou, for their unwavering love and support. I would also like to acknowledge my best friends back in China, especially Rongrong Tang and Jian Xu for traveling thousands of miles to visit me when I needed you the most, thank you all so much for always being there for the nonacademic challenges and adventures. Without any of your help, I would have stopped long ago.

## CONTRIBUTION OF AUTHORS

The research presented in this dissertation is a product of the work of many researchers and could not have been completed without their help. Amy Bortvedt and Lauren Crandon contributed experimental and editorial support to the study presented in Chapter 3. Lindsay Denluck provided written support on the work presented in Chapter 6. Sumit Saha, Bettye Maddux, and Douglas Keszler characterized and provided the organotin and coated wafers presented in Chapter 7. Stacey Harper and Bryan Harper have provided technical, analytical, and editorial support for all the research comprising this dissertation.



## TABLE OF CONTENTS

	<u>Page</u>
Chapter 1. Introduction .....	1
1.1 Nanomaterials and environmental concerns.....	1
1.2 Challenges to evaluating the environmental impacts of nanomaterials .....	3
1.3 Document Organization.....	4
Chapter 2. Current and future approaches to evaluate the ecotoxicity of NPs .....	6
2.1 Single species toxicity testing.....	6
2.2 Environmentally relevant exposures .....	7
2.3 Introducing the nanocosm assay.....	11
2.4 NP selection.....	14
Chapter 3. Uptake and toxicity of CuO nanoparticles to <i>Daphnia magna</i> varies between indirect dietary and direct waterborne exposures.....	17
3.1 Graphical Abstract.....	18
3.2 Abstract.....	19
3.3 Introduction .....	21
3.4 Materials and Methods .....	24
3.4.1 Test organisms.....	24
3.4.2 Nanoparticle characterization.....	24
3.4.3 Preparation of CuO NP incubated algae (Cu-algae) .....	25
3.4.4 Experimental design for toxicity evaluations.....	26
3.4.5 Determination of dissolved and organismal Cu content .....	28
3.5 Results .....	29
3.5.1 Nanoparticle characterization.....	29
3.5.2 Removal of non-attached CuO NPs from algae .....	29
3.5.3 CuO NPs dissolution and uptake in <i>D. magna</i> .....	30

## TABLE OF CONTENTS (Continued)

	<u>Page</u>
3.5.4 Chronic toxicity of CuO NPs to <i>D. magna</i> .....	35
3.6 Discussion.....	37
3.7 Conclusion .....	43
3.8 References .....	45
3.9 Appendix .....	51
Chapter 4. Comparison of the dissolution, uptake and toxicity of nano- and micron-sized zinc oxide particles .....	59
4.1 Abstract.....	60
4.2 Introduction .....	61
4.3 Materials and methods.....	64
4.3.1 Exposure media and organism maintenance .....	64
4.3.2 Test organisms.....	65
4.3.3 Nanoparticles characterization .....	66
4.3.4 Experiment setup and toxicity evaluations.....	66
4.3.5 Measurement of dissolved Zn concentrations and uptake .....	68
4.3.6 Statistical analysis .....	69
4.4 Results .....	70
4.4.1 Nanoparticle Characterization.....	70
4.4.2 Nanoparticle Dissolution.....	71
4.4.3 Biotic .....	72
4.4.4 Zn uptake.....	74
4.4.5 Organism Toxicity.....	75
4.4.6 Integrated comparison.....	80
4.5 Discussion.....	83

## TABLE OF CONTENTS (Continued)

	<u>Page</u>
4.5.1 NP characterization .....	83
4.5.2 Dissolved Zn and organismal uptake .....	83
4.5.3 Toxicity .....	85
4.6 Conclusion .....	88
4.7 Reference .....	89
4.8 Appendix .....	96
Chapter 5. Differential dissolution and toxicity of surface functionalized silver nanoparticles in small-scale microcosms: impacts of community complexity .....	100
5.1 Abstract.....	101
5.2 Introduction .....	102
5.3 Materials and methods.....	107
5.3.1 Nanoparticles characterization .....	107
5.3.2 Preparation of exposure media.....	108
5.3.3 Test organisms.....	108
5.3.4 Experimental design.....	109
5.3.5 Toxicity evaluations .....	110
5.3.6 Measurement of AgNP dissolution, uptake and dissolved Ag concentrations ...	111
5.3.7 Data analysis .....	112
5.4 Results .....	114
5.4.1 Nanoparticle characterization.....	114
5.4.2 Nanoparticle dissolution.....	115
5.4.3 Toxicity of AgNPs .....	118
5.4.4 Dissolved Ag concentration – response relationship .....	126
5.5 Discussion.....	129

## TABLE OF CONTENTS (Continued)

	<u>Page</u>
5.5.1 Exposure characterization .....	129
5.5.2 <i>D. magna</i> and zebrafish silver uptake .....	134
5.5.3 Toxicity of AgNPs in nanocosms.....	135
5.6 Conclusion .....	138
5.7 Acknowledgements .....	139
5.8 References .....	140
5.9 Appendix .....	148
Chapter 6. Evaluation of Cu and CuO nanoparticle environmental impacts using laboratory small scale microcosms .....	164
6.1 Introduction .....	165
6.2 Materials and Methods .....	167
6.2.1 Nanoparticle characterization.....	167
6.2.2 Exposure setup and toxicity evaluation.....	168
6.2.3 Dissolution and organism uptake measurements .....	169
6.2.4 Statistics .....	170
6.3 Results .....	171
6.3.1 NP characterization .....	171
6.3.2 Dissolved Cu measured in abiotic and biotic environment.....	172
6.3.3 Cu uptake in <i>D. magna</i> and zebrafish .....	175
6.3.4 Toxicity results.....	176
6.4 Discussion.....	179
6.5 Conclusion .....	182
6.6 Reference .....	183
6.7 Appendix .....	186

## TABLE OF CONTENTS (Continued)

	<u>Page</u>
Chapter 7. Monoalkyl tin cluster films: High-resolution patterning materials with low environmental impact under simulated natural conditions .....	187
7.1 Abstract.....	188
7.2 Introduction .....	189
7.3 Materials and Methods .....	190
7.3.1 Synthesis of [(BuSn) <sub>12</sub> O <sub>14</sub> (OH) <sub>6</sub> ][OH] <sub>2</sub> .....	190
7.3.2 Film preparation .....	191
7.3.3 Toxicity testing.....	192
7.3.4 Leachate collection.....	193
7.4 Results and Discussion .....	194
7.4.1 Toxicity of (BuSn) <sub>12</sub> (OH) <sub>6</sub> clusters.....	194
7.4.2 Leachate characterization.....	195
7.4.3 Toxicity of leachate.....	199
7.5 Appendix .....	204
7.6 Reference .....	201
Chapter 8. Validation and Summary.....	208
8.1 Nanocosm Validation .....	208
8.1.1 Comparison of control species for standardization.....	208
8.1.2 Dissolved Oxygen .....	212
8.2 Summary of the fate and toxicity of tested NPs .....	213
8.3 Nanocosm modeling.....	216
8.4 Cost-benefit analysis.....	221
8.5 The advantages and disadvantages of the approaches.....	222
8.6 Summary.....	225

## TABLE OF CONTENTS (Continued)

	<u>Page</u>
Chapter 9. Bibliography.....	227

## LIST OF FIGURES

<u>Figure</u>	<u>Page</u>
2-1. The potential interactions of the four species in the nanocosm assay. ....	13
3-1. a) Identification of CuO NPs using HSI and the corresponding spectral profile of bare CuO NPs, algae cells, and CuO NPs associated with algae cells. Dark field images b) before and c) after the centrifugation and filtration rinsing steps. ....	32
3-2. Total Cu in <i>D. magna</i> following low and high exposure concentrations through feeding and direct exposure scenarios.....	33
3-3. Total Cu measured in a) molted carapaces, and b) produced neonates from both delivery scenarios. ....	35
3-4. Chronic effects of CuO NPs to <i>D. magna</i> following feeding and direct exposure for 14 days (a. percent survival; b. # neonates / adult; c. # brood / adult). ....	36
S3-1. Hydrodynamic diameter (HDD) and zeta potential (ZP) of CuO NPs in <i>Daphnia</i> water (panel a, b) and algal media (panel c, d). ....	52
S3-2. Percentage of Cu remaining associated with algae after serial filtration. ....	53
S3-3. Percentage Cu remaining with EDTA and without EDTA ( <i>Daphnia</i> media) following one time filtration. ....	54
S3-4. Cu associated with algae in the amounts of algae fed to individual <i>D. magna</i> .....	55
S3-5. Dark field images of <i>D. magna</i> molted carapaces and typical spectral profiles in a) control, b) feeding exposure, and c) direct exposure scenarios. ....	56
S3-6. <i>D. magna</i> daily reproduction in a) direct exposure and b) feeding exposure over 14 days.	57
S3-7. <i>D. magna</i> body length in a) direct exposure and b) feeding exposure. ....	58
4-1. Hydrodynamic diameter (a) of 10 mg L <sup>-1</sup> ZnO NPs in NCM and MQW and zeta potential (b) over 120 hours. ....	71
4-2. Dissolved zinc concentrations for all three types of Zn exposures (normalized at 10 mg ZnO/L) measured in NCM over 120 hours. ....	72
4-3. Dissolved zinc fraction (based on measured initial stock Zn concentrations) measured in NCM at 24 (a) and 120 (b) hours under each exposure scenario. ....	73
4-4. Zebrafish uptake in individual exposure scenario (a) and community exposure scenario (b) with Zn exposures at 0.1, 1, and 10 mg ZnO/L.....	75

## LIST OF FIGURES (Continued)

<u>Figure</u>	<u>Page</u>
4-6. Zebrafish hatching rate in single (a) and community (b) exposure conditions after 120 hours. ....	80
4-7. The overall 120-hour comparison of each species in single and NC group exposed at 10 mg ZnO/L. ....	82
S4-1. <i>D. magna</i> uptake in community exposure scenario with Zn exposures at 0.1 and 1 mg ZnO/L. ....	98
S4-2. <i>D. magna</i> survival over 48 hours in single (a) and NC (b) exposures to ZnCl <sub>2</sub> , ZnO NPs and ZnO MPs (b). ....	99
5-1. a) Hydrodynamic diameter (HDD) and b) zeta potential (ZP) of PEG-Ag, Si-Ag, and Ami-Si-Ag in NCM over 120 hours at 10 mg L <sup>-1</sup> .....	115
5-2. Dissolution of PEG, Si, and Ami-Si coated AgNPs at 1 mg L <sup>-1</sup> in NCM over 120 hours. .	116
5-3. Dissolved Ag concentration in NCM after 120 hours with 0.1 mg L <sup>-1</sup> (a), 1 mg L <sup>-1</sup> (b), 5 mg L <sup>-1</sup> (c) AgNP exposures under three different community exposure scenarios. ....	118
5-4. 120 hour growth rates of algae (panels a, b, c) and bacteria (panels d, e, f) under three different exposure scenarios: algae and bacteria (A+B), algae, bacteria and daphnids (A+B+D), and algae, bacteria, daphnia and zebrafish (A+B+D+Z). ....	120
5-5. Algal survival at 120 hours after normalized based on control in a) A+B; b) A+B+D; and c) A+B+D+Z exposure scenarios. ....	121
5-6. Bacterial survival at 120 hours normalized based on control survival in a) A+B; b) A+B+D; and c) A+B+D+Z exposure scenarios. ....	121
5-7. <i>Daphnia</i> survival following exposure to PEG-Ag, Si-Ag, and Ami-Si-Ag in algae, bacteria and daphnia (A+B+D) (Panel a, c, e), and algae, bacteria, daphnids and zebrafish (A+B+D+Z) (Panel b, d, f) community exposure scenarios. ....	127
5-8. Hatching probability of zebrafish in control and Si-Ag exposure at 5 mg L <sup>-1</sup> . ....	128
5-9. The proportion of symptomatic fish following AgNP exposures.....	128
S5-1. The potential interactions of the four species in the nanocosm assay.....	153
S5-2. AgNP surface chemistry, TEM images and primary particle sizes as reported by the manufacturer.....	154



## LIST OF FIGURES (Continued)

<u>Figure</u>	<u>Page</u>
S5-3. Zeta potential (ZP) of PEG-Ag (orange circle), Si-Ag (green triangle), and Ami-Si-Ag (blue square) in NCM over 120 hours at 10 mg L <sup>-1</sup> . .....	155
S5-4. Normalized algal survival in exposure scenarios containing algae and bacteria (A+B), as well as those that added Daphnia (A+B+D) and zebrafish (A+B+D+Z) using three different surface functionalized AgNPs. ....	156
S5-5. Normalized bacterial survival in three different exposure scenarios with three types of AgNPs. ....	157
S5-6. Images of 120-hour <i>D. magna</i> after exposure to 5 mg L <sup>-1</sup> Ami-Si-Ag exposure; .....	158
S5-7. Percent of zebrafish mortality and malformation following 120-hours exposure to three different surface functionalized silver nanoparticles.....	158
S5-8. Ag content (%) in unhatched zebrafish chorion (blue) and fish body (green) with 5 mg L <sup>-1</sup> Si-AgNP exposure after 120 hours under A+B+D+Z exposure scenario. ....	159
S5-9. The relationship between the dissolved Ag concentration in the exposure environment and the Daphnia (a) and zebrafish (b) silver uptake.....	160
S5-10. Concentration-response relationship between the dissolved Ag concentration in each exposure nanocosm and algal survival. ....	161
S5-11. Concentration-response relationship between the dissolved Ag concentration in each exposure nanocosm and bacterial survival. ....	161
S5-12. Concentration-response relationship between <i>D. magna</i> survival and the dissolved Ag concentration in each exposure nanocosm. ....	162
S5-13. Concentration-response relationship between zebrafish survival and the dissolved Ag concentration in each exposure nanocosm. ....	162
S5-14. Species sensitivity distributions (SSDs) of organisms in nanocosm using the mean LC <sub>50</sub> value calculated from Table 2 and the dissolved Ag concentration in the exposure vessels. ....	163
6-1. Hydrodynamic diameter (a) and zeta potential (b) of Cu and CuO NP measured in nanocosm media at 10 mg/L averaged over five days.....	172
6-2. Abiotic Cu NP and CuO NP dissolution were measured in nanocosm media at 10 mg/L..	173

## LIST OF FIGURES (Continued)

<u>Figure</u>	<u>Page</u>
6-3. Dissolved Cu measured from Cu NPs and CuO NP at 1, 5, and 10 mg/L at 120 hours. ....	174
6-4. Cu uptake in <i>D. magna</i> from a) ionic Cu, b) CuO NP, and c) CuO NP at multiple exposure concentration. ....	175
6-5. Cu uptake in manually dethatched chorions (from delay hatched zebrafish) and hatched zebrafish from CuNP, CuO NP, and ionic Cu at 10 mg L <sup>-1</sup> . ....	176
6-6. Toxicity endpoint in each tested organism using the measured dissolved Cu from each exposure type. ....	178
S6-1. Hydrodynamic diameter (a) and zeta potential (b) of Cu and CuO NP measured in nanocosm media at 10 mg/L over 120 hours. ....	186
7-1. Toxicity of (BuSn) <sub>12</sub> (OH) <sub>6</sub> clusters measured as <i>C. reinhardtii</i> growth rates (a) and <i>D. magna</i> immobilization and mortality (b). ....	195
7-2. Releasing kinetic of tin coated wafers (a), modeled leaching capacity over 90 days (b), and the leaching rate of tin from wafers (c) under four different environmental scenarios. ....	197
7-3. The ratio of algal growth rates after exposing to control and tin wafer leachate under each incubation scenario. ....	198
7-4. <i>D. magna</i> 48-hour immobilization and mortality after exposed to simulated leachate after 14 (a) and 90 (b) days. (CW: Control wafer; TW: Tin wafer). ....	198
S7-1. Chemical Structure of [(BuSn) <sub>12</sub> O <sub>14</sub> (OH) <sub>6</sub> ][OH] <sub>2</sub> . ....	204
S7-2. Sonication time versus the corresponding particle HDDs. ....	204
S7-3. Four different incubation scenarios with control wafers and tin-coated wafers (a. 20°C, pH = 7, b. 20°C, pH = 5.6, c. 37°C, pH = 7, and d. 37°C, pH = 5.6). ....	205
S7-4. Total tin (mass) leached from control and tin-coated wafers through four different incubation conditions (a. Temp = 20°C, pH = 7; b. Temp = 20°C, pH = 5.6; c. Temp = 37°C, pH = 7; d. Temp = 37°C, pH = 5.6). ....	206
S7-5. Algae growth rate with the exposure of simulated leachate under varying scenarios: a. Temp = 20°C, pH = 7; b. Temp = 20°C, pH = 5.6; c. Temp = 37°C, pH = 7; d. Temp = 37°C, pH = 5.6. ....	207

## LIST OF FIGURES (Continued)

<u>Figure</u>	<u>Page</u>
8-1. Combined algal growth rates (a) and 120-hour algal survival probability (b) from different trials of experiments with multiple replicates. ....	209
8-2. Combined bacterial growth rates (a) and 120-hour bacterial survival probability (b) different trials of experiments with multiple replicates. ....	209
8-3. Combined <i>D. magna</i> survival rate from different trials of experiments with multiple replicates. ....	211
8-4. 120-hour zebrafish survival (blue bars) and hatching rate (red bars) from different trials of experiments with multiple replicates. ....	212
8-5. Dissolved oxygen measured in each species and NC community after 120 hours (Dissolved oxygen measured in <i>D. magna</i> were measured at 48 hour). ....	213
8-6. Summary of the toxicity, uptake, and dissolved fraction of all evaluated NPs using nanocosm assay. ....	214
8-7. <i>D. magna</i> uptake in different types of NP exposures at 0.1 (a) and 1 (b) mg/L. ....	215
8-8. The potential interactions of the four species in the nanocosm assay including the distribution of NP under exposures. ....	220

## LIST OF TABLES

<u>Table</u>	<u>Page</u>
2-1. Organism selection and evaluated endpoints.....	14
S3-1. Standardized information for determining the zeta potential measurements in algae and <i>D. magna</i> media .....	51
S4-1. Standardized information for determining nanoparticle zeta potential in NCM.....	96
S4-2. Theoretical Zn speciation calculated with Visual-MINTEQ assuming equilibrium in NCM using the exposed Zn concentrations.....	97
5-1. Summary of AgNPs uptake in individual daphnids and zebrafish in algae, bacteria and daphnids (A+B+D) and algae, bacteria, daphnia and zebrafish (A+B+D+Z) exposure scenarios after 120 hours. ....	125
5-2. The calculated LC <sub>50</sub> of each species using the dissolved silver concentration measured in each exposure nanocosm. ....	129
S5-1. Metadata associated with zeta potential measurements. ....	148
S5-2. AgNP digestion recovery rates.....	149
S5-3. AgNP hydrodynamic diameters (HDDs) and the corresponding polydispersity index ....	150
S5-4. Theoretical Ag speciation calculated with Visual-MINTEQ assuming equilibrium in NCM. AgCl <sub>(s)</sub> highlight in red indicates the percentage of precipitates that can be formed at the modeled concentrations. ....	151
S5-5. Theoretical Ag speciation calculated with Visual-MINTEQ using measured dissolved silver concentrations in the presence of organisms for each type of AgNP in NCM at each exposure concentration.....	152
S6-1. The dissolution rates and predicted maximum dissolved Cu released in the exposure media. ....	186
8-1. Cost benefit analysis comparing nanocosm assay to ASTM microcosm assay. ....	221

# Novel Approaches to Evaluate the Environmental Impacts of Nanomaterials

## Chapter 1. Introduction

### 1.1 Nanomaterials and environmental concerns

Nanotechnology has been defined as one of the key emerging technologies identified in the Europe 2020 Strategy, and as one of the fastest growing industries in the history, nanotechnology has been referred to as the next industrial revolution (European Parliament 2010). Nanoparticles are defined as particles have one or more external dimension in the size range of 1-100 nm. At such scale, materials usually have different or enhanced properties compared to their bulk counterparts due to an increase in surface-volume ratio that translates into higher reactivity (Nel, Xia et al. 2006). For instance, bulk materials with the same surface area usually constitute only a few percent of the total number of atoms at the surface compared to nano-size materials, where most of atoms lay close to or at the surface (Casals, Gonzalez et al. 2012). The large surface-to-volume ratio makes NPs have high surface reactivity (Hotze, Phenrat et al. 2010), tensile strength (Eatemadi, Daraee et al. 2014), and high atomic precision (Jin 2015), etc.

With those advantages, nanomaterials are widely used in a broad range of consumer products such as cosmetics, consumer electronics, filters, antibacterial products, and industrial products such as semiconductors (Mitrano, Motellier et al. 2015). With the ever-expanding

applications of nanomaterials, industrial production volumes have increased every year (Mueller and Nowack 2008; Sun, Gottschalk et al. 2014). Piccinno et al. estimated that the worldwide production of four metal and metal oxide NPs, and carbon nanotubes (CNTs) to be between 100 and 1000 t/year, and up to 10000 t/year for TiO<sub>2</sub> NPs (Piccinno, Gottschalk et al. 2012).

Increasing NPs production volumes and the growing likelihood of occupational and environmental exposure to nanomaterials, particularly metal and metal oxide NPs such as ZnO, Ag, and CuO NPs, results in their inevitable release into aquatic environments and raises environmental concerns (Blaser, Scheringer et al. 2008). Modeled estimates of ZnO NP concentrations in surface waters range from 0.001 to 0.058  $\mu\text{g L}^{-1}$ , with much higher estimated quantities in soil (0.24-0.661  $\mu\text{g kg}^{-1}$  soil per year) and sewage treatment plant effluent (0.22-1.42  $\mu\text{g L}^{-1}$ ) (Gottschalk, Sonderer et al. 2009). Exposure models also have predicted environmental concentration of AgNPs in water could reach tens to hundreds of  $\text{ng L}^{-1}$  (Mueller and Nowack 2008).

Numerous studies have shown that some nanomaterials are highly toxic to aquatic organisms and can potentially disrupt overall community health (Colman, Espinasse et al. 2014; Bour, Mouchet et al. 2015). Thus, it is of primary importance to elucidate the potential effects of nanomaterials on the health of ecosystems. A significant amount of research has focused on the toxicity of nanoparticles to individual freshwater organisms. For instance, ZnO NPs have been classified as “extremely toxic” to freshwater organisms (Blinova, Ivask et al. 2010); however, the reported toxicity of ZnO NPs to aquatic organisms belonging to various trophic levels varies considerably (Adams, Lyon et al. 2006; Brayner, Ferrari-Iliou et al. 2006; Franklin, Rogers et al. 2007; Zhang, Jiang et al. 2007; Heinlaan, Ivask et al. 2008; Huang, Zheng et al. 2008; Aruoja,

Dubourguier et al. 2009; Blinova, Ivask et al. 2010; Wong, Leung et al. 2010; Xiong, Fang et al. 2011). According to Bondarenko et al., the reported EC<sub>50</sub> values of ZnO NPs for bacteria (multiple species) range from 50-1000 mg L<sup>-1</sup>, algae (multiple species) from 0.052-4.56 mg L<sup>-1</sup>, crustaceans (*Daphnia magna*) range from 0.62-22 mg L<sup>-1</sup>, and fish (*Danio rerio*) vary from 1.79-4.92 mg L<sup>-1</sup> (Bondarenko, Juganson et al. 2013). For AgNPs, median L(E)C<sub>50</sub> values have been summarized as 0.01 mg L<sup>-1</sup> for crustaceans; 0.36 mg L<sup>-1</sup> for algae; 1.36 mg L<sup>-1</sup> for fish; and the median minimum inhibitory concentration for bacteria is 7.1 mg L<sup>-1</sup>. CuO NPs have a relatively lower toxicity compared to AgNPs, with L(E)C<sub>50</sub> values of 2.1 mg L<sup>-1</sup> for crustaceans, 2.8 mg L<sup>-1</sup> for algae, and 200 mg L<sup>-1</sup> for bacteria (Bondarenko, Juganson et al. 2013). The variations in toxicity are likely due to the difference in exposure media, NP shape, size, surface coatings, etc.

## 1.2 Challenges to evaluating the environmental impacts of nanomaterials

Although toxicity data based on individual species provides baseline information for assessing the potential risks of NPs, toxicity studies conducted in controlled laboratory experiments with a single biological model are not a realistic representation of the complexity in nature environments. Individual organism exposure-response relationships are essential for elucidating the mechanisms of toxicity and are what is typically done to inform risk assessments. However, it is quite difficult to extrapolate these findings to natural ecosystems (Colman, Espinasse et al. 2014). Interspecies interactions, such as interspecies competition and prey/predator interaction, cannot be assessed with individual species tests. One the most commonly recognized challenges in evaluating nanomaterial fate and environmental impacts in

aquatic ecosystems is the lack of standardized methods to detect and quantify NPs in experimental media, or environmental and biological samples (Von der Kammer, Ferguson et al. 2012). Existing methods that are employed are time consuming, require specialized equipment, generate large amounts of waste, and are generally not applicable for complex matrices. For instance, particle exposures may not remain consistent due to particle agglomeration kinetics which can result in high inter-laboratory variance.

NPs are currently still regulated as if they were identical to their bulk counterparts and thus have the same CAS (chemical abstract service) number, thus they are not recognized as a new class of chemicals (Bondarenko, Juganson et al. 2013). It is urgent for the nanoscience community to develop a rapid, but cost-effective assay that can systematically evaluate the toxicity of nanomaterials released to the environment. In addition, the assay needs to generate a large enough dataset to allow for modeling the changes in NP properties, and easy enough to be adapted under standard laboratory conditions.

### **1.3 Document Organization**

In this dissertation, Chapter 2 presents a brief overview of all current testing paradigms for evaluating the environmental impacts and fate and transport of NPs; it also lists out the corresponding advantages and disadvantages of each method. To highlight the importance of using more environmental relevant exposure scenarios, Chapter 3 elucidates differences in uptake and toxicity of CuO NP by comparing chronic waterborne exposure to an indirect feeding exposure. Chapter 4 introduces a small-scale, multi-species microcosm community (the



nanocosm assay), which is a more environmentally relevant approach to testing the environmental impacts of NPs. We compared nano- and micro-ZnO particles in the nanocosm assay to improve our understanding of how the agglomeration status affects the dissolution and toxicity to single species or within a community setting. Using the same nanocosm assay, Chapter 5 presents a thorough investigation on differences in organism responses that are due to community complexity, and additionally explores how surface functionalization of AgNPs dictates the toxicity and uptake by organisms in small communities. Chapter 6 further validates the nanocosm assay through an evaluation of the environmental impacts of Cu and CuO NPs. Chapter 7 provides a different perspective of evaluating the toxicity of nanotechnology-containing materials by simulating the end-of-life cycle for an organotin-coated thin film. Finally, Chapter 8 provides summary of this body of work and concludes with an evaluation of the consistency achieved in the developed nanocosm assay, as well as a forecast of the further work that should be addressed moving forward to assay standardization.

## **Chapter 2. Current and future approaches to evaluate the ecotoxicity of NPs**

### **2.1 Single species toxicity testing**

Single species toxicity testing provides basic information on the dose-response relationship of NPs to target organisms. Although these studies are particularly important for understanding mechanisms of toxicity, they do not provide a comprehensive understanding of the fate and transformation of NPs in the environment, nor the impacts in functioning ecosystems. The complexity of the natural aquatic environments impacts NP fate (Tiede, Hassellöv et al. 2009; Aiken, Hsu-Kim et al. 2011), bioavailability (Saikia, Yazdimamaghani et al. 2016; Jiang, Castellon et al. 2017), and toxicity (Maurer-Jones, Gunsolus et al. 2013), particularly water parameters such as pH (Levard, Hotze et al. 2012), dissolved organic matter (Wang, Li et al. 2011), ionic strength (Bian, Mudunkotuwa et al. 2011), and natural buffering capacity (Bone, Matson et al. 2015). The responses of an organism to NP exposures can be affected by the route of exposure: whether NPs are added directly into the exposure solution or added as a complex with algae or other food source, or both simultaneously. Organisms living in contaminated ecosystems are likely to be exposed directly as well as feed on contaminated food. The ingestion of contaminants can have effects that differ from those observed following direct exposure in the environment. In addition, the interactions among organisms can significantly change the actual “dose” (bioavailability) to target and non-target organisms (Bone, Matson et al. 2015). Moreover, the sensitivity of organisms to contaminants are different in an ecosystem, and affected species at one trophic level can influence the whole community balance. Thus,

environmentally relevant exposures are urgently needed to improve our understanding of the impact of NPs to aquatic environments.

## 2.2 Environmentally relevant exposures

Bour and colleagues reviewed 40 existing environmentally relevant approaches to evaluate the impacts of engineered NPs (Bour, Mouchet et al. 2015). They suggest that the current existing environmentally relevant approaches for evaluating NP environmental impact can be sorted into three categories: 1) trophic level exposure which allows for multiple trophic routes under laboratory conditions, 2) multi-species exposures under laboratory conditions, 3) outdoor microcosms and mesocosms (Bour, Mouchet et al. 2015).

Controlled laboratory exposures conducted with species at multiple trophic levels can enhance our determination of NP accumulation in the food chain and its implications for organismal toxicity. This exposure approach assesses the potential of NPs to bioaccumulate or transfer through the food chain, which is particularly important to inform risk assessment. This approach has been performed in multiple aquatic organisms with a variety of different NPs. TiO<sub>2</sub> NPs, for example, have been shown to bioaccumulate in some fish species - *Oncorhynchus mykiss* (Ramsden, Smith et al. 2009), but not others - *Danio rerio* (Fouqueray, Noury et al. 2013), when fed TiO<sub>2</sub> NP contaminated inert food. Other studies fed algae contaminated with NPs to the primary consumer and delivered NPs directly through a dietary route, where accumulation has been observed in using Ag (Zhao and Wang 2010; Buffet, Pan et al. 2013; McTeer, Dean et al. 2014), and TiO<sub>2</sub> NPs exposures (Zhu, Chang et al. 2010). Jackson et al. observed significant

mortality among amphipods fed algae contaminated with CdSe/ZnS quantum dots at concentrations equivalent to 3.6 mg Cd/L of culture medium (Jackson, Bugge et al. 2012). This approach provides a higher level of environmental complexity compared to traditional single species toxicity testing; however, a common disadvantage of this exposure approach is that they usually require a lot of materials and are extremely time consuming and labor intensive to perform. In Chapter 3, we performed a similar study to demonstrate differences in uptake and toxicological impacts between exposure routes which highlight the importance of performing environmentally relevant exposures. However, trophic level exposures are usually chronic experiments, which are not realistic to be utilized to test all nanomaterials and standardized for inter-laboratory comparisons.

Laboratory approaches using multi-species exposures (laboratory microcosms) have multiple advantages. First, simultaneous exposure of multiple species might lead to more complex toxicity responses and provide more integrated results due to species interaction that are not occurring in single species exposures. Second, this method allows for the control of abiotic factors, such as pH and ionic strength, which are important in NP toxicity research since the properties of NP tend to change significantly with minor changes in water parameters (e.g., temperature, pH, ionic strength, hardness, etc.). Third, competition for food or nutrients can be considered in this approach and species sensitivity can be evaluated, which is not possible in single species tests. However, with these advantages, laboratory multi-species exposures also have some drawbacks. In considering logistics, large containers and high volumes of media and materials are required. Although the experiments and replicates can be tightly controlled, sometimes species can be unintentionally added to the system, especially in microbial

communities. Additionally, experiments are still conducted under laboratory conditions, which are not as representative as field studies. Thus, only limited number of freshwater multi-species studies have been performed under laboratory conditions. Three AgNPs were studied using this type of multi-species community approach. Polymer coated AgNPs elicited a decrease in community richness in marine microbial communities (Doiron, Pelletier et al. 2012). Colman et al. observed similar results where a decrease in microbial respiration in stream water microbial community was observed at 75 mg L<sup>-1</sup> PVP-AgNP exposure (Colman, Wang et al. 2012). However, Bradford et al. did not find a significant impact on prokaryotic abundance or bacterial diversity after 20 days of exposure at 25 and 1000 µg/L of AgNPs exposure (Bradford, Handy et al. 2009). Unfortunately, although these studies included multiple microbial communities to investigate interspecies competition, none of these studies investigated a multi-species exposure including a trophic chain.

The third approach to evaluate ecosystem health is outdoor large-scale microcosms and mesocosms. This exposure scenario provides the most comprehensive understanding for NP ecological impact and simulates the most realistic conditions, even consideration of weather and climatic factors. Few studies have investigated the NP environmental impacts using outdoor mesocosms. Pakrashi et al. found Al<sub>2</sub>O<sub>3</sub> NPs decreased algal viability at 1 mg L<sup>-1</sup> in outdoor fresh water microcosm initially, then recovered after long-term exposure (Pakrashi, Dalai et al. 2012). Kulacki et al. investigated the toxicity of TiO<sub>2</sub> NPs in stream mesocosms using three algal species individually or as a community and did not see any toxicity on algal growth or final dry mass from 0.1 – 1 mg L<sup>-1</sup>. In addition, no differences were observed between single and multi-culture exposures (Kulacki, Cardinale et al. 2012). Two other studies researched AgNPs

environmental impacts which did show toxicity and accumulation in aquatic plants (Colman, Espinasse et al. 2014) and fish species (Lowry, Espinasse et al. 2012), using mesocosms and simulated large scale fresh water emergent wetlands, respectively. However, there are a few disadvantages that limit this approach from being widely applied. First, detection methods and quantification methods can be very challenging for NPs in the environment. Second, this exposure scenario is very difficult to conduct and offers limited controls, especially in terms of abiotic factors, which might lead to low repeatability, and the localized parameters make the study hard to translate to other aquatic environments. Third, this approach is extremely time consuming and labor intensive (days to months), making the studies hard to perform and too long to be considered for the rapid pace at which we need to be evaluating NP environmental impacts. Fourth, it is hard to unequivocally interpret the results due to the high complexity of the exposure environment and the multiple confounding factors that can interact and impact the results.

In summary, studies using complex aquatic exposure systems to model environmental conditions and test NPs, such as microcosm or mesocosms, are very scarce. These studies vary widely and concern different types of NP and utilize many different biological models, which prevents the comparison of the results and makes it very difficult to establish general trends regarding NP toxicity and toxicity mechanisms. Besides, many uncertainties and artifacts can occur during outdoor nano-ecotoxicity studies and complicate the comparison among studies. Moreover, the most commonly reported disadvantages for all the studies described above are time and materials necessary to conduct the studies that are labor intensive and generate substantial waste. In order to overcome these limitations, here we introduce a small-scale freshwater microcosm (termed the nanocosm assay) comprised of algae, bacteria, invertebrate,

and vertebrate but also provide enough resolution to evaluate the acute toxicity of NPs to a complex aquatic environment. This nanocosm assay allows rapid and cost-effective evaluation of NPs environmental impacts by assessing the uptake and toxicity. Although the environmental relevancy is not as high as the field micro- or mesocosm experiments, it has highly controlled abiotic factors and can be widely adopted and implemented under basic laboratory conditions. The overarching objective of this dissertation is to develop and validate this rapid, cost-effective nanocosm assay to systematically evaluate the environmental impacts of ENMs.

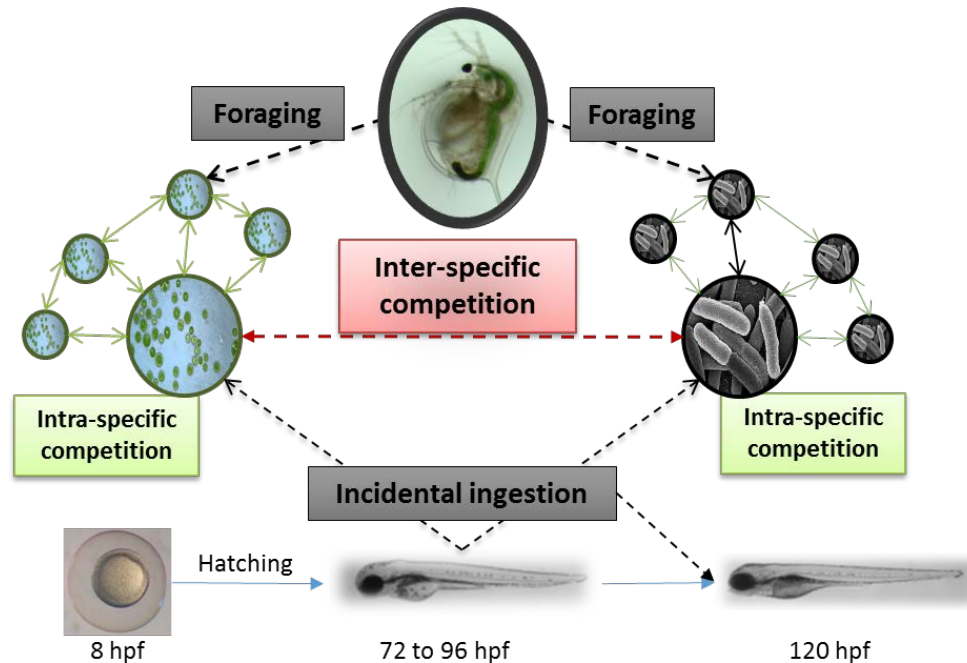
### **2.3 Introducing the nanocosm assay**

A rapid and cost-effective microcosm (multi-species community) including a primary producer, decomposer, and primary consumer will be introduced in this dissertation. Four species (*Chlamydomonas reinhardtii*, *Escherchia coli*, *Daphnia magna*, *Danio rerio*) were selected as test species based on their extensive use in aquatic nanotoxicity tests and represent a broad spectrum of trophic levels (Sondi and Salopek-Sondi 2004; Adams, Lyon et al. 2006; Harper, Usenko et al. 2008; Heinlaan, Ivask et al. 2008; Navarro, Piccapietra et al. 2008; Chen, Zhou et al. 2012; Perreault, Oukarroum et al. 2012; Colman, Arnaout et al. 2013). *C. reinhardtii* and *E. coli* were chosen to represent primary producers and decomposers, respectively. Both species have a simple life cycle, are inexpensive to maintain, are commonly found in aquatic environments and interspecific competition between the two species has been reported (Levy, Stauber et al. 2009). While bacteria and plankton compete for resources, both also serve as food for the primary consumer *D. magna*. *D. magna* are small aquatic crustaceans ubiquitous in

freshwater lotic environments and were included as a primary grazer of the microorganisms. *D. magna* are sensitive to chemical stressors and have long been utilized as an indicator species for assessing aquatic contamination. Embryonic zebrafish were selected as an ideal developing vertebrate model due to their: (i) rapid development, (ii) relatively high sensitivity to anthropogenic contaminants at embryonic stage, (iii) transparency for visual observations, and (iv) well-studied sub-lethal endpoints elicited from NP exposures (Harper, Carriere et al. 2011). Although the embryonic zebrafish do not actively participate in the food web given the short timeframe of these studies, they are exposed to the microcosm contaminants throughout the experiment and following hatching. Mouth-gaping behavior begins around the time of hatching which can lead to oral ingestion of contaminants, despite not actively feeding.

An illustration of the potential species interactions in the nanocosm is presented in Figure 2-1. The detailed procedure of nanocosm community setup is presented in the materials and methods sections in Chapters 4, 5, and 6. Briefly, algae and bacteria are added into a culture flask in 15 mL of nanocosm media. Following that, five *D. magna* neonates and eight embryonic zebrafish at the same developmental stage are added to the nanocosm. Multiple sub-lethal toxicological endpoints are used to evaluate the impacts of NPs as summarized in Table. 2-1.





**Figure 2-1.** The potential interactions of the four species in the nanocosm assay. Algae serve as primary producers and provide oxygen for other species in the system. Bacteria are the representative decomposers of the system. Both algae and bacteria are a primary food source of *D. magna*. Zebrafish do not interact with other species directly before they hatch as their chorion serves as a barrier to those interactions. After zebrafish hatching at 80 hours, they start mouth gaping behavior and can potentially ingest some algae and bacteria.

**Table 2-1.** Organism selection and evaluated endpoints

<b>Organism level</b>	<b>Species name</b>	<b>Reason for selection</b>	<b>Endpoints</b>
<b>Primary producer</b>	<i>Chlamydomonas reinhardtii</i>	Easy to maintain; short life cycle; well-studied; multiple endpoints	Growth rate; cell viability
<b>Decomposer</b>	<i>Escherichia coli</i>	Well studied in nanotoxicity testing; short life cycle; easy to culture;	Growth rate; cell viability
<b>Primary consumer</b>	<i>Daphnia magna</i>	Indicator species for assessing aquatic contamination; widely existing in aquatic ecosystems; transparent body allows easily observed endpoints	Survivability; immobilization; body length; uptake; reproduction
<b>Secondary consumer (indirect)</b>	<i>Danio rerio</i>	Alternative animal model, rapidly develop, easy for observation	Mortality, developmental progression; malformation; behavior; uptake

## 2.4 NP selection

ZnO, Ag, Cu and CuO NPs were selected as model NPs due to their high production volume, known toxicity to aquatic organisms, and relatively large single species toxicity database for comparing our findings. The worldwide annual production of ZnO NPs is estimated

to be 550 tons, ranking as the third most produced NPs (Piccinno, Gottschalk et al. 2012). AgNPs has seen the most wide application, with more than 300 out of 1300 nanotechnological consumer products on the market containing AgNPs (Consumer Products Inventory 2012). Even though Cu and CuO NPs may not have as large production volume as some other two NPs, they have wide industrial application in products such as gas sensors (Li, Liang et al. 2008) and catalysts (Carnes and Klabunde 2003). They are applied in electronics as semiconductors, electronic chips, and are used as heat transfer nanofluids due to their excellent thermophysical properties (Ebrahimnia-Bajestan, Niazmand et al. 2011). In addition, there are other joint nominators for these NPs. All three NPs have metallic elemental composition, and applied in antimicrobial field (Kahru and Dubourguier 2010). Besides, ZnO, Cu, and CuO NPs have negatively charged surface due to the hydroxo and oxo groups on their surface (Levard, Hotze et al. 2012), which allow us to minimize the change in surface charge and the interaction of NPs with organisms. Furthermore, they are all soluble to some extent in aqueous media. Solubility is considered as the key issue in the toxicity of many metal oxide nanoparticles, which stresses that the solubility of NP is important to be considered as one property to enhance our understanding on NP environmental impacts (Aruoja, Dubourguier et al. 2009; Bondarenko, Juganson et al. 2013). Although with these joint criteria, selected NPs have different chemical composition and properties to distinguish the behaviors and impacts in a given environment. Cu and Zn are essential trace elements for almost all types of living cells but Ag is not. In addition, although the primary size are similar in the nano range, the toxicity can be quite different due to their aggregation status which is dynamic in the environment. Besides, Cu is a redox element having common valences of +2 or +1, which is different from Zn and Ag. The surfaces of these

NPs are negatively charged; however, surface coatings attached to the surface to modify their agglomeration potential can dictate NP behavior and their toxicity when interacting with organisms (Bonventre, Pryor et al. 2014). In Chapters 4, 5, and 6, we will investigate the environmental impact of each NP, and explore the influence of minor changes in NP physicochemical features, such size, surface coating and dissolution on organismal uptake and toxicity.

### **Chapter 3. Uptake and toxicity of CuO nanoparticles to *Daphnia magna* varies between indirect dietary and direct waterborne exposures**

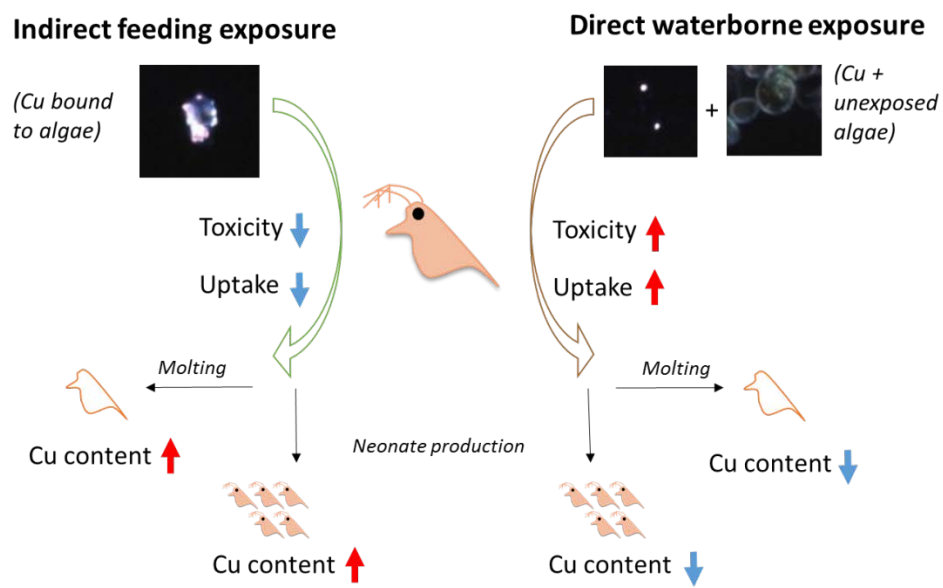
Fan Wu<sup>1</sup>, Amy Bortvedt<sup>2</sup>, Bryan J. Harper<sup>3</sup>, Lauren Crandon<sup>1</sup>, Stacey L. Harper<sup>1,3,4\*</sup>

<sup>1</sup>*School of Chemical, Biological and Environmental Engineering*, <sup>2</sup>*Department of Integrated Biology*, <sup>3</sup>*Department of Environmental and Molecular Toxicology, Oregon State University, Corvallis, OR, United States*; <sup>4</sup>*Oregon Nanoscience and Microtechnologies Institute, Eugene, Oregon, United States*

Aquatic Toxicology

Submitted April 2017

### 3.1 Graphical Abstract



### 3.2 Abstract

Research examining the direct and indirect ecological effects of nanomaterials in aquatic ecosystems is important for developing a more realistic understanding of the environmental implications of nanotechnology. Copper oxide nanoparticles (CuO NPs) are being used extensively in many industries but are considered highly toxic to aquatic species residing in surface waters. Few studies have addressed whether CuO NPs can be transferred through the aquatic food chain, and if such indirect exposure to nanomaterials impacts their toxicity. We investigated the uptake and trophic transfer of CuO NPs from the algae *Chlorella vulgaris* to the crustacean *Daphnia magna* and assessed bio-partitioning and resulting toxicity. We hypothesized that CuO NPs can be associated with algal cells and be transported to predators through feeding, and that the chronic toxicity can be altered in comparison to direct CuO NP exposure. For the indirect feeding exposure, algae pre-incubated with CuO NPs (Cu-algae) were washed to remove loose NPs and fed to *D. magna* while Cu uptake and toxicity were evaluated. For the direct waterborne exposures, a parallel group of *D. magna* were exposed to equivalent concentrations of CuO NPs while being fed unexposed algae. Using hyperspectral imaging we observed strong surface associations between pre-incubated CuO NPs and algae used in the feeding exposure, and quantified the average Cu content (0.15 mg Cu/L) with ICP-OES. Cu accumulated in daphnid bodies to a greater extent in direct exposures, whereas molted carapaces and neonate offspring had more copper following the indirect feeding exposure, implying that *D. magna* may regulate internal Cu differently depending on the method of CuO NP delivery. Significantly higher *D. magna* mortality was observed following direct exposure relative to feeding exposure, and neonate production from adult daphnids exposed indirectly to CuO NPs was significantly

reduced. Thus, nanoparticle interaction with biota at one trophic level may alter the biological response at the next trophic level in a way that is dependent on the delivery scenario. This study highlights the importance of evaluating potential ecological impacts of nanomaterials in more relevant, complex exposure scenarios.

**Keywords:** copper oxide, *Daphnia magna*, hyperspectral imaging, exposure route, chronic toxicity, trophic transfer



### 3.3 Introduction

Copper oxide nanoparticles (CuO NPs) possess excellent thermophysical properties (Ebrahimnia-Bajestan, Niazmand et al. 2011), catalytic activity (Prasad, Kanchi et al. 2016), and physical strength (Xiao, Vijver et al. 2015), making their use widespread in industrial and consumer products. CuO NPs are utilized as sensors (49%), catalysts (20%), surfactants (6%), antimicrobials (4%), and for other purposes (21%) (Bondarenko, Juganson et al. 2013). The aquatic environment is particularly at risk to engineered nanomaterials as is it a natural sink for pollutants and a natural vehicle for pollutant migration. This includes CuO nanoparticles entering wastewater streams following industrial and commercial use (Nowack and Bucheli 2007; Scown, Van Aerle et al. 2010; Keller and Lazareva 2013). Because CuO NPs can be highly toxic to aquatic organisms (Ivask, Juganson et al. 2014), there are concerns about their environmental fate and toxicity following their release into the environment.

The acute toxicity of CuO NPs to aquatic organisms has been evaluated in a variety of studies with reported  $EC_{50}$  values ranging from 0.54 – 37.55 mg Cu/L for algae, 0.06 – 9.8 mg Cu/L for crustaceans, and up to 79.9 mg Cu/L for fish (Bondarenko, Juganson et al. 2013). Reported aquatic toxicity results vary considerably among these studies, likely due to the differences in the specific CuO NPs tested, water quality (e.g. pH, ionic strength), and exposure conditions (e.g. temperature, duration, concentration); all of which can alter dynamic physicochemical processes such as agglomeration and dissolution (Xiao, Peijnenburg et al. 2016). Although acute toxicity studies provide useful information on material or chemical hazards, chronic toxicity testing across varying exposure conditions can provide a more

comprehensive understanding of the potential ecotoxicity of a given nanomaterial. Since chronic toxicity testing is expensive, time consuming and labor intensive, few studies have evaluated the chronic toxicity of CuO or Cu-containing NPs to aquatic organisms (de O.F. Rossetto, Melegari et al. 2014; Adam, Vakurov et al. 2015; Ates, Arslan et al. 2015; Nations, Long et al. 2015; Wang, Fan et al. 2015), only one of these studies that evaluated the chronic toxicity of CuO NPs in the crustacean *Daphnia magna* reported a 21 day EC<sub>50</sub> of 1.04 mg Cu/L (Adam, Vakurov et al. 2015); however, an understanding of the impacts of chronic exposure to CuO NPs on aquatic species remains largely unknown.

Research examining the direct and indirect ecological effects of nanomaterials in aquatic ecosystems is important for developing a more realistic understanding of the environmental implications of nanotechnology (Bernhardt, Colman et al. 2010). While many NP toxicity studies have focused on directly exposing organisms to test substances (Harper, Carriere et al. 2011), organisms living in NP contaminated ecosystems are exposed to contaminants indirectly through bioaccumulation and transfer through the food chain. Contaminants such as CuO NPs ingested in conjunction with food may cause effects that differ from those observed following direct exposures due to potential alterations in the type and degree of environmental transformation occurring within each type of nanoparticle exposure. Evidence suggests that indirect or secondary toxicity may result from interactions of NPs with other chemical, physical, and biological constituents already present in the environment (Geitner, Marinakos et al. 2016; Ribeiro, Van Gestel et al. 2017).

Nanomaterials associated with a food source (feeding exposure) have been shown to affect organismal health at higher trophic levels. When *D. magna* exposed to TiO<sub>2</sub> NPs were fed to zebrafish, results revealed a negative impact on exposed zebrafish digestive enzyme activity (Fouqueray, Noury et al. 2013). In another study, Ramsden and colleagues introduced TiO<sub>2</sub> NPs to juvenile rainbow trout through their diet, which resulted in Ti accumulation in the gill, gut, liver, brain and spleen (Ramsden, Smith et al. 2009). Studies in marine ragworms found differences in the toxicity of cadmium sulfide NPs following direct waterborne and dietary exposures (Buffet, Poirier et al. 2014). Evidence also suggests that dietary metal exposure often shows inconsistent toxicity compared to direct exposure, and that dietary and waterborne metal exposures sometimes show synergistic toxicity (Clearwater, Farag et al. 2002; DeForest and Meyer 2015). These findings suggest that differential exposure and toxicity may be expected between direct waterborne exposures and indirect dietary exposures, especially over chronic exposure timeframes.

We established two chronic exposure scenarios for this study, an indirect feeding exposure and a direct waterborne exposure. In the feeding exposure, *Daphnia magna* were exposed to CuO NPs that were strongly associated with (surface bound or internalized) an algal food source (*Chlorella vulgaris*) (Gersich and Milazzo 1990). Unbound and loosely bound CuO NPs were removed through rinsing so that ingestion was the dominant delivery route in the feeding exposure. In comparison, the direct waterborne exposures constituted the same concentration of CuO NPs bound to the algae in the indirect feeding study, only the CuO NPs were added directly to the media while *D. magna* were fed an equivalent amount of unexposed algae. We hypothesized that CuO NPs can be associated with algal cells resulting in predators

being exposed during feeding, and that the chronic toxicity of CuO NPs to *D. magna* would be altered by changes in copper uptake and partitioning relative to direct NP exposure. The major aim of this study was to improve our understanding of the ecological risk and biological behavior of CuO NPs in aquatic environments under two different exposure scenarios. To our knowledge, this is the first study comparing chronic toxicity of CuO NPs to aquatic organisms using both indirect feeding exposures and direct waterborne exposures.

### 3.4 Materials and Methods

#### 3.4.1 Test organisms

*C. vulgaris* was purchased from the University of Texas Culture Collection (UTEX 2714) and cultured in TAP media (Gorman and Levine 1965). *D. magna* obtained from Carolina Biological Supply Company (Burlington, NC) were maintained in 2 L plastic beakers with 1.5 L of culture media. *Daphnia* culture media was reconstituted hard water consisting of final salt concentrations of 120 mg L<sup>-1</sup> CaSO<sub>4</sub>•2H<sub>2</sub>O, 120 mg L<sup>-1</sup> MgSO<sub>4</sub>, 192 mg L<sup>-1</sup> NaHCO<sub>3</sub>, and 8 mg L<sup>-1</sup> KCl prepared in reverse osmosis water (Weber 1991). pH was maintained in the range of 7.8 ± 0.2. All organisms were maintained at room temperature 20.5 ± 0.5 °C with a 16:8-h light:dark photoperiod under 1690 ± 246 lux light intensity provided by full-spectrum growth lights. *D. magna* were fed *C. vulgaris* daily, with 50% of the culture media refreshed every other day.

#### 3.4.2 Nanoparticle characterization

CuO NPs (primary particle size < 50 nm) were purchased from Sigma Aldrich (St. Louis, MO). Stock suspensions of 1000 mg L<sup>-1</sup> CuO NPs in 10 mL algae or *D. magna* culture media were ultra-sonicated for 2 minutes at 40% intensity using a VCX 750 Vibra-Cell sonicator (Sonics & Materials Inc., Newtown, CT) then diluted to a CuO NP concentration of 50 mg L<sup>-1</sup>. The hydrodynamic diameter (HDD) and the zeta potential (ZP) as a function of electrophoretic mobility (ASTM 2012), were measured by dynamic light scattering using a Zetasizer Nano ZS (Malvern Instruments, Worcestershire, UK) in both types of culture media (algae and *D. magna*) immediately after sonication, and at 24 and 48 hours. Samples were taken from 1 cm below the surface without resuspension. The detailed parameters for HDD and ZP measurements are described in Table S1.

### 3.4.3 Preparation of CuO NP incubated algae (Cu-algae)

Algae associated with CuO NPs were cultured for use in the indirect feeding exposure studies. To prepare the Cu-algae, *C. vulgaris* was grown in TAP media until the cells reached the exponential growth phase (~ day 4), at which time 50 mg L<sup>-1</sup> of CuO NPs were added to each 200 mL algae culture. The mixture was gently shaken at 120 rpm for 24 hours to allow for algae-particle interaction, and then samples were centrifuged in 50 mL conical tubes at 600 x g for 10 minutes to pellet algal cells. After centrifugation, the supernatant was removed and the remaining algal pellets were re-suspended in fresh *D. magna* culture media. The centrifugation and resuspension process was then performed two more times, for a total of three washes. To further remove the free and loosely bound CuO NPs or dissolved copper remaining in the algae

solution, the re-suspended algae was filtered through a 2  $\mu$ m filter (Whatman Nuclepore Track-Etched Membranes GE Healthcare, Pittsburgh, PA) to collect the cells on the filter and washed with 0.05M EDTA. Excess EDTA was removed by additional centrifugation and resuspension in *D. magna* media. The Cu-algae food was prepared fresh daily and sub-samples were preserved at -4° C for later determination of Cu content with inductively coupled plasma optical emission spectrometry (ICP-OES) (ThermoFisher Scientific Inc., Waltham, MA). The average Cu concentration quantified in the algae was used to determine the amount of CuO NPs needed for a comparable direct exposure.

NP and algal associations were analyzed and verified using enhanced darkfield microscopy and hyperspectral imaging (Cytoviva, Inc., Auburn, AL) before and after the washing process. In brief, a 10  $\mu$ L droplet of each algae or nanoparticle solution was mounted on the middle of a clean glass slide, with a cover slip carefully placed on top of the droplet. Prepared slides were viewed at 60 and 100X magnification using dark-field and hyperspectral imaging techniques. CuO NPs associated with algal spectral signatures were verified with spectral images of algae and CuO NPs alone in the exposure media.

#### 3.4.4 Experimental design for toxicity evaluations

Individual *D. magna* neonates (<24 hours old, n=48) were transferred to 50 mL *D. magna* media in 100 mL plastic beakers (VWR, Radnor, PA), with the water in the beaker completely renewed every 48 hours during the 14 day experimental period. Each exposure treatment included a total of 48 replicate beakers. In the feeding studies, control algae and Cu-algae were

used to feed *D. magna* in control, low, and high Cu treatments with the control group receiving the CuO NP free algae source, the low exposure group being fed 50% control + 50% Cu-algae, and the high exposure group was fed 100% Cu-algae. Algal cell concentration was determined spectrophotometrically using a SpectraMax M2 (Molecular Devices, Sunnyvale, CA) at a wavelength of 440 nm in order to provide individual *D. magna* 0.1mg C per day as algae (OECD 2012). We fed each *D. magna* the same amount of algae (~ 0.1 mg C/day) in order to maintain *D. magna* health (Mackevica, Skjolding et al. 2013). In the direct waterborne exposures, an equivalent amount of control algae as was fed to *D. magna*, followed immediately by direct addition of CuO NPs to the media at a concentration equivalent to the daily amount received in the Cu-algae feeding exposures.

*D. magna* mortality, body length, and neonate production were monitored and recorded over the experimental period. Offspring were removed from the exposure beakers daily. Molted carapaces from *D. magna* were also collected from the beakers throughout the experiment. Ten *D. magna* from each treatment were imaged on days 4, 9, and 14 using an Olympus SZX10 microscope (Center Valley, PA) equipped with a SC100 digital camera and body length was analyzed with ImageJ software (Rasband 1997-2016). After imaging, daphnids were thoroughly rinsed with ultrapure water three times, then placed into 1 ml centrifuge tubes and dried at 60 °C until dry weight remained unchanged, at which time Cu quantification was performed. Neonate offspring and molted carapaces collected from experimental beakers were also similarly washed with ultrapure water and dried prior to Cu quantification.

### 3.4.5 Determination of dissolved and organismal Cu content

CuO NP dissolution in the exposure beakers was measured at three time points (0, 24 and 48 hours) throughout the experiment. At each time point, a 0.5 mL aliquot was taken from each beaker and centrifuged at 13,000×g for 10 minutes through a 3 kDa centrifugal polyethersulfone (PES) membrane filter (VWR #82031-346, Radnor, PA) to remove any CuO NPs or precipitates. The process was repeated nine more times in order to get a total collection of 4.5 mL of filtered water sample for ICP-OES. Water samples were adjusted with 70% trace-metal grade HNO<sub>3</sub> to a final concentration of 3% HNO<sub>3</sub>. The algae, *D. magna* adults and neonates, and molted carapace samples were digested in Teflon tubes (Wu, Harper et al. 2017). Samples were heated to 200 °C and the acid was allowed to completely evaporate. This process was repeated three times and the digested samples were dissolved in 5 mL of 3% HNO<sub>3</sub> prior to ICP-OES analysis. Copper ICP standards were purchased from RICCA Chemical Company (Arlington, TX). All measurements were conducted in triplicate.

### 3.4.6 Data analysis

SigmaPlot version 13.0 (Systat Software, San Jose, CA, USA) was used to perform all statistical analyses. Differences among delivery scenarios, concentrations, Cu uptake, body length, average brood size, total number of broods, and time to first brood were compared using analysis of variance (ANOVA) with Dunnett's post-hoc analysis. Fisher's exact test was used to identify significant differences in the number of surviving *D. magna* relative to control daily from day 0 to day 14. All differences were considered statistically significant at  $p \leq 0.05$ . Copper



bioaccumulation factors were calculated using equation 3.1, assuming the CuO NP taken up by *D. magna* were from the total exposed CuO NPs over the 14 days without the consideration of depuration.

$$\text{Bioaccumulation Factor} = \frac{\text{Total Cu measured in } D. magna}{\text{Exposed CuO NPs over 14 days}} \quad (\text{equation 3.1})$$

### 3.5 Results

#### 3.5.1 Nanoparticle characterization

HDD and ZP were characterized in both algae and *Daphnia* culture media over 48 hours to monitor particle agglomeration in each media (Figure S3-1). In the *Daphnia* exposure media, CuO NPs had significant agglomeration over time with an initial HDD of  $926 \pm 35$  nm (polydispersity index of  $0.57 \pm 0.03$ ) and a ZP of  $-22.7 \pm 1.1$  mV. After 24 hours, agglomerate size decreased significantly to  $751 \pm 31$  nm, followed by an increase to  $1095 \pm 119$  nm after 48 hours. The corresponding ZP was  $-26.4 \pm 0.8$  mV and  $-9.6 \pm 0.8$  mV at 24 and 48 hours, respectively. However, in the algae media, CuO NPs had significantly larger agglomerates of  $1040 \pm 99$  nm at time 0, which then decreased to  $823 \pm 100$  nm at 24 hours and remained relatively constant with agglomerates measuring  $879 \pm 92$  nm after 48 hours. Initial ZP in the algae media was negative ( $-31.6 \pm 2.1$  mV) then became more neutral and stabilized to  $-19.2 \pm 0.1$  mV and  $-19.7 \pm 2.5$  mV at 24 and 48 hours, respectively.

#### 3.5.2 Removal of non-attached CuO NPs from algae

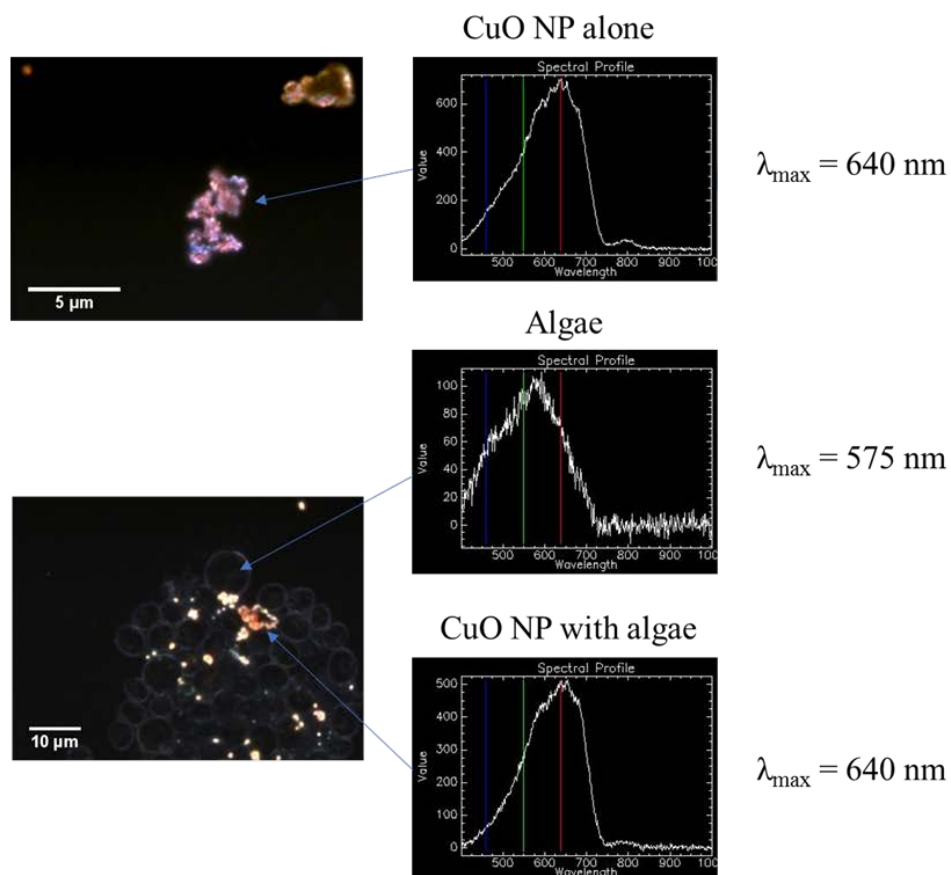
To effectively remove non-attached CuO NPs, serial filtration was performed on the prepared Cu-algae. As is shown in Figure S3-2, more than 70% of CuO NPs loosely bound to algal surfaces and free in solution were removed after the first round of centrifugation and filtration, with the strongly bounded CuO NPs/Cu concentration remaining relatively consistent following further filtrations (Figure S3-2). In addition, adding the EDTA wash step significantly decreased the percent of Cu in the remaining algae (Figure S3-3). Dark field microscopy and HSI (Figure 3-1a) were used before (Figure 3-1b) and after (Figure 3-1c) centrifugation and filtration to image the algal cells and verify that free particles were effectively removed. The amount of Cu associated with the Cu-algae fed to individual *D. magna* was quantified with ICP-OES daily and is shown in Figure S3-4. The mean value over 14 days was used to determine the exposure concentration for the corresponding direct waterborne exposures (0.07 mg Cu/L for low and 0.15 mg Cu/L for high concentration exposure).

### 3.5.3 CuO NPs dissolution and uptake in *D. magna*

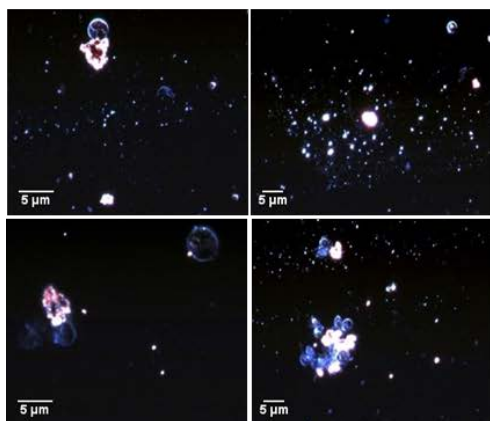
Dissolved Cu concentration was below the 5 µg/L detection limit of the ICP-OES in both the feeding and direct exposures, indicating that the freely dissolved Cu fraction was less than 1.7% of the total CuO NPs added. The total Cu content in *D. magna* was quantified at days 4, 9 and 14 for both exposure scenarios (Figure 3-2). Significantly higher Cu concentrations were found in *D. magna* bodies with increasing exposure concentrations in both delivery scenarios over time. However, the dynamics of Cu concentration in *D. magna* over time between the two delivery scenarios were largely different. In the feeding exposure, the total Cu content reached a

maximum at day 9 (with 1.84 mg Cu/g and 2.36 mg Cu/g in the low and high concentration exposure, respectively), and then significantly decreased at day 14. In contrast, Cu concentration in *D. magna* bodies continued to increase in the direct exposure, with the peak Cu content found at day 14. Interestingly, the final Cu concentration in *D. magna* at day 14 in both the feeding (0.88 and 1.39 mg Cu/g in low and high exposures, respectively) and direct (1.1 and 1.48 mg Cu/g in low and high exposures, respectively) chronic studies reached similar final values.

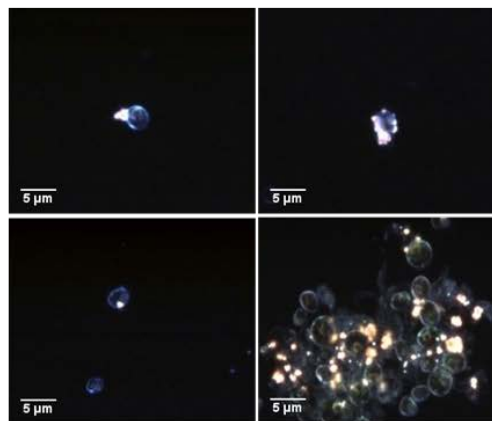
## a. Identification of CuO NP



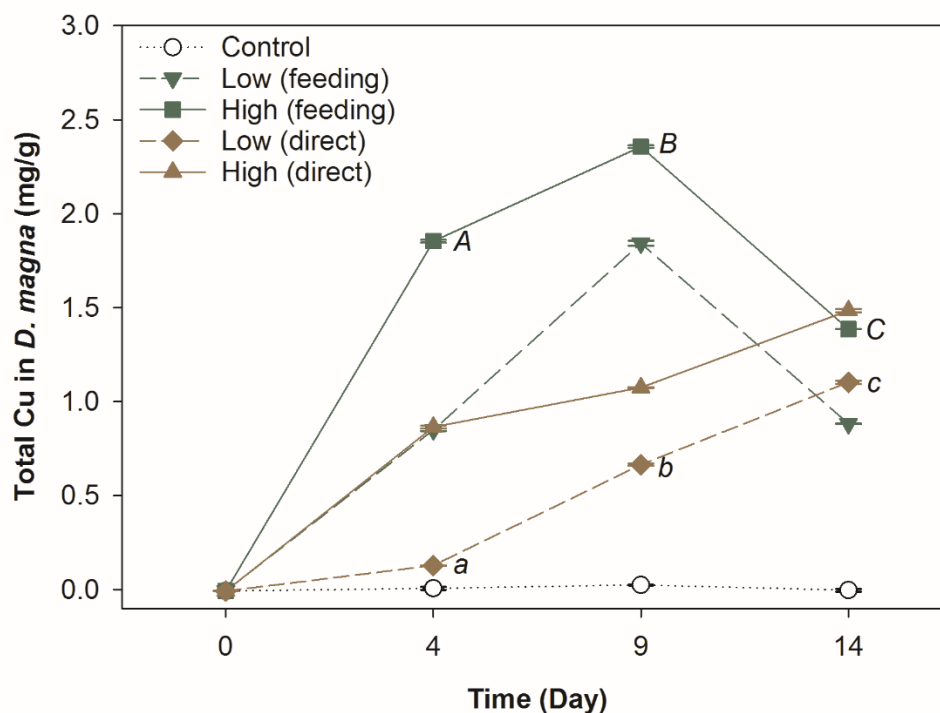
## b. Unfiltered



## c. Filtered



**Figure 3-1.** a) Identification of CuO NPs using HSI and the corresponding spectral profile of bare CuO NPs, algae cells, and CuO NPs associated with algae cells. Dark field images b) before and c) after the centrifugation and filtration rinsing steps.

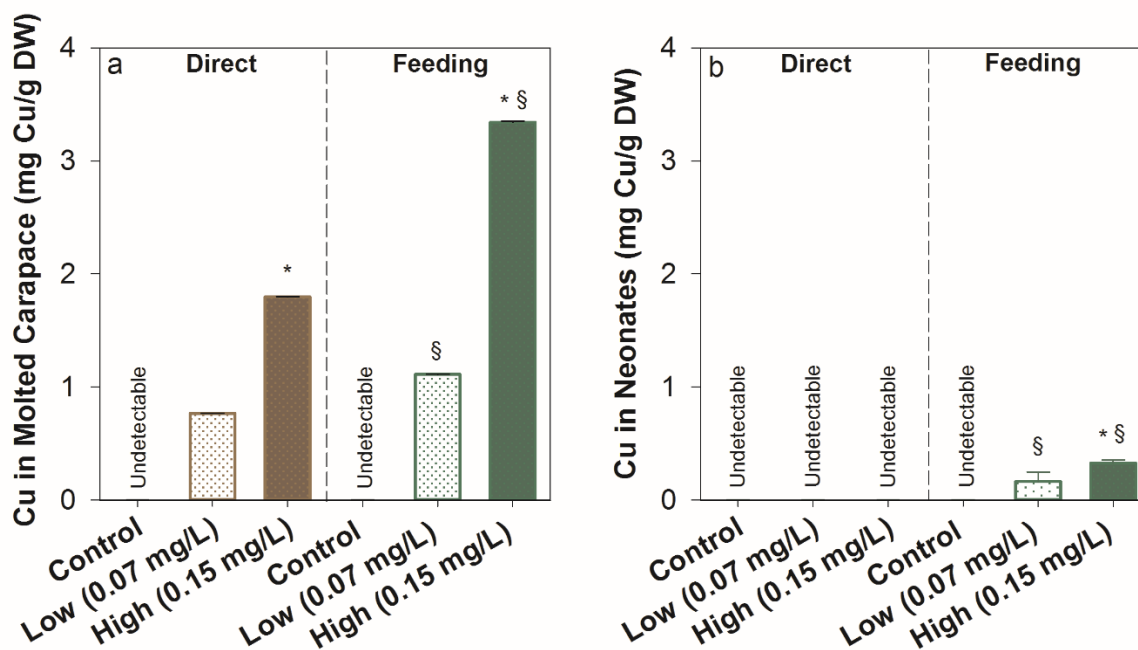


**Figure 3-2.** Total Cu in *D. magna* following low (dash line) and high (solid line) exposure concentrations through feeding (green) and direct (brown) exposure scenarios (DW = Dry Weight). The error bar represents the standard error of three sample replicates. Lowercase (a, b, c) characters indicate significant differences in Cu concentration between feeding and direct exposure, and uppercase (A, B, C) indicate significant difference between low and high exposure concentrations, respectively.

As *D. magna* typically molt every two days, carapaces were collected throughout the experiments and the Cu concentration in the molted carapaces from each exposure scenario are presented in Figure 3-3a. Cu content in the carapaces significantly increased with exposure concentration in both exposure scenarios. In addition, the carapaces from the feeding exposure had significantly more Cu overall than was found in the direct exposure carapaces. The measured

Cu concentrations in the carapaces were similar to the copper content in the bodies. Although Cu was found in the molted carapaces in both feeding and direct exposure, only carapaces collected from direct exposure had observable CuO NPs attached, whereas no CuO NPs were observed on the carapaces from the feeding exposure (Figure S3-5).

*D. magna* started to reproduce at day 9 of the experiment (Figure S3-6). Neonates were collected and distributed to three sample replicates by exposure concentration and feeding group, and the measured Cu content in neonates is presented in Figure 3-3b. There was no significant Cu accumulation in neonates collected from the direct NP exposures compared to control; however, the feeding exposure resulted in a significantly elevated Cu concentration compared to control and direct exposure neonates. Overall, neonates had much lower copper concentrations per unit mass than was found in either the adult bodies or carapaces. In the feeding exposure, Cu content in neonates was approximately 8.9% and 13.8% of what was found in the adult bodies (day 14) under the low and high exposure concentration, respectively.

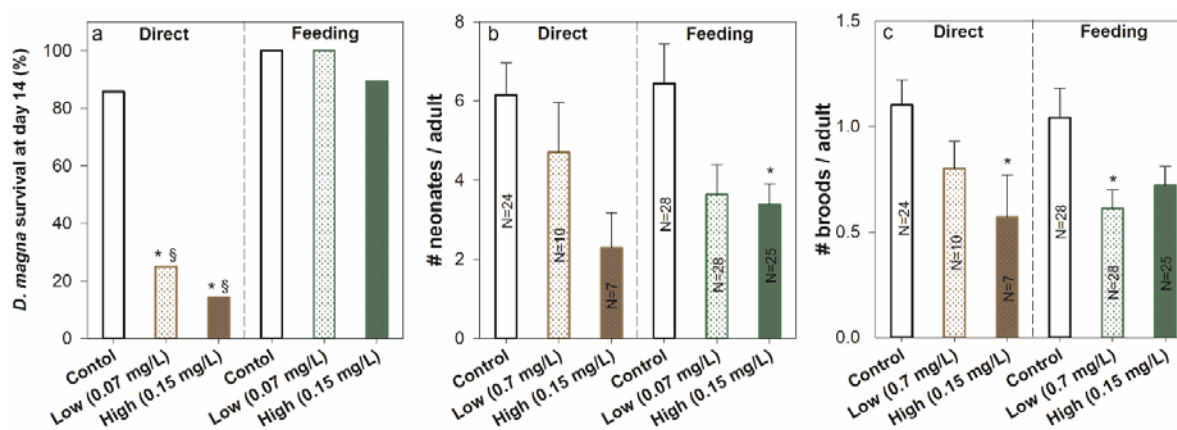


**Figure 3-3.** Total Cu measured in a) molted carapaces, and b) produced neonates from both delivery scenarios. The error bar represents the standard error of three measurement replicates in molted carapaces and three sample replicates in produced neonates. Asterisk symbol \* indicates significantly increased Cu concentration in the high concentration exposures compared to low concentration exposures, and symbol § indicates a significant difference in Cu concentration between feeding and direct exposures at a given exposure concentration. All exposures had significantly higher Cu concentration compared to corresponding controls except Cu in neonates (b) in the direct exposure (not labeled in Figure 3-3).

#### 3.5.4 Chronic toxicity of CuO NPs to *D. magna*

*D. magna* body length was significantly decreased in the direct exposure group at the high exposure concentration compared to control *D. magna* at day 14 (Figure S3-7a); however, there was no significant difference in *D. magna* body length in the feeding exposure (Figure S3-7b). By comparing both delivery scenarios, significantly reduced body length was found in the direct exposure at the same exposure concentration. The chronic toxicity of CuO NPs to *D.*

*magna* following feeding and direct exposures is shown in Figure 3-4. Direct exposure resulted in high mortality to *D. magna*, with nearly 70% and 90% mortality occurring in the low (0.07 mg L<sup>-1</sup>) and high (0.15 mg L<sup>-1</sup>) exposure concentrations, respectively (Figure 3-4a). In contrast, the feeding exposures showed no significant difference in mortality compared to control *D. magna* at any exposure concentration. In addition, there was no significant difference in average number of neonates and broods produced per adult between the two delivery scenarios. However, the high concentration feeding exposure significantly reduced the average number of neonates produced per adult by 50% relative to the corresponding control (Figure 3-4b). The total number of broods produced per adult was significantly lower in the direct exposure at the high concentration, and at the low exposure concentration in the feeding exposure (Figure 3-4c). This indicates that CuO NP exposures could impact the reproduction of *D. magna* regardless of the exposure scenario.



**Figure 3-4.** Chronic effects of CuO NPs to *D. magna* following feeding and direct exposure for 14 days (a. percent survival; b. # neonates / adult; c. # brood / adult). The error bar represents the standard error of all sample replicates. Asterisk (\*) indicate significant differences among treatments compared to corresponding controls, and symbol § indicates significant difference between direct and feeding exposure under the same exposed Cu concentrations. Detailed statistics are described in the supplemental information.



### 3.6 Discussion

In order to interpret the findings and improve our understanding of the ecological risks and biological behavior of CuO NPs in aquatic environments, all the factors contributing to the exposure should be fully characterized throughout the exposure period. Here, we hypothesized that indirect feeding exposures and direct waterborne exposures would have different effects on *D. magna* due to association with algal cells. Overall, we found that toxicity and partitioning was different between the two exposure scenarios, thus, nanoparticle interaction with biota at one trophic level may alter the biological response to that nanoparticle at the next trophic level in a way that is dependent on the delivery scenario.

The high ionic strength of algae media and the presence of divalent cations ( $\text{Ca}^{2+}$  and  $\text{Mg}^{2+}$ ) in *D. magna* water likely contributed to the formation of large agglomerates (Figure S3-1) since agglomeration state is known to be largely dependent on the ionic strength, pH, and hardness (French, Jacobson et al. 2009; Badawy, Luxton et al. 2010). In algae media, the agglomerated particles were smaller than the pore size of the membrane filter used to collect Cu-algae cells, supporting our selection of the 2  $\mu\text{m}$  filter to collect algal cells while allowing NP agglomerates to pass. The washing process effectively removed background NPs and loosely bound NPs on the algae cells, leaving only NPs strongly bound to the algae surface and possibly internalized (Figure 3-1). After removing the background and loosely bound CuO NPs, approximately  $9.6 \pm 2.2$  % of the initial exposed CuO NPs remained associated with algal cells.

It should be noted that the 50 mg L<sup>-1</sup> CuO NP incubation concentration is approximately three orders of magnitude higher than expected environmental concentrations (0.06 mg Cu/L) (Chio, Chen et al. 2012); however, the final exposure concentrations to each *D. magna* were in the range of estimated environmental concentrations (0.07 and 0.15 mg Cu/L) consistently throughout the feeding experiment (Figure S3-4). The exposure concentrations obtained were also comparable to concentrations used in the toxicological research database (ranging from 0.32–569 mg L<sup>-1</sup> as acute EC<sub>50</sub> to multiple species in NanoE-Tox database) (Juganson, Ivask et al. 2015). Although nanoparticle internalization was not visually confirmed in this study, small NPs do have the potential to be internalized in algal cells. Studies have demonstrated that NPs are predominantly taken up by algae via endocytosis (Wang, Li et al. 2011; Zhao, Cao et al. 2016), where phagocytosis enables ingestion of large particles (> 250 nm in diameter), and pinocytosis allows algal cells to ingest solutes and small particles (<100 nm) via small pinocytic vesicles (Bruce Alberts 2002). Smaller NPs can also diffuse across the ion/voltage channels (Chang, Zhang et al. 2012), and transporter proteins can permit NPs to cross the plasma membrane (De Jong, Hagens et al. 2008; Kwon, Hwang et al. 2008). However, agglomeration likely minimized these processes in our experiments. Rather, it is likely that the larger agglomerated CuO particles were strongly bound to the algae surface, as is shown in Figure 3-1.

All NP zeta potentials were initially negative in the exposure media and the magnitude decreased over time, likely due to interactions of cations with the NP surface. ZP values ranged from -10 to -30 mV, indicating relative instability in both algae and *Daphnia* culture media. Indeed, we see significant agglomeration occurring (HDD values ranging from 751-1095 nm) in both types of exposure media (Figure S3-1). Since the HDD and ZP were measured in abiotic

exposure media, it is worth noting that the presence of organisms could further alter the stability and surface charge of the NPs. Algae have a negatively charged cell surface (Hadjoudja, Deluchat et al. 2010), the repulsive force of the negatively charged CuO NPs could hinder the interaction between CuO NPs and algae cells and lead to a low attachment tendency (Zhao, Cao et al. 2016). However, dissolved organic matter, such as algal exudates, can alter the surface charge of NPs by binding to the NP surface via electrostatic interaction and consequently affect the bioavailability of those NPs to organisms (Collin, Oostveen et al. 2014; Wang, Zhang et al. 2016).

There was no detectable ionic Cu in either exposure scenario at any time during our study. This may be because CuO dissolution is a process promoted by acidic conditions that is limited at or above neutral pH (7.8 in this study) (Wang, Von Dem Bussche et al. 2013; Kaweeteerawat, Chang et al. 2015). Additionally, extracellular organic matter could have coated the CuO NPs, inhibiting ion release by preventing interaction of the NP surface with the exposure media and reducing the availability of  $H^+$  (Ostermeyer, Kostigen Mumuper et al. 2013; Adeleye, Conway et al. 2014). Furthermore, NP hetero-agglomeration with algae and homo-agglomeration can further decrease the surface area exposed to the aquatic environment, resulting in lower dissolution (Bian, Mudunkotuwa et al. 2011). Lastly, dissolved Cu has a high affinity for amino acids and proteins so dissolved Cu species may have bound to large proteins and been removed through the filtration process with a 3kDa filter (Wang, Von Dem Bussche et al. 2013).

In both exposure scenarios, there was a concentration dependent uptake of copper by *D. magna*; however, by the end of the 14 day exposure, there was higher Cu content in the direct exposures relative to the feeding exposures. The elevated Cu content found in the direct exposures could be attributed to CuO NP association with *D. magna* external and internal structures. Even in the direct exposures, it is likely that some NPs were ingested directly, as others have shown in *D. magna* that some particles could have associated with the food being grazed (Zhu, Chang et al. 2010; Adam, Leroux et al. 2015).

Cu found in *D. magna* from the feeding exposures showed a significantly more rapid accumulation over the first 9 days. It is likely that CuO NPs were easily taken up by *D. magna* in the feeding exposure through preying on the CuO NP associated algae. Interestingly, Cu accumulated in *D. magna* continuously throughout the direct exposures, whereas in the feeding exposures, Cu concentration reached a peak at day 9 and then decreased by day 14. This is likely attributed to regulatory mechanisms within individual *D. magna*, as the decrease in Cu content between days 9 and 14 in the feeding exposure coincides with the onset of neonate production. Thus, maternal transfer to offspring may have served as a major pathway for Cu regulation following ingestion that did not seem to occur when *D. magna* were directly exposed to the NPs. Geitner et al. also observed maternal transfer of AuNPs to neonates (2.5 mg/g) by conducting 24 hour feeding studies with AuNP contaminated algae (Geitner, Marinakos et al. 2016). Maternal transfer of metal contaminants can significantly affect the offspring in terms of their growth, survival, and metal tolerance (Tsui and Wang 2007), which have the potential to ultimately impact ecosystem health.

Studies have shown that possible pathways of Cu loss from *D. magna* include excretion, molting, feces, and transfer to neonates (Zhao, Fan et al. 2009). Cu was detected in *D. magna* carapaces in both exposure scenarios, but was significantly higher in the feeding exposures. Despite this finding, hyperspectral imaging revealed observable CuO NPs on the carapaces from the direct exposures only (Figure S3-5), suggesting that the high Cu concentration in the feeding carapaces was not in NP form, and that molting is one mechanism for regulating maternal copper. In addition, the concentration of copper found in carapaces from both exposures was similar to what was found in the adult bodies, further supporting molting as one of the main mechanisms of decreasing internal Cu concentration. Bossuyt and Janssen have shown that *D. magna* can actively regulate absorbed copper to maintain homeostasis when exposure is less than 150 µg Cu/L (Bossuyt and Janssen 2005), which is similar to our highest exposure concentration, suggesting the *D. magna* in our study were likely able to regulate their internal copper concentration. The regulatory mechanisms that dominate following differential exposures is worth pursuing in future studies.

We observed significantly higher *D. magna* mortality and lower body lengths in the direct exposure compared to the feeding exposure. Some studies suggest that Cu<sup>2+</sup> released from the CuO core dominates toxicity of CuO NPs (Ebrahimnia-Bajestan, Niazmand et al. 2011; Jo, Choi et al. 2012); however, there was no detectable ionic Cu in either exposure scenario in our study. This could be due to either suggesting a lack of dissolution or the rapid uptake of ionic copper. The surface attachment of CuO NPs to algae may have contributed to the corresponding lower toxicity observed in the feeding exposure scenario. Reduced toxicity observed in the feeding exposure may be related to passivation of the NP surface by organic matter. Extracellular

organic matter released from algae produced during the incubation period could interact with NPs to reduce their toxicity, as has been shown for CuO and other metal oxide NPs (Henderson, Baker et al. 2008). Zhao et al. revealed that fulvic acid significantly reduced the damage of CuO NPs to bacterial membranes by reducing the leakage of  $K^+$  ions caused by CuO NPs (Zhao, Wang et al. 2013). In addition, organic matter can coat the NPs, quenching the production of reactive oxygen species to reduce toxicity, creating an electrostatic repulsive force by changing the surface charge or by reducing the reactivity by hindering the direct contact between NPs and organisms (Louie, Tilton et al. 2016). Although algae extracellular organic matter was present in both exposure scenarios, this process may have had a greater contribution in the feeding exposure due to the 24 hour incubation period. Hetero-agglomeration between algae and CuO NPs in the feeding exposures could lead to a decrease in available reactive surface area. Studies have shown that agglomerated NPs tend to have reduced reactivity and correspondingly lower cellular uptake and toxicity (Albanese and Chan 2011; Jassby, Farner Budarz et al. 2012). The interaction of nanoparticles with environmental constituents (e.g., particulates, microorganisms) is often described in terms of surface attachment efficiency, which could be an important indicator of nanoparticle trophic level interactions (Geitner, Marinakos et al. 2016).

The interaction of NPs with lower trophic level aquatic organisms could be a critical route of nanomaterial exposure and persistence that can impact ecosystem health at higher trophic levels (Ferry, Craig et al. 2009; Dabrunz, Duester et al. 2011). In our study, the feeding exposure delivered largely hetero-agglomerated CuO NPs to *D. magna*, leading to significantly decreased *D. magna* reproduction. Similar results have also been observed with  $Cu^{2+}$  exposures, where *D. magna* showed a decrease in growth and reproduction from elevated Cu in their diet of

green algae *Pseudokirchneriella subcapitata* (De Schamphelaere, Forrez et al. 2007). Based on our knowledge,  $\text{Cu}^{2+}$  has the capacity to transfer through the food chain, but not always in sufficient quantities to biomagnify due to internal regulation of copper (De Schamphelaere and Janssen 2004; De Schamphelaere, Forrez et al. 2007). CuO NPs that are internalized with food in *D. magna* can be excreted quickly through the feces when the exposure stops (Adam, Vakurov et al. 2015), but in this study *D. magna* were continuously exposed with no depuration period. In reality, each delivery scenario that we simulated here could underestimate the overall chronic impacts in the natural environment, since multiple delivery scenarios can occur in the same ecosystem simultaneously. By assuming equilibrium and no excretion in this 14-day study, we obtained bioaccumulation factors of 710 and 660 for direct and feeding exposures, respectively. The high tendency of Cu to accumulate in *D. magna* provides us information that CuO NP exposures could lead to biomagnification in a continuously contaminated food web, potentially affecting higher-level organism health.

### 3.7 Conclusion

This study highlights some of the critical ecological responses that may be overlooked when conducting individual species toxicity testing. In this study, we emphasized the role of exposure time, trophic transfer, and environmental fate on the toxicity and behavior of NPs. Current testing paradigms do not emphasize the importance of evaluating the ecological impacts of NPs in a multi-species community, which allows for organismal transformations of the NPs themselves, the trophic transfer of NPs, as well as the potential for mitigation of effects by

extracellular exudates. The combined direct and indirect effects of nanomaterial exposure have the potential to modify both the exposure and the toxicity in comparison to results from traditional single-species tests that feed into current risk assessments. Thus, to truly understand how nanomaterials behave in complex aquatic food chains, it will require additional studies like this, which examine both the interspecies and generational transfer of nanomaterials and their components.



### 3.8 References

- Adam, N., F. Leroux, et al. (2015). "The uptake and elimination of ZnO and CuO nanoparticles in *Daphnia magna* under chronic exposure scenarios." Water research **68**: 249-261.
- Adam, N., A. Vakurov, et al. (2015). "The chronic toxicity of CuO nanoparticles and copper salt to *Daphnia magna*." Journal of hazardous materials **283**: 416-422.
- Adeleye, A. S., J. R. Conway, et al. (2014). "Influence of extracellular polymeric substances on the long-term fate, dissolution, and speciation of copper-based nanoparticles." Environmental science & technology **48**(21): 12561-12568.
- Albanese, A. and W. C. Chan (2011). "Effect of gold nanoparticle aggregation on cell uptake and toxicity." ACS nano **5**(7): 5478-5489.
- ASTM (2012). Standard Guide for Measurement of Electrophoretic Mobility and Zeta Potential of Nanosized Biological Materials, ASTM International.
- Ates, M., Z. Arslan, et al. (2015). "Accumulation and toxicity of CuO and ZnO nanoparticles through waterborne and dietary exposure of goldfish (*Carassius auratus*)." Environmental toxicology **30**(1): 119-128.
- Badawy, A. M. E., T. P. Luxton, et al. (2010). "Impact of environmental conditions (pH, ionic strength, and electrolyte type) on the surface charge and aggregation of silver nanoparticles suspensions." Environmental science & technology **44**(4): 1260-1266.
- Bernhardt, E. S., B. P. Colman, et al. (2010). "An ecological perspective on nanomaterial impacts in the environment." Journal of environmental quality **39**(6): 1954-1965.
- Bian, S.-W., I. A. Mudunkotuwa, et al. (2011). "Aggregation and dissolution of 4 nm ZnO nanoparticles in aqueous environments: influence of pH, ionic strength, size, and adsorption of humic acid." Langmuir **27**(10): 6059-6068.
- Bondarenko, O., K. Juganson, et al. (2013). "Toxicity of Ag, CuO and ZnO nanoparticles to selected environmentally relevant test organisms and mammalian cells in vitro: a critical review." Archives of toxicology **87**(7): 1181-1200.
- Bossuyt, B. T. and C. R. Janssen (2005). "Copper regulation and homeostasis of *Daphnia magna* and *Pseudokirchneriella subcapitata*: influence of acclimation." Environmental pollution **136**(1): 135-144.

- Bruce Alberts, D. B., Julian Lewis, Martin Raff, Keith Roberts, James D. Watson, and A. V. Grimstone (2002). Transport into the Cell from the Plasma Membrane: Endocytosis. Molecular Biology of the Cell. New York, Garland Science.
- Buffet, P.-E., L. Poirier, et al. (2014). "Biochemical and behavioural responses of the marine polychaete *Hediste diversicolor* to cadmium sulfide quantum dots (CdS QDs): waterborne and dietary exposure." Chemosphere **100**: 63-70.
- Chang, Y.-N., M. Zhang, et al. (2012). "The toxic effects and mechanisms of CuO and ZnO nanoparticles." Materials **5**(12): 2850-2871.
- Chio, C.-P., W.-Y. Chen, et al. (2012). "Assessing the potential risks to zebrafish posed by environmentally relevant copper and silver nanoparticles." Science of The Total Environment **420**: 111-118.
- Clearwater, S. J., A. Farag, et al. (2002). "Bioavailability and toxicity of dietborne copper and zinc to fish." Comparative Biochemistry and Physiology Part C: Toxicology & Pharmacology **132**(3): 269-313.
- Collin, B., E. Oostveen, et al. (2014). "Influence of natural organic matter and surface charge on the toxicity and bioaccumulation of functionalized ceria nanoparticles in *Caenorhabditis elegans*." Environmental science & technology **48**(2): 1280-1289.
- Dabrunz, A., L. Duester, et al. (2011). "Biological surface coating and molting inhibition as mechanisms of TiO<sub>2</sub> nanoparticle toxicity in *Daphnia magna*." PloS one **6**(5): e20112.
- De Jong, W. H., W. I. Hagens, et al. (2008). "Particle size-dependent organ distribution of gold nanoparticles after intravenous administration." Biomaterials **29**(12): 1912-1919.
- de O.F. Rossetto, A. L., S. P. Melegari, et al. (2014). "Comparative evaluation of acute and chronic toxicities of CuO nanoparticles and bulk using *Daphnia magna* and *Vibrio fischeri*." Science of The Total Environment **490**: 807-814.
- De Schamphelaere, K., I. Forrez, et al. (2007). "Chronic toxicity of dietary copper to *Daphnia magna*." Aquatic Toxicology **81**(4): 409-418.
- De Schamphelaere, K. A. and C. R. Janssen (2004). "Effects of chronic dietary copper exposure on growth and reproduction of *Daphnia magna*." Environmental toxicology and chemistry **23**(8): 2038-2047.
- DeForest, D. K. and J. S. Meyer (2015). "Critical review: toxicity of dietborne metals to aquatic organisms." Critical Reviews in Environmental Science and Technology **45**(11): 1176-1241.

- Ebrahimnia-Bajestan, E., H. Niazmand, et al. (2011). "Numerical investigation of effective parameters in convective heat transfer of nanofluids flowing under a laminar flow regime." International journal of heat and mass transfer **54**(19): 4376-4388.
- Ferry, J. L., P. Craig, et al. (2009). "Transfer of gold nanoparticles from the water column to the estuarine food web." Nature Nanotechnology **4**(7): 441-444.
- Fouqueray, M., P. Noury, et al. (2013). "Exposure of juvenile Danio rerio to aged TiO<sub>2</sub> nanomaterial from sunscreen." Environmental Science and Pollution Research **20**(5): 3340-3350.
- French, R. A., A. R. Jacobson, et al. (2009). "Influence of ionic strength, pH, and cation valence on aggregation kinetics of titanium dioxide nanoparticles." Environmental science & technology **43**(5): 1354-1359.
- Geitner, N. K., S. M. Marinakos, et al. (2016). "Nanoparticle Surface Affinity as a Predictor of Trophic Transfer." Environmental science & technology.
- Gersich, F. and D. Milazzo (1990). "Evaluation of a 14-day static renewal toxicity test with *Daphnia magna* Straus." Archives of environmental contamination and toxicology **19**(1): 72-76.
- Gorman, D. S. and R. Levine (1965). "Cytochrome f and plastocyanin: their sequence in the photosynthetic electron transport chain of *Chlamydomonas reinhardtii*." Proceedings of the National Academy of Sciences of the United States of America **54**(6): 1665.
- Hadjoudja, S., V. Deluchat, et al. (2010). "Cell surface characterisation of *Microcystis aeruginosa* and *Chlorella vulgaris*." Journal of colloid and interface science **342**(2): 293-299.
- Harper, S. L., J. L. Carriere, et al. (2011). "Systematic evaluation of nanomaterial toxicity: utility of standardized materials and rapid assays." ACS nano **5**(6): 4688-4697.
- Henderson, R. K., A. Baker, et al. (2008). "Characterisation of algogenic organic matter extracted from cyanobacteria, green algae and diatoms." Water research **42**(13): 3435-3445.
- Ivask, A., K. Juganson, et al. (2014). "Mechanisms of toxic action of Ag, ZnO and CuO nanoparticles to selected ecotoxicological test organisms and mammalian cells in vitro: A comparative review." Nanotoxicology **8**(sup1): 57-71.
- Jassby, D., J. Farner Budarz, et al. (2012). "Impact of aggregate size and structure on the photocatalytic properties of TiO<sub>2</sub> and ZnO nanoparticles." Environmental science & technology **46**(13): 6934-6941.

- Jo, H. J., J. W. Choi, et al. (2012). "Acute toxicity of Ag and CuO nanoparticle suspensions against *Daphnia magna*: the importance of their dissolved fraction varying with preparation methods." Journal of hazardous materials **227**: 301-308.
- Juganson, K., A. Ivask, et al. (2015). "NanoE-Tox: New and in-depth database concerning ecotoxicity of nanomaterials." Beilstein journal of nanotechnology **6**(1): 1788-1804.
- Kaweeteerawat, C., C. H. Chang, et al. (2015). "Cu nanoparticles have different impacts in *Escherichia coli* and *Lactobacillus brevis* than their micro-sized and ionic analogues." ACS nano **9**(7): 7215-7225.
- Keller, A. A. and A. Lazareva (2013). "Predicted releases of engineered nanomaterials: from global to regional to local." Environmental Science & Technology Letters **1**(1): 65-70.
- Kwon, J.-T., S.-K. Hwang, et al. (2008). "Body distribution of inhaled fluorescent magnetic nanoparticles in the mice." Journal of occupational health **50**(1): 1-6.
- Louie, S. M., R. D. Tilton, et al. (2016). "Critical review: impacts of macromolecular coatings on critical physicochemical processes controlling environmental fate of nanomaterials." Environmental Science: Nano **3**(2): 283-310.
- Mackevica, A., L. M. Skjolding, et al. (2013). The effects of food availability on growth and reproduction of *Daphnia magna* exposed to silver nanoparticles. 8th International Conference on the Environmental Effects of Nanoparticles and Nanomaterials.
- Nations, S., M. Long, et al. (2015). "Subchronic and chronic developmental effects of copper oxide (CuO) nanoparticles on *Xenopus laevis*." Chemosphere **135**: 166-174.
- Nowack, B. and T. D. Bucheli (2007). "Occurrence, behavior and effects of nanoparticles in the environment." Environmental Pollution **150**(1): 5-22.
- OECD (2012). Test No. 211: *Daphnia magna* Reproduction Test, OECD Publishing.
- Ostermeyer, A.-K., C. Kostigen Mumuper, et al. (2013). "Influence of bovine serum albumin and alginate on silver nanoparticle dissolution and toxicity to *Nitrosomonas europaea*." Environmental science & technology **47**(24): 14403-14410.
- Prasad, P. R., S. Kanchi, et al. (2016). "In-vitro evaluation of copper nanoparticles cytotoxicity on prostate cancer cell lines and their antioxidant, sensing and catalytic activity: One-pot green approach." Journal of Photochemistry and Photobiology B: Biology.

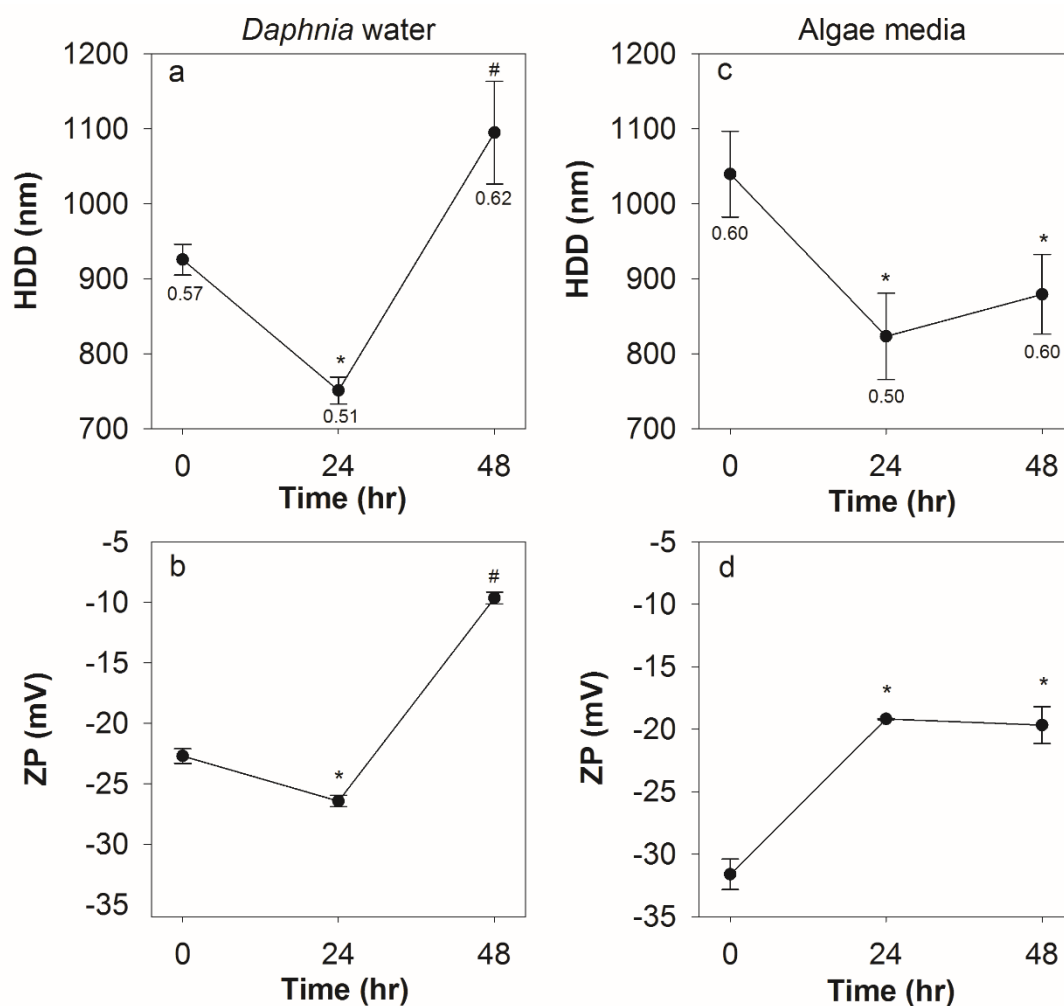
- Ramsden, C. S., T. J. Smith, et al. (2009). "Dietary exposure to titanium dioxide nanoparticles in rainbow trout, (*Oncorhynchus mykiss*): no effect on growth, but subtle biochemical disturbances in the brain." Ecotoxicology **18**(7): 939-951.
- Rasband, W. S. (1997-2016). ImageJ. Bethesda, Maryland, USA, U. S. National Institutes of Health.
- Ribeiro, F., C. A. Van Gestel, et al. (2017). "Bioaccumulation of silver in *Daphnia magna*: Waterborne and dietary exposure to nanoparticles and dissolved silver." Science of The Total Environment **574**: 1633-1639.
- Scown, T., R. Van Aerle, et al. (2010). "Review: do engineered nanoparticles pose a significant threat to the aquatic environment?" Critical reviews in toxicology **40**(7): 653-670.
- Tsui, M. T. K. and W. X. Wang (2007). "Biokinetics and tolerance development of toxic metals in *Daphnia magna*." Environmental toxicology and chemistry **26**(5): 1023-1032.
- Wang, H., W. Fan, et al. (2015). "Chronic effects of six micro/nano-Cu<sub>2</sub>O crystals with different structures and shapes on *Daphnia magna*." Environmental pollution **203**: 60-68.
- Wang, Z., J. Li, et al. (2011). "Toxicity and internalization of CuO nanoparticles to prokaryotic alga *Microcystis aeruginosa* as affected by dissolved organic matter." Environmental science & technology **45**(14): 6032-6040.
- Wang, Z., A. Von Dem Bussche, et al. (2013). "Biological and environmental transformations of copper-based nanomaterials." ACS nano **7**(10): 8715-8727.
- Wang, Z., L. Zhang, et al. (2016). "Environmental processes and toxicity of metallic nanoparticles in aquatic systems as affected by natural organic matter." Environmental Science: Nano **3**(2): 240-255.
- Weber, C. I. (1991). Methods for measuring the acute toxicity of effluents and receiving waters to freshwater and marine organisms, Environmental Monitoring Systems Laboratory, Office of Research and Development, US Environmental Protection Agency.
- Wu, F., B. J. Harper, et al. (2017). "Differential dissolution and toxicity of surface functionalized silver nanoparticles in small-scale microcosms: impacts of community complexity." Environmental Science: Nano.
- Xiao, Y., W. J. Peijnenburg, et al. (2016). "Toxicity of copper nanoparticles to *Daphnia magna* under different exposure conditions." Science of The Total Environment **563**: 81-88.
- Xiao, Y., M. G. Vijver, et al. (2015). "Toxicity and Accumulation of Cu and ZnO nanoparticles in *Daphnia magna*." Environmental science & technology **49**(7): 4657-4664.

- Zhao, C. M., W. H. Fan, et al. (2009). "Aqueous and dietary copper uptake and elimination in *Daphnia magna* determined by the  $^{67}\text{Cu}$  radiotracer." Environmental toxicology and chemistry **28**(11): 2360-2366.
- Zhao, J., X. Cao, et al. (2016). "Interactions of CuO nanoparticles with the algae *Chlorella pyrenoidosa*: adhesion, uptake, and toxicity." Nanotoxicology **10**(9): 1297-1305.
- Zhao, J., Z. Wang, et al. (2013). "Mitigation of CuO nanoparticle-induced bacterial membrane damage by dissolved organic matter." Water research **47**(12): 4169-4178.
- Zhu, X., Y. Chang, et al. (2010). "Toxicity and bioaccumulation of  $\text{TiO}_2$  nanoparticle aggregates in *Daphnia magna*." Chemosphere **78**(3): 209-215.

### 3.9 Appendix

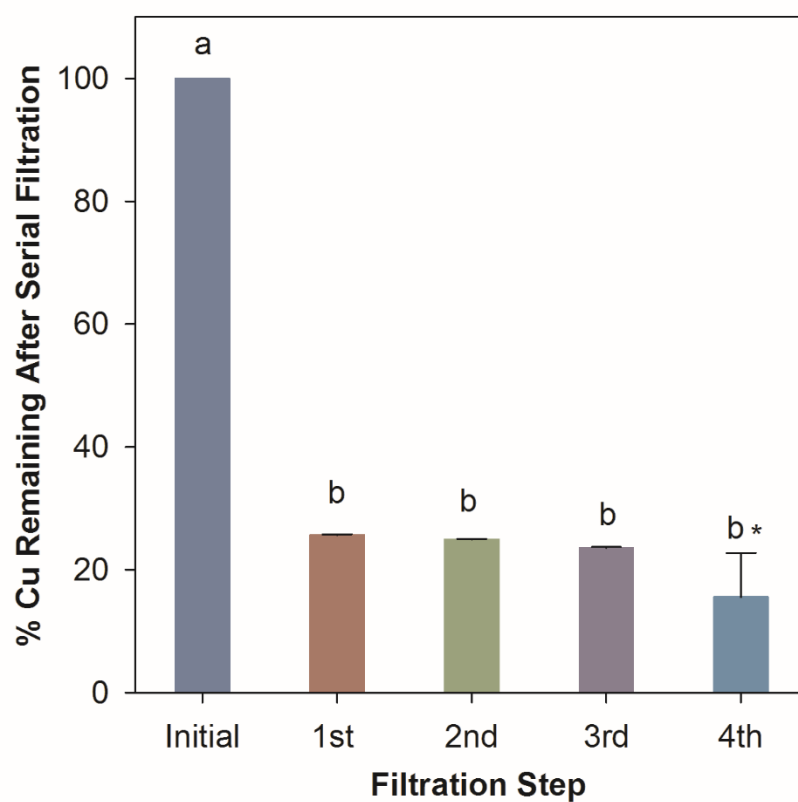
**Table S3-1.** Standardized information for determining the zeta potential measurements in algae and *D. magna* media:

Surface functionalization	None	
Shape	spherical	
Model used to compute the zeta potential	Henry's Equation (Smoluchowski approximation)	
<i>D. magna</i> media		
pH	7.8 ± 0.2	
Ionic strength	0.00616 mol/L	
Ionic composition	111 mg L <sup>-1</sup> CaSO <sub>4</sub> , 42.65 mg L <sup>-1</sup> MgSO <sub>4</sub> , 117.6 mg L <sup>-1</sup> NaHCO <sub>3</sub> , and 6 mg L <sup>-1</sup> KCl	
Electrophoretic mobility (mV)	0 hour	-1.78 ± 0.08
	24 hours	-2.07 ± 0.07
	48 hours	-0.76 ± 0.07
Algae media		
pH	7.2 ± 0.2	
Ionic strength	0.013 mol/L	
Ionic composition	Ref. 25	
Electrophoretic mobility (mV)	0 hour	-2.48 ± 0.17
	24 hours	-1.50 ± 0.01
	48 hours	-1.54 ± 0.20
Duration of measurement	90 seconds for single measurement	
Applied voltage	148 V	
Number of measurements made and averaged to determine each ZP	12	
Total number of replicate measurements	3	

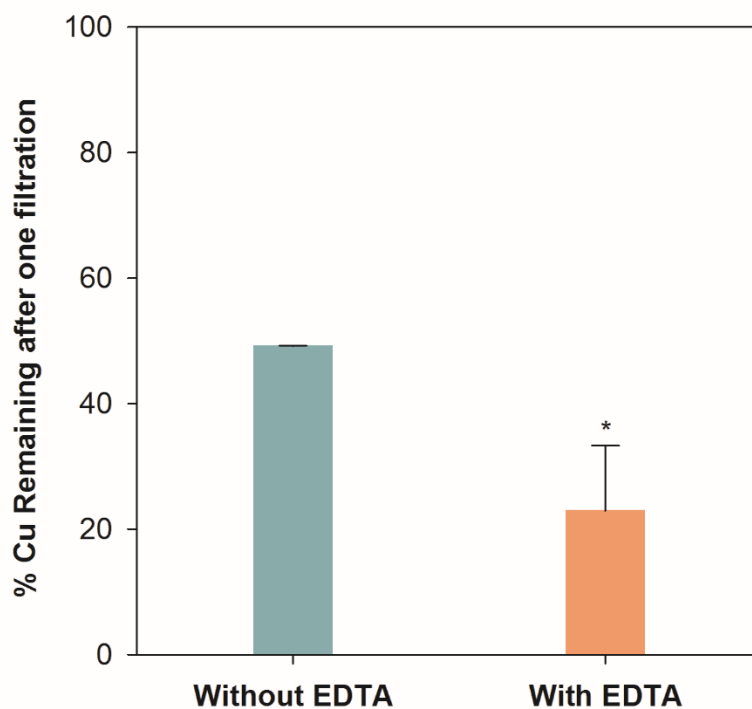


**Figure S3-1.** Hydrodynamic diameter (HDD) and zeta potential (ZP) of CuO NPs in *Daphnia* water (panel a, b) and algal media (panel c, d). The error bar represents the standard error of three measurement replicates. Asterisk (\*) and Octothorpe (#) indicate significant differences among measurements over time, and numbers below HDD in panel a and c are the corresponding mean polydispersity index of CuO NPs at the measured time point.

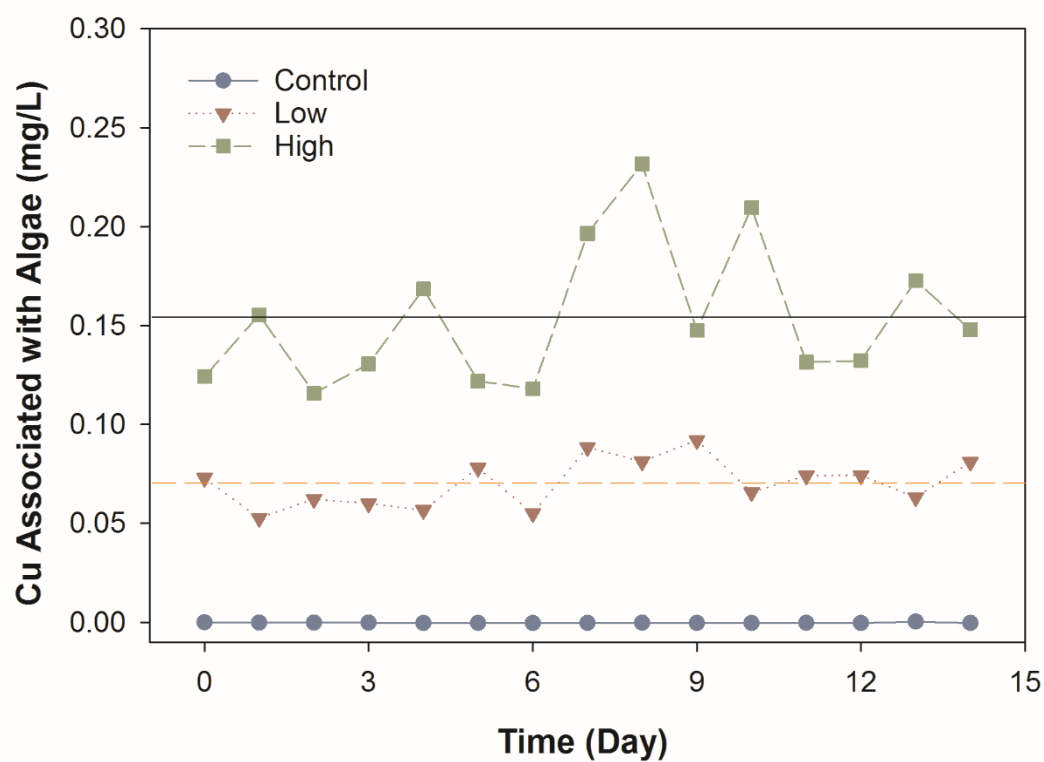




**Figure S3-2.** Percentage of Cu remaining associated with algae after serial filtration. The error bar represents the standard error of three sample replicates. The initial concentration was before centrifugation and filtration ( $50 \text{ mg L}^{-1}$  CuO NPs). Lowercase letters indicate significant differences between filtered algae and initial unfiltered algae, \* indicates a significant difference from the first filtration step.

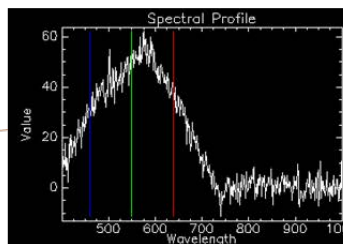
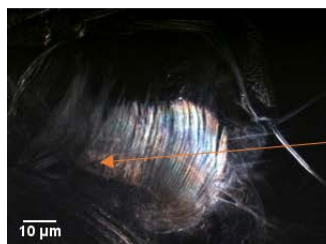


**Figure S3-3.** Percentage Cu remaining with EDTA and without EDTA (*Daphnia media*) following one time filtration. The error bar represents the standard error of three measurement replicates. \* indicates a significant difference between with and without EDTA wash.



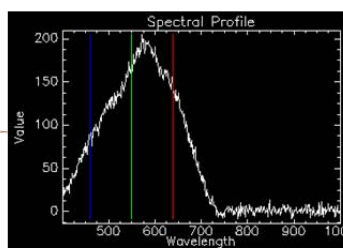
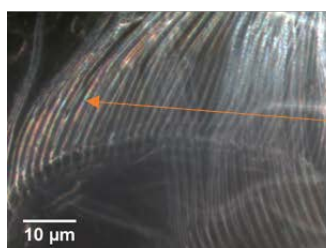
**Figure S3-4.** Cu associated with algae in the amounts of algae fed to individual *D. magna*. The solid and dashed lines indicate the average high and low exposure concentrations used in the direct exposures.

a. Control carapace



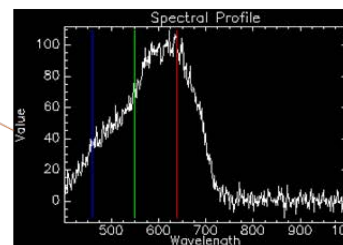
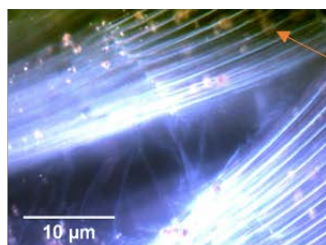
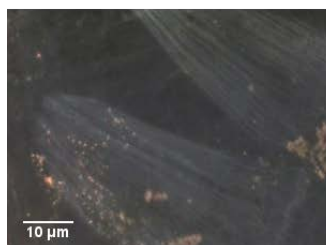
$$\lambda_{\max} = 575 \text{ nm}$$

b. Feeding exposure carapace



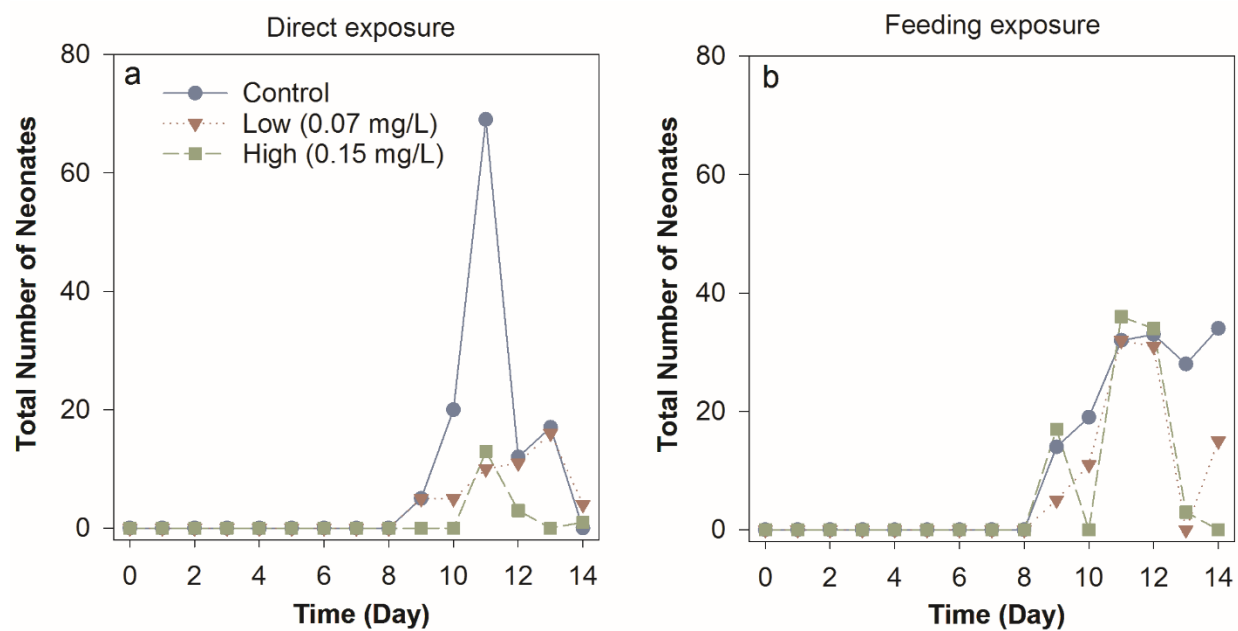
$$\lambda_{\max} = 575 \text{ nm}$$

c. Direct exposure carapace

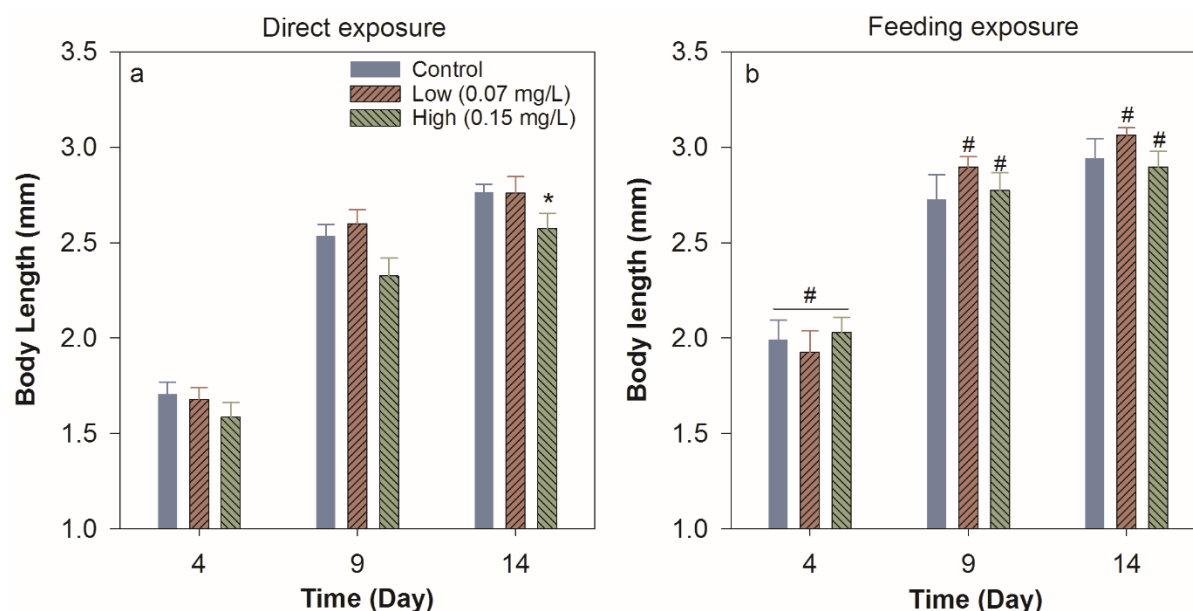


$$\lambda_{\max} = 635 \text{ nm}$$

**Figure S3-5.** Dark field images of *D. magna* molted carapaces and typical spectral profiles in a) control, b) feeding exposure, and c) direct exposure scenarios.



**Figure S3-6.** *D. magna* daily reproduction in a) direct exposure and b) feeding exposure over 14 days.



**Figure S3-7.** *D. magna* body length in a) direct exposure and b) feeding exposure. \* indicates a significant difference between the treatment and control. # indicates a significant difference between direct and feeding exposures at same exposure concentration.

*Statistics information for Figure 3-4:*

Fisher's exact test indicating significant difference for the number of survival after 14 days of exposure (In direct exposure,  $p = 0.0011$  and  $< 0.0001$  for low and high exposure concentration, respectively). One-way ANOVA with Dunnett's post hoc tests indicating significant differences from the blank for average brood size ( $p = 0.015$  for feeding exposure,  $p = 0.054$  for direct exposure), but no significant difference for the time to first brood ( $p = 0.548$  for feeding exposure,  $p = 0.271$  for direct exposure). One way RM ANOVA with Holm-Sidak post hoc test indicates significant difference in number of broods per adults compared to corresponding control ( $p = 0.02$  for feeding exposure,  $p = 0.018$  for direct exposure).

## **Chapter 4. Comparison of the dissolution, uptake and toxicity of nano- and micron-sized zinc oxide particles**

Fan Wu<sup>1</sup>, Bryan J. Harper<sup>2</sup>, Stacey L. Harper<sup>1,2,3\*</sup>

*<sup>1</sup>School of Chemical, Biological and Environmental Engineering, Oregon State University, Corvallis, OR, United States; <sup>2</sup>Department of Environmental and Molecular Toxicology, Oregon State University, Corvallis, OR, United States; <sup>3</sup>Oregon Nanoscience and Microtechnologies Institute, Eugene, Oregon, United States*

**Keywords:** Zinc oxide; multi-species; dissolution; uptake; toxicity; nanoparticle

Submittal expected June 2017

#### 4.1 Abstract

Zinc nanoparticles (ZnO NPs) are known to be highly toxic to aquatic organisms, yet their fate and toxicity in a complex community comprised of multiple organisms is still unclear. The lack of environmental realism in individual species laboratory exposures precludes thorough understanding of ZnO NP risk to aquatic environments. Potential differences in species susceptibility to NP contaminants make the use of multi-species community toxicity testing strategies beneficial in understanding the ecological risk. Here, we conducted multi-species microcosm exposures and compared the responses of individual species to the same species in a mixed community exposure. The microcosm was comprised of *C. reinhardtii*, *E. coli*, *D. magna*, and *D. rerio*. In addition, different sized ZnO particles ionic Zn were compared to investigate the contribution of NP toxicity and dissolved Zn to aquatic organisms. Each organism and community was exposed to ZnO NPs (50 nm), macroparticles (MPs, 5  $\mu$ m), and ionic Zn at 0.1, 1 and 10 mg ZnO/L (0.08, 0.8, and 8 mg Zn/L). Our results identified *D. magna* as the most sensitive species to Zn exposures due to the high mortality observed at 10 mg ZnO/L. In addition, all three types of zinc exposures elicited differential toxicity among test organisms, with stronger adverse outcomes observed in single species than within a community. The community (nanocosm) we developed showed 5 to 10% environmental resistance to all Zn exposures compared to individual exposures at effective concentrations, and the dissolved Zn released from ZnO NP and MP likely drove their toxicities. Overall, our findings indicate that both engineered ZnO NPs and ZnO MPs could disrupt community balance by causing toxicity to organisms through releasing of Zn ions. The multi-species community assay could be useful to rapidly assess and screen the ecological impacts of nanomaterials in complex environments.



## 4.2 Introduction

Zinc oxide nanoparticles (ZnO NPs) are the third highest production nanoparticles worldwide (estimates range from 550 to 10000 tons per year) due to their wide ranging applications in cosmetics, solar cells, pigments, electronics and textiles (Wang 2004; Aschberger, Micheletti et al. 2011; Piccinno, Gottschalk et al. 2012). The rapid development of the nano-industry and the diverse engineering capabilities, such as shape (Hsiao and Huang 2011), size (Hanley, Thurber et al. 2009), crystallinity (Hariharan 2006), and surface chemistry variations (Khrenov, Klapper et al. 2005), available to modify ZnO NPs for a myriad of uses have led to the development of numerous types of ZnO nanoparticles. Thus, ZnO NPs will eventually enter aquatic environments through wastewater streams following industrial and commercial uses (Nowack and Bucheli 2007; Scown, Van Aerle et al. 2010; Keller and Lazareva 2013). The likely increase in both the diversity and quantity of ZnO NPs entering the environment necessitates further study of their ecological impacts. Modeled estimates of ZnO NP concentrations in surface waters range from 0.001 to 0.058  $\mu\text{g L}^{-1}$ , 0.24-0.661  $\mu\text{g kg}^{-1}$  in soil, and 0.22-1.42  $\mu\text{g L}^{-1}$  in sewage treatment plant effluent, where the concentrations are expected to continuously increasing (Gottschalk, Sonderer et al. 2009).

ZnO NPs have been classified as “extremely toxic” ( $\text{L(E)C}_{50} < 0.1 \text{ mg L}^{-1}$ ) to aquatic organisms (Kahru and Dubourguier 2010); however, the reported toxicity of ZnO NPs to aquatic organisms belonging to various trophic levels varies considerably (Adams, Lyon et al. 2006; Brayner, Ferrari-Iliou et al. 2006; Franklin, Rogers et al. 2007; Zhang, Jiang et al. 2007; Heinlaan, Ivask et al. 2008; Huang, Zheng et al. 2008; Aruoja, Dubourguier et al. 2009; Blinova, Ivask et al. 2010; Wong, Leung et al. 2010; Xiong, Fang et al. 2011). According to a review by

Bondarenko et al., the reported L(E)C<sub>50</sub> values of ZnO NPs for bacteria (multiple species), algae (multiple species), crustaceans (*Daphnia magna*), and fish (*Danio rerio*) varied from 50-1000, 0.052-4.56, 0.62-22 and 1.79-4.92 mg L<sup>-1</sup>, respectively (Bondarenko, Juganson et al. 2013), and the high variation was mainly dependent on the testing species and experimental conditions, such as pH, media composition, temperature, and other factors. ZnO NP toxicity is well studied, and it has been demonstrated that the toxic mechanisms are mainly associated with the dissolution and release of ionic Zn (Bacchetta, Maran et al. 2016). Generation of reactive oxygen species (ROS) by ZnO NPs have also shown to induce DNA damages in zebrafish (Bai, Zhang et al. 2010; Zhao, Wang et al. 2013). Additionally, the small size of nanomaterials has the potential to influence the uptake by organisms (Gliga, Skoglund et al. 2014) (Abdelmonem, Pelaz et al. 2015), dissolution behavior in aquatic systems (Lopes, Ribeiro et al. 2014), and potentially impact the toxicity of nanoparticles compared to their bulk counterparts (Nair, Sasidharan et al. 2009; Sharma, Anderson et al. 2012; Kononenko, Repar et al. 2017).

Studies are typically conducted under laboratory exposures with individual organisms, which do not provide a comprehensive understanding of how ZnO NPs influence environmental health due to the lack of environmental realism. Exposures conducted in environmentally relevant conditions, such as within a community of organisms, can provide us detailed information on how nanomaterial exposures impact population and trophic level interactions. Although individual species based ZnO NP toxicity data provides baseline information for assessing the potential risks of ZnO NPs, multi-species toxicity tests can assess the potential impacts of toxicants across trophic levels, identify any indirect effects caused by species interactions (Mackay, Holmes et al. 1989) (Boxall, Brown et al. 2002), capture the variability of

exposure routes and the range of sensitivities among organisms (De Zwart and Posthuma 2005). Information can be gained from changes in organisms, populations, and communities simultaneously. Given the complex nature of ecosystems, it is expected that multi-species toxicity tests would provide a more realistic estimation of community and ecosystem-level responses to the toxicant.

Despite the recognition that the sensitivity of organisms to NP contaminants can be altered in the presence of other species (Levy, Stauber et al. 2009), knowledge of the impacts of engineered nanoparticles to aquatic ecosystems as a whole is still quite limited (Bernhardt, Colman et al. 2010). Few investigations have been conducted at environmentally relevant concentrations of ZnO NPs utilizing a microcosm experimental design. One such study showed that low concentrations of ZnO NPs caused adverse effects on soybean growth using soil microcosms (Yoon, Kwak et al. 2014); however, to our knowledge, no study has investigated environmental impacts of ZnO NPs to organisms includes trophic level within a freshwater microcosm.

Aquatic microcosm assays have not been commonly applied to nanomaterials due to they are costly, time consuming, require large quantities of nanomaterials, and generate large amounts of waste (ASTM 2011). To overcome these barriers, our approach was to develop a rapid, small-volume multi-species screening level mixed species assessment (hereafter referred to as the nanocosm assay) that requires minimal quantities of test nanomaterials. In this study, we compared the responses of individual species including algae (*Chlamydomonas reinhardtii*), bacteria (*Escherichia coli*), invertebrates (*Daphnia magna*), and developing vertebrates (*Danio rerio*) to the responses of mixed-species exposures to determine the biological impacts of ZnO

NPs in a community setting to further validate the function of our nanocosm assay. Test species were selected because they represent a broad spectrum of trophic levels as is discussed in a previous publication (Wu, Harper et al. 2017), and are among the most commonly used in aquatic toxicity testing, particularly for nanoparticles (Sondi and Salopek-Sondi 2004; Adams, Lyon et al. 2006; Harper, Usenko et al. 2008; Heinlaan, Ivask et al. 2008; Navarro, Piccapietra et al. 2008; Chen, Zhou et al. 2012; Perreault, Oukarroum et al. 2012; Colman, Arnaout et al. 2013). The potential interactions among species were explained in early publication (Wu, Harper et al. 2017). Multiple sub-lethal toxicological endpoints (cell growth rate, survival proportion, fish malformation, etc.) were used to evaluate the impacts of ZnO NPs at environmentally relevant concentrations. The long-term goal of this study is to establish a validated method for assessing nanomaterial ecological risk to rapidly identify nanoparticle hazards and species at risk.

In this study, commercially available ZnO NPs, ZnO microparticles (ZnO MPs), and ZnCl<sub>2</sub> as the dissolved Zn control were selected to investigate the influence of dissolved Zn and size scale of particles in aquatic toxicity. We hypothesized that the toxicity of ZnO nanoparticles would vary in single and community exposures due to differential species susceptibility and interspecies interactions, and that dissolved Zn dictates the toxicity of the ZnO particles.

## **4.3 Materials and methods**

### *4.3.1 Exposure media and organism maintenance*

The exposure media, hereafter referred to as the nanocosm media (NCM) (Wu, Harper et al. 2017), was prepared by mixing 50% of Taub's #36 solution (Taub and Dollar 1968) with 50% of 5 mM HEPES buffer (EMD Chemicals Inc., Gibbstown, NJ) ensuring the pH of NCM was maintained at 7.2 before use. The media is selected to optimize the growth rate of algae, and HEPES buffer is used because it is often used as biological buffer in cell culture. NCM was stored at 4 °C and was autoclaved at 120 °C for 20 min and cooled to room temperature prior to use.

#### 4.3.2 Test organisms

*C. reinhardtii* was purchased from the University of Texas Culture Collection (UTEX 2243 and 2244) and cultured in TAP media (Gorman and Levine 1965). *E. coli* was purchased from Carolina Biological Supply Company (MicroKwik culture, Burlington, NC, USA) and cultured in LB media (consisted of 10 mg/L tryptone, 5 mg/L yeast extract, and 10 mg/L sodium chloride) on a shaker at 37°C. *D. magna* were maintained in reconstituted moderately hard water consisting of final salt concentrations of 111 mg/L CaSO<sub>4</sub>, 42.65 mg/L MgSO<sub>4</sub>, 117.6 mg/L NaHCO<sub>3</sub>, and 6 mg/L KCl in reverse osmosis water and fed with dry spirulina daily. The pH was maintained in the range of  $7.8 \pm 0.2$ . *D. magna* neonates (<24 hours old) were collected from the stock culture and placed in NCM for 24 hours prior to toxicity testing to acclimate to the new media prior to the onset of testing. Adult wild-type zebrafish were maintained at the Sinnhuber Aquatic Research Laboratory (SARL) at Oregon State University. Embryos were collected from group spawns and staged to ensure all embryos were 6–8 hours post-fertilization (hpf) at the start of the experiment (Kimmel, Ballard et al. 1995). All the organisms were maintained at room

temperature of  $20.5 \pm 0.5$  °C with a 16:8-h light:dark photoperiod under  $1690 \pm 246$  lux light intensity provided by full-spectrum growth lights.

#### *4.3.3 Nanoparticles characterization*

ZnO NPs (average primary particle size specified by the manufacturers as  $<50$  nm), ZnO MPs ( $< 5$   $\mu$ m particle size), and ZnCl<sub>2</sub> were all purchased in powder form from Sigma-Aldrich (St. Louis, MO). ZnO source stock suspensions and ZnCl<sub>2</sub> solution were prepared at a concentration of 1000 mg ZnO/L in NCM, and ZnO NPs were then sonicated for 2 minutes at 40% intensity with VCX 750 Vibra-Cell sonicator (Sonics & Materials Inc., Newtown, CT) equipped with a cup-horn probe and recirculating water bath to maintain temperature. ZnO NP suspensions in NCM were prepared at 10 mg/L for characterization of hydrodynamic diameter (HDD) and zeta potential (ZP) by dynamic light scattering using a Zetasizer Nano ZS (Malvern Instruments Ltd, Worcestershire, UK) with measurements taken every 24 hours for 5 days. The HDDs of same concentration of ZnO NPs suspended in Milli-Q ultrapure water (MQW) (EMD Millipore Corporation, Billerica, MA) were also measured for comparing the impact of media type on particle agglomeration.

#### *4.3.4 Experiment setup and toxicity evaluations*

*C. reinhardtii* cells grown in TAP media were collected during steady growth and centrifuged at  $600\times g$  for 5 minutes to pellet the cells. Following removal of the supernatant, the algal cells were re-suspended in NCM. For individual and mixed-species toxicity tests with

algae, *C. reinhardtii* cells were inoculated into 50 ml Falcon® vented tissue culture flasks (Fisher Scientific, Pittsburgh, PA) at a starting density of  $\sim 2 \times 10^4$  cells mL<sup>-1</sup>, and acclimated for 1 day before starting the experiment. Vented caps were chosen to equalize air pressure inside and outside the container and to prevent contamination from airborne particles and microbes. The total volume of each flask was adjusted to 15 mL, leaving approximately 35 cc of headspace to allow for ventilation through the filter cap. For tests incorporating bacteria, *E. coli* inoculates were added to the 50 ml flasks as mentioned above to provide a final density of  $5 \times 10^5$  cells mL<sup>-1</sup>. Initial algal and bacterial cell densities were quantified using an Accuri C6 flow cytometer (BD Biosciences, San Jose, CA) to ensure consistency in our initial cell densities at the start of the experiment. For *D. magna* and zebrafish exposures (alone or in conjunction with algae and bacteria), five neonate *D. magna* and eight zebrafish embryos were introduced into each 50 ml flask. Triplicate flasks were prepared for each exposure scenario at 0, 0.1, 1, and 10 mg ZnO/L (as 0.08, 0.8, and 8 mg Zn/L) of each type of Zn exposure, ZnCl<sub>2</sub> concentrations were chosen to match the amount of Zn present in the particle concentrations (as 0.08, 0.8, and 8 mg Zn/L). Five replicates were prepared for nanocosms and each individual exposures at each exposure concentration.

Algal and bacterial viability was measured using SYTOX Green cell stain (Life Technologies, Grand Island, NY) in conjunction with flow cytometry after 2 and 6 hours of exposure for bacteria, then daily for the remainder of the experiment for both algae and bacteria. *D. magna* mortality and immobilization was recorded daily. *D. rerio* embryo hatching rate and mortality were monitored daily. At the end of the five day exposure, zebrafish embryos were examined under a dissecting microscope for malformations (body axis, brain, heart, eyes, fins,

jaw, trunk, somite), physiological abnormalities (pigmentation, circulatory system, pericardial edema, yolk sac edema) and behaviors (touch response, hatching rate). *D. rerio* embryo developmental stage was corrected according to Kimmel et al. due to the change in experimental temperature,

$$H_T = h / (0.055T - 0.57) \quad (1)$$

where  $H_T$  represents the hours of development at temperature  $T$ , and  $h$  represents the hours of development to reach that stage at 28.5°C (Kimmel, Ballard et al. 1995).

#### *4.3.5 Measurement of dissolved Zn concentrations and uptake*

The abiotic dissolution of ZnO particles (both nano and micro) at 10 mg ZnO/L was measured in NCM initially and after 1 and 5 days. Dissolved Zn concentrations in each exposure scenario was measured at day 1 and 5 at all concentrations. In detail, nanocosm flasks were gently agitated prior to sampling to resuspend any settled particles at each time point, then a 0.5 ml aliquot was taken from the exposure and centrifuged at 8000 rpm for 10 minutes through a 3 kDa centrifugation filter (VWR) to remove undissolved particles. Filtered media was transferred to a polystyrene tube and acidified with trace-metal grade nitric acid (Fisher Scientific, Pittsburgh, PA) prior to analysis of Zn content by inductively coupled plasma optical emission spectrometry (ICP-OES, Teledyne Technologies, Hudson, NH). A zinc ICP standard was purchased from Sigma-Aldrich and prepared from 0 to 10 mg Zn/L (St. Louis, MO). Further, Zn speciation in the NCM was modeled using the maximum measured dissolved Zn concentration from exposures with Visual MINTEQ 3.1 (downloaded from <https://vminteq.lwr.kth.se/>). Zinc uptake by organisms was measured following toxicological observations at the end of the



experiment. Individual daphnids and zebrafish were rinsed three times with MQW to remove loosely attached algae, bacteria, and particles. Unhatched zebrafish were dissected to remove the chorionic membrane. Chorionic membranes, zebrafish embryos, and daphnids were stored at  $-4^{\circ}\text{C}$  in polystyrene tubes prior to acid digestion. The acid digestion procedure was described in detail previously with average recovery at  $101.6 \pm 1.6\%$  (Wu, Harper et al. 2017). After digestion, all samples contained a final proportion of 3% nitric acid and were analyzed with ICP-OES. Three sample replicates were prepared for each exposure scenario at each exposure concentration.

#### 4.3.6 Statistical analysis

The algae and bacteria survival was calculated using the Henderson-Tilton formula (equation 2) to compensate for possible differences in the surviving proportion of organisms occurring post-treatment.

$$\text{Corrected survival \%} = \left( \frac{n_{Cb} \times n_{Ta}}{n_{Ca} \times n_{Tb}} \right) \times 100 \quad (2)$$

where  $n_C$  is the survival proportion (live cell/total cell) in the control group,  $n_T$  is the survival proportion in the treatment group, and a and b designate after and before treatment, respectively (Henderson and Tilton 1955). The intrinsic growth rates of algae and bacteria were calculated using an three parameter logistic model in equation 3 (Paine, Marthews et al. 2012):

$$M = \frac{k}{(1 + (\frac{k}{M_0 - 1})) \times e^{-rt}} \quad (3)$$

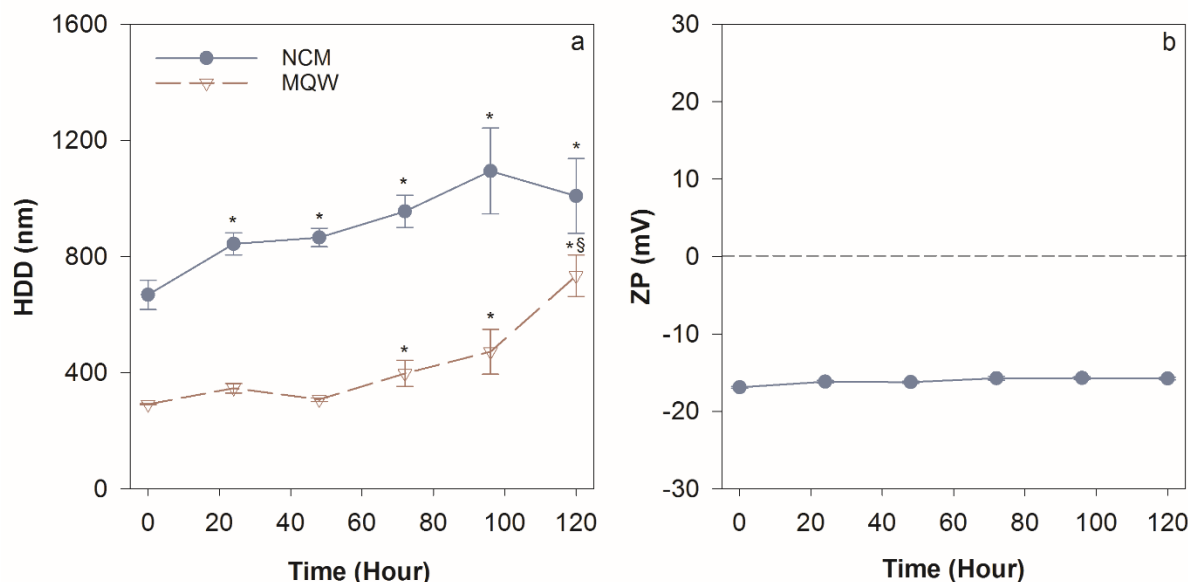
where  $r$  is the specific growth rate ( $\text{h}^{-1}$ ),  $t$  is the time (h),  $k$  represents the maximum capacity of cells,  $M_0$  is the initial cell counts at time ( $t$ ) = 0, and  $M$  represents the cell count at  $t = t$ .

SigmaPlot (Systat Software, San Jose, CA, USA) was used to perform statistical analysis of the changes in algal and bacterial survival over time using the Kruskal-Wallis rank sum test followed in conjunction with a Tukey post-hoc test. Differences in the frequency of developmental abnormalities in *D. rerio* between treatments and the corresponding control were analyzed with the Fisher's exact test. The difference of integrated organismal response ( $X$ ) = (each organism survival in NC community exposure) – (organism survival in individual exposure). Differences were considered statistically significant at  $p \leq 0.05$  for all analyses.

## 4.4 Results

### 4.4.1 Nanoparticle Characterization

The measured HDD and ZP of the ZnO NPs at 10 mg/L are presented in Figure 4-1. The initial HDD of ZnO NPs suspended in MQW were  $291 \pm 2$  nm (Fig. 1a). In contrast, the HDD of the ZnO NPs suspended in the NCM was much larger ( $668 \pm 51$  nm). ZnO NP agglomeration significantly increased at 72 hours in the MQW, and the final HDD reached  $734 \pm 72$  nm after 120 hours. Significantly larger agglomerates were observed in the NCM, and the HDD increased to  $1008 \pm 128$  nm after 120 hours. While the ZP in the MQW does not reflect the real stability due to the lack of ionic strength (Lowry, Hill et al. 2016), the ZP measured in NCM was consistently in the range of  $-15.7$  to  $-16.9$  mV throughout the 120 hour period.



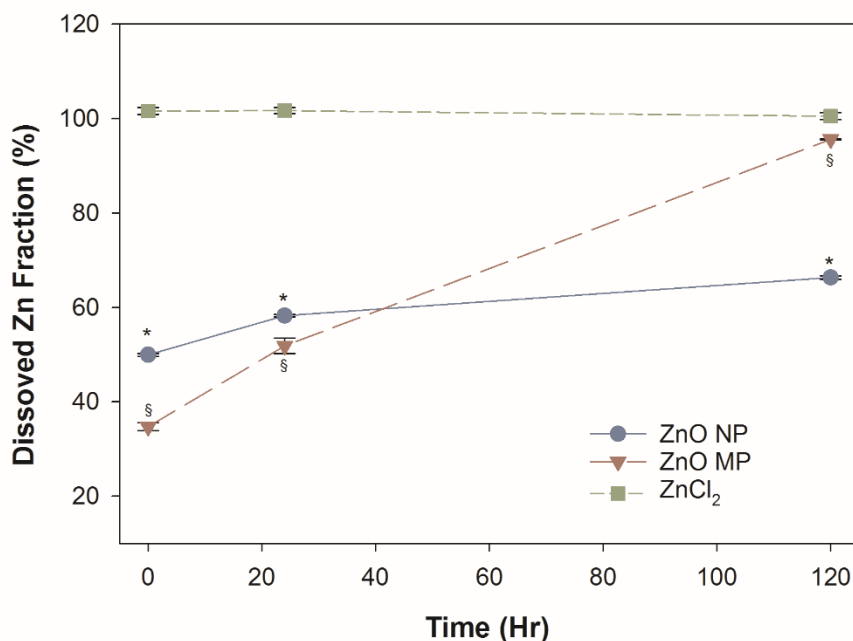
**Figure 4-1.** Hydrodynamic diameter (a) of  $10 \text{ mg L}^{-1}$  ZnO NPs in NCM and MQW and zeta potential in NCM (b) over 120 hours. The solid lines with filled circle represent responses measured in NCM and dashed lines with open triangle represent the responses measured in MQW. Error bars correspond to the standard error for each set of measurements. The asterisk (\*) represents significant differences compared to corresponding initial measurements, and symbol § indicates significantly difference from previous time point in MQW.

#### 4.4.2 Nanoparticle Dissolution

##### 4.4.2.1 Abiotic

Figure 4-2 presents the dissolved Zn measurements from each abiotic Zn exposure in NCM.  $\text{ZnCl}_2$  had near instantaneous complete dissolution, revealing a consistent near 100% dissolved Zn concentration throughout the 120 hours; whereas the ZnO NPs and MPs had initial dissolved Zn concentrations representing 50% and 35% of the initial concentration, respectively. After 24 hours, there was a significant increase in the dissolved Zn concentration for both ZnO NP and MP. The final 120 hour dissolved Zn concentration was significantly higher for the ZnO MPs, with nearly 95% of the particles dissolved relative to 66% of the total concentration for the

NPs. By linearizing the release of dissolved Zn, ZnO MPs had a higher dissolution rate (0.045 mg/hr) compared to ZnO NPs (0.0095 mg/hr), leading to a significantly higher final dissolved Zn concentration.

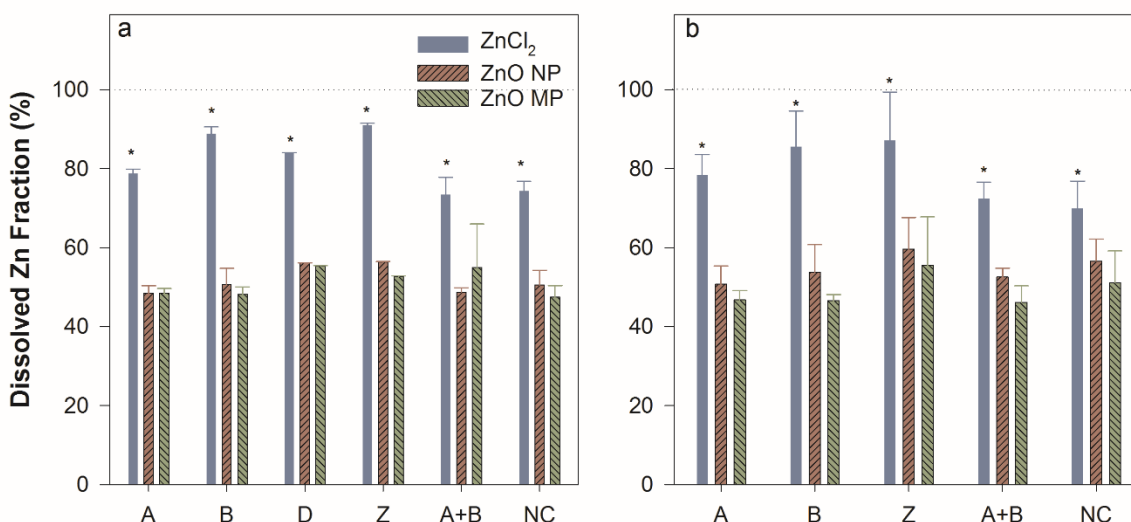


**Figure 4-2.** Dissolved zinc concentrations for all three types of Zn exposures (normalized at 10 mg ZnO/L) measured in NCM over 120 hours. Error bars represent the standard error derived for triplicate samples. Letters indicate significant differences between ZnCl<sub>2</sub>, ZnO NP and ZnO MP, as well significant difference in dissolved Zn over time.

#### 4.4.3 Biotic

Dissolved Zn in each level of organismal complexity was measured at both 24 hours and 120 hours for all three types of Zn exposures (Figure 4-3). At 10 mg ZnO/L, the dissolved Zn in ZnCl<sub>2</sub> exposures was nearly 13 to 30% lower compared to the initial exposed Zn (dash line in figure 4-3) depending on the type organism exposure. Comparing the biotic and abiotic dissolved

Zn concentrations, the presence of organisms significantly decreased the dissolved Zn concentrations in ZnO NP at 24 hours (Figure 4-3a), and MPs at 120 hours (Figure 4-3b). However, there is no clear trend indicating which organism had the most impact on Zn dissolution. Although organisms decreased the dissolved Zn fraction,  $\text{ZnCl}_2$  still had significantly more dissolved Zn than both NP and MP exposures. In biotic environment, there was no significant difference between 24 and 120 hours in all exposure scenarios. Although all species affected the dissolution of ZnO NP and MP, the effects were not additive since the community did not elicit significantly different dissolved Zn compared to other single exposure scenarios. The chemical equilibrium model, Visual MINTEQ V3.1 was employed to investigate how zinc ions may speciate within the NCM following release from the dissolving ZnO particles (Table S4-2). According to the model, majority of the Zn speciations were remained present as dissolved Zn as free Zn ions and ionic complexes, where zinc precipitates were minimized.

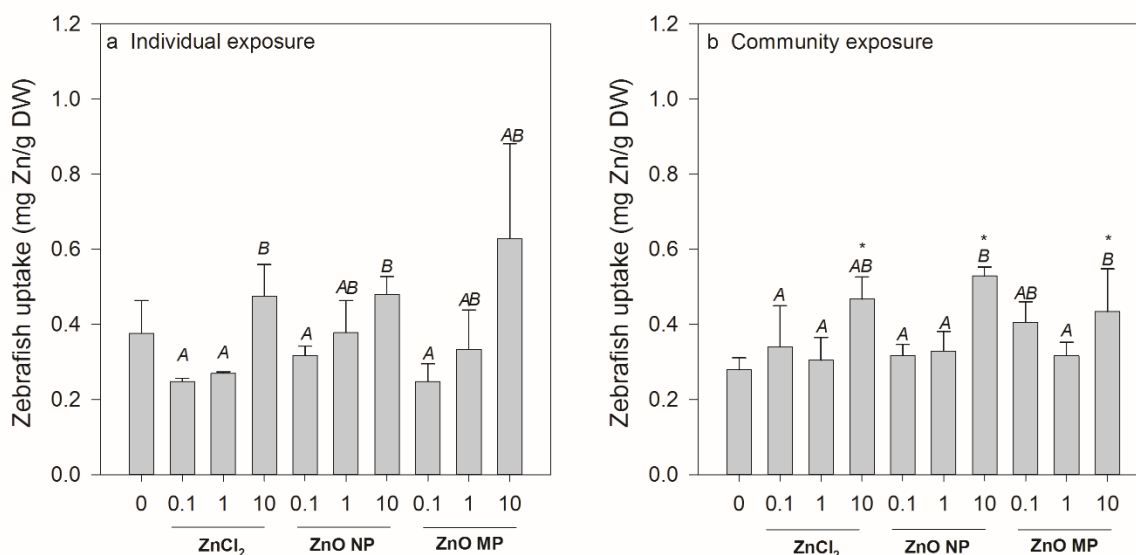


**Figure 4-3.** Dissolved zinc fraction (based on measured initial stock Zn concentrations) measured in NCM at 24 (a) and 120 (b) hours under each exposure scenario. Error bars

represent the standard error derived for triplicate samples. The asterisk (\*) indicates significant differences among each exposure types. Dissolved Zn fraction in individual *Daphnia* at day 5 were not measured due to the limitation of animal survival after 48 hours.

#### 4.4.4 Zn uptake

*D. magna* and zebrafish zinc uptake following all three types of Zn exposure are shown in Figure S4-1 and 4-4, respectively. *D. magna* uptake was only measured at 120 hours in the community exposure at exposure concentrations of 0, 0.1, and 1 mg ZnO/L due to the 100% mortality that occurred at 10 mg/L. There was a concentration dependent increase in Zn uptake in *D. magna*; ZnCl<sub>2</sub> exposures had significantly higher uptake in *D. magna* than ZnO NP and MPs, however, there was no significant difference in *D. magna* uptake among the three different types of Zn exposures at 1 mg/L. Zebrafish uptake in single exposure and community exposure are presented in Figure 4-4 a and b, respectively. Zn concentration in zebrafish showed concentration dependent uptake. Significantly higher Zn concentration was measured in zebrafish at 10 mg ZnO/L exposures in community exposure, but not individual exposure scenario.



**Figure 4-4.** Zebrafish uptake in individual exposure scenario (a) and community exposure scenario (b) with Zn exposures at 0.1, 1, and 10 mg ZnO/L. Error bars represent the standard error derived from triplicate samples. Uppercase letters indicate significant difference among exposure types at varying concentrations. The asterisk (\*) indicates significant difference compared to Zn concentration measured in control zebrafish.

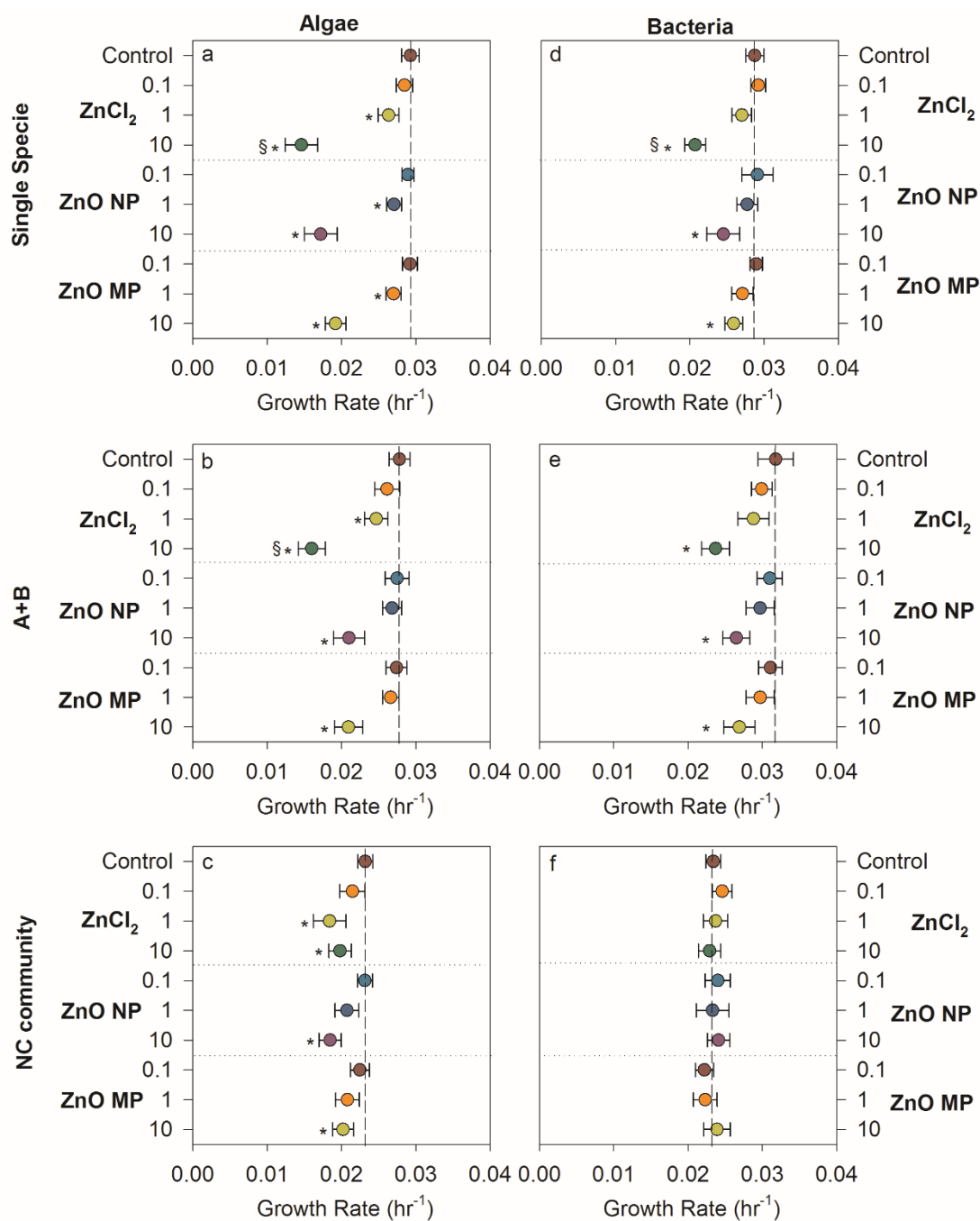
#### 4.4.5 Organism Toxicity

##### 4.4.5.1 Single algae vs A+B vs Community

All three types of Zn exposures showed a significant concentration dependent impact on algae growth rates (Figure 4-5a, b, c). The growth rate of algae in the individual exposure scenario was significantly decreased compared to control growth rates by all types of Zn exposures at concentrations equal or greater than 1 mg/L (Figure 4-5a). ZnCl<sub>2</sub> exposure elicited significantly higher impacts than ZnO MPs at 10 mg ZnO/L. When bacteria and algae were combined (A+B exposure scenario), similar responses were observed in algae growth rates (Figure 5b), where all three Zn exposures significantly decreased the algal growth rates at 10 mg ZnO/L exposures. In addition, significant growth inhibition was also observed at 1 mg/L of

ZnCl<sub>2</sub> exposure. In the nanocosm community exposure (Figure 5c), *D. magna* predation significantly decreased the growth rates of algae compared to single algae and A+B exposure scenarios by comparing the controls in different exposure scenarios. ZnCl<sub>2</sub> significantly inhibited algae growth rates at 1 mg/L and 10 mg/L, where ZnO NP and MP inhibited algae growth at 10 mg/L in the nanocosm community.





**Figure 4-5.** Growth rates of algae (left panel) and bacteria (right panel) in three different exposure scenarios: single species (a, d), algae+bacteria (A+B) (b, e), all four species combined (NC) (c, f). The vertical reference lines indicate control growth rates, and the horizontal reference lines separate the type of Zn exposures. Error bars represent the standard error derived from triplicate samples. The asterisk (\*) represents a significant difference from the corresponding control, and

symbol § indicates significant lower growth rate among the three Zn exposures at the same concentration.

#### 4.4.5.2 Bacteria Responses (Single vs Mix vs Community)

A significant decline in bacterial growth was found in single bacteria exposures at 10 mg/L in all three types of Zn exposures, but not at any of the other concentrations (Figure 4-5d). In the A+B toxicity testing, the presence of algae did not affect the control bacterial growth. The population growth rate of bacteria was significantly decreased by all types of Zn exposures at 10 mg/L compared to control (Figure 4-5e). In the nanocosm community exposure, *D. magna* predation also significantly reduced bacteria growth rates compared to what found in single and A+B exposure scenarios (Figure 4-5f); however, there was no significant difference in bacteria growth rates at any exposure concentrations.

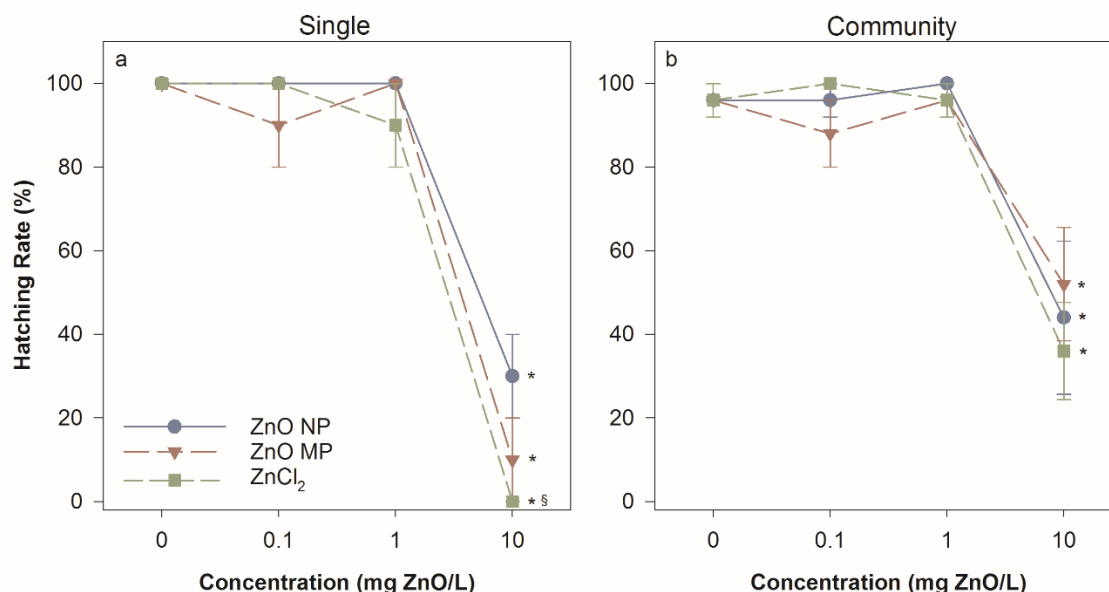
#### 4.4.5.3 Daphnia Response (Single vs Community)

The toxicity of zinc materials to *Daphnia magna* in individual and community exposures was compared at 48 hours due to the limitation of nutrients and food source (algae and bacteria) in the individual exposures (Figure S4-2). In contrast, abundant algae and bacteria in NC exposures served as a primary food source, leading to high *D. magna* survival throughout the 120-hour exposure period. In both the single and community exposure scenarios, no significant adverse effect to *D. magna* was observed for any type of Zn exposure at 0.1 and 1 mg/L, whereas 100% mortality was observed at 10 mg ZnO/L (Figure S4-2a). In the single *D. magna* exposure, ZnCl<sub>2</sub> elicited higher mortality compared to ZnO NP and MP exposure at 24 hours, but 100% mortality was observed for all three Zn exposures at 48 hours. In comparison, lower toxicity was

observed in *D. magna* with the same exposure concentrations in the community exposure (Figure S4-2b).  $\text{ZnCl}_2$  again elicited the highest toxicity to *D. magna* compared to other two types of Zn exposures, where 20% mortality and 90% mortality observed at 24 and 48 hours, respectively. ZnO NPs and MPs showed delayed toxicity compared to single species exposures, with 30% and 50% mortality after 48 hours, respectively.

#### 4.4.5.4 Zebrafish Responses (Single vs Community)

There was no significant difference in mortality or sub-lethal malformations at exposure concentrations up to 10 mg ZnO/L, regardless of the type of zinc in both single and community scenarios. However, the hatching rate was significantly delayed at 10 mg/L in all Zn exposures at both single and community scenarios (Figure 4-6). In this single zebrafish exposure,  $\text{ZnCl}_2$  led to a significantly higher hatching delay than the ZnO NPs and MPs. However, there was no significant difference in hatching delay among the three Zn types in the NC exposure. In addition, zebrafish hatching rate is significantly lower in the single species exposure than in the community with  $\text{ZnCl}_2$  exposure at 10 mg/L.

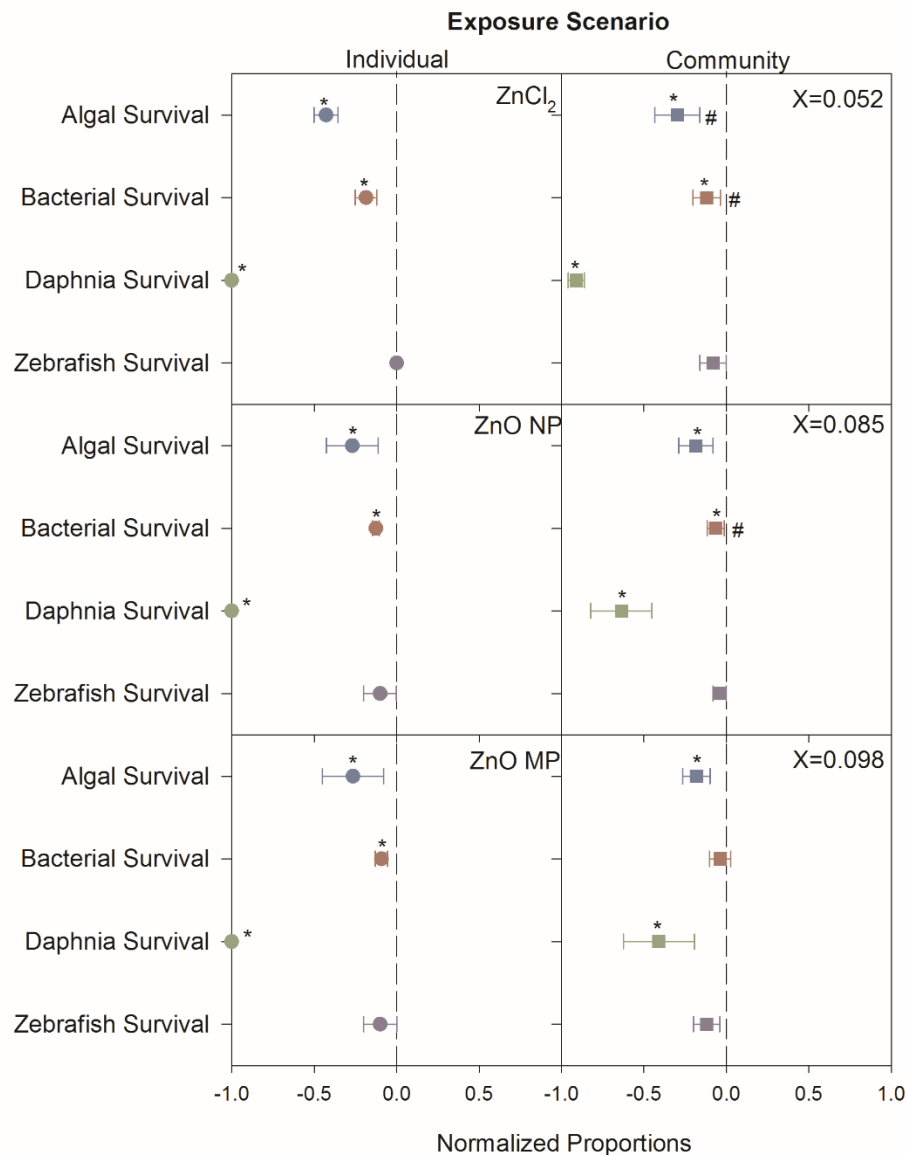


**Figure 4-6.** Zebrafish hatching rate in single (a) and community (b) exposure conditions after 120 hours. The asterisk (\*) represents a significant difference from corresponding control, and symbol § indicates significant difference between ZnCl<sub>2</sub> and ZnO MP exposure. Error bars represent the standard error derived from three sample replicates.

#### 4.4.6 Integrated comparison

The population level endpoints measured depended on the species interactions in the system. For instance, the growth rates of algae and bacteria are dependent on the predation of *D. magna*. Individual level organismal endpoints (120 hour algae and bacteria survival, *D. magna* survival at 48 hours, and 120-hour zebrafish hatching rate) were used to compare the response of each species to Zn exposures in single and NC exposures (Figure 4-7). 120 hour algae and bacteria survival were normalized using equation 2. The corresponding control of each species was set to 0 (dash lines in the center of each panel), and all organism responses were normalized based on each corresponding control. The deviation from the control indicates positive (>0) or negative (<0) impacts by Zn exposures compared to corresponding controls. At lower exposure

concentrations (0.1 and 1 mg/L), the deviation of each organismal toxicity was not significantly different in single or NC community exposures. However, there was a significant reduction in toxicity in the NC community exposure at 10 mg/L compared to single species exposures. By comparing the deviation of each organism in NC to single exposure, the overall resistance was calculated as percent deviation of species response in the NC to single species. The resistance of community exposure was 8.5%, 9.8%, and 5.2% for ZnO NP, MP, and ZnCl<sub>2</sub>, respectively for organism survival.



**Figure 4-7.** The overall 120-hour comparison of each species in single and NC group exposed at 10 mg ZnO/L. The dashed line is the corrected controls for single and NC responses. Error bars represent the standard error derived from triplicate samples. The asterisk \* represents a significant difference compared to corresponding control. Symbol # indicates significant difference between organism responses between individual species exposure and community exposures. X and the following values are the mean mitigated toxicity shifts of all four species in NC community compared to single exposure scenario.

## 4.5 Discussion

### 4.5.1 NP characterization

The large HDD of ZnO NPs in NCM indicates significant agglomeration of ZnO NPs occurred over the experimental period. Significantly higher agglomeration was measured in NCM than MQ water, likely attributed to the presence of various cations in the NCM, which compress the electrical double layer and increase the likelihood of particle–particle interactions (Prathna, Chandrasekaran et al. 2011). Divalent cations have been demonstrated to impact the stability of NPs in aqueous media (Baalousha, Nur et al. 2013; Miao, Wang et al. 2016). Large agglomerates were inevitably formed due to the moderate hardness of the nanocosm media, and the HDD of ZnO NPs reached the micro scale after 72 hours.

The ZP of ZnO NPs in the NCM was negative and consistent over time. The point of zero charge for ZnO NPs is known to be at a pH range of 8.7 to 10.3 depending on media composition (Kosmulski 2001), where some researchers have specified pH 9 as the closest to the point of zero charge for ZnO NPs (Bian, Mudunkotuwa et al. 2011; Omar, Aziz et al. 2014). The negative ZP values of ZnO NPs in the NCM could be attributed to the neutralization of the positively charged zinc ions by anionic species in the medium, resulting in a negatively charged nanoparticle surface.

### 4.5.2 Dissolved Zn and organismal uptake

In abiotic nanocosm media, both sizes of ZnO particles showed high initial dissolved zinc concentrations indicating rapid dissolution in the NCM. This high initial dissolved Zn

concentrations were similar to the dissolution kinetics previously reported for ZnO NPs in other types of suspension media (Xia, Kovochich et al. 2008; Adam, Leroux et al. 2014; Xiao, Vijver et al. 2015). The amount of dissolved zinc released from ZnO NPs was also similar to that reported by Merdzan et al. (Merdzan, Domingos et al. 2014), who found more than 85% of zinc ions were released from bare ZnO NPs in HEPES buffer after 24 hours of sample equilibration . Combined effects of the NP surface coating (Merdzan, Domingos et al. 2014), particle size (Meulenkamp 1998), and water parameters of the exposure media (Li and Wang 2013) have been reported to critically impact NP dissolution. The difference in dissolved Zn concentrations between ZnO NPs and MPs is potentially attributed to high agglomeration tendency of nanoparticles, which lead to variation in the available surface for Zn dissolution. ZnO NPs had a more rapid release of dissolved Zn than MPs, but MPs had a more consistent releasing rate overtime than NPs.

In the biotic environment, the dissolved Zn measurements in ZnCl<sub>2</sub> exposure suggests that organisms actively took up Zn as micronutrient. Thus, the actual dissolved Zn concentrations should be higher than the measured dissolved Zn in NP and MP exposures due to the utilization of Zn by organisms. In addition, the released free zinc ions could also interact with exudates from the organisms, and may not be measured as dissolved Zn after 3 kDa filter centrifugation. Organic matter can also coat NPs and MPs and prevent them from further releasing ions (Adeleye, Conway et al. 2014). In a previous study, we showed biotic environments significantly promoted the release of dissolved Ag from silver NPs, which posed potentially higher risks to aquatic environments (Wu, Harper et al. 2017). Surprisingly, no significant difference was found between ZnO NP and MP dissolution in biotic environment.



This may be due to the high agglomeration observed in the NPs, which lead to a decrease in reactive surface area, and possible shadowing effects. By using visual MINTEQ, we predicted more than 90% of the measured Zn was present as free  $\text{Zn}^{2+}$  assuming equilibrium, implying that  $\text{Zn}^{2+}$  may play an important role dominating the toxicity of ZnO particles to organisms. In addition, the measured Zn uptake in *D. magna* and zebrafish was also not significantly different among three Zn source at the same exposure concentrations, suggesting that dissolved Zn species were readily taken up and attributed for the Zn measured in the organisms.

#### 4.5.3 Toxicity

Generally, the mechanisms of ZnO NP toxicity to organisms are attributed to the release of Zn ions disrupting homeostasis (Chevallet, Gallet et al. 2016), generation of reactive oxygen species (ROS) interacting with membrane proteins (Zhang, Jiang et al. 2010), and direct particle-cell contact which causes membrane disorganization and internalization (Adams, Lyon et al. 2006; Huang, Zheng et al. 2008). The toxicity of exposures to all four species are highly dependent on the dissolved Zn fraction, implying that dissolved Zn dictated the toxicity. In addition,  $\text{ZnCl}_2$  elicited higher toxicity in the nanocosm compared to both nano and micro sized particles, suggesting the toxicity from the ZnO NPs was mostly attributed to the dissolved Zn released from ZnO NPs since no particle specific impact was observed in this study.

Studies have shown that *C. reinhardtii* is more susceptible to soluble species than suspended solid particulates (Gunawan, Sirimanoonphan et al. 2013). ZnO NPs contained more smaller, membrane permeable particles, which potentially could be internalized by algae and bacteria and cause toxicity (Gunawan, Sirimanoonphan et al. 2013). However, the large HDDs at

10 mg ZnO/L and comparable toxicity with the MP exposures indicates the particles themselves were likely not serving as the major toxic agent.

Despite previous studies reporting *E.coli* to have low sensitivity to ZnO NP exposures (Bondarenko, Juganson et al. 2013), ZnO NPs inhibited the growth of *E. coli* in the individual exposure. The toxicity of ZnO NPs to *E.coli* could vary depending on the composition of the test media. For instance, CeO<sub>2</sub> NPs were highly toxic to *E. coli* in pure water (Thill, Zeyons et al. 2006), but no effect on *E.coli* was found in culture media because the CeO<sub>2</sub> NPs formed large aggregates (Zeyons, Thill et al. 2009).

*D. magna* were much more susceptible to Zn exposures than algae and bacteria. Due to their filter feeding behavior, they were exposed to Zn from suspended particles in the water column exposures, and from preying on Zn contaminated food sources. ZnCl<sub>2</sub> elicited higher toxicity to *D. magna* than ZnO NPs and MPs, where higher Zn concentration was also measured within *D. magna* body under ZnCl<sub>2</sub> exposures. This is consistent with what was observed in previous studies that concluded the toxicity of ZnO NPs was triggered by the release of ionic Zn from NPs (Ergonul, Atasagun et al. 2012; Bondarenko, Juganson et al. 2013; Seo, Kim et al. 2014).

Significant hatching delay in Zebrafish was observed in both individual and community exposures. This is likely due to the high concentrations of dissolved Zn released from ZnO particles. Bai and colleagues reported a concentration dependent decrease in hatching rate of zebrafish embryos for ZnO NPs, and suggested that delayed hatching might be caused by the disturbance of the hatching enzyme by released ionic Zn, and hypoxia induced by ZnO NPs (Bai, Zhang et al. 2010). Given the large HDD of ZnO NPs and primary size of MPs, the rapid

settlement of ZnO particles can coat the chorion, which can interfere with embryo oxygen exchange (Cheng, Flahaut et al. 2007). However, due to the rapid dissolution of ZnO particles, it is more likely that dissolved Zn species were responsible for the observed delayed hatching. It is also established that  $\text{Zn}^{2+}$  is essential to zebrafish embryos for both development and fertilization (Zhao, Xia et al. 2014); however, abundant  $\text{Zn}^{2+}$  has been shown to inhibit the development of embryonic zebrafish, and a high concentration of  $\text{Zn}^{2+}$  may cause ionic competition altering the nutrient uptake and eventually disrupting the normal hatching function of zebrafish. Significantly more zebrafish showed delayed hatching in  $\text{ZnCl}_2$  exposure also suggests dissolved Zn likely caused hatching delay.

The single and NC exposure scenarios had different limiting factors. In the single species exposures, toxicity was elicited directly from the Zn exposures. However, in the NC, the effective Zn exposure was impacted by the interactions among species, including trophic transfer and interspecies interaction, therefore altering toxicity. The interaction among species and NP-organism interaction could potentially decrease the overall exposure due to the presence of more biological sinks, which provides environmental resistance to a given ecosystem. The nanocosm community assay we developed here has shown environmental resistance to all three Zn exposures compared to single species. Similar results have also been discovered in another study, who compared the toxicity of AgNP in outdoor mesocosm, microcosm, and conventional laboratory studies, where lower toxicity was observed in larger scale mesocosms (Bone, Matson et al. 2015). For example, the secretion of extracellular organic carbon by *C. reinhardtii* and *E. coli* can coat NPs (Baba, Suzuki et al. 2011; Kadar, Rooks et al. 2012), significantly reducing dissolution with concomitant impacts on the toxicity of NPs (Stevenson, Dickson et al. 2013). In

addition, metal NP toxicity can be reduced in the presence of DOC (Blinova, Niskanen et al. 2013), with the potential of more DOC generated in the nanocosm than individual species scenario, toxicity can also be mitigated. The nanocosm assay is a rapid, and cost-effective method to screen and evaluate the acute toxicity of NPs.

#### **4.6 Conclusion**

Overall, our study demonstrated that dissolved Zn dictates the uptake behavior and toxicity of ZnO particles to the simulated community due to the high solubility and rapid dissolution. Lower toxicity and delayed impacts were observed for each species in the NC group compared to the single exposures. This validated our nanocosm assay as a rapid assay for assessing the acute environmental impact of NPs, and demonstrated environment resistance to Zn exposures. Future work will consider using Zn isotope to separate the contribution of Zn ion and NP impacts and trace their distribution in an ecosystem due to the high background concentration in the nature and the high dissolution rates.

## 4.7 Reference

- Abdelmonem, A. M., B. Pelaz, et al. (2015). "Charge and agglomeration dependent in vitro uptake and cytotoxicity of zinc oxide nanoparticles." Journal of inorganic biochemistry **153**: 334-338.
- Adam, N., F. Leroux, et al. (2014). "The uptake of ZnO and CuO nanoparticles in the water-flea *Daphnia magna* under acute exposure scenarios." Environmental Pollution **194**: 130-137.
- Adams, L. K., D. Y. Lyon, et al. (2006). "Comparative eco-toxicity of nanoscale TiO<sub>2</sub>, SiO<sub>2</sub>, and ZnO water suspensions." Water research **40**(19): 3527-3532.
- Adeleye, A. S., J. R. Conway, et al. (2014). "Influence of extracellular polymeric substances on the long-term fate, dissolution, and speciation of copper-based nanoparticles." Environmental science & technology **48**(21): 12561-12568.
- Aruoja, V., H.-C. Dubourguier, et al. (2009). "Toxicity of nanoparticles of CuO, ZnO and TiO<sub>2</sub> to microalgae *Pseudokirchneriella subcapitata*." Science of the Total Environment **407**(4): 1461-1468.
- Aschberger, K., C. Micheletti, et al. (2011). "Analysis of currently available data for characterising the risk of engineered nanomaterials to the environment and human health—lessons learned from four case studies." Environment international **37**(6): 1143-1156.
- ASTM (2011). Standard Practice for Standardized Aquatic Microcosms: Fresh Water. West Conshohocken, PA, ASTM International.
- Baalousha, M., Y. Nur, et al. (2013). "Effect of monovalent and divalent cations, anions and fulvic acid on aggregation of citrate-coated silver nanoparticles." Science of the total environment **454**: 119-131.
- Baba, M., I. Suzuki, et al. (2011). "Proteomic analysis of high-CO<sub>2</sub>-inducible extracellular proteins in the unicellular green alga, *Chlamydomonas reinhardtii*." Plant and cell physiology **52**(8): 1302-1314.
- Bacchetta, R., B. Maran, et al. (2016). "Role of soluble zinc in ZnO nanoparticle cytotoxicity in *Daphnia magna*: A morphological approach." Environmental research **148**: 376-385.
- Bai, W., Z. Zhang, et al. (2010). "Toxicity of zinc oxide nanoparticles to zebrafish embryo: a physicochemical study of toxicity mechanism." Journal of Nanoparticle Research **12**(5): 1645-1654.

- Bernhardt, E. S., B. P. Colman, et al. (2010). "An ecological perspective on nanomaterial impacts in the environment." Journal of environmental quality **39**(6): 1954-1965.
- Bian, S.-W., I. A. Mudunkotuwa, et al. (2011). "Aggregation and dissolution of 4 nm ZnO nanoparticles in aqueous environments: influence of pH, ionic strength, size, and adsorption of humic acid." Langmuir **27**(10): 6059-6068.
- Blinova, I., A. Ivask, et al. (2010). "Ecotoxicity of nanoparticles of CuO and ZnO in natural water." Environmental Pollution **158**(1): 41-47.
- Blinova, I., J. Niskanen, et al. (2013). "Toxicity of two types of silver nanoparticles to aquatic crustaceans *Daphnia magna* and *Thamnocephalus platyurus*." Environmental Science and Pollution Research **20**(5): 3456-3463.
- Bondarenko, O., K. Juganson, et al. (2013). "Toxicity of Ag, CuO and ZnO nanoparticles to selected environmentally relevant test organisms and mammalian cells in vitro: a critical review." Archives of toxicology **87**(7): 1181-1200.
- Bone, A. J., C. W. Matson, et al. (2015). "Silver nanoparticle toxicity to Atlantic killifish (*Fundulus heteroclitus*) and *Caenorhabditis elegans*: A comparison of mesocosm, microcosm, and conventional laboratory studies." Environmental Toxicology and Chemistry **34**(2): 275-282.
- Boxall, A., C. D. Brown, et al. (2002). "Higher-tier laboratory methods for assessing the aquatic toxicity of pesticides." Pest management science **58**(7): 637-648.
- Brayner, R., R. Ferrari-Iliou, et al. (2006). "Toxicological impact studies based on *Escherichia coli* bacteria in ultrafine ZnO nanoparticles colloidal medium." Nano Letters **6**(4): 866-870.
- Chen, L., L. Zhou, et al. (2012). "Toxicological effects of nanometer titanium dioxide (nano-TiO<sub>2</sub>) on *Chlamydomonas reinhardtii*." Ecotoxicology and environmental safety **84**: 155-162.
- Cheng, J., E. Flahaut, et al. (2007). "Effect of carbon nanotubes on developing zebrafish (*Danio rerio*) embryos." Environmental Toxicology and Chemistry **26**(4): 708-716.
- Chevallet, M., B. Gallet, et al. (2016). "Metal homeostasis disruption and mitochondrial dysfunction in hepatocytes exposed to sub-toxic doses of zinc oxide nanoparticles." Nanoscale **8**(43): 18495-18506.
- Colman, B. P., C. L. Arnaout, et al. (2013). "Low Concentrations of Silver Nanoparticles in Biosolids Cause Adverse Ecosystem Responses under Realistic Field Scenario." PloS one **8**(2): e57189.

- De Zwart, D. and L. Posthuma (2005). "Complex mixture toxicity for single and multiple species: proposed methodologies." Environmental Toxicology and Chemistry **24**(10): 2665-2676.
- Ergonul, M. B., S. Atasagun, et al. (2012). "The Acute Toxicity of Zinc chloride on *Daphnia magna* Straus." Gazi University Journal of Science **25**(2): 313-316.
- Franklin, N. M., N. J. Rogers, et al. (2007). "Comparative toxicity of nanoparticulate ZnO, bulk ZnO, and ZnCl<sub>2</sub> to a freshwater microalga (*Pseudokirchneriella subcapitata*): the importance of particle solubility." Environmental science & technology **41**(24): 8484-8490.
- Gliga, A. R., S. Skoglund, et al. (2014). "Size-dependent cytotoxicity of silver nanoparticles in human lung cells: the role of cellular uptake, agglomeration and Ag release." Particle and fibre toxicology **11**(1): 11.
- Gorman, D. S. and R. Levine (1965). "Cytochrome f and plastocyanin: their sequence in the photosynthetic electron transport chain of *Chlamydomonas reinhardtii*." Proceedings of the National Academy of Sciences of the United States of America **54**(6): 1665.
- Gottschalk, F., T. Sonderer, et al. (2009). "Modeled environmental concentrations of engineered nanomaterials (TiO<sub>2</sub>, ZnO, Ag, CNT, fullerenes) for different regions." Environmental science & technology **43**(24): 9216-9222.
- Gunawan, C., A. Sirimanoonphan, et al. (2013). "Submicron and nano formulations of titanium dioxide and zinc oxide stimulate unique cellular toxicological responses in the green microalga *Chlamydomonas reinhardtii*." Journal of hazardous materials **260**: 984-992.
- Hanley, C., A. Thurber, et al. (2009). "The influences of cell type and ZnO nanoparticle size on immune cell cytotoxicity and cytokine induction." Nanoscale research letters **4**(12): 1409.
- Hariharan, C. (2006). "Photocatalytic degradation of organic contaminants in water by ZnO nanoparticles: Revisited." Applied Catalysis A: General **304**: 55-61.
- Harper, S., C. Usenko, et al. (2008). "In vivo biodistribution and toxicity depends on nanomaterial composition, size, surface functionalisation and route of exposure." Journal of Experimental Nanoscience **3**(3): 195-206.
- Heinlaan, M., A. Ivask, et al. (2008). "Toxicity of nanosized and bulk ZnO, CuO and TiO<sub>2</sub> to bacteria *Vibrio fischeri* and crustaceans *Daphnia magna* and *Thamnocephalus platyurus*." Chemosphere **71**(7): 1308-1316.

- Henderson, C. F. and E. W. Tilton (1955). "Tests with acaricides against the brown wheat mite." Journal of Economic Entomology **48**(2): 157-161.
- Hsiao, I.-L. and Y.-J. Huang (2011). "Effects of various physicochemical characteristics on the toxicities of ZnO and TiO<sub>2</sub> nanoparticles toward human lung epithelial cells." Science of the total environment **409**(7): 1219-1228.
- Huang, Z., X. Zheng, et al. (2008). "Toxicological effect of ZnO nanoparticles based on bacteria." Langmuir **24**(8): 4140-4144.
- Kadar, E., P. Rooks, et al. (2012). "The effect of engineered iron nanoparticles on growth and metabolic status of marine microalgae cultures." Science of the total environment **439**: 8-17.
- Kahru, A. and H.-C. Dubourguier (2010). "From ecotoxicology to nanoecotoxicology." Toxicology **269**(2): 105-119.
- Keller, A. A. and A. Lazareva (2013). "Predicted releases of engineered nanomaterials: from global to regional to local." Environmental Science & Technology Letters **1**(1): 65-70.
- Khrenov, V., M. Klapper, et al. (2005). "Surface functionalized ZnO particles designed for the use in transparent nanocomposites." Macromolecular chemistry and physics **206**(1): 95-101.
- Kimmel, C. B., W. W. Ballard, et al. (1995). "Stages of embryonic development of the zebrafish." Developmental dynamics **203**(3): 253-310.
- Kononenko, V., N. Repar, et al. (2017). "Comparative in vitro genotoxicity study of ZnO nanoparticles, ZnO macroparticles and ZnCl<sub>2</sub> to MDCK kidney cells: Size matters." Toxicology in Vitro **40**: 256-263.
- Kosmulski, M. (2001). Chemical properties of material surfaces, CRC press.
- Levy, J. L., J. L. Stauber, et al. (2009). "The effect of bacteria on the sensitivity of microalgae to copper in laboratory bioassays." Chemosphere **74**(9): 1266-1274.
- Li, W.-M. and W.-X. Wang (2013). "Distinct biokinetic behavior of ZnO nanoparticles in *Daphnia magna* quantified by synthesizing 65 Zn tracer." Water research **47**(2): 895-902.
- Lopes, S., F. Ribeiro, et al. (2014). "Zinc oxide nanoparticles toxicity to *Daphnia magna*: size - dependent effects and dissolution." Environmental Toxicology and Chemistry **33**(1): 190-198.



- Lowry, G. V., R. J. Hill, et al. (2016). "Guidance to improve the scientific value of zeta-potential measurements in nanoEHS." Environmental Science: Nano **3**(5): 953-965.
- Mackay, D., P. Holmes, et al. (1989). The application of bioassay techniques to water pollution problems—The United Kingdom experience. Environmental Bioassay Techniques and their Application, Springer: 77-86.
- Merdzan, V., R. F. Domingos, et al. (2014). "The effects of different coatings on zinc oxide nanoparticles and their influence on dissolution and bioaccumulation by the green alga, *C. reinhardtii*." Science of the total environment **488**: 316-324.
- Meulenkamp, E. A. (1998). "Size dependence of the dissolution of ZnO nanoparticles." The Journal of Physical Chemistry B **102**(40): 7764-7769.
- Miao, L., C. Wang, et al. (2016). "Effect of alginate on the aggregation kinetics of copper oxide nanoparticles (CuO NPs): bridging interaction and hetero-aggregation induced by Ca<sup>2+</sup>." Environmental Science and Pollution Research **23**(12): 11611-11619.
- Nair, S., A. Sasidharan, et al. (2009). "Role of size scale of ZnO nanoparticles and microparticles on toxicity toward bacteria and osteoblast cancer cells." Journal of Materials Science: Materials in Medicine **20**(1): 235.
- Navarro, E., F. Piccapietra, et al. (2008). "Toxicity of silver nanoparticles to *Chlamydomonas reinhardtii*." Environmental science & technology **42**(23): 8959-8964.
- Nowack, B. and T. D. Bucheli (2007). "Occurrence, behavior and effects of nanoparticles in the environment." Environmental Pollution **150**(1): 5-22.
- Omar, F. M., H. A. Aziz, et al. (2014). "Aggregation and disaggregation of ZnO nanoparticles: influence of pH and adsorption of Suwannee River humic acid." Science of the total environment **468**: 195-201.
- Paine, C., T. R. Marthews, et al. (2012). "How to fit nonlinear plant growth models and calculate growth rates: an update for ecologists." Methods in Ecology and Evolution **3**(2): 245-256.
- Perreault, F., A. Oukarroum, et al. (2012). "Polymer coating of copper oxide nanoparticles increases nanoparticles uptake and toxicity in the green alga *Chlamydomonas reinhardtii*." Chemosphere **87**(11): 1388-1394.
- Piccinno, F., F. Gottschalk, et al. (2012). "Industrial production quantities and uses of ten engineered nanomaterials in Europe and the world." Journal of Nanoparticle Research **14**(9): 1-11.

- Prathna, T., N. Chandrasekaran, et al. (2011). "Studies on aggregation behaviour of silver nanoparticles in aqueous matrices: effect of surface functionalization and matrix composition." Colloids and Surfaces A: Physicochemical and Engineering Aspects **390**(1): 216-224.
- Scown, T., R. Van Aerle, et al. (2010). "Review: do engineered nanoparticles pose a significant threat to the aquatic environment?" Critical reviews in toxicology **40**(7): 653-670.
- Seo, J., S. Kim, et al. (2014). "Effects of Physiochemical Properties of Test Media on Nanoparticle Toxicity to *Daphnia magna* Straus." Bulletin of environmental contamination and toxicology **93**(3): 257-262.
- Sharma, V., D. Anderson, et al. (2012). "Zinc oxide nanoparticles induce oxidative DNA damage and ROS-triggered mitochondria mediated apoptosis in human liver cells (HepG2)." Apoptosis **17**(8): 852-870.
- Sondi, I. and B. Salopek-Sondi (2004). "Silver nanoparticles as antimicrobial agent: a case study on *E. coli* as a model for Gram-negative bacteria." Journal of colloid and interface science **275**(1): 177-182.
- Stevenson, L. M., H. Dickson, et al. (2013). "Environmental Feedbacks and Engineered Nanoparticles: Mitigation of Silver Nanoparticle Toxicity to *Chlamydomonas reinhardtii* by Algal-Produced Organic Compounds." PloS one **8**(9): e74456.
- Taub, F. B. and A. M. Dollar (1968). "The nutritional inadequacy of *Chlorella* and *Chlamydomonas* as food for *Daphnia pulex*." Limnol. Oceanogr **13**(4): 607-617.
- Thill, A., O. Zeyons, et al. (2006). "Cytotoxicity of CeO<sub>2</sub> nanoparticles for *Escherichia coli*. Physico-chemical insight of the cytotoxicity mechanism." Environmental science & technology **40**(19): 6151-6156.
- Wang, Z. L. (2004). "Zinc oxide nanostructures: growth, properties and applications." Journal of Physics: Condensed Matter **16**(25): R829.
- Wong, S. W., P. T. Leung, et al. (2010). "Toxicities of nano zinc oxide to five marine organisms: influences of aggregate size and ion solubility." Analytical and bioanalytical chemistry **396**(2): 609-618.
- Wu, F., B. J. Harper, et al. (2017). "Differential dissolution and toxicity of surface functionalized silver nanoparticles in small-scale microcosms: impacts of community complexity." Environmental Science: Nano.

- Xia, T., M. Kovoichich, et al. (2008). "Comparison of the mechanism of toxicity of zinc oxide and cerium oxide nanoparticles based on dissolution and oxidative stress properties." ACS Nano **2**(10): 2121-2134.
- Xiao, Y., M. G. Vijver, et al. (2015). "Toxicity and Accumulation of Cu and ZnO nanoparticles in *Daphnia magna*." Environmental science & technology **49**(7): 4657-4664.
- Xiong, D., T. Fang, et al. (2011). "Effects of nano-scale TiO<sub>2</sub>, ZnO and their bulk counterparts on zebrafish: Acute toxicity, oxidative stress and oxidative damage." Science of the total environment **409**(8): 1444-1452.
- Yoon, S.-J., J. I. Kwak, et al. (2014). "Zinc oxide nanoparticles delay soybean development: A standard soil microcosm study." Ecotoxicology and environmental safety **100**: 131-137.
- Zeyons, O., A. Thill, et al. (2009). "Direct and indirect CeO<sub>2</sub> nanoparticles toxicity for *Escherichia coli* and *Synechocystis*." Nanotoxicology **3**(4): 284-295.
- Zhang, L., Y. Jiang, et al. (2010). "Mechanistic investigation into antibacterial behaviour of suspensions of ZnO nanoparticles against *E. coli*." Journal of Nanoparticle Research **12**(5): 1625-1636.
- Zhang, L., Y. Jiang, et al. (2007). "Investigation into the antibacterial behaviour of suspensions of ZnO nanoparticles (ZnO nanofluids)." Journal of Nanoparticle Research **9**(3): 479-489.
- Zhao, L., Z. Xia, et al. (2014). "Zebrafish in the sea of mineral (iron, zinc, and copper) metabolism." Frontiers in pharmacology **5**.
- Zhao, X., S. Wang, et al. (2013). "Acute ZnO nanoparticles exposure induces developmental toxicity, oxidative stress and DNA damage in embryo-larval zebrafish." Aquatic toxicology **136**: 49-59.

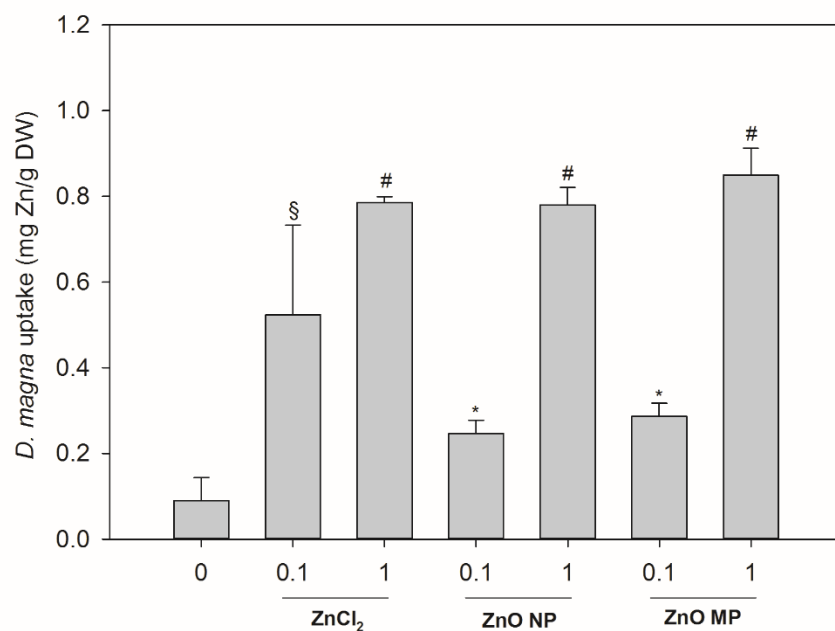
## 4.8 Appendix

**Table S4-1.** Standardized information for determining nanoparticle zeta potential in NCM.

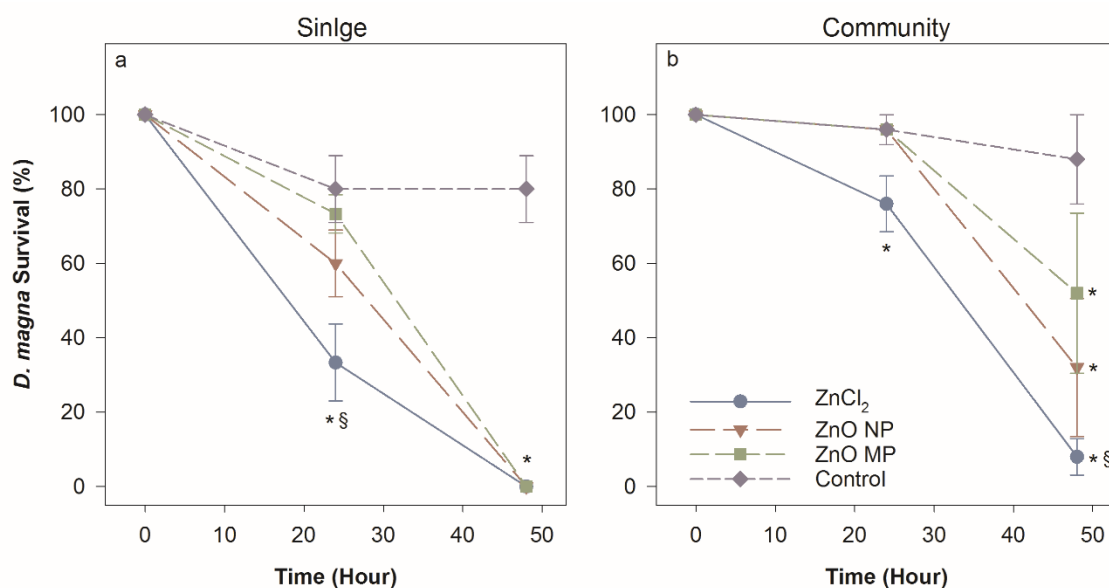
Surface functionalization	None
Shape	spherical
Model used to compute the zeta potential	Henry's Equation (Smoluchowski approximation)
Duration of measurement	90 seconds for single measurement
Applied voltage	148 V
Number of measurements made and averaged to determine each ZP	12
Total number of replicate measurements	3
pH	$7.2 \pm 0.2$
Ionic strength	0.01 mol/L
Ionic composition	Made according to Ref. 47
Temperature	25 °C
Total number of replicate measurements	3
Applied voltage	148 V

**Table S4-2.** Theoretical Zn speciation calculated with Visual-MINTEQ assuming equilibrium in NCM using the exposed Zn concentrations.

Input concentration (8 mg Zn/L)			Input concentration (0.8 mg Zn/L)			Input concentration (0.08 mg Zn/L)		
Zn speciation	Mass (mg/L)	Percent Total	Zn speciation	Mass (mg/L)	Percent Total	Zn speciation	Mass (mg/L)	Percent Total
Zn(H <sub>2</sub> BO <sub>3</sub> ) <sub>2</sub> (aq)	1.08E-09	0%	Zn(H <sub>2</sub> BO <sub>3</sub> ) <sub>2</sub> (aq)	8.63E-06	0%	Zn(H <sub>2</sub> BO <sub>3</sub> ) <sub>2</sub> (aq)	7.4E-14	0%
Zn(NO <sub>3</sub> ) <sub>2</sub> (aq)	5.13E-07	0%	Zn(NO <sub>3</sub> ) <sub>2</sub> (aq)	4.09E-03	0%	Zn(NO <sub>3</sub> ) <sub>2</sub> (aq)	3.5E-11	0%
Zn(OH) <sub>2</sub> (aq)	1.57E-02	0%	Zn(OH) <sub>2</sub> (aq)	1.25E+02	0%	Zn(OH) <sub>2</sub> (aq)	1.1E-06	0%
Zn(OH) <sub>3</sub> <sup>-</sup>	8.66E-07	0%	Zn(OH) <sub>3</sub> <sup>-</sup>	6.90E-03	0%	Zn(OH) <sub>3</sub> <sup>-</sup>	5.9E-11	0%
Zn(OH) <sub>4</sub> <sup>2-</sup>	2.84E-12	0%	Zn(OH) <sub>4</sub> <sup>2-</sup>	2.27E-08	0%	Zn(OH) <sub>4</sub> <sup>2-</sup>	1.9E-16	0%
Zn(SO <sub>4</sub> ) <sub>2</sub> <sup>2-</sup>	5.13E-05	0%	Zn(SO <sub>4</sub> ) <sub>2</sub> <sup>2-</sup>	4.09E-01	0%	Zn(SO <sub>4</sub> ) <sub>2</sub> <sup>2-</sup>	3.6E-09	0%
Zn <sup>+2</sup>	6.96E+00	87%	Zn <sup>+2</sup>	5.54E+04	53%	Zn <sup>+2</sup>	4.7E-04	0%
Zn <sub>2</sub> OH <sup>+</sup>	1.32E-05	0%	Zn <sub>2</sub> OH <sup>+</sup>	1.05E-01	0%	Zn <sub>2</sub> OH <sup>+</sup>	6.1E-14	0%
ZnCl <sup>+</sup>	6.36E-02	1%	ZnCl <sup>+</sup>	5.07E+02	0%	ZnCl <sup>+</sup>	4.3E-06	0%
ZnCl <sub>2</sub> (aq)	2.34E-04	0%	ZnCl <sub>2</sub> (aq)	1.87E+00	0%	ZnCl <sub>2</sub> (aq)	1.6E-08	0%
ZnCl <sub>3</sub> <sup>-</sup>	1.18E-06	0%	ZnCl <sub>3</sub> <sup>-</sup>	9.44E-03	0%	ZnCl <sub>3</sub> <sup>-</sup>	8.1E-11	0%
ZnCl <sub>4</sub> <sup>2-</sup>	3.18E-09	0%	ZnCl <sub>4</sub> <sup>2-</sup>	2.53E-05	0%	ZnCl <sub>4</sub> <sup>2-</sup>	2.2E-13	0%
ZnEDTA <sup>2-</sup>	3.11E-01	4%	ZnEDTA <sup>2-</sup>	2.48E+03	37%	ZnEDTA <sup>2-</sup>	7.8E-02	71%
ZnH <sub>2</sub> BO <sub>3</sub> <sup>+</sup>	1.82E-05	0%	ZnH <sub>2</sub> BO <sub>3</sub> <sup>+</sup>	1.45E-01	0%	ZnH <sub>2</sub> BO <sub>3</sub> <sup>+</sup>	1.2E-09	0%
ZnH <sub>2</sub> EDTA (aq)	5.90E-11	0%	ZnH <sub>2</sub> EDTA (aq)	4.70E-07	0%	ZnH <sub>2</sub> EDTA (aq)	1.5E-11	0%
ZnHEDTA <sup>-</sup>	4.07E-05	0%	ZnHEDTA <sup>-</sup>	3.24E-01	0%	ZnHEDTA <sup>-</sup>	1.0E-05	0%
ZnHPO <sub>4</sub> (aq)	3.27E-01	4%	ZnHPO <sub>4</sub> (aq)	2.61E+03	3%	ZnHPO <sub>4</sub> (aq)	2.4E-05	0%
ZnNO <sub>3</sub> <sup>+</sup>	6.15E-03	0%	ZnNO <sub>3</sub> <sup>+</sup>	4.90E+01	0%	ZnNO <sub>3</sub> <sup>+</sup>	4.2E-07	0%
ZnOH <sup>+</sup>	8.55E-02	1%	ZnOH <sup>+</sup>	6.81E+02	1%	ZnOH <sup>+</sup>	5.8E-06	0%
ZnOHEDTA <sup>-3</sup>	4.41E-06	0%	ZnOHEDTA <sup>-3</sup>	3.52E-02	0%	ZnOHEDTA <sup>-3</sup>	1.1E-06	0%
ZnSO <sub>4</sub> (aq)	6.67E-02	1%	ZnSO <sub>4</sub> (aq)	5.32E+02	1%	ZnSO <sub>4</sub> (aq)	4.6E-06	0%



**Figure S4-1.** *D. magna* uptake in community exposure scenario with Zn exposures at 0.1 and 1 mg ZnO/L. Error bars represent the standard error derived from triplicate samples. All exposures had significant higher Zn in *D. magna*, and symbols \*, § and # indicates significant difference among exposure type and varied exposure concentrations.



**Figure S4-2.** *D. magna* survival over 48 hours in single (a) and NC (b) exposures to ZnCl<sub>2</sub> (Green square), ZnO NPs and ZnO MPs (b). The asterisk (\*) represents a significant difference from corresponding control, and symbol § indicates significant difference of ZnCl<sub>2</sub> with ZnO NP and MP exposures. Error bars represent the standard error derived from triplicate samples.

## **Chapter 5. Differential dissolution and toxicity of surface functionalized silver nanoparticles in small-scale microcosms: impacts of community complexity**

Fan Wu,<sup>a</sup> Bryan J. Harper,<sup>b</sup> and Stacey L. Harper<sup>a,b,c\*</sup>

<sup>a</sup> *School of Chemical, Biological and Environmental Engineering, Oregon State University, Corvallis, Oregon, United States*

<sup>b</sup> *Environmental and Molecular Toxicology, Oregon State University, Corvallis, Oregon, United States*

<sup>c</sup> *Oregon Nanoscience and Microtechnologies Institute, Eugene, Oregon, United States*

Environmental Science: Nano  
Royal Society of Chemistry  
1050 Connecticut Ave NW, Suite 500 Washington DC 20036  
Published: 2017,4, 359-372  
DOI: 10.1039/C6EN00324A



## 5.1 Abstract

Surface functionalization can minimize nanoparticle agglomeration and expand their applications; however, these modifications can also alter particle stability, dissolution, bioavailability and toxicity. Here we investigated how silver nanoparticles (AgNPs) with different surface chemistries affect community health, and how increased trophic complexity affects the interactions between organisms and nanomaterials. We compared AgNP exposures in simple microcosms comprised of algae (*Chlamydomonas reinhardtii*) and bacteria (*Escherichia coli*) to increasingly complex microcosms containing predatory invertebrates (*Daphnia magna*) and developing vertebrates (*Danio rerio*). Each microcosm was exposed to one of three 70 nm AgNPs [polyethylene glycol (PEG –AgNP), silica (Si-AgNP), or aminated silica-coated AgNP (Ami-Si-AgNP)] at 0, 0.1, 1, and 5 mg L<sup>-1</sup> to investigate the relative influence of surface charge, composition and dissolution on organismal uptake and toxicity. All three AgNPs released more dissolved Ag into solution when organisms were present than was measured in the same media without organisms. PEG-AgNPs had the highest overall toxicity in all scenarios, followed by Si-AgNPs, and lastly Ami-Si-AgNPs. Toxicity correlated with the amount of Ag measured in the exposure media and the amount taken up by the organisms. Our findings indicate that surface functionalization plays an important role in determining dissolution, uptake and toxicity of AgNPs. Increasing trophic complexity decreased organismal susceptibility under the same AgNP concentration exposures, likely due to the change in bioavailable Ag that each organism experienced. This implies that tests using individual species provide conservative estimates of environmental impacts, while exposure may be mitigated in more realistic multi-species scenarios like those found in nature.

## 5.2 Introduction

Understanding the physicochemical features of nanoparticles that drive their biological interactions is important to the development of novel, sustainable and biocompatible nanotechnology. Silver nanoparticles (AgNPs), although most commonly used for their antimicrobial properties, also have a wide range of current and potential future applications as catalysts, conductive inks and to aid medicine in diagnosis, imaging, treatment and drug delivery (Ho, Tobis et al. 2004; Ge, Li et al. 2014; Lü, Pu et al. 2015; Dong, Zhang et al. 2016). AgNPs are frequently coated with surface stabilizers during the synthesis processes to avoid aggregation that can affect their desired performance (Kvitek, Panáček et al. 2008; Kittler, Greulich et al. 2009). For instance, Ag nanoclusters coated with a carbon shell, form nanostructures that exhibit excellent catalytic activity and stability (Dong, Zhang et al. 2016). Silica coatings on AgNPs allow for diverse surface modification options which can alter their hydrophobicity, facilitate uptake, and limit dissolution and aggregation of AgNPs in order to achieve better performance in biomedical applications (Legrand, Catheline et al. 2008; Fruijtier-Pöllöth 2012; Agnihotri, Mukherji et al. 2013). Changes to particle surface chemistry are known to alter particle stability, dissolution rates, bioavailability and toxicity (Brunner, Wick et al. 2006; Franklin, Rogers et al. 2007; Kvitek, Panáček et al. 2008; El Badawy, Luxton et al. 2010; Tejamaya, Römer et al. 2012). Studies have also shown that variations in surface charge resulting from surface functionalization can impact cellular uptake, translocation to different tissues, and cytotoxicity (Fabrega, Luoma et al. 2011; Fröhlich 2012; Ivask, ElBadawy et al. 2013; Bonventre, Pryor et al. 2014). The magnitude of the surface charge, as measured by zeta potential, can influence the amount and the mechanism of nanoparticle uptake into cells (Slowing, Trewyn et al. 2006). In

addition, the zeta potential of NPs in the environmental media influences particle agglomeration processes and thus the exposure to water-column species. Taken together, this implies that surface chemistry of NPs has compelling potential to dominate the fate and the toxicity of nanoparticles in the natural environment (Louie, Tilton et al. 2016).

The ever growing production and applications of AgNPs will inevitably result in release to aquatic environments raising ecological concerns (Blaser, Scheringer et al. 2008) (Mueller and Nowack 2008). There is minimal information available on the risks associated with AgNP surface functionalization to mixed aquatic communities. The median L(E)C<sub>50</sub> values of AgNPs to a number of aquatic species have been determined and were recently summarized in a review as 0.01 mg L<sup>-1</sup> for crustaceans; 0.36 mg L<sup>-1</sup> for algae; 1.36 mg L<sup>-1</sup> for fish; and the median minimum inhibitory concentration (MIC) for bacteria was 7.1 mg L<sup>-1</sup>; however, these studies constituted laboratory exposures with individual organisms to establish a baseline exposure-response relationship (Bondarenko, Juganson et al. 2013). Recently it has been reported that concentration-effect thresholds may be lower in more complex test systems (Bundschuh, Seitz et al. 2016). Significant impacts of AgNPs on lake bacterioplankton have been shown to occur at exposure concentrations higher than would be predicted based on laboratory studies. As such, it is quite difficult to extrapolate the findings from laboratory studies to aquatic risk in natural environments (Colman, Espinasse et al. 2014). Exposures conducted under environmentally relevant conditions, such as a community of organisms comprised of varied populations and trophic levels, can provide detailed information on organism responses to AgNP exposure, as well as the impacts on the community as a whole (Sheehan 1984).

Common AgNP toxicity mechanisms have been summarized as 1) the release of  $\text{Ag}^+$  from AgNPs; 2) the generation of reactive oxygen species (ROS) from AgNPs and  $\text{Ag}^+$ ; and 3) cell membrane damage caused by direct interaction with AgNPs (Hwang, Lee et al. 2008). Since one of the most important mechanisms of toxicity for AgNP is reportedly the release of  $\text{Ag}^+$  (Xiu, Zhang et al. 2012), changes in AgNP dissolution have the potential to alter Ag speciation and precipitation, and thus impact toxicity to aquatic organisms. Natural waters often have sufficient anions present in solution that can interact with NP released  $\text{Ag}^+$ . For example,  $\text{Cl}^-$  in a system could result in AgCl precipitation. Thus, understanding the potential speciation of silver following dissolution in the environmental media is critical to understanding the organismal exposure to  $\text{Ag}^+$ . Despite this knowledge, information on the environmental dissolution and subsequent risk of AgNPs to organisms within a community setting remains unclear. Large-scale mesocosm studies can provide more realistic information on ecosystem risk and interspecies trophic interactions; however, many environmental variables cannot be controlled and the amount of materials required to perform a study limits the ability to test across multiple concentrations and locations. Bour et al. recently reviewed 40 papers published on indoor (laboratory) or outdoor (field) experiments under environmentally relevant approaches to assess nanoparticle ecotoxicity; however, none of those studies investigated multi-species exposures at various levels of trophic complexity in a laboratory freshwater system (Bour, Mouchet et al. 2015). Thus, this study was designed to fill this data gap by assessing nanoparticle ecotoxicity to freshwater organisms and determining the impacts of community structure on organismal susceptibility using a microcosm approach.

Guidelines have been established for conducting aquatic microcosm assays, yet these approaches have not been commonly applied to nanomaterials as they are costly, time-consuming, require large quantities of nanomaterials, and generate large amounts of waste (ASTM 2011). To overcome these barriers, we developed small-scale microcosms (termed ‘nanocosms’) with organisms from multiple trophic levels and tested the impact of three different surface-coated AgNPs under different exposure scenarios. Nanocosms comprised of algae (*Chlamydomonas reinhardtii*) and bacteria (*Escherichia coli*) were compared to increasingly complex nanocosms comprised of algae, bacteria, predatory invertebrates (*Daphnia magna*) and developing vertebrates (*Danio rerio*). Test species were selected because they represent a broad spectrum of trophic levels and are accepted as good model organisms for aquatic toxicity testing, particularly for nanoparticles (Sondi and Salopek-Sondi 2004; Adams, Lyon et al. 2006; Harper, Usenko et al. 2008; Heinlaan, Ivask et al. 2008; Navarro, Piccapietra et al. 2008; Chen, Zhou et al. 2012; Perreault, Oukarroum et al. 2012; Colman, Arnaout et al. 2013). *C. reinhardtii* and *E. coli* were chosen to represent primary producers and decomposers, respectively. Both species have a simple life cycle, are inexpensive to maintain, are commonly found in aquatic environments and interspecific competition between the two species has been reported (Levy, Stauber et al. 2009). While bacteria and plankton compete with each other for resources, both serve as food for the secondary consumer *D. magna*. *D. magna* are small aquatic crustaceans ubiquitous in freshwater lotic environments and were included as a primary grazer of the microorganisms. *D. magna* are sensitive to chemical stressors and have long been utilized as an indicator species for assessing aquatic contamination (Warren 1900; Peltier, Weber et al. 1985; Bury, Shaw et al. 2002). Embryonic zebrafish were selected as an ideal developing

vertebrate model due to their rapid development, relatively high sensitivity to anthropogenic contaminants during development, transparency for visual observations, and well-studied sublethal endpoints elicited from NP exposures (Harper, Carriere et al. 2011). Although the embryonic zebrafish do not actively participate in the food web given the short timeframe of these studies, they are exposed to the microcosm contaminants throughout the experiment and following hatching, begin mouth-gaping behavior that can lead to oral ingestion of contaminants, despite not actively feeding. An illustration of the potential species interactions in the nanocosm is presented in Figure S5-1 of the supplementary information.

Nanocosms were exposed to 70 nm polyethylene glycol (PEG-AgNP), silica (Si-AgNP), and aminated silica-coated AgNP (Ami-Si-AgNP). These surface stabilizer coatings were selected as each is covalently bound to the particle, with PEG representing an organic chemical stabilizing shell and silica representing an inorganic stabilizing shell. The aminated silica shell was chosen to provide a cationic surface charge to the silica shell. These surface functionalities were predicted to alter the particle dissolution as well as to modify the surface charge, in order to determine the impacts of these features on uptake and toxicity to the organisms. Nanocosms comprised of algae (*C. reinhardtii*) and bacteria (*E. coli*) were compared to increasingly complex nanocosms comprised of algae, bacteria, predatory invertebrates (*D. magna*) and developing vertebrates (*D. rerio*).

Exposure models have predicted environmental concentrations of AgNPs in the ng L<sup>-1</sup> to µg L<sup>-1</sup> range, with higher concentrations being found locally around spills or locations where treatment plant effluent is released (Mueller and Nowack 2008; Gottschalk, Sun et al. 2013). In addition, estimated environmental concentrations have increased over the past years as the uses

of AgNPs expand (Sun, Gottschalk et al. 2014). Three concentrations were selected for our exposures to represent scenarios for 1) an environmentally relevant exposure representing the highest possible estimated concentration for fresh waters ( $0.1 \text{ mg L}^{-1}$ ), 2) a concentration that mimics a local spill or effluent concentrations ( $1 \text{ mg L}^{-1}$ ), and 3) a high concentration that is expected to elicit lethal responses in most of the studied species ( $5 \text{ mg L}^{-1}$ ) to allow for comparison of our results with the existing toxicological literature based on lethality (Bondarenko, Juganson et al. 2013). We hypothesized that the surface coating on AgNPs would dictate its toxicity through alterations in dissolution. In addition, varying community complexity was anticipated to alter individual organism responses to AgNP exposure due to potential changes in bioavailable Ag and interspecies interactions.

## 5.3 Materials and methods

### 5.3.1 Nanoparticles characterization

Three different surface modified silver nanoparticles, PEG-AgNP, Si-AgNP, and Ami-Si-AgNP, were purchased from nanoComposix (San Diego, CA) as BioPure suspensions (Figure 5-2). All three AgNPs were composed of the same Ag core with a primary particle size of 70 nm; however, the Si-Ag and Ami-Si-Ag had a 20 nm silica shell surrounding the core. The primary particle sizes measured by TEM were provided by nanoComposix (Figure S5-2). Hydrodynamic diameter (HDD) and zeta potential (ZP) were measured by dynamic light scattering (DLS) using a Zetasizer Nano ZS (Malvern Instruments, Worcestershire, UK) every 24 hours up to 120 hours at  $10 \text{ mg L}^{-1}$  particle concentration. Detailed parameters for ZP measurements are provided in

Table S1. HDD is defined as the size of a hypothetical hard sphere that diffuses in the same fashion as that of the particle being measured, and ZP as the electrostatic potential on the surface of hydrodynamic shear, measured as electrophilic mobility using DLS (ASTM 2012). HDD in both Milli-Q water (MQW) and exposure media, hereafter referred to as nanocosm media (NCM) was determined. ZP was measured only in NCM samples since Milli-Q water does not contain sufficient conductivity to accurately determine particle electrophoretic mobility (ASTM 2012; Lowry, Hill et al. 2016). All measurements were conducted in triplicate.

### 5.3.2 Preparation of exposure media

Nanocosm media (NCM) was prepared by mixing 50% of Taub's #36 solution (Taub and Dollar 1968) with 50% of 5 mM HEPES buffer (EMD Chemicals Inc., Gibbstown, NJ) and adjusting the pH to 7.2 with 0.1 M NaOH. Taub media was selected to minimize NP aggregation due to its low ionic strength and to optimize the growth of algae and daphnids. HEPES buffer was chosen due its compatibility as a biological buffer. Prior to experimentation, NCM was autoclaved at 120 °C for 20 minutes and then cooled to room temperature for use.

### 5.3.3 Test organisms

*C. reinhardtii* was purchased from the University of Texas Culture Collection (UTEX 2243 and 2244) and cultured in TAP media (Gorman and Levine 1965). *E. coli* was purchased from Carolina Biological Supply Company (MicroKwik culture, Burlington, NC, USA), and cultured in lysogeny broth (10 mg L<sup>-1</sup> tryptone, 5 mg L<sup>-1</sup> yeast extract, and 10 mg L<sup>-1</sup> sodium



chloride) on a shaker at 37 °C. *D. magna* were cultured in modified International Organization for Standardization (ISO, 2012) media, consisting of calcium chloride (195.87 mg L<sup>-1</sup>), magnesium sulfate (82.20 mg L<sup>-1</sup>), sodium carbonate (64.80 mg L<sup>-1</sup>), potassium chloride (5.80 mg L<sup>-1</sup>) and sodium selenite (0.002 mg L<sup>-1</sup>). *D. rerio* embryos were collected from group spawns of adult wild-type zebrafish maintained at the Sinnhuber Aquatic Research Laboratory (SARL) at Oregon State University. Embryos were staged to ensure uniform age of 8 hours post-fertilization (hpf) at the beginning of the experiment (Kimmel, Ballard et al. 1995). All organisms and experiments were maintained and conducted at 20.5 ± 0.5 °C with a 16:8-h light:dark photoperiod under 1690 ± 246 lux light intensity provided by full-spectrum fluorescent grow lights.

#### 5.3.4 Experimental design

*C. reinhardtii* were inoculated into 50 ml Falcon® vented tissue culture flasks (Fisher Scientific, Pittsburgh, PA) at a starting density of ~2×10<sup>4</sup> cells mL<sup>-1</sup> to avoid any effect of the initial cell density on measured growth rates (Franklin, Stauber et al. 2002). *D. magna* neonates (<24 hours old) were collected from the stock culture and placed in NCM for a 24 hour acclimation period prior to toxicity testing. After 24 hours of incubation, *E. coli* inoculates were added to the flasks at a density of 5×10<sup>5</sup> cells mL<sup>-1</sup>. Initial algal and bacterial cell densities were quantified using an Accuri C6 flow cytometer (BD Biosciences, San Jose, CA) to ensure consistent densities at the start of the experiment. Five NCM-acclimated daphnid neonates (24 – 48 hours life stage) and eight zebrafish embryos (8 hpf) were introduced into corresponding flasks to sequentially increase community complexity. Triplicate flasks were prepared for each

community exposure scenario and exposed to 0, 0.1, 1 or 5 mg L<sup>-1</sup> of each of the three types of AgNPs. The total volume of each flask was adjusted to 15 mL, leaving approximately 35 cc of headspace to allow for ventilation through the filter cap. Vented caps were used to equalize the air pressure inside and outside the container and prevent contamination from airborne particles and microbes. A dissolved oxygen meter with a micro-oxygen electrode (Lazar Research Laboratories, Inc., Los Angeles, CA) was used to measure the dissolved oxygen at the end of the experiment in each exposure flask. All experiments were performed in compliance with national and university care and use guidelines regarding the use of live organisms

#### *5.3.5 Toxicity evaluations*

Algal and bacterial viability was measured using SYTOX Green dead cell stain (Life Technologies, Grand Island, NY) in conjunction with flow cytometry every 24 hours for the remainder of the experiment. Live and dead cell counts were determined by collecting 200 µL of sample from each exposure flask and adding 0.2 µL SYTOX green dead cell stain to each sample. Samples were incubated in the dark for 15-20 minutes prior to being analyzed by flow cytometry. *D. magna* mortality was recorded daily. Dead daphnia and zebrafish were removed from the nanocosm at the end of the experiment and were not used for Ag uptake analysis. At the end of the 120 hour experimental period, live daphnids were removed from the experimental flasks and imaged using an Olympus SC100 high-resolution digital color camera (Olympus Corporation, Center Valley, PA). Zebrafish embryo hatching rate and mortality were monitored daily. At the end of the five-day exposure, zebrafish embryos were examined under a dissecting microscope for malformations (body axis, brain, heart, eyes, fins, jaw, trunk, and somite),

physiological abnormalities (pigmentation, impaired circulation, pericardial edema, and yolk sac edema), and the presence of a touch response. Zebrafish developmental stage at our experimental temperature was corrected using equation 5.1:

$$H_T = \left( \frac{h}{0.055T - 0.57} \right) \quad (\text{equation 5.1})$$

where  $H_T$  represents the hours of development at temperature  $T$ , and  $h$  represents the hours of development to reach that stage at 28.5 °C (Kimmel, Ballard et al. 1995).

### *5.3.6 Measurement of AgNP dissolution, uptake and dissolved Ag concentrations*

Nanoparticle dissolution in the NCM was measured by collecting 1 mL of a 1 mg L<sup>-1</sup> suspension of each type of AgNP at 0 hours and repeated daily up to 120 hours (without organisms present). To measure dissolved Ag in the exposure media when organisms were present, a 1 ml aliquot of exposure media was collected at the end of the toxicity experiments. Nanocosms were gently agitated prior to sampling to resuspend any settled NPs, then a 1 ml sample was collected from each replicate nanocosm flask. All samples were centrifuged at 20,000×g for 60 minutes to pellet undissolved particles. After centrifugation, 0.2 ml of the supernatant was transferred to a polystyrene tube and stored at -4 °C until sample digestion was performed. Ag uptake by organisms was measured following toxicological observations at the end of the experiment. Individual daphnids and zebrafish were rinsed three times with Milli-Q water to remove loosely attached algae, bacteria, and particles. Unhatched zebrafish were dissected to remove the chorionic membrane. Chorionic membranes, zebrafish embryos, and daphnids were stored at -4 °C in polystyrene tubes until acid digestion was performed to prepare

the samples for inductively coupled plasma mass spectrometry (ICP-MS) analysis of silver content.

Samples were thawed and digested in teflon tubes at 200 °C with 3 ml 70% trace-metal grade nitric acid (Kim, Truong et al. 2013). Once the acid had completely evaporated, the acidification and evaporation process was performed two more times. Trace-metal grade nitric acid (0.3 ml) was added to each teflon tube while the tube was still hot, followed by 4.7 ml Milli-Q water, bringing the final sample volume to 5 ml. Samples with a 3% nitric acid final proportion and 1  $\mu\text{g L}^{-1}$  internal indium standard were analyzed for dissolved Ag concentration by ICP-MS (Thermo Fisher Scientific, Waltham, MA). Silver and indium ICP standards were purchased from Ricca Chemical Company (Arlington, TX). All samples were measured in triplicate. Digestion efficiency was verified, with 100% recovery of Ag from each type after acid digestion (Table S2). *D. magna* mean dry mass was obtained from the mean weight of 6 groups of daphnids (each group containing 10 daphnids). Zebrafish dry mass was estimated based on work by Hachicho et al. 2015, using the normalized development at the experimental temperature of 20.5 °C (Hachicho, Reithel et al. 2015). Further, Ag speciation and complexation was estimated using the mean measured dissolved Ag concentration from each exposure using Visual MINTEQ 3.1 (downloaded from <https://vminteq.lwr.kth.se/>). Equilibrium was assumed and cerargyrite (AgCl) was added as a possible solid formed.

### 5.3.7 Data analysis

Algal and bacterial growth rates were modelled using a three parameter logistic model in equation 5.2:

$$M = \frac{k}{(1 + (\frac{k}{M_0 - 1})) \times e^{-rt}} \quad (\text{equation 5.2})$$

where  $r$  is the specific growth rate ( $\text{h}^{-1}$ ),  $t$  is the time (hr),  $k$  represents the maximum capacity of cells,  $M_0$  is the initial cell counts at  $t = 0$ , and  $M$  represents the cell count at  $t = t$  (Paine, Marthews et al. 2012). Algal and bacterial survival was corrected using equation 5.3 to compensate for possible differences in the surviving proportion of organisms occurring post-treatment:

$$\text{Corrected survival \%} = \left( \frac{n_{Cb} \times n_{Ta}}{n_{Ca} \times n_{Tb}} \right) \times 100 \quad (\text{equation 5.3})$$

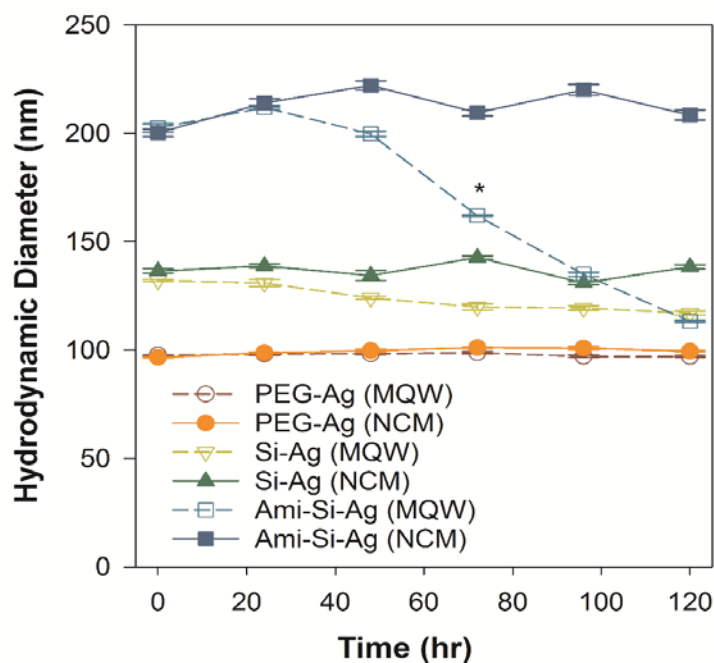
where  $n_C$  is the survival proportion (live cell/total cell) in the control group,  $n_T$  is the survival proportion in the treatment group, and  $a$  and  $b$  designate after and before treatment, respectively (Henderson and Tilton 1955). SigmaPlot version 13.0 (Systat Software, San Jose, CA, USA) was used to perform statistical analyses. The corrected algal and bacterial cell mortality in the presence of nanoparticles were compared to control responses using a Kruskal-Wallis rank sum test followed by a Tukey post-hoc test. The growth rates of algae and bacteria were calculated in SAS 9.3 (SAS Institute, Cary NC) using a sigmoid growth model (Gauss-Newton method) (Nyholm and Källqvist 1989). *D. magna* survival among the control and treatments was compared using a two-way ANOVA with a Tukey post-hoc test. Developmental abnormalities in zebrafish were compared between treatments and the corresponding controls using a Fisher's exact test. Dissolved Ag concentration of each AgNP in NCM and exposure vessels were

compared using a simple linear regression model in R version 3.1.2 (Team. 2014). All differences were considered statistically significant at  $p \leq 0.05$  for all analyses.

## 5.4 Results

### 5.4.1 Nanoparticle characterization

All three AgNPs formed small agglomerates, which remained stable over the 120 hour exposure period (Figure 5-1). In Milli-Q water, PEG–Ag had the smallest HDD ( $97.9 \pm 0.3$  nm), followed by the Si–Ag ( $124.0 \pm 2.6$  nm), and Ami–Si–Ag had the greatest HDD ( $170.7.4 \pm 16.5$  nm). Similar results were found in NCM, with PEG–Ag having the smallest HDD ( $99.4 \pm 0.7$  nm), followed by the Si–Ag ( $137.0 \pm 1.6$  nm), and Ami–Si–Ag still having the greatest HDD ( $212.4 \pm 3.3$  nm). There was no significant change in HDD over time in either media, except for the Ami–Si–Ag in Milli-Q water, which showed a significant decrease in size after 48 hours. The measured HDDs and the corresponding polydispersity index (PDI) were provided in the Table S3. Different ZP ranges were observed for the three AgNPs in NCM, with PEG–Ag being close to neutral initially ( $-3.7 \pm 0.2$  mV), Ami–Si–Ag having a positive zeta potential ( $12.7 \pm 0.2$  mV), and Si–Ag being negative ( $-15.2 \pm 0.3$  mV) (Fig. S3). Ami–Si–Ag was the only particle to show a significant change in ZP over time, increasing to  $26.3 \pm 0.4$  at 48 hours then remaining relatively constant for the duration of the experiment.



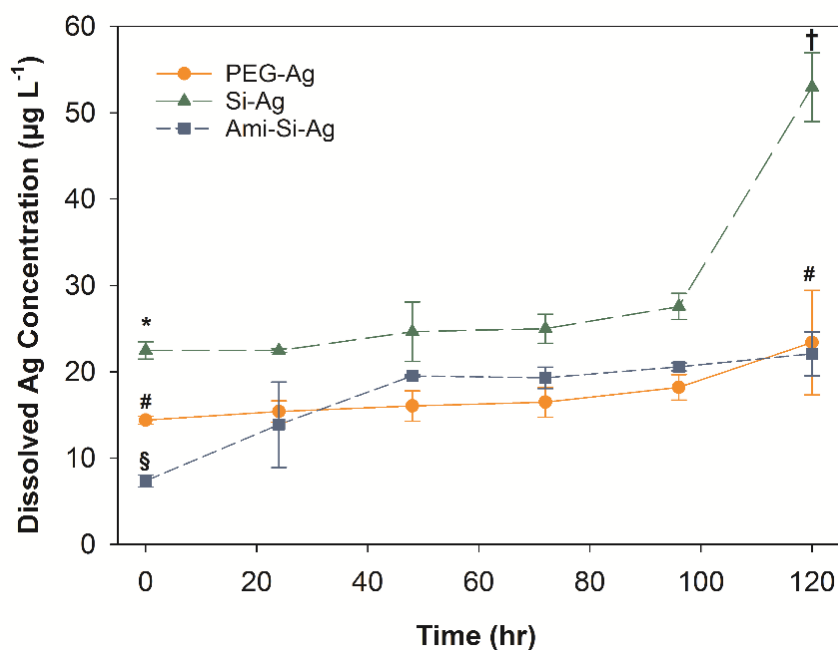
**Figure 5-1.** a) Hydrodynamic diameter (HDD) and b) zeta potential (ZP) of PEG-Ag (solid line orange circle), Si-Ag (solid line green triangle – face up), and Ami-Si-Ag (blue square with solid line) in NCM over 120 hours at  $10 \text{ mg L}^{-1}$ . PEG-Ag in dash line red circle, Si-Ag in yellow triangle – face down with dash line, and Ami-Si-Ag with dash line blue unfilled square represents the HDD of the same particles measured in MQW. Standard errors were derived for triplicate measures on each AgNP. Asterisk (\*) indicates a significant change in HDD from initial measurements at time 0, and octothorpe (#) represents a change in zeta potential from time 0.

## 5.4.2 Nanoparticle dissolution

### 5.4.2.1 Dissolution in NCM

The dissolved Ag concentration resulting from the dissolution of each AgNP ( $1 \text{ mg L}^{-1}$ ) in NCM was measured daily (Figure 5-2). The AgNPs generally had low dissolution rates in the NCM, with 2.4 %, 5.3 %, and 2.2% dissolved Ag based on the  $1 \text{ mg L}^{-1}$  nominal exposure concentration for PEG, Si, and Ami-Si AgNP after 120 hours, respectively. Si-Ag had the highest initial dissolved Ag concentration ( $22.4 \pm 1.0 \mu\text{g L}^{-1}$ ), followed by PEG-Ag ( $14.4 \pm 0.47$

$\mu\text{g L}^{-1}$ ), while Ami-Si-Ag had the lowest ( $7.3 \pm 0.7 \mu\text{g L}^{-1}$ ) initial concentration. PEG-Ag and Ami-Si-Ag showed similar dissolution trends over time. After 120 hours, the dissolved Ag concentration for PEG-Ag increased to  $23.4 \pm 6.1 \mu\text{g L}^{-1}$ , and Ami-Si-Ag increased to  $22.1 \pm 2.5 \mu\text{g L}^{-1}$ ; however, dissolved Ag from Si-Ag remained higher than the other AgNPs over time, with the final concentration being two-fold higher than the PEG-Ag and Ami-Si-Ag particles ( $53.0 \pm 4.0 \mu\text{g L}^{-1}$ ).

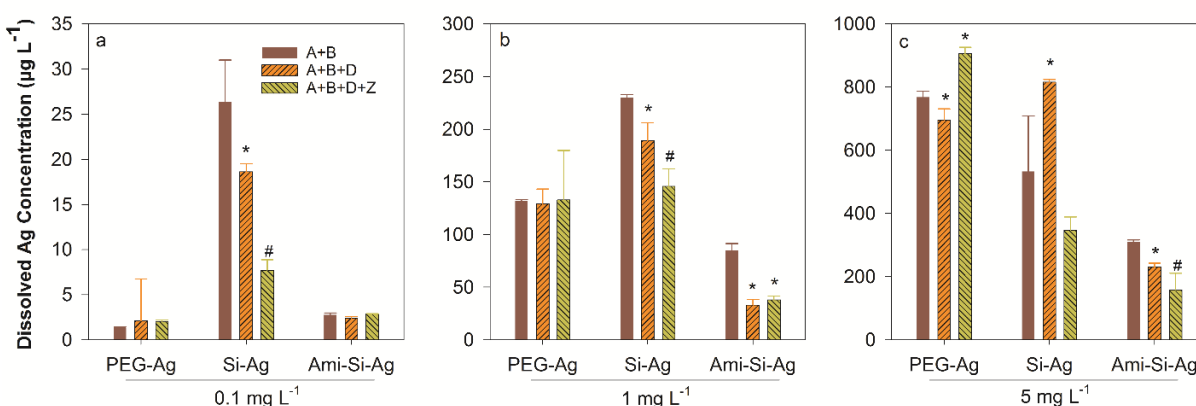


**Figure 5-2.** Dissolution of PEG (circle), Si (triangle), and Ami-Si (square) coated AgNPs at  $1 \text{ mg L}^{-1}$  in NCM over 120 hours. Symbols (\*, #, §) indicate significant differences in dissolved Ag among three AgNPs at 0 and 120 hours. Symbol † represents significantly higher dissolved Ag in Ami-Si-Ag compared to other two AgNPs after 120 hours. Error bars represent the standard error derived from three sample replicates

#### 5.4.2.2 Quantification of dissolved Ag in nanocosm experiments



Dissolved Ag concentration was measured in each exposure scenario at the end of the experiment to determine the influence of the organisms on available dissolved Ag concentrations (Figure 5-3). By comparing the concentrations in Figure 5-3b with the dissolved Ag concentration in Figure 5-2, the 120 hour dissolved Ag concentration for all three AgNPs were significantly enhanced compared to the dissolved Ag in the abiotic environments at 1 mg L<sup>-1</sup>. Both PEG-Ag and Si-Ag had significantly higher dissolved Ag concentrations than Ami-Si-Ag at 1 and 5 mg L<sup>-1</sup> exposure concentration in all three exposure scenarios. Si-Ag also had the highest dissolved Ag concentration at 0.1 mg L<sup>-1</sup> exposure concentration. In addition, the dissolved Ag concentration from PEG-Ag did not change with an increase in community complexity, whereas the dissolved Ag concentration was highly dependent on the community complexity. Increasing community complexity significantly decreased the dissolved Ag concentration at 0.1 and 1 mg L<sup>-1</sup> Si-Ag exposures, but a similar trend was not observed at 5 mg L<sup>-1</sup>. In Ami-Si-Ag, enhanced dissolved Ag concentration was observed in the algae and bacteria exposure scenario and decreased in both 1 and 5 mg L<sup>-1</sup> with increasing community complexity, and the dissolved Ag from PEG-Ag changed significantly and was depended on community complexity at 5 mg L<sup>-1</sup>. In Ami-Si-Ag, enhanced dissolved Ag concentration was observed in the algae and bacteria exposure scenario and decreased in both 1 and 5 mg L<sup>-1</sup> with increasing community complexity, and the dissolved Ag from PEG-Ag changed significantly and was dependent on community complexity at 5 mg L<sup>-1</sup>. Ag speciation calculations using measured dissolved Ag concentrations are presented in Table S5. Dissolved Ag concentration measured at 1 and 5 mg L<sup>-1</sup> predict a high percentage of Ag precipitates (cerargyrite), but at 0.1 mg L<sup>-1</sup> all dissolved forms of Ag should preferentially form aqueous complexes.



**Figure 5-3.** Dissolved Ag concentration in NCM after 120 hours with 0.1 mg L<sup>-1</sup> (a), 1 mg L<sup>-1</sup> (b), 5 mg L<sup>-1</sup> (c) AgNP exposures under three different community exposure scenarios (algae and bacteria, A+B: red; algae, bacteria and daphnia, A+B+D: orange; and algae, bacteria, daphnia and zebrafish, A+B+D+Z: dark yellow). Octothorpe (#) indicates a significant difference among exposure scenarios within the same AgNP. Asterisk (\*) indicates significant difference compared to the corresponding A+B exposure scenarios. Error bars represent the standard error derived from the mean of three sample replicates.

### 5.4.3 Toxicity of AgNPs

#### 5.4.3.1 Algae + Bacteria (A+B) exposure scenarios

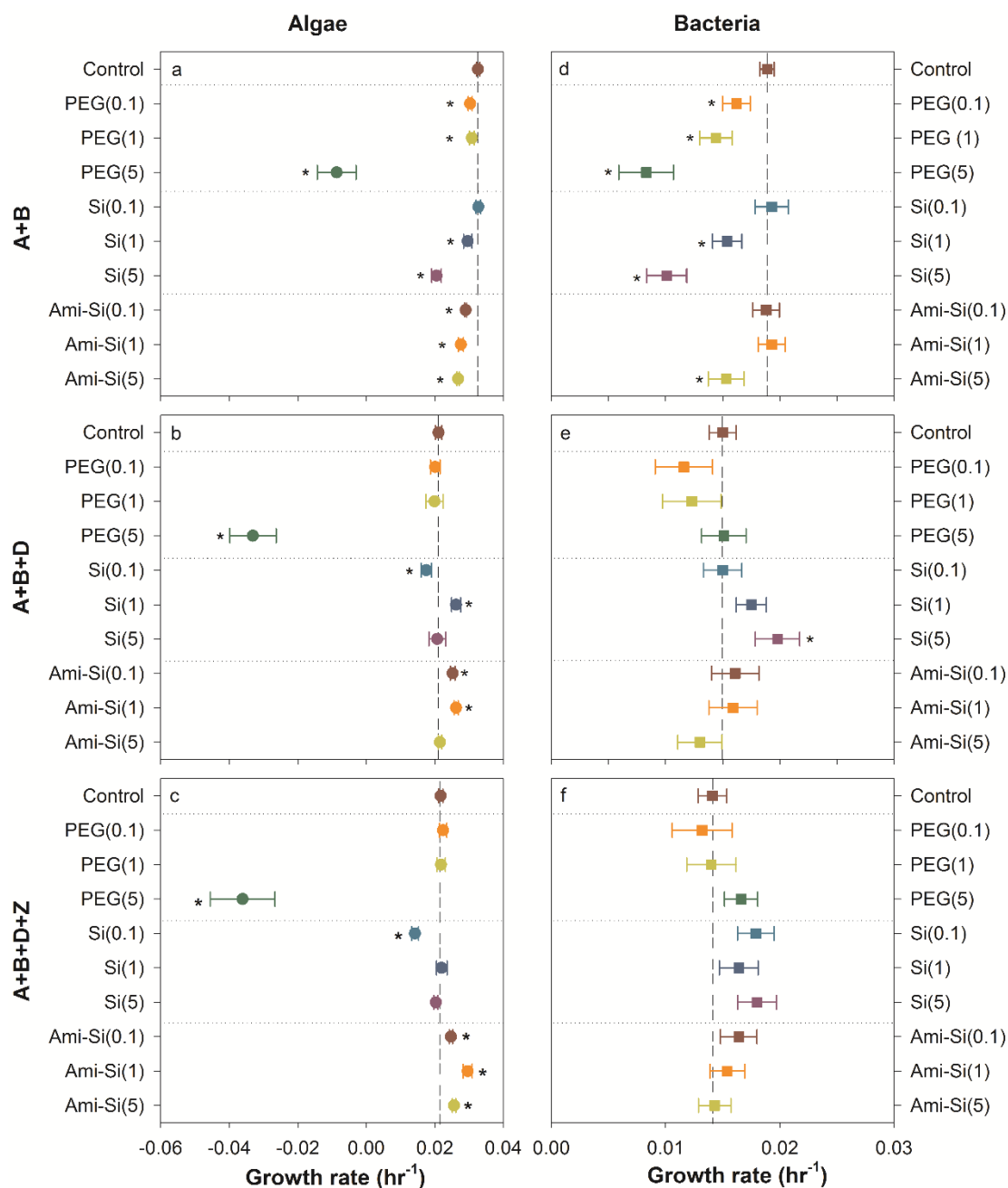
##### 5.4.3.1.1 Algal responses

Calculated algal population growth rates based on the number of live cells at 120 hours are shown in Figure 5-4a. There was a significant concentration-dependent decrease in algal growth rates with each of the tested AgNPs. By cross comparing the three different coated AgNP exposures at 5 mg L<sup>-1</sup>, PEG-Ag showed the largest effects on algae growth rate, followed by Si-Ag and Ami-Si-Ag. Algal survival was normalized by taking into account the relative control cell survival using equation 5.2 and is presented over the 120 hours experimental period in Figure S5-4 and normalized survival at 120 hour is presented in Figure 5-5. PEG-Ag exposed algae showed \100% cell mortality after 72 hours at 5 mg L<sup>-1</sup> exposures (Figure S5-4). The Si-Ag

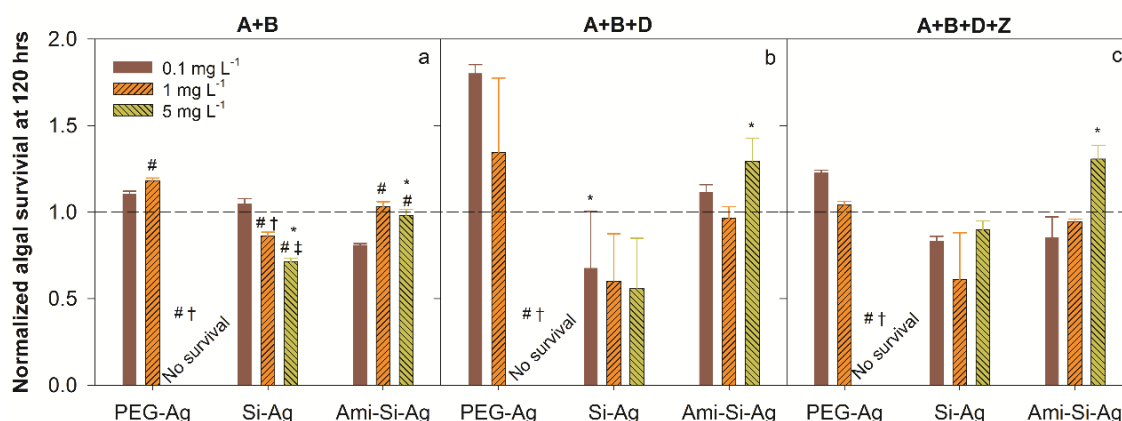
was less toxic to algae compared to PEG-Ag; however, it still significantly decreased algal survival compared to control, but the population recovered after 48 hours. Ami-Si-Ag did not inhibit algal growth in the A+B exposures (Figure S5-4 and Figure 5-5, panel a), but did in the more complex exposure scenarios (see sections 3.3.2.1. and 3.3.3.1).

#### 5.4.3.1.2 Bacterial responses

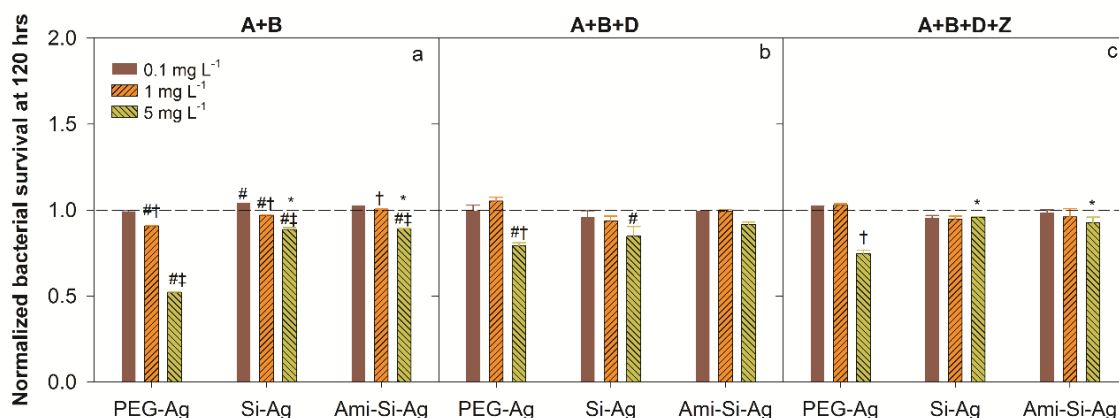
Similar to algae, bacteria also showed concentration dependent growth inhibition in all three AgNP exposures (Figure 5-4d). All three PEG-Ag concentrations significantly inhibited bacterial growth rates, and Si-Ag treated samples had significant lower growth rates at 1 and 5 mg L<sup>-1</sup> exposures compared to the control, whereas Ami-Si-Ag only showed significant inhibition at 5 mg L<sup>-1</sup>. Normalized bacterial survival in each exposure scenario over the 120 hour experiment is provided in Figure S5-4. The 120 hour normalized survival of bacteria in PEG-Ag exposure at 5 mg L<sup>-1</sup> was nearly 50% lower than the control (Figure 5-6). Taken together, the results suggest that all three AgNPs were toxic to bacteria at a high exposure concentration (5 mg L<sup>-1</sup>), but PEG-Ag and Si-Ag were more toxic to bacteria than Ami-Si-AgNP.



**Figure 5-4.** 120 hour growth rates of algae (panels a, b, c) and bacteria (panels d, e, f) under three different exposure scenarios: algae and bacteria (A+B), algae, bacteria and daphnia (A+B+D), and algae, bacteria, daphnia and zebrafish (A+B+D+Z). Error bars represent the standard error among sample replicates. Asterisk (\*) indicates significant differences compared to control growth. The vertical reference lines indicate control growth rates, and the horizontal reference lines separate the type of AgNP exposures.



**Figure 5-5.** Algal survival at 120 hours after normalized based on control in a) A+B; b) A+B+D; and c) A+B+D+Z exposure scenarios. The dashed line is the normalized control algal survival. ANOVA on ranks (Tukey post-hoc test) was used to compare the difference among the exposures and the controls (symbol #), and different concentrations (symbol † and ‡). Two-way ANOVA was used to compare among difference NP coatings at the same concentration with PEG as the reference (\*). A significance level of  $p \leq 0.05$  was maintained for all analyses.



**Figure 5-6.** Bacterial survival at 120 hours normalized based on control survival in a) A+B; b) A+B+D; and c) A+B+D+Z exposure scenarios. The dashed line is the normalized control bacterial survival. ANOVA on ranks (Tukey post-hoc test) was used to compare the difference among the exposures and the controls (symbol #), and different concentrations (symbol † and ‡). Two-way ANOVA was used to compare among difference NP surfaces at the same concentration with PEG as the reference (\*). A significance level of  $p \leq 0.05$  was maintained for all analyses.

### 5.4.3.2 Algae + Bacteria + *Daphnia* (A+B+D) exposure scenarios

#### 5.4.3.2.1 Algal response

When predatory *D. magna* were added to the community (A+B+D), the control algal growth rate was significantly lower compared to the control in A+B scenario (Figure 5-4a & b). Similar to the A+B exposures, a negative growth rate was observed for PEG-Ag exposures at 5 mg L<sup>-1</sup> compared to corresponding control, but no significant effects were observed at 0.1 and 1 mg L<sup>-1</sup> exposure concentrations. Si-Ag significantly affected algal growth at 0.1 and 1 mg L<sup>-1</sup>, but had no effect on algal growth at 5 mg L<sup>-1</sup>. Ami-Si-Ag exposure significantly increased algal growth at 0.1 and 1 mg L<sup>-1</sup>, but had no effect at the 5 mg L<sup>-1</sup>. Only 5 mg L<sup>-1</sup> PEG-Ag exposure showed significantly lower normalized algal survival compared to the control (Figure 5-5b), with Si-Ag and Ami-Si-Ag failing to elicit any significant impacts on algal survival.

#### 5.4.3.2.2 Bacterial response

Among the three AgNPs, only Si-Ag elicited significant impacts on bacterial growth rate. Si-Ag exposures significantly increased growth rates at 5 mg L<sup>-1</sup> but remained unchanged at the lower exposure concentrations (Figure 5-4e). However, the normalized bacterial survival reveals that both PEG-Ag and Si-Ag exposures at 5 mg L<sup>-1</sup> showed decreased bacteria survival compared to the control (Figure 5-6). After 120 hours, PEG-Ag elicited the strongest anti-bacterial effects, which showed 20% lower bacterial survival at 5 mg L<sup>-1</sup>. Si-Ag also significantly decreased bacterial survival at 5 mg L<sup>-1</sup> but only by 15% after 120 hours.

#### 5.4.3.2.3 *Daphnid response*

Daphnid survival during the AgNP exposures is presented in Figure 5-7 (a, c & e). PEG-Ag caused 100% mortality after 48 hours of exposure to 5 mg L<sup>-1</sup>. Si-Ag elicited significant mortality at both 1 and 5 mg L<sup>-1</sup> with rapid mortality being observed after 10 minutes of exposure to 5 mg L<sup>-1</sup>. Interestingly, Ami-Si-Ag did not elicit significant mortality at any test concentration, but a brownish color was observed in the gut and thoracopods at 5 mg L<sup>-1</sup> (Figure S5-6). After quantification with ICP-MS, *Daphnia* silver uptake was calculated (Table 1). The uptake concentration is considered to be the total Ag tightly adsorbed on the carapace, ingested, and/or internalized in the daphnid. With increased exposure concentration, there was a corresponding increase in silver accumulated in daphnids bodies, with *D. magna* having an almost 20 fold increase in uptake following 5 mg L<sup>-1</sup> exposures relative to 1 mg L<sup>-1</sup> Ami-Si-Ag exposures.

#### 5.4.3.3 Algae + Bacteria + *Daphnia* + Zebrafish (A+B+D+Z) exposure scenarios

##### 5.4.3.3.1 *Algal response*

The control algal growth rate was similar to the control in the A+B+D exposure scenario (Figure 5-4b&c). PEG-Ag exposure still elicited significant toxicity on algae by inhibiting the growth rate at 5 mg L<sup>-1</sup> but not at lower exposure concentrations. Si-Ag significantly inhibited growth at 0.1 mg L<sup>-1</sup>, but not at 1 and 5 mg L<sup>-1</sup> compared to control algal growth rates. All Ami-Si-Ag exposure concentrations significantly enhanced the growth rate of algae. No algae survived after 72 hours with PEG-Ag exposure at 5 mg L<sup>-1</sup> (Figure S5-4); however, there was no impact on algal survival in any of the other concentrations (Figure 5-5c).

#### 5.4.3.3.2 Bacterial response

The control bacterial growth rate was similar to the control rate in the A+B+D scenario (Figure 5-4f); however, unlike the other exposure scenarios, there was no significant difference for bacterial growth rate among treatments at any of the tested exposure concentrations. For normalized bacterial survival at 120 hours, PEG-Ag still significantly decreased bacterial survival by about 20% relative to control (Figure 5-6), but no other exposures showed impacts on bacterial survival after 120 hours of exposure.

#### 5.4.3.3.3 Daphnid response

Daphnid responses with zebrafish present were similar to those responses in the A+B+D scenario (Figure 5-7b, d & f). Si-Ag was still lethal to daphnids immediately after the exposure at 5 mg L<sup>-1</sup>, while PEG-Ag showed significantly lower survival only after 48 hours. Ami-Si-Ag again showed the highest accumulation at 5 mg L<sup>-1</sup> (Table 5-1, Figure S5-6), but the accumulation of Ag did not cause significant mortality to daphnids at that concentration.

#### 5.4.3.3.4 Zebrafish response

PEG-Ag resulted in 100% zebrafish mortality after 72 hours at 5 mg L<sup>-1</sup>, but none of the other exposures resulted in significant mortality (Figure S5-7), suggesting that PEG-Ag was the most toxic AgNP to embryonic zebrafish. In addition, all controls and exposures showed 100% hatching except the Si-Ag exposures at 5 mg L<sup>-1</sup>, which only had a hatching rate of 40 % (Figure 5-8). A significant proportion of fish with one or more sub-lethal malformations were observed at 1 and 5 mg L<sup>-1</sup> Si-Ag exposure, and 5 mg L<sup>-1</sup> Ami-Si-Ag exposure (Figure 5-9). Yolk sac



edema, pericardial edema, and disrupted blood circulation were the specific sub-lethal effects we observed, but were not individually significant at any exposure concentration (Figure S5-7).

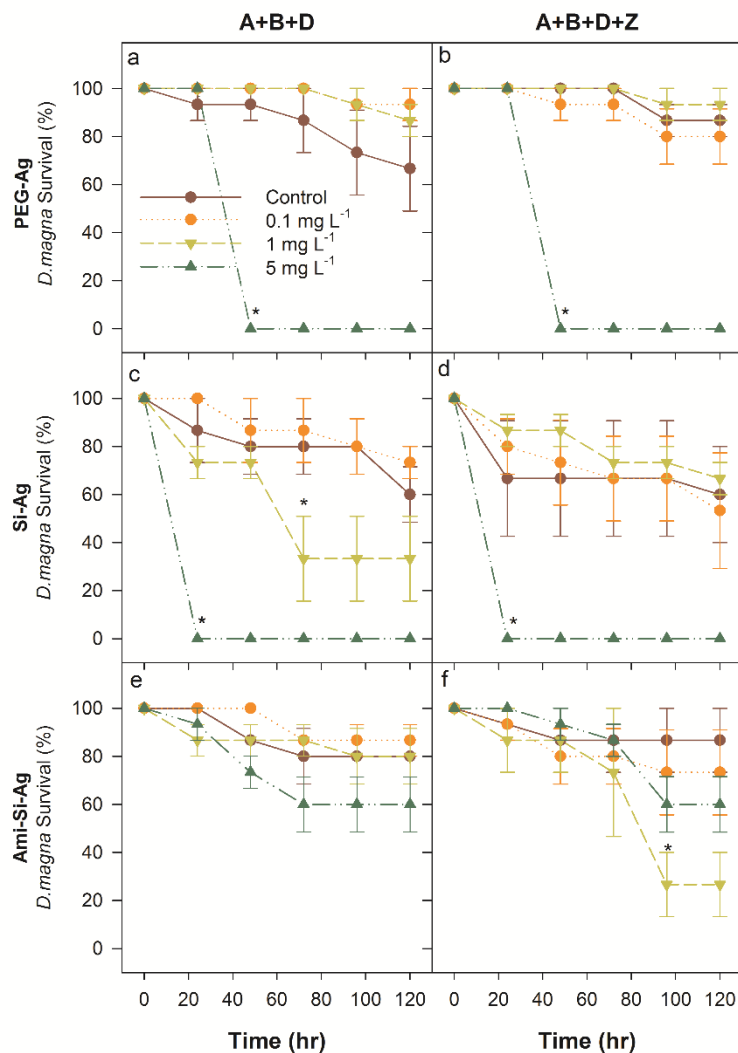
The amount of Ag in daphnids from the same exposure flask was 20 to 38238 times higher on a per mass basis than in zebrafish (Table 5-1). The uptake concentration measured in hatched zebrafish was close to the ICP-MS detection limits with all three types of AgNPs, indicating low Ag uptake by zebrafish. However, high Ag content was measured in Si-Ag exposed zebrafish (unhatched) at 5 mg L<sup>-1</sup>. By separating chorion from the unhatched fish from Si-Ag exposure, the result showed less than 4% of the Ag content in the zebrafish body while nearly 96% was retained by the chorion (Figure S5-8).

**Table 5-1.** Summary of AgNPs uptake in individual daphnids and zebrafish in algae, bacteria and daphnia (A+B+D) and algae, bacteria, daphnia and zebrafish (A+B+D+Z) exposure scenarios after 120 hours. The ratio indicates the quantitative relationship of Ag taken up by Daphnia and zebrafish within the same exposure flask. N/A indicates unavailable to measure due to animal mortality, and \* indicates the zebrafish showed delayed hatching and remained inside chorion after 120 hours. Standard deviations from machine replicates were below 10<sup>-3</sup> µg g<sup>-1</sup>.

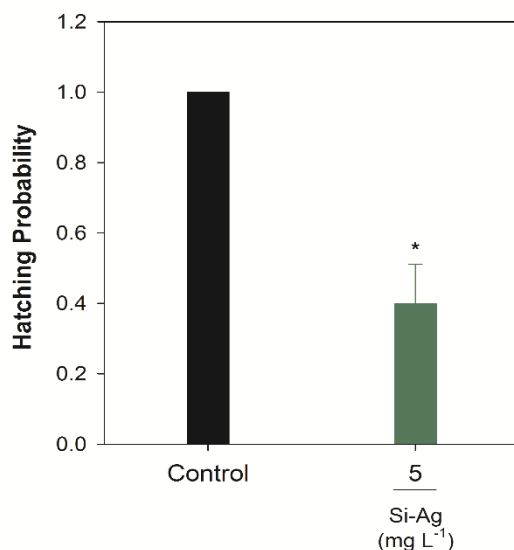
AgNP	Concentration (mg L <sup>-1</sup> )	A+B+D	A+B+D+Z		
		Daphnid (µg g <sup>-1</sup> )	Daphnid (µg g <sup>-1</sup> )	Zebrafish (µg g <sup>-1</sup> )	Ratio
PEG-Ag	0.1	6.3	6.4	0.080	80
	1	50.2	99.8	0.150	665
	5	N/A	N/A	N/A	N/A
Si-Ag	0.1	13.2	4.8	0.24	20
	1	37.8	140.1	2.4	58
	5	N/A	N/A	*	N/A
Ami-Si-Ag	0.1	14.7	8.1	0.065	125
	1	45.8	17.7	0.34	52
	5	797.5	611.8	0.016	38238

#### 5.4.4 Dissolved Ag concentration – response relationship

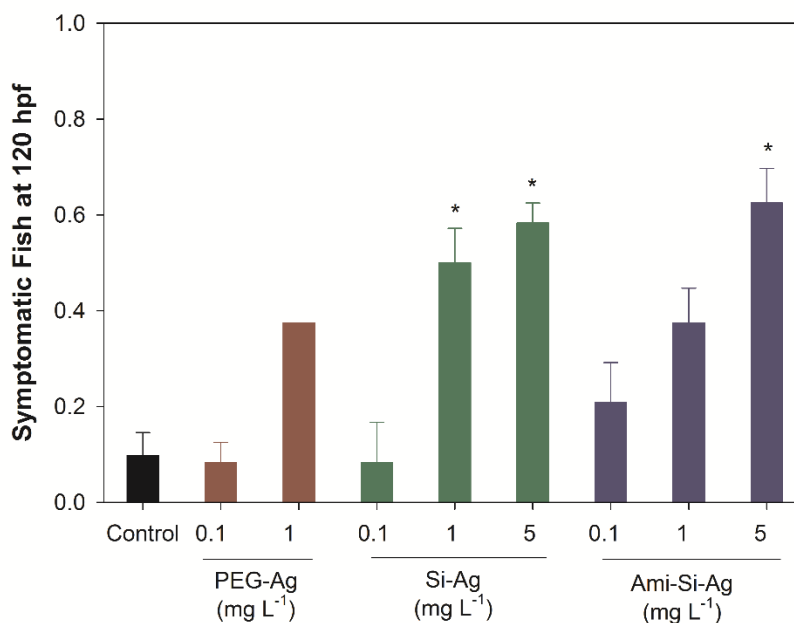
The relationship between total Ag taken up by both *D. magna* and zebrafish relative to the dissolved Ag concentration measured in the A+B+D and A+B+D+Z nanocosm reveals that there was a trend towards increasing uptake in *Daphnia* with increased dissolved Ag concentration; however, this trend did not exist with respect to the exposed zebrafish (Figure S9). Estimated LC<sub>50</sub> values were calculated at the end of each exposure nanocosm against the proportion of lethal responses (Figure S10-S13, Table 2). The calculated mean LC<sub>50</sub> values were fit to a species sensitivity distributions (SSDs) model (Stephan 2002; Kwak, Cui et al. 2016), which identified *D. magna* as the most sensitive species to AgNPs/Ag<sup>+</sup> exposure in the nanocosm system, followed by zebrafish, algae and bacteria, respectively (Figure S5-14). This result is consistent with the relative sensitivity of AgNP/Ag<sup>+</sup> to variety of species from literature (Bondarenko, Juganson et al. 2013).



**Figure 5-7.** *Daphnia* survival following exposure to PEG-Ag, Si-Ag, and Ami-Si-Ag in algae, bacteria and daphnia (A+B+D) (Panel a, c, e), and algae, bacteria, daphnia and zebrafish (A+B+D+Z) (Panel b, d, f) community exposure scenarios. Error bars represent the standard error among sample replicates. Asterisk (\*) indicates the time point after which there is a significant difference from control response.



**Figure 5-8.** Hatching probability of zebrafish in control and Si-Ag exposure at 5 mg L<sup>-1</sup>. Error bars represent the standard error among sample replicates. Asterisk (\*) indicates significantly lower hatching probability compared to control.



**Figure 5-9.** The proportion of symptomatic fish (number of symptomatic fish / total number of live fish) following AgNP exposures. Error bars represent the standard error among sample

replicates. Asterisk (\*) indicates statistical difference compared to control with one-way ANOVA test ( $p \leq 0.05$ ).

**Table 5-2.** The calculated  $LC_{50}$  of each species using the dissolved silver concentration measured in each exposure nanocosm.

Species	$LC_{50}$ Mean ( $\mu\text{g L}^{-1}$ )	SE ( $\mu\text{g L}^{-1}$ )
<i>Chlamydomonas reinhardtii</i>	605	38
<i>Escherichia coli</i>	903	171
<i>Daphnia magna</i>	220	38
<i>Danio rerio</i>	434	82

## 5.5 Discussion

### 5.5.1 Exposure characterization

In this study, we compared the dissolution and toxicity of AgNPs with varied surface coatings in nanocosms with differing community complexity. Surface coating played a dominant role in the zeta potential measured in the NCM. Despite low zeta potential indicating a high potential for particle agglomeration (Letterman 1999), all three surface coatings stabilized the AgNPs, either by repulsion force or steric hindrance, and minimized the particle agglomeration in the exposure media. The relatively small and consistent HDDs over time suggests that the NPs were well-dispersed in the exposure media. Although the initial HDD of Ami-Si-Ag NPs were similar in both MQW and NCM, the size of agglomerates significantly decreased over the 5 days

in MQW but not NCM. Although the initial HDD of Ami-Si-Ag NPs were similar in both MQW and NCM, the size of agglomerates significantly decreased over the 5 days in MQW but not NCM. The large initial HDD of the aminated particles in both MQ water and NCM suggests the cationic charge was not sufficient to prevent agglomeration. Agglomerates that formed in the NCM appear to be stabilized by the ions in the media; whereas, in MQ water aggregate stability decreased over time such that by 120 hours the HDD was comparable to primary size and the AgNPs with other surface coatings (Figure 5-1).

The small HDD differences among particle types can be attributed to the thickness of the silica shell (~20 nm) and the varied surface chemistry once NP surfaces react with the exposure media. PEG sterically stabilizes AgNPs, and provides excellent dispersibility in water and increases compatibility in biological systems (Tejamaya, Römer et al. 2012). Silica is added as a coating or shell on the AgNPs to control or reduce ion release from the Ag core and enhance the particle stability; however, the nanoporous structure still allows low molecular weight molecules to be loaded into, and released out of this shell based on the manufacturer. Ami-Si-AgNPs functionalized with amine groups on the surface of the silica shell provides a strong positively charged surface evidenced by the measures of zeta potential in the NCM (Figure 5-1b). The addition of amine groups to the silica shells may salinize the surface and further reduce the potential for dissolved Ag leaching.

AgNP surface coatings played a significant role in determining the dissolution rate for the various particles. dissolved Ag concentrations measured during the dissolution study showed a slow release of Ag over time. Dissolution in the NCM for all three particle types was in the range of 2.2 to 5.3% of the total silver, which is relatively low over the 120 hour experimental period

compared to other studies, which report ranging from 3% of the total silver content to complete dissolution over similar timeframes, depending on the solution chemistry (Lok, Ho et al. 2007; Choi, Deng et al. 2008; Liu and Hurt 2010; Xiu, Zhang et al. 2012). It should be noted that the high  $\text{Cl}^-$  concentration in the NCM could minimize the free  $\text{Ag}^+$  present in solution through the formation of  $\text{AgCl}$  precipitates. The modeled threshold concentration of free Ag needed to form precipitates is above  $59 \mu\text{g L}^{-1}$  (Table S4). The dissolved Ag concentration measured without organisms present was below that threshold concentration, indicating minimal precipitation. In the biotic dissolved Ag measurements (Table S4), precipitates could settle out from the exposure media over time. Since centrifugation can easily remove these precipitates, Ag concentrations in the form of precipitates are not represented in the measured dissolved Ag concentration in this study. In addition, the uptake into or complexation of the particles or free ions could also reduce the amount of measured dissolved Ag. Thus, our measured dissolved Ag concentrations in the NCM with the presence of organisms may have underestimated the actual released Ag fraction from AgNPs when exposure concentrations were at 1 and  $5 \text{ mg L}^{-1}$  (Table S5).

The total dissolved Ag in Si-Ag NP exposures were either higher, or comparable to PEG-Ag (Figure 5-3). Xiu et. al demonstrated that PEG coating of AgNPs did not prevent the continuous release of  $\text{Ag}^+$  in their abiotic media (Xiu, Zhang et al. 2012). Studies have suggested the use of silica shells as a method to reduce the release of destructive  $\text{Ag}^+$  from the core (Bahadur, Furusawa et al. 2011). In our study, Si-Ag released a large quantity of dissolved Ag from the core, indicating that the porosity of the silica shell allowed for silver ionic exchange with the surrounding media. However, lower initial and final dissolved Ag concentration in Ami-Si-Ag exposures implies that the silinated monolayer of the aminated-silica AgNP surfaces can

better prevent ion release from the silver core than the silica shell alone, as has been reported by others studying the dissolution of similar particles (Agnihotri, Mukherji et al. 2013; Taglietti, Arciola et al. 2014). The amine functional groups on the surface may help seal the porosity of the silica shell, which could physically block the ionic exchange between the particle surface and the surrounding media, preventing the release of  $\text{Ag}^+$ . Overall, the relatively high dissolution of the Si-Ag NPs compared to the other surface coatings suggests that this particle might be beneficial in applications that require silver ion release to achieve their function; however, the other coatings may be more appropriate for applications such as medical imaging where the release of silver ions is not part of the particle's intended use.

A significantly higher dissolved Ag concentration was found in the biotic exposures than was found in the abiotic dissolution study, highlighting the importance of understanding how organisms impact the release of dissolved ions from NPs. The dissolved Ag concentration at the end of the experiment represents the combination of particle dissolution and the potential release of dissolved silver from organisms. Other factors, such as lysosomal or intestinal degradation of NPs and the subsequent release of dissolved silver may play a role in the relatively high levels of dissolved silver found in the NCM at the end of the experiments (Baird, Kurz et al. 2006; Park, Yi et al. 2010; Soenen, Rivera-Gil et al. 2011; Hsiao, Hsieh et al. 2015). Increased AgNP dissolution has been suggested by other researchers working in aquatic environments rich with algae and plants. (Zook, Long et al. 2011; He, Dorantes-Aranda et al. 2012; Unrine, Colman et al. 2012) Navarro et al. measured higher concentrations of dissolved Ag during toxicity experiments when particles were in contact with *C. reinhardtii* (Navarro, Wagner et al. 2015), and they claim that the production and secretion of ROS by algae might lead to increased dissolution through



enhanced oxidation at the particle surface since ROS is a much more efficient agent at dissolving AgNPs than oxygen (Pospíšil 2009; Liu and Hurt 2010; Sigg and Lindauer 2015) AgNPs can be internalized by *C. reinhardtii*, resulting in an increased sequestration of Ag in the cytoplasm, which can then be released upon cell lysis (Wang, Lv et al. 2016). Thus, dead and broken algae and bacteria cells can serve as additional source of dissolved Ag to the aqueous environment. It is important to emphasize additional aspects that likely play a role in the dissolved Ag in such complex systems. The amount of living and/or dead organisms can alter dissolved Ag concentrations as the organisms can serve as biological sinks and organic ligands released from organisms can sorb available Ag. A thorough mass balance of dissolved, total and accumulated silver in all organisms and all media fractions would be needed to provide more quantitative information.

The impact of organisms on the dissolved Ag released from AgNPs suggests that measuring dissolved Ag concentration in an abiotic environment could overlook the increased rate of Ag ion release from AgNP, and the subsequent toxicity. For instance, the same Si-Ag and Ami-Si-Ag NPs studied in our experiments have been investigated in a previous zebrafish study, where Ami-Si-Ag was found to be more toxic than Si-Ag to developing fish (Bonventre, Pryor et al. 2014). However, when the exposure scenario was changed to a multi-species community, rich in algae and bacteria, the impacts on developing zebrafish embryos were not in complete accord. In another study, He et al. reported a synergistic toxicity to fish gill cells when *C. marina* and AgNP/Ag<sup>+</sup> exposure were both present (He, Dorantes-Aranda et al. 2012). It is likely that the enhancement of ROS produced by algae and bacteria after exposure to AgNPs and Ag<sup>+</sup>, and the release of toxic species from collapsed cells (fatty acids), can enhance the overall toxicity in a

multispecies system. Changing community complexity significantly influenced the amount of dissolved Ag at varying exposure concentrations, likely due to the change in the amount of biological sinks present in the small-scale system.

#### 5.5.2 *D. magna* and zebrafish silver uptake

The concentration of Ag in daphnids was similar under both A+B+D and A+B+D+Z exposure scenarios, suggesting that daphnid uptake was unaffected by the presence of zebrafish. Zebrafish had lower Ag uptake compared to the daphnids in all exposures, which is not surprising since daphnid filter feeding behaviour allows them to incidentally take up small particles while feeding on algae and bacteria (Gophen and Geller 1984). Detectable, but extremely low Ag concentrations in the zebrafish suggests that their dermal and oral uptake through mouth gaping were not significant routes of exposure to AgNPs after hatching, and that the chorion served as a barrier to block the particles and regulate the Ag concentrations during early development. Lee et al. found that AgNPs are transported into and out of the chorionic membrane through pores via Brownian diffusion rather than active transport (Lee, Nallathamby et al. 2007). The particles have the potential to physically block the chorion pores and restrict the diffusion of oxygen, causing hypoxia and delaying hatching (Cheng, Flahaut et al. 2007; Asharani, Wu et al. 2008). The mean dissolved oxygen measured at the end of the experiment was  $8.79 \pm 1.1 \text{ mg L}^{-1}$  at 20 °C, and as hypoxia-induced developmental effects such as cardiac arrhythmia and axis malformations which were not observed (Shang and Wu 2004). it is not likely that chorionic blockage occurred in our experiments. Dissolved silver ions are known to cause delayed hatching in zebrafish (Powers, Slotkin et al. 2011; Massarsky, Dupuis et al. 2013),

however this is typically associated with mortality, axis curvature and other cardiovascular effects not occurring at significant levels in our experiments (Asharani, Wu et al. 2008; George, Lin et al. 2012). Thus, there may have been some disruption of hatching by the particles generating high dissolved Ag concentrations, yet the typical developmental toxicity of dissolved Ag to zebrafish embryos was mediated by the other organisms present during the exposure and the ability of the chorionic membrane to sequester metal ions and minimize embryonic exposure (Lin, Zhao et al. 2011).

Unlike zebrafish, *Daphnia* are filter feeders, which have higher potential to accumulate suspended NPs in their intestines during feeding, and their constant movement provides the opportunity for NPs to accumulate in their antennae and thoracopods. The high Ag concentration in daphnids measured by ICP-MS corresponded with daphnid pictures in Figure S5-6, suggesting that they could accumulate AgNPs. Ribeiro, et al. also showed a high Ag content in *D. magna* with AgNP water born exposures (Ribeiro, Van Gestel et al. 2016); meanwhile, a simultaneous water and dietary exposure to AgNPs induced higher Ag concentration in *D. magna* compared to AgNO<sub>3</sub>, which is considered more likely in natural environments and was simulated in the nanocosm. The particular nature of the AgNPs also likely contributed to their sensitivity relative to the other organisms in the nanocosm (Figure S5-14). Given their role in hierarchical food webs, this bioaccumulation has the potential to lead to biomagnification in predators.

### 5.5.3 Toxicity of AgNPs in nanocosms

The three surface coated AgNPs elicited significantly different responses to test organisms. Surface interactions between AgNP surface chemistry and organisms is an important

consideration in understanding AgNP toxicity to organisms (El Badawy, Silva et al. 2010). It has been shown that positively charged nanoparticles have higher potential to interact with cells which results in higher cytotoxicity than negatively charged particles (Liu, Li et al. 2011; Fröhlich 2012). They are also purportedly more likely to be internalized in cells, and preferentially localized in the lysosomes to become more toxic due to the activation of oxidase activity by the NPs in the acidic environment (Luyts, Napierska et al. 2013). However, our findings are not consistent with those studies. We found that positively charged Ami-Si-Ag were the least toxic and had the lowest dissolved Ag at all concentrations and exposure scenarios. We believe the reason for the observed toxicity was due to the relatively high dissolved Ag released from those AgNPs, which may have overwhelmed the toxicity caused by cell-particle surface interactions. In other reports, PEG only demonstrated toxicity to algae and bacteria at very high concentrations (460 - 1000 mg L<sup>-1</sup>) compared to our exposure concentrations (0.1 – 5 mg L<sup>-1</sup>) (Kent, Andersen et al. 1999; Harford, Hogan et al. 2011). Therefore, direct toxicity caused by PEG in our study was unlikely, and not observed, at the test concentrations. Si-Ag was expected to have reduced toxicity compared to AgNPs lacking a silica shell due to reduced ion release from the AgNP core and the fact that the much less toxic silica shell, not the Ag, would have greater contact with the media and the organisms (Bahadur, Furusawa et al. 2011; Fuertes, Sánchez-Munoz et al. 2011).

Toxic responses were highly correlated to the amount of dissolved Ag in the exposure media measured at the conclusion of the study (Figure S5-10 to S5-13). High toxicity was observed with PEG-Ag and Si-Ag, which matched with their high ionic Ag concentration, whereas less toxicity was observed with Ami-Si-Ag with the lowest dissolution rate among three

different AgNPs. Many studies propose that the AgNP toxicity was primarily dominated by free ionic Ag (Xiu, Ma et al. 2011; Xiu, Zhang et al. 2012), and a linear correlation between AgNP toxicity and dissolved Ag released from AgNP has also been proposed (Yang, Gondikas et al. 2011). In our study, AgNPs dissolution was also highly related to their surface coatings, implying that surface coatings influence AgNP toxicity by controlling the rate of Ag dissolution. The SSDs model in this study revealed the relative sensitivity of species in the nanocosm based on final measured dissolved Ag concentration in the exposure vessels. Thus, combining the nanocosm assay with the traditional toxicological models may help better predict the ecotoxicity of nanomaterials in complex environments.

Increasing community complexity mitigated the toxicity elicited by AgNPs. AgNP toxicity to algae and bacteria was less with the additional complexity in the exposure scenario when daphnids and zebrafish were introduced into the system to increase community complexity. The predation from daphnids decreased the growth rates of algal and bacterial cells, despite the fact that excretions from the daphnids could serve as an additional nutrient source for the microorganisms present in the nanocosms. The predation of contaminated microorganisms provided *D. magna* another potential route for bioaccumulating AgNP and dissolved Ag (Ribeiro, Van Gestel et al. 2016). Embryonic zebrafish did not have direct interaction with other organisms in the system prior to hatching, but did serve as a potential biological sink for AgNPs and dissolved Ag in solution. Increasing trophic complexity altered the apparent organismal susceptibility to AgNP exposures. We believe this is due to the decrease in bioavailable Ag (both dissolved Ag and AgNPs) when compared to low trophic complexity communities. Bone et al. compared the toxicity of AgNP under mesocosm, microcosm, and conventional laboratory

settings, and they found that increasing the environment complexity of the mesocosms resulted in reduced toxicity to atlantic killifish (*Fundulus heteroclitus*) embryos (Bone, Matson et al. 2015). Within more complex exposure communities, organism interactions and other environmental factors have greater potential to modify a given organisms response to nanoparticles. This implies single toxicity tests may be conservative in estimating the realistic ecological responses to nanomaterials; however, surface functionalization cannot be ignored due to direct interactions and potential alterations to processes such as dissolution.

## 5.6 Conclusion

Overall, this study stresses the importance of conducting toxicity evaluations within a community setting to fill important data gaps for more complex ecosystem responses to nanomaterial exposure. A key finding was that quantifying dissolved metal concentrations in specific exposure scenarios is critical to understand the toxicity mechanisms of metal/metal oxide NPs. The nanocosm approach we have introduced here is not intended to simulate a naturally occurring ecosystem, but instead to create a multi-species community for toxicity testing and for providing valuable insight beyond single species toxicity testing, such as toxicity caused by bioaccumulation and biomagnification. Rapid, low-cost and efficient microcosm assays, like the nanocosm assay, are urgently needed to assess potential ecological responses to NP exposures. This type of assay could be implemented in inter-laboratory testing strategies and potentially become a standardized method for rapidly assessing potential community impacts from nanoparticle exposure.

## **5.7 Acknowledgements**

This work is funded by the National Science Foundation (NSF Grant #1438165). We thank the Sinnhuber Aquatic Research laboratory (SARL) at Oregon State University for providing zebrafish embryos (NIEHS Grant # P30 ES000210). The authors would like to thank Lindsay Denluck, Lauren Crandon, Amy Bortvedt for support in manuscript editing.

## 5.8 References

- Adams, L. K., D. Y. Lyon, et al. (2006). "Comparative eco-toxicity of nanoscale TiO<sub>2</sub>, SiO<sub>2</sub>, and ZnO water suspensions." Water research **40**(19): 3527-3532.
- Agnihotri, S., S. Mukherji, et al. (2013). "Immobilized silver nanoparticles enhance contact killing and show highest efficacy: elucidation of the mechanism of bactericidal action of silver." Nanoscale **5**(16): 7328-7340.
- Asharani, P., Y. L. Wu, et al. (2008). "Toxicity of silver nanoparticles in zebrafish models." Nanotechnology **19**(25): 255102.
- ASTM (2011). Standard Practice for Standardized Aquatic Microcosms: Fresh Water. West Conshohocken, PA, ASTM International.
- ASTM (2012). Standard Guide for Measurement of Electrophoretic Mobility and Zeta Potential of Nanosized Biological Materials, ASTM International.
- Bahadur, N. M., T. Furusawa, et al. (2011). "Fast and facile synthesis of silica coated silver nanoparticles by microwave irradiation." Journal of colloid and interface science **355**(2): 312-320.
- Baird, S., T. Kurz, et al. (2006). "Metallothionein protects against oxidative stress-induced lysosomal destabilization." Biochem. J **394**: 275-283.
- Blaser, S. A., M. Scheringer, et al. (2008). "Estimation of cumulative aquatic exposure and risk due to silver: contribution of nano-functionalized plastics and textiles." Science of the total environment **390**(2): 396-409.
- Bondarenko, O., K. Juganson, et al. (2013). "Toxicity of Ag, CuO and ZnO nanoparticles to selected environmentally relevant test organisms and mammalian cells in vitro: a critical review." Archives of toxicology **87**(7): 1181-1200.
- Bone, A. J., C. W. Matson, et al. (2015). "Silver nanoparticle toxicity to Atlantic killifish (*Fundulus heteroclitus*) and *Caenorhabditis elegans*: A comparison of mesocosm, microcosm, and conventional laboratory studies." Environmental Toxicology and Chemistry **34**(2): 275-282.
- Bonventre, J. A., J. B. Pryor, et al. (2014). "The impact of aminated surface ligands and silica shells on the stability, uptake, and toxicity of engineered silver nanoparticles." Journal of Nanoparticle Research **16**(12): 1-15.



- Bour, A., F. Mouchet, et al. (2015). "Environmentally relevant approaches to assess nanoparticles ecotoxicity: A review." Journal of hazardous materials **283**: 764-777.
- Brunner, T. J., P. Wick, et al. (2006). "In vitro cytotoxicity of oxide nanoparticles: comparison to asbestos, silica, and the effect of particle solubility." Environmental science & technology **40**(14): 4374-4381.
- Bundschuh, M., F. Seitz, et al. (2016). "Effects of nanoparticles in fresh waters: risks, mechanisms and interactions." Freshwater Biology.
- Bury, N., J. Shaw, et al. (2002). "Derivation of a toxicity-based model to predict how water chemistry influences silver toxicity to invertebrates." Comparative Biochemistry and Physiology Part C: Toxicology & Pharmacology **133**(1): 259-270.
- Chen, L., L. Zhou, et al. (2012). "Toxicological effects of nanometer titanium dioxide (nano-TiO<sub>2</sub>) on *Chlamydomonas reinhardtii*." Ecotoxicology and environmental safety **84**: 155-162.
- Cheng, J., E. Flahaut, et al. (2007). "Effect of carbon nanotubes on developing zebrafish (*Danio rerio*) embryos." Environmental Toxicology and Chemistry **26**(4): 708-716.
- Choi, O., K. K. Deng, et al. (2008). "The inhibitory effects of silver nanoparticles, silver ions, and silver chloride colloids on microbial growth." Water research **42**(12): 3066-3074.
- Colman, B. P., C. L. Arnaout, et al. (2013). "Low Concentrations of Silver Nanoparticles in Biosolids Cause Adverse Ecosystem Responses under Realistic Field Scenario." PloS one **8**(2): e57189.
- Colman, B. P., B. Espinasse, et al. (2014). "Emerging contaminant or an old toxin in disguise? Silver nanoparticle impacts on ecosystems." Environmental science & technology **48**(9): 5229-5236.
- Dong, W., L. Zhang, et al. (2016). "Preparation of hollow multiple-Ag-nanoclusters-C-shell nanostructures and their catalytic properties." Applied Catalysis B: Environmental **180**: 13-19.
- El Badawy, A. M., T. P. Luxton, et al. (2010). "Impact of environmental conditions (pH, ionic strength, and electrolyte type) on the surface charge and aggregation of silver nanoparticles suspensions." Environmental science & technology **44**(4): 1260-1266.
- El Badawy, A. M., R. G. Silva, et al. (2010). "Surface charge-dependent toxicity of silver nanoparticles." Environmental science & technology **45**(1): 283-287.
- Fabrega, J., S. N. Luoma, et al. (2011). "Silver nanoparticles: behaviour and effects in the aquatic environment." Environment international **37**(2): 517-531.

- Franklin, N. M., N. J. Rogers, et al. (2007). "Comparative toxicity of nanoparticulate ZnO, bulk ZnO, and ZnCl<sub>2</sub> to a freshwater microalga (*Pseudokirchneriella subcapitata*): the importance of particle solubility." Environmental science & technology **41**(24): 8484-8490.
- Franklin, N. M., J. L. Stauber, et al. (2002). "Effect of initial cell density on the bioavailability and toxicity of copper in microalgal bioassays." Environmental Toxicology and Chemistry **21**(4): 742-751.
- Fröhlich, E. (2012). "The role of surface charge in cellular uptake and cytotoxicity of medical nanoparticles." International journal of nanomedicine **7**: 5577.
- Fruijtier-Pölloth, C. (2012). "The toxicological mode of action and the safety of synthetic amorphous silica—A nanostructured material." Toxicology **294**(2): 61-79.
- Fuertes, G., O. L. Sánchez-Munoz, et al. (2011). "Switchable bactericidal effects from novel silica-coated silver nanoparticles mediated by light irradiation." Langmuir **27**(6): 2826-2833.
- Ge, L., Q. Li, et al. (2014). "Nanosilver particles in medical applications: synthesis, performance, and toxicity." International journal of nanomedicine **9**: 2399.
- George, S., S. Lin, et al. (2012). "Surface defects on plate-shaped silver nanoparticles contribute to its hazard potential in a fish gill cell line and zebrafish embryos." ACS nano **6**(5): 3745-3759.
- Gophen, M. and W. Geller (1984). "Filter mesh size and food particle uptake by *Daphnia*." Oecologia **64**(3): 408-412.
- Gorman, D. S. and R. Levine (1965). "Cytochrome f and plastocyanin: their sequence in the photosynthetic electron transport chain of *Chlamydomonas reinhardtii*." Proceedings of the National Academy of Sciences of the United States of America **54**(6): 1665.
- Gottschalk, F., T. Sun, et al. (2013). "Environmental concentrations of engineered nanomaterials: review of modeling and analytical studies." Environmental Pollution **181**: 287-300.
- Hachicho, N., S. Reithel, et al. (2015). "Body mass parameters, lipid profiles and protein contents of zebrafish embryos and effects of 2, 4-dinitrophenol exposure." PloS one **10**(8): e0134755.
- Harford, A. J., A. C. Hogan, et al. (2011). "Ecotoxicological assessment of a polyelectrolyte flocculant." Water research **45**(19): 6393-6402.

- Harper, S., C. Usenko, et al. (2008). "In vivo biodistribution and toxicity depends on nanomaterial composition, size, surface functionalisation and route of exposure." Journal of Experimental Nanoscience **3**(3): 195-206.
- Harper, S. L., J. L. Carriere, et al. (2011). "Systematic evaluation of nanomaterial toxicity: utility of standardized materials and rapid assays." ACS nano **5**(6): 4688-4697.
- He, D., J. J. Dorantes-Aranda, et al. (2012). "Silver nanoparticle-algae interactions: oxidative dissolution, reactive oxygen species generation and synergistic toxic effects." Environmental science & technology **46**(16): 8731-8738.
- Heinlaan, M., A. Ivask, et al. (2008). "Toxicity of nanosized and bulk ZnO, CuO and TiO<sub>2</sub> to bacteria *Vibrio fischeri* and crustaceans *Daphnia magna* and *Thamnocephalus platyurus*." Chemosphere **71**(7): 1308-1316.
- Henderson, C. F. and E. W. Tilton (1955). "Tests with acaricides against the brown wheat mite." Journal of Economic Entomology **48**(2): 157-161.
- Ho, C. H., J. Tobis, et al. (2004). "Nanoseparated polymeric networks with multiple antimicrobial properties." Advanced materials **16**(12): 957-961.
- Hsiao, I.-L., Y.-K. Hsieh, et al. (2015). "Trojan-horse mechanism in the cellular uptake of silver nanoparticles verified by direct intra-and extracellular silver speciation analysis." Environmental science & technology **49**(6): 3813-3821.
- Hwang, E. T., J. H. Lee, et al. (2008). "Analysis of the Toxic Mode of Action of Silver Nanoparticles Using Stress-Specific Bioluminescent Bacteria." Small **4**(6): 746-750.
- Ivask, A., A. ElBadawy, et al. (2013). "Toxicity mechanisms in *Escherichia coli* vary for silver nanoparticles and differ from ionic silver." ACS nano **8**(1): 374-386.
- Kent, R. A., D. Andersen, et al. (1999). "Canadian water quality guidelines for glycols—An ecotoxicological review of glycols and associated aircraft anti-icing and deicing fluids." Environmental Toxicology **14**(5): 481-522.
- Kim, K.-T., L. Truong, et al. (2013). "Silver nanoparticle toxicity in the embryonic zebrafish is governed by particle dispersion and ionic environment." Nanotechnology **24**(11): 115101.
- Kimmel, C. B., W. W. Ballard, et al. (1995). "Stages of embryonic development of the zebrafish." Developmental dynamics **203**(3): 253-310.
- Kittler, S., C. Greulich, et al. (2009). "Synthesis of PVP-coated silver nanoparticles and their biological activity towards human mesenchymal stem cells." Materialwissenschaft und Werkstofftechnik **40**(4): 258-264.

- Kvitek, L., A. Panáček, et al. (2008). "Effect of surfactants and polymers on stability and antibacterial activity of silver nanoparticles (NPs)." The Journal of Physical Chemistry C **112**(15): 5825-5834.
- Kwak, J. I., R. Cui, et al. (2016). "Multispecies toxicity test for silver nanoparticles to derive hazardous concentration based on species sensitivity distribution for the protection of aquatic ecosystems." Nanotoxicology **10**(5): 521-530.
- Lee, K. J., P. D. Nallathamby, et al. (2007). "In vivo imaging of transport and biocompatibility of single silver nanoparticles in early development of zebrafish embryos." ACS nano **1**(2): 133-143.
- Legrand, S., A. Catheline, et al. (2008). "Controlling silica nanoparticle properties for biomedical applications through surface modification." New Journal of Chemistry **32**(4): 588-593.
- Letterman, R. D. (1999). Water quality and treatment: a handbook of community water supplies, McGraw-Hill Professional.
- Levy, J. L., J. L. Stauber, et al. (2009). "The effect of bacteria on the sensitivity of microalgae to copper in laboratory bioassays." Chemosphere **74**(9): 1266-1274.
- Lin, S., Y. Zhao, et al. (2011). "High content screening in zebrafish speeds up hazard ranking of transition metal oxide nanoparticles." ACS nano **5**(9): 7284-7295.
- Liu, J. and R. H. Hurt (2010). "Ion release kinetics and particle persistence in aqueous nano-silver colloids." Environmental science & technology **44**(6): 2169-2175.
- Liu, Y., W. Li, et al. (2011). "Intracellular dynamics of cationic and anionic polystyrene nanoparticles without direct interaction with mitotic spindle and chromosomes." Biomaterials **32**(32): 8291-8303.
- Lok, C. N., C. M. Ho, et al. (2007). "Silver nanoparticles: partial oxidation and antibacterial activities." JBIC Journal of Biological Inorganic Chemistry **12**(4): 527-534.
- Louie, S. M., R. D. Tilton, et al. (2016). "Critical Review: Impacts of Macromolecular Coatings on Critical Physicochemical Processes Controlling Environmental Fate of Nanomaterials." Environmental Science: Nano.
- Lowry, G. V., R. J. Hill, et al. (2016). "Guidance to improve the scientific value of zeta-potential measurements in nanoEHS." Environmental Science: Nano.
- Lü, Z., T. Pu, et al. (2015). "Flexible ferroelectric polymer devices based on inkjet-printed electrodes from nanosilver ink." Nanotechnology **26**(5): 055202.

- Luyts, K., D. Napierska, et al. (2013). "How physico-chemical characteristics of nanoparticles cause their toxicity: complex and unresolved interrelations." Environmental Science: Processes & Impacts **15**(1): 23-38.
- Massarsky, A., L. Dupuis, et al. (2013). "Assessment of nanosilver toxicity during zebrafish (*Danio rerio*) development." Chemosphere **92**(1): 59-66.
- Mueller, N. C. and B. Nowack (2008). "Exposure modeling of engineered nanoparticles in the environment." Environmental science & technology **42**(12): 4447-4453.
- Navarro, E., F. Piccapietra, et al. (2008). "Toxicity of silver nanoparticles to *Chlamydomonas reinhardtii*." Environmental science & technology **42**(23): 8959-8964.
- Navarro, E., B. Wagner, et al. (2015). "Effects of differently coated silver nanoparticles on the photosynthesis of *Chlamydomonas reinhardtii*." Environmental science & technology.
- Nyholm, N. and T. Källqvist (1989). "Methods for growth inhibition toxicity tests with freshwater algae." Environmental Toxicology and Chemistry **8**(8): 689-703.
- Paine, C., T. R. Marthews, et al. (2012). "How to fit nonlinear plant growth models and calculate growth rates: an update for ecologists." Methods in Ecology and Evolution **3**(2): 245-256.
- Park, E.-J., J. Yi, et al. (2010). "Silver nanoparticles induce cytotoxicity by a Trojan-horse type mechanism." Toxicology in Vitro **24**(3): 872-878.
- Peltier, W. H., C. I. Weber, et al. (1985). Methods for measuring the acute toxicity of effluents to freshwater and marine organisms, Environmental Monitoring and Support Laboratory, Office of Research and Development, US Environmental Protection Agency.
- Perreault, F., A. Oukarroum, et al. (2012). "Polymer coating of copper oxide nanoparticles increases nanoparticles uptake and toxicity in the green alga *Chlamydomonas reinhardtii*." Chemosphere **87**(11): 1388-1394.
- Pospíšil, P. (2009). "Production of reactive oxygen species by photosystem II." Biochimica et Biophysica Acta (BBA)-Bioenergetics **1787**(10): 1151-1160.
- Powers, C. M., T. A. Slotkin, et al. (2011). "Silver nanoparticles alter zebrafish development and larval behavior: distinct roles for particle size, coating and composition." Neurotoxicology and teratology **33**(6): 708-714.
- Ribeiro, F., C. A. Van Gestel, et al. (2016). "Bioaccumulation of silver in *Daphnia magna*: Waterborne and dietary exposure to nanoparticles and dissolved silver." Science of the total environment.

- Shang, E. H. and R. S. Wu (2004). "Aquatic hypoxia is a teratogen and affects fish embryonic development." Environmental science & technology **38**(18): 4763-4767.
- Sheehan, P. J. (1984). Effects of Pollutants at the Ecosystem Level. New York, John Wiley & Sons Ltd.
- Sigg, L. and U. Lindauer (2015). "Silver nanoparticle dissolution in the presence of ligands and of hydrogen peroxide." Environmental Pollution **206**: 582-587.
- Slowing, I., B. G. Trewyn, et al. (2006). "Effect of surface functionalization of MCM-41-type mesoporous silica nanoparticles on the endocytosis by human cancer cells." Journal of the American Chemical Society **128**(46): 14792-14793.
- Soenen, S. J., P. Rivera-Gil, et al. (2011). "Cellular toxicity of inorganic nanoparticles: common aspects and guidelines for improved nanotoxicity evaluation." Nano Today **6**(5): 446-465.
- Sondi, I. and B. Salopek-Sondi (2004). "Silver nanoparticles as antimicrobial agent: a case study on *E. coli* as a model for Gram-negative bacteria." Journal of colloid and interface science **275**(1): 177-182.
- Stephan, C. (2002). "Use of species sensitivity distributions in the derivation of water quality criteria for aquatic life by the US Environmental Protection Agency." Species Sensitivity Distributions in Ecotoxicology. Lewis, Boca Raton, FL, USA: 211-220.
- Sun, T. Y., F. Gottschalk, et al. (2014). "Comprehensive probabilistic modelling of environmental emissions of engineered nanomaterials." Environmental Pollution **185**: 69-76.
- Taglietti, A., C. R. Arciola, et al. (2014). "Antibiofilm activity of a monolayer of silver nanoparticles anchored to an amino-silanized glass surface." Biomaterials **35**(6): 1779-1788.
- Taub, F. B. and A. M. Dollar (1968). "The nutritional inadequacy of *Chlorella* and *Chlamydomonas* as food for *Daphnia pulex*." Limnol. Oceanogr **13**(4): 607-617.
- Team., R. D. C. (2014). R: A language and environment for statistical computing. . Vienna, Austria, R Fundation for Statistical Computing.
- Tejamaya, M., I. Römer, et al. (2012). "Stability of citrate, PVP, and PEG coated silver nanoparticles in ecotoxicology media." Environmental science & technology **46**(13): 7011-7017.
- Unrine, J. M., B. P. Colman, et al. (2012). "Biotic and abiotic interactions in aquatic microcosms determine fate and toxicity of Ag nanoparticles. Part 1. Aggregation and dissolution." Environmental science & technology **46**(13): 6915-6924.

- Wang, S., J. Lv, et al. (2016). "Cellular internalization and intracellular biotransformation of silver nanoparticles in *Chlamydomonas reinhardtii*." Nanotoxicology: 1-7.
- Warren, E. (1900). "On the reaction of *Daphnia magna* (Straus) to certain changes in its environment." Quart. J. Microsc. Sci **43**: 199-224.
- Xiu, Z. M., J. Ma, et al. (2011). "Differential effect of common ligands and molecular oxygen on antimicrobial activity of silver nanoparticles versus silver ions." Environmental science & technology **45**(20): 9003-9008.
- Xiu, Z. M., Q. B. Zhang, et al. (2012). "Negligible particle-specific antibacterial activity of silver nanoparticles." NANO LETTERS **12**(8): 4271-4275.
- Yang, X., A. P. Gondikas, et al. (2011). "Mechanism of silver nanoparticle toxicity is dependent on dissolved silver and surface coating in *Caenorhabditis elegans*." Environmental science & technology **46**(2): 1119-1127.
- Zook, J. M., S. E. Long, et al. (2011). "Measuring silver nanoparticle dissolution in complex biological and environmental matrices using UV-visible absorbance." Analytical and bioanalytical chemistry **401**(6): 1993-2002.

## 5.9 Appendix

**Table S5-1.** Metadata associated with zeta potential measurements.

Surface functionalization	PEG; Silanol; Amine terminated Silica	
Shape	Spherical	
Size distribution (minimum - maximum)	PEG-Ag	50 - 220 nm
	Si-Ag	68 - 295 nm
	Ami-Si-Ag	68 - 615 nm
Initial hydrodynamic diameter (mean)	PEG-Ag	96.6
	Si-Ag	136.5
	Ami-Si-Ag	200.2
Particle concentration from the manufacturer	PEG-Ag	5.9E+9 particles/ml
	Si-Ag	5.1E+9 particles/ml
	Ami-Si-Ag	5.9E+9 particles/ml
Electrophoretic mobility (initial: 0 hour - final: 120 hours)	PEG-Ag	-0.287 - -0.199
	Si-Ag	-1.193 - 1.04
	Ami-Si-Ag	0.992 - 2.213
Model used to compute the zeta potential	Smoluchowski equation	
pH	7.2	
Ionic strength	0.01 mol/L	
Ionic composition	Made according to reference 36	
Temperature	25 °C	
Viscosity	0.8872 mPa	
Macromolecules/NOM	None	
Duration of measurement	4 minutes	
Applied voltage	148 V	
Number of instrument measurements made and averaged to determine each ZP	12	
Total number of replicate measurements	3	



*Table S5-2. AgNP digestion recovery rates.*

NP type	Recovery rate (%)	Standard deviation (%)
PEG-Ag	105.4	5.1
Si-Ag	104.2	2.6
Ami-Si-Ag	104.1	2.3

**Table S5-3.** AgNP hydrodynamic diameters (HDD) and the corresponding polydispersity index (PDI) measured every 24 hours throughout the experimental period ( $\pm$  indicates the standard error of three sample replicates).

Time (hr)	PEG-Ag (MQW)		PEG-Ag (NCM)		Si-Ag (MQW)		Si-Ag (NCM)		Ami-Si-Ag (MQW)		Ami-Si-Ag (NCM)	
	HDD (nm)	PDI	HDD (nm)	PDI	HDD (nm)	PDI	HDD (nm)	PDI	HDD (nm)	PDI	HDD (nm)	PDI
0	97.7 $\pm$ 0.17	0.058 $\pm$ 0.006	96.6 $\pm$ 0.15	0.041 $\pm$ 0.007	132.2 $\pm$ 0.5	0.014 $\pm$ 0.01	136.5 $\pm$ 1.1	0.033 $\pm$ 0.009	202.5 $\pm$ 2	0.152 $\pm$ 0.019	200.2 $\pm$ 1.7	0.162 $\pm$ 0.005
24	98.2 $\pm$ 0.65	0.063 $\pm$ 0.008	98.8 $\pm$ 0.32	0.053 $\pm$ 0.002	131 $\pm$ 1.7	0.037 $\pm$ 0.002	138.8 $\pm$ 0.9	0.078 $\pm$ 0.008	211.9 $\pm$ 1.1	0.128 $\pm$ 0.023	214.1 $\pm$ 2	0.161 $\pm$ 0.017
48	98.3 $\pm$ 0.32	0.058 $\pm$ 0.011	99.7 $\pm$ 0.61	0.058 $\pm$ 0.001	124.1 $\pm$ 0.67	0.044 $\pm$ 0.01	134.4 $\pm$ 2.4	0.107 $\pm$ 0.014	199.7 $\pm$ 1.23	0.171 $\pm$ 0.009	222.1 $\pm$ 2.1	0.176 $\pm$ 0.013
72	98.8 $\pm$ 0.56	0.061 $\pm$ 0.004	101.1 $\pm$ 0.25	0.06 $\pm$ 0.004	120 $\pm$ 1.41	0.051 $\pm$ 0.007	142.7 $\pm$ 0.76	0.173 $\pm$ 0.012	162 $\pm$ 0.33	0.184 $\pm$ 0.01	209.5 $\pm$ 1.5	0.174 $\pm$ 0.011
96	97.1 $\pm$ 0.51	0.07 $\pm$ 0.005	100.9 $\pm$ 0.82	0.045 $\pm$ 0.005	119.4 $\pm$ 1.02	0.07 $\pm$ 0.01	131 $\pm$ 0.76	0.106 $\pm$ 0.017	135 $\pm$ 0.9	0.155 $\pm$ 0.011	220 $\pm$ 2.6	0.197 $\pm$ 0.011
120	97.1 $\pm$ 0.35	0.062 $\pm$ 0.01	99.5 $\pm$ 0.31	0.058 $\pm$ 0.016	117.1 $\pm$ 0.92	0.045 $\pm$ 0.004	138.4 $\pm$ 1.02	0.12 $\pm$ 0.012	113.3 $\pm$ 0.52	0.149 $\pm$ 0.013	208.4 $\pm$ 2.3	0.19 $\pm$ 0.021

**Table S5-4.** Theoretical Ag speciation calculated with Visual-MINTEQ assuming equilibrium in NCM.  $\text{AgCl}_{(s)}$  highlight in red indicates the percentage of precipitates that can be formed at the modeled concentrations.

a)  $\text{AgCl}_{(s)}$  starts to form when the input  $\text{Ag}^+$  concentration is above  $59 \mu\text{g L}^{-1}$ .

Input Ag+ concentration (59 $\mu\text{g/L}$ )			Input Ag+ concentration (60 $\mu\text{g/L}$ )		
Ag Speciation	$\mu\text{g Ag/L}$	% Total	Ag Speciation	$\mu\text{g Ag/L}$	% Total
$\text{Ag}(\text{OH})_2^-$	1.25E-09	0%	$\text{Ag}(\text{OH})_2^-$	1.26E-09	0%
$\text{Ag}^+$	5.02E+00	9%	$\text{Ag}^+$	5.07E+00	8%
$\text{Ag}_2\text{MoO}_4$ (aq)	4.27E-14	0%	$\text{Ag}_2\text{MoO}_4$ (aq)	4.36E-14	0%
$\text{AgCl}$ (aq)	3.88E+01	66%	$\text{AgCl}$ (aq)	3.92E+01	65%
$\text{AgCl}_2^-$	1.52E+01	26%	$\text{AgCl}_2^-$	1.54E+01	26%
$\text{AgCl}_3^-$	7.23E-02	0%	$\text{AgCl}_3^-$	7.31E-02	0%
$\text{AgEDTA}^-$	2.75E-07	0%	$\text{AgEDTA}^-$	2.78E-07	0%
$\text{AgH}_2\text{BO}_3$ (aq)	9.89E-06	0%	$\text{AgH}_2\text{BO}_3$ (aq)	9.99E-06	0%
$\text{AgHEDTA}^-$	5.53E-08	0%	$\text{AgHEDTA}^-$	5.58E-08	0%
$\text{AgNO}_3$ (aq)	1.67E-03	0%	$\text{AgNO}_3$ (aq)	1.69E-03	0%
$\text{AgOH}$ (aq)	7.34E-05	0%	$\text{AgOH}$ (aq)	7.42E-05	0%
$\text{AgSO}_4^-$	6.33E-03	0%	$\text{AgSO}_4^-$	6.39E-03	0%
$\text{AgCl}$ (s)	0.00E+00	0%	$\text{AgCl}$ (s)	4.13E-01	1%
Total	59.07	100%	Total	60.07	100%

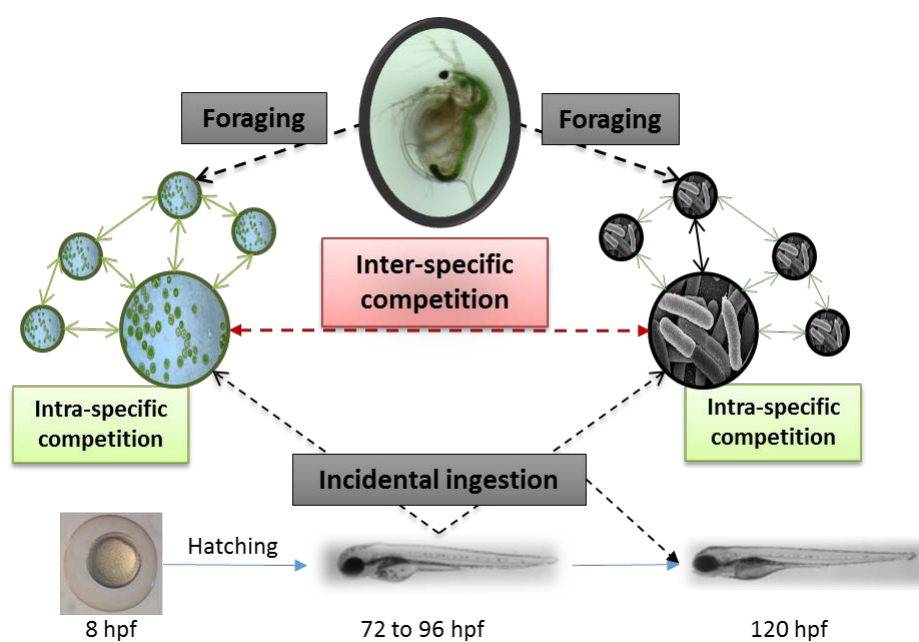
b) Ag speciation calculated using the highest abiotic dissolved Ag concentration measured in NCM (Figure 5-2) for each AgNP.

PEG-AgNP (24 $\mu\text{g/L}$ )			Si-AgNP (53 $\mu\text{g/L}$ )			Ami-Si-AgNP (22 $\mu\text{g/L}$ )		
Ag Speciation	$\mu\text{g Ag/L}$	% Total	Ag Speciation	$\mu\text{g Ag/L}$	% Total	Ag Speciation	$\mu\text{g Ag/L}$	% Total
$\text{Ag}(\text{OH})_2^-$	5.08E-10	0%	$\text{Ag}(\text{OH})_2^-$	1.12E-09	0%	$\text{Ag}(\text{OH})_2^-$	4.66E-10	0%
$\text{Ag}^+$	2.04E+00	9%	$\text{Ag}^+$	4.51E+00	9%	$\text{Ag}^+$	1.87E+00	9%
$\text{Ag}_2\text{MoO}_4$ (aq)	7.07E-15	0%	$\text{Ag}_2\text{MoO}_4$ (aq)	3.45E-14	0%	$\text{Ag}_2\text{MoO}_4$ (aq)	5.94E-15	0%
$\text{AgCl}$ (aq)	1.58E+01	66%	$\text{AgCl}$ (aq)	3.48E+01	66%	$\text{AgCl}$ (aq)	1.45E+01	66%
$\text{AgCl}_2^-$	6.18E+00	26%	$\text{AgCl}_2^-$	1.37E+01	26%	$\text{AgCl}_2^-$	5.67E+00	26%
$\text{AgCl}_3^-$	2.94E-02	0%	$\text{AgCl}_3^-$	6.50E-02	0%	$\text{AgCl}_3^-$	2.70E-02	0%
$\text{AgEDTA}^-$	1.12E-07	0%	$\text{AgEDTA}^-$	2.47E-07	0%	$\text{AgEDTA}^-$	1.02E-07	0%
$\text{AgH}_2\text{BO}_3$ (aq)	4.02E-06	0%	$\text{AgH}_2\text{BO}_3$ (aq)	8.88E-06	0%	$\text{AgH}_2\text{BO}_3$ (aq)	3.69E-06	0%
$\text{AgHEDTA}^-$	2.25E-08	0%	$\text{AgHEDTA}^-$	4.97E-08	0%	$\text{AgHEDTA}^-$	2.06E-08	0%
$\text{AgNO}_3$ (aq)	6.80E-04	0%	$\text{AgNO}_3$ (aq)	1.50E-03	0%	$\text{AgNO}_3$ (aq)	6.24E-04	0%
$\text{AgOH}$ (aq)	2.99E-05	0%	$\text{AgOH}$ (aq)	6.60E-05	0%	$\text{AgOH}$ (aq)	2.74E-05	0%
$\text{AgSO}_4^-$	2.57E-03	0%	$\text{AgSO}_4^-$	5.68E-03	0%	$\text{AgSO}_4^-$	2.36E-03	0%
$\text{AgCl}$ (s)	0.00E+00	0%	$\text{AgCl}$ (s)	0.00E+00	0%	$\text{AgCl}$ (s)	0.00E+00	0%
Total	24.03	100%	Total	53.07	100%	Total	22.03	100%

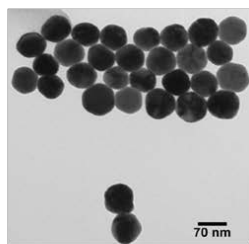
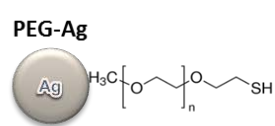
**Table S5-5.** Theoretical Ag speciation calculated with Visual-MINTEQ using measured dissolved silver concentrations in the presence of oprganisms for each type of AgNP in NCM at each exposure concentration (Figure 5-3). AgCl<sub>(s)</sub> highlight in red indicates the percentage of precipitates that can be formed at the modeled concentrations.

PEG-Ag (Exposure con. 100 µg/L)			PEG-Ag (Exposure con. 1000 µg/L)			PEG-Ag (Exposure con. 5000 µg/L)		
Dissolved Ag measured in NC (2.1 µg/L)			Dissolved Ag measured in NC (132.9 µg/L)			Dissolved Ag measured in NC (906.2 µg/L)		
Ag Speciation	Mass (µg/L)	% Total	Ag Speciation	Mass (µg/L)	% Total	Ag Speciation	Mass (µg/L)	% Total
Ag(OH)2-	4.36E-11	0%	Ag(OH)2-	1.26E-09	0%	Ag(OH)2-	1.26E-09	0%
Ag+1	1.75E-01	9%	Ag+1	5.07E+00	4%	Ag+1	5.08E+00	1%
Ag2MoO4 (aq)	5.21E-17	0%	Ag2MoO4 (aq)	4.36E-14	0%	Ag2MoO4 (aq)	4.38E-14	0%
AgCl (aq)	1.35E+00	66%	AgCl (aq)	3.92E+01	29%	AgCl (aq)	3.92E+01	4%
AgCl2-	5.31E-01	26%	AgCl2-	1.54E+01	12%	AgCl2-	1.53E+01	2%
AgCl3-2	2.53E-03	0%	AgCl3-2	7.30E-02	0%	AgCl3-2	7.28E-02	0%
AgEDTA-3	9.60E-09	0%	AgEDTA-3	2.78E-07	0%	AgEDTA-3	2.78E-07	0%
AgH2BO3 (aq)	3.45E-07	0%	AgH2BO3 (aq)	9.99E-06	0%	AgH2BO3 (aq)	1.00E-05	0%
AgHEDTA-2	1.93E-09	0%	AgHEDTA-2	5.59E-08	4.20E-10	AgHEDTA-2	5.59E-08	0%
AgNO3 (aq)	5.84E-05	0%	AgNO3 (aq)	1.69E-03	0%	AgNO3 (aq)	1.69E-03	0%
AgOH (aq)	2.56E-06	0%	AgOH (aq)	7.42E-05	0%	AgOH (aq)	7.43E-05	0%
AgSO4-	2.21E-04	0%	AgSO4-	6.39E-03	0%	AgSO4-	6.40E-03	0%
AgCl (s)	0.00E+00	0%	AgCl (s)	7.34E+01	55%	AgCl (s)	8.48E+02	93%
Total	2.06	100%	Total	133.03	100%	Total	907.29	100%
Si-Ag (Exposure con. 100 µg/L)			Si-Ag (Exposure con. 1000 µg/L)			Si-Ag (Exposure con. 5000 µg/L)		
Dissolved Ag measured in NC (26.4 µg/L)			Dissolved Ag measured in NC (229.9 µg/L)			Dissolved Ag measured in NC (815.96 µg/L)		
Ag Speciation	Mass (µg/L)	% Total	Ag Speciation	Mass (µg/L)	% Total	Ag Speciation	Mass (µg/L)	% Total
Ag+1	2.25E+00	9%	Ag+1	5.07E+00	2%	Ag+1	5.08E+00	1%
Ag2MoO4 (aq)	8.56E-15	0%	Ag2MoO4 (aq)	4.36E-14	0%	Ag2MoO4 (aq)	4.37E-14	0%
AgCl (aq)	1.74E+01	66%	AgCl (aq)	3.92E+01	17%	AgCl (aq)	3.92E+01	5%
AgCl2-	6.81E+00	26%	AgCl2-	1.53E+01	7%	AgCl2-	1.53E+01	2%
AgCl3-2	3.24E-02	0%	AgCl3-2	7.30E-02	0%	AgCl3-2	7.28E-02	0%
AgEDTA-3	1.23E-07	0%	AgEDTA-3	2.78E-07	0%	AgEDTA-3	2.78E-07	0%
AgH2BO3 (aq)	4.43E-06	0%	AgH2BO3 (aq)	9.99E-06	0%	AgH2BO3 (aq)	1.00E-05	0%
AgHEDTA-2	2.47E-08	0%	AgHEDTA-2	5.59E-08	0%	AgHEDTA-2	5.59E-08	0%
AgNO3 (aq)	7.49E-04	0%	AgNO3 (aq)	1.69E-03	0%	AgNO3 (aq)	1.69E-03	0%
AgOH (aq)	3.29E-05	0%	AgOH (aq)	7.42E-05	0%	AgOH (aq)	7.43E-05	0%
AgSO4-	2.83E-03	0%	AgSO4-	6.39E-03	0%	AgSO4-	6.40E-03	0%
AgCl (s)	0.00E+00	0%	AgCl (s)	1.71E+02	74%	AgCl (s)	7.57E+02	93%
Total	26.44	100%	Total	230.22	100%	Total	816.96	100%
Ami-Si-Ag (Exposure con. 100 µg/L)			Ami-Si-Ag (Exposure con. 1000 µg/L)			Ami-Si-Ag (Exposure con. 5000 µg/L)		
Dissolved Ag measured in NC (7.7 µg/L)			Dissolved Ag measured in NC (84.6 µg/L)			Dissolved Ag measured in NC (309.8 µg/L)		
Ag Speciation	Mass (µg/L)	% Total	Ag Speciation	Mass (µg/L)	% Total	Ag Speciation	Mass (µg/L)	% Total
Ag+1	6.57E-01	9%	Ag+1	5.07E+00	6%	Ag+1	5.08E+00	2%
Ag2MoO4 (aq)	7.32E-16	0%	Ag2MoO4 (aq)	4.36E-14	0%	Ag2MoO4 (aq)	4.36E-14	0%
AgCl (aq)	5.07E+00	66%	AgCl (aq)	3.92E+01	46%	AgCl (aq)	3.92E+01	13%
AgCl2-	1.99E+00	26%	AgCl2-	1.54E+01	18%	AgCl2-	1.53E+01	5%
AgCl3-2	9.47E-03	0%	AgCl3-2	7.30E-02	0%	AgCl3-2	7.30E-02	0%
AgEDTA-3	3.60E-08	0%	AgEDTA-3	2.78E-07	0%	AgEDTA-3	2.78E-07	0%
AgH2BO3 (aq)	1.29E-06	0%	AgH2BO3 (aq)	9.99E-06	0%	AgH2BO3 (aq)	9.99E-06	0%
AgHEDTA-2	7.23E-09	0%	AgHEDTA-2	5.58E-08	0%	AgHEDTA-2	5.59E-08	0%
AgNO3 (aq)	2.19E-04	0%	AgNO3 (aq)	1.69E-03	0%	AgNO3 (aq)	1.69E-03	0%
AgOH (aq)	9.61E-06	0%	AgOH (aq)	7.42E-05	0%	AgOH (aq)	7.42E-05	0%
AgSO4-	8.28E-04	0%	AgSO4-	6.39E-03	0%	AgSO4-	6.39E-03	0%
AgCl (s)	0.00E+00	0%	AgCl (s)	2.50E+01	30%	AgCl (s)	2.51E+02	81%
Total	7.73	100%	Total	84.68	100%	Total	310.20	100%

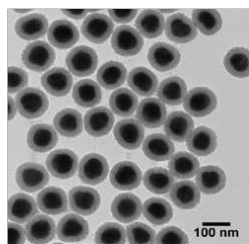
**Figure S5-1.** The potential interactions of the four species in the nanocosm assay. Algae serves as primary producer and produces oxygen for other species in the system. Bacteria are the representative decomposers of the system. Both algae and bacteria are a primary food source of *D. magna*. Zebrafish do not interact with other species directly before they hatch as their chorion serves as a barrier to those interactions. After zebrafish hatching at 80 hours, they start mouth gaping behavior and can potentially ingest some algae and bacteria.



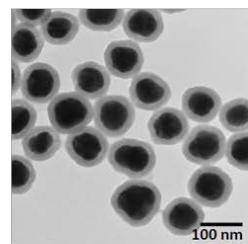
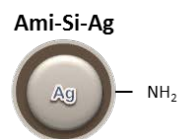
**Figure S5-2.** AgNP surface chemistry, TEM images and primary particle sizes as reported by the manufacturer.



Mean diameter: 73.2 nm  
Particle surface: mPEG 5 kDa

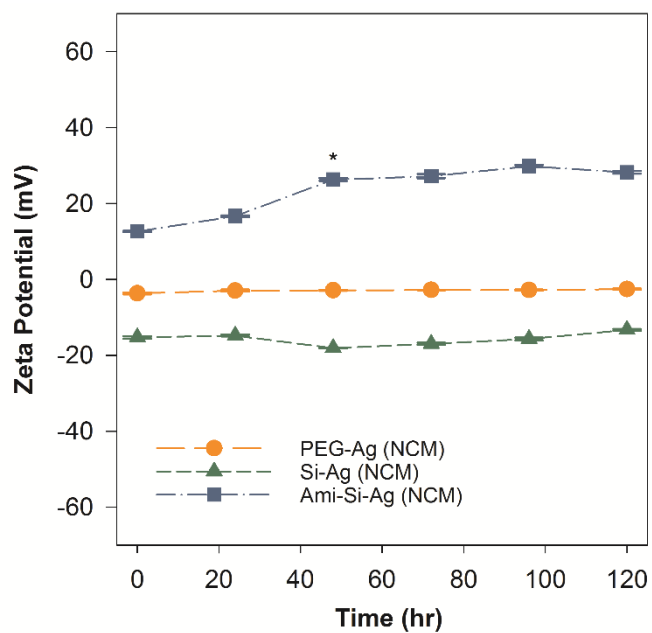


Mean diameter : 72.3 nm  
Mean shell thickness: 22.6 nm  
Particle surface: Silanol

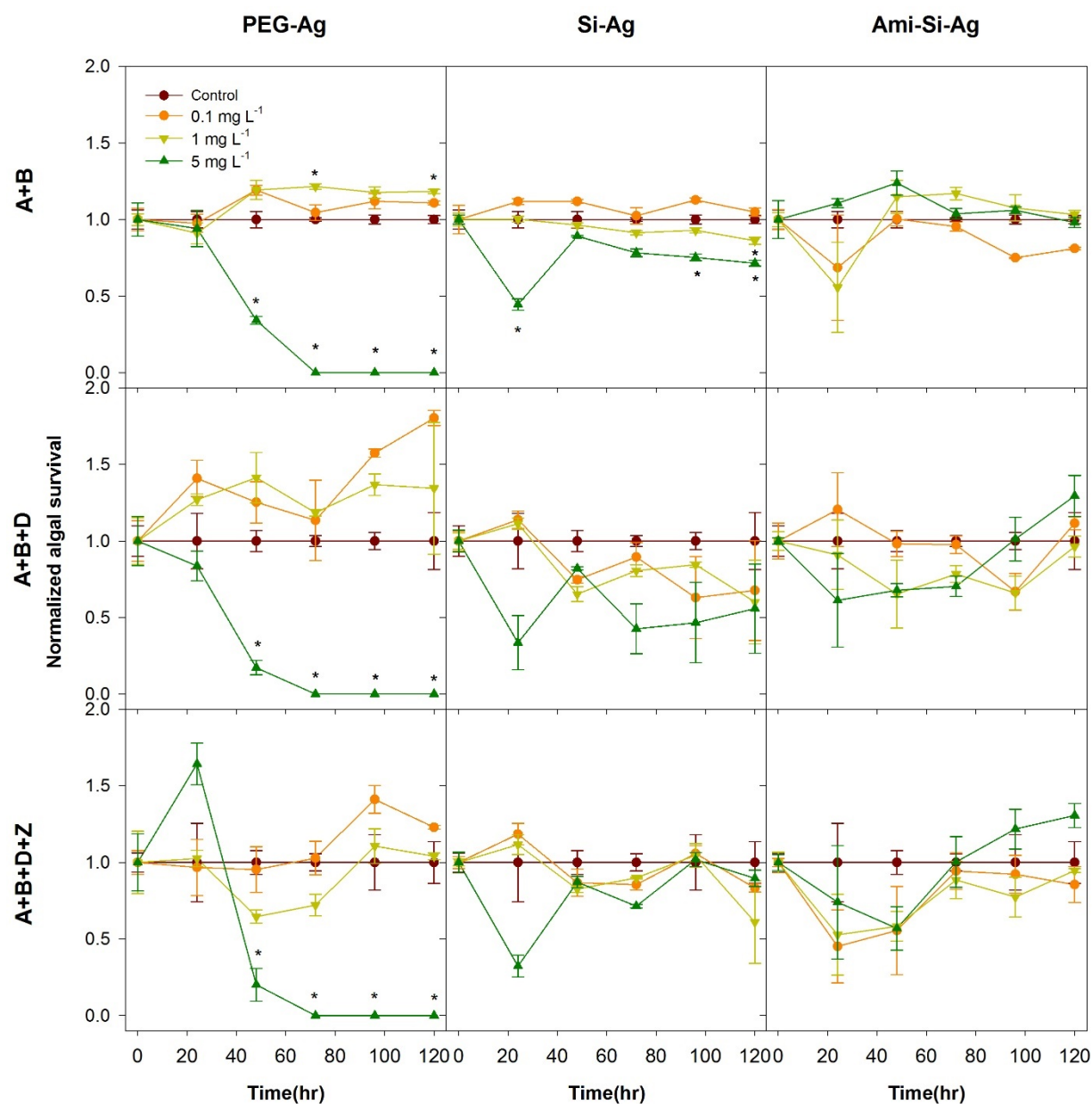


Mean diameter: 67.7 nm  
Mean shell thickness: 20 nm  
Particle surface: Amine-terminated Silica

**Figure S5-3.** Zeta potential (ZP) of PEG-Ag (orange circle), Si-Ag (green triangle), and Ami-Si-Ag (blue square) in NCM over 120 hours at  $10 \text{ mg L}^{-1}$ . Standard errors were derived for triplicate measures on each AgNP. Asterisk (\*) represents a change in zeta potential from time 0 in Ami-Si-Ag.

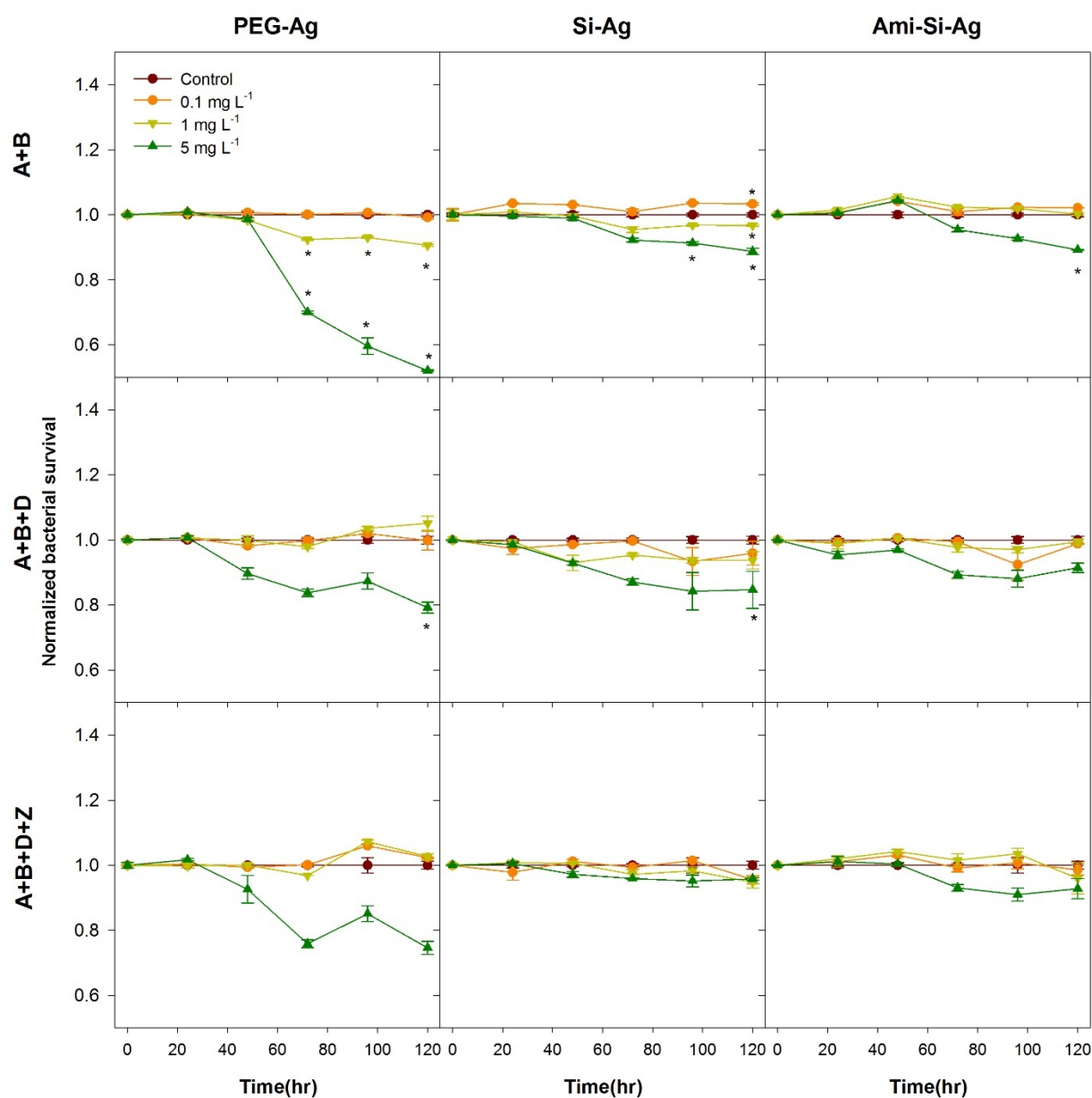


**Figure S5-4.** Normalized algal survival in exposure scenarios containing algae and bacteria (A+B), as well as those that added *Daphnia* (A+B+D) and zebrafish (A+B+D+Z) using three different surface functionalized AgNPs. Asterisk (\*) indicates significant difference among treatments and the corresponding control.

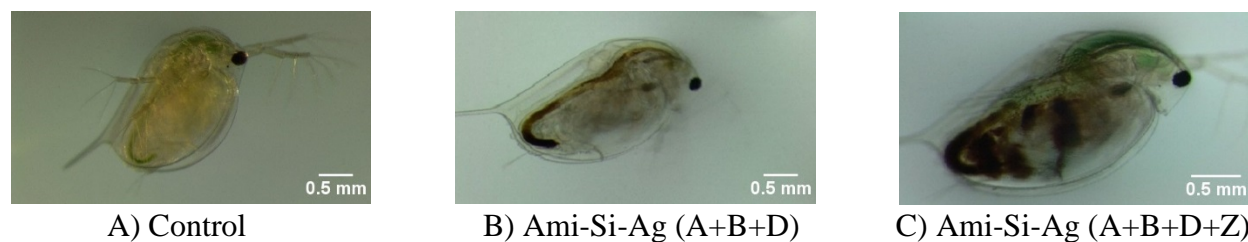




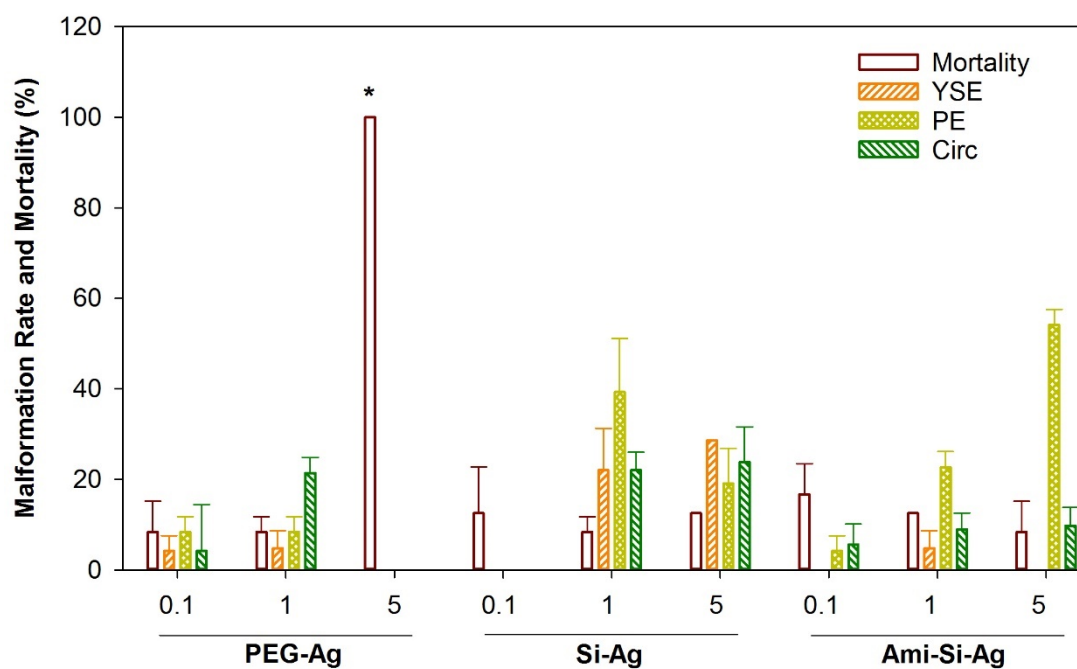
**Figure S5-5.** Normalized bacterial survival in three different exposure scenarios with three types of AgNPs. Asterisk (\*) indicates significant difference among treatments and the corresponding control.



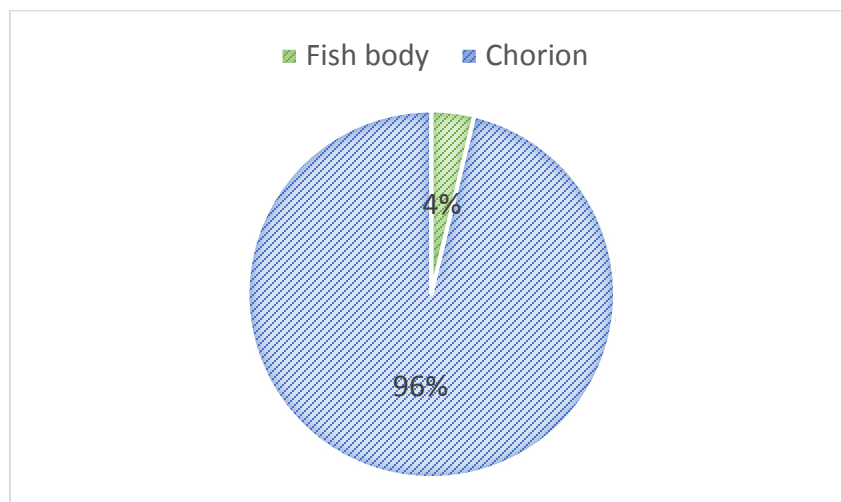
**Figure S5-6.** Images of 120-hour *D. magna* after exposure to 5 mg L<sup>-1</sup> Ami-Si-Ag exposure; A) control; B) *D. magna* in A+B+D exposure scenario; C) *D. magna* in A+B+D+Z exposure scenario.



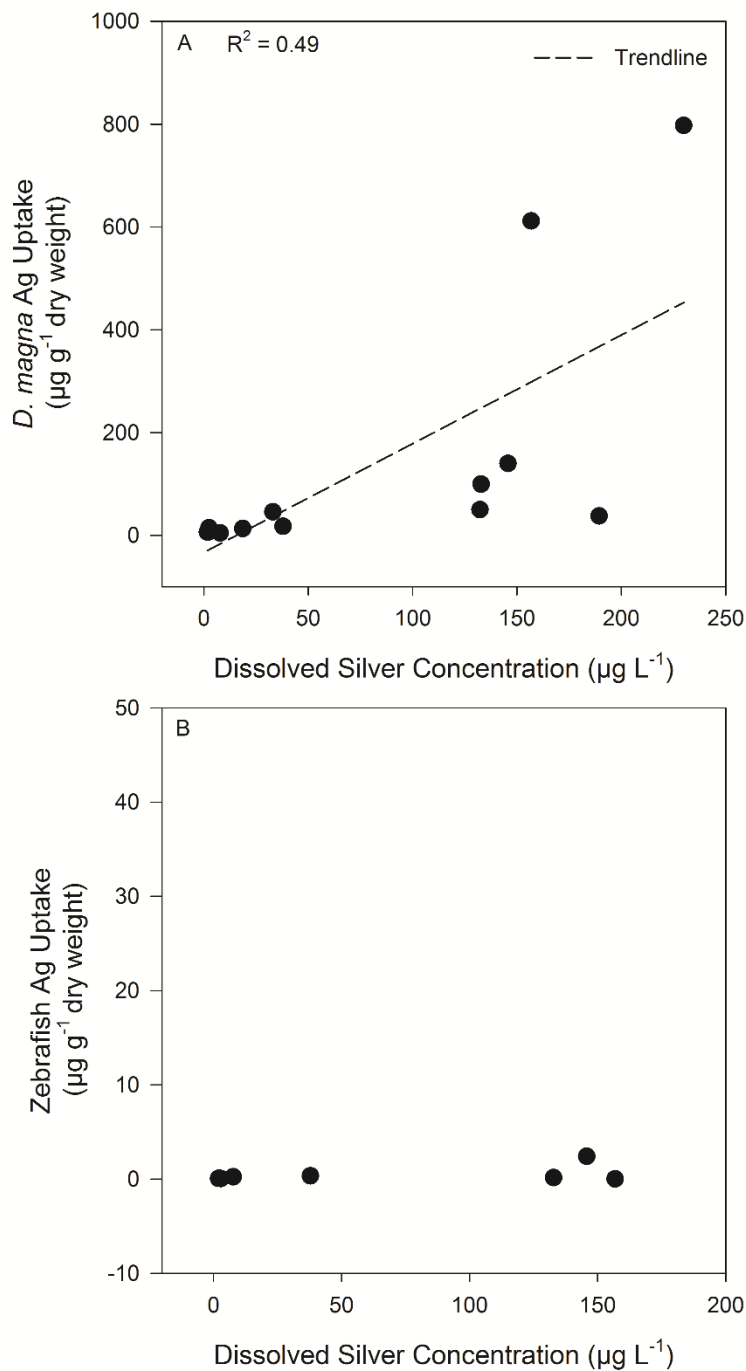
**Figure S5-7.** Percent of zebrafish mortality and malformation following 120-hours exposure to three different surface functionalized silver nanoparticles. \* indicates significant difference from control values. YSE-yolk sac edema; PE-pericardial edema; Circ-circulation.



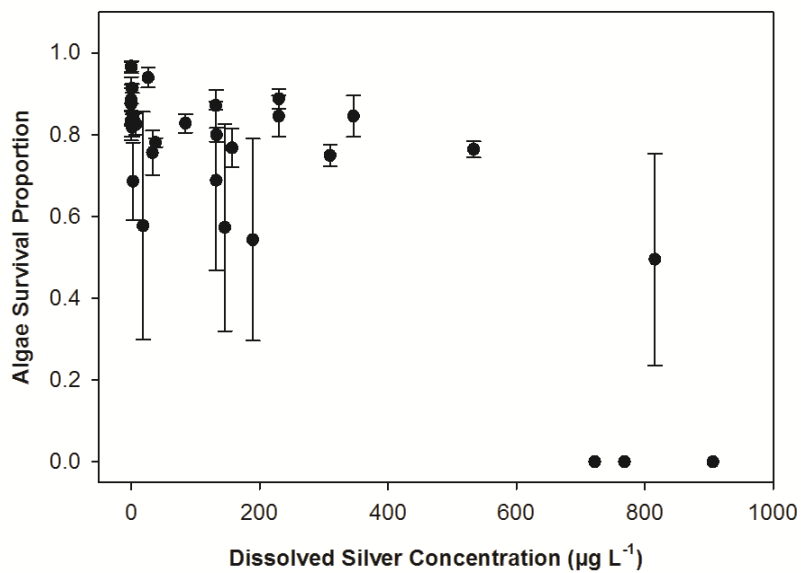
**Figure S5-8.** Ag content (%) in unhatched zebrafish chorion (blue) and fish body (green) with 5 mg L<sup>-1</sup> Si-AgNP exposure after 120 hours under A+B+D+Z exposure scenario.



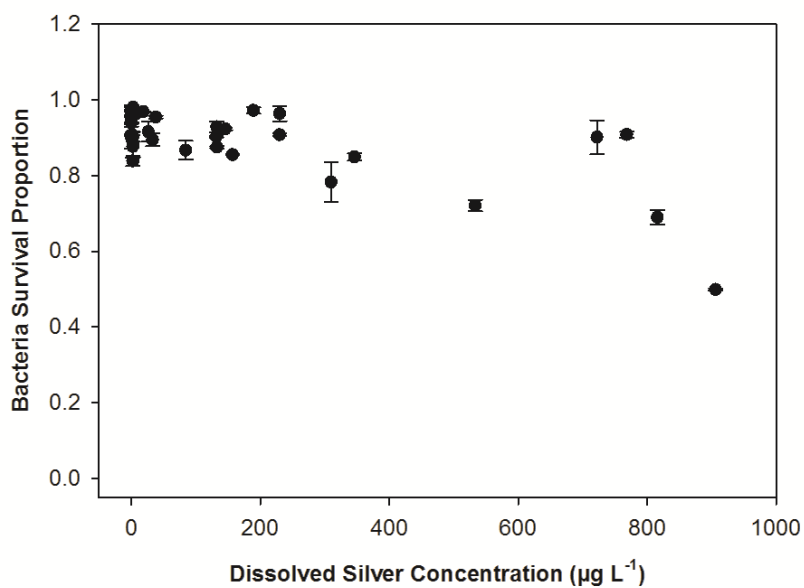
**Figure S5-9.** The relationship between the dissolved Ag concentration in the exposure environment and the *Daphnia* (a) and zebrafish (b) silver uptake.



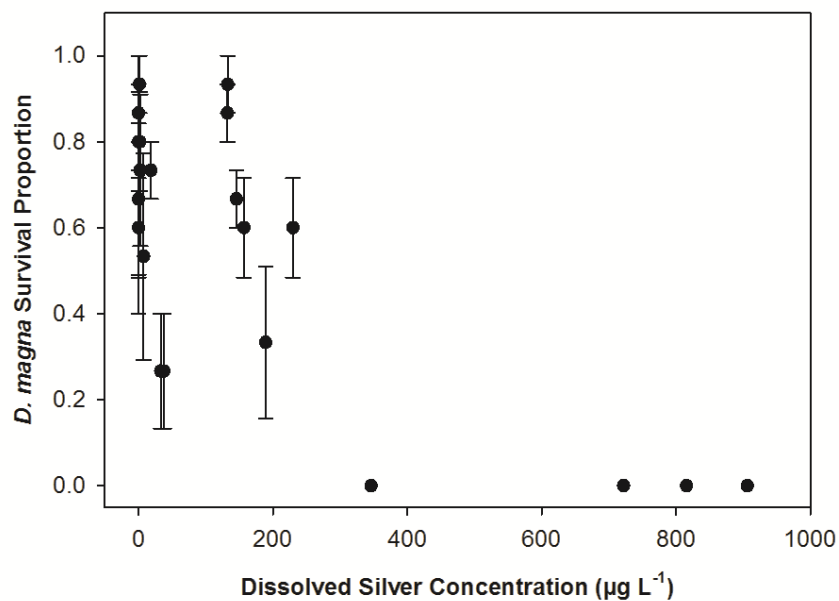
**Figure S5-10.** Concentration-response relationship between the dissolved Ag concentration in each exposure nanocosm and algal survival.



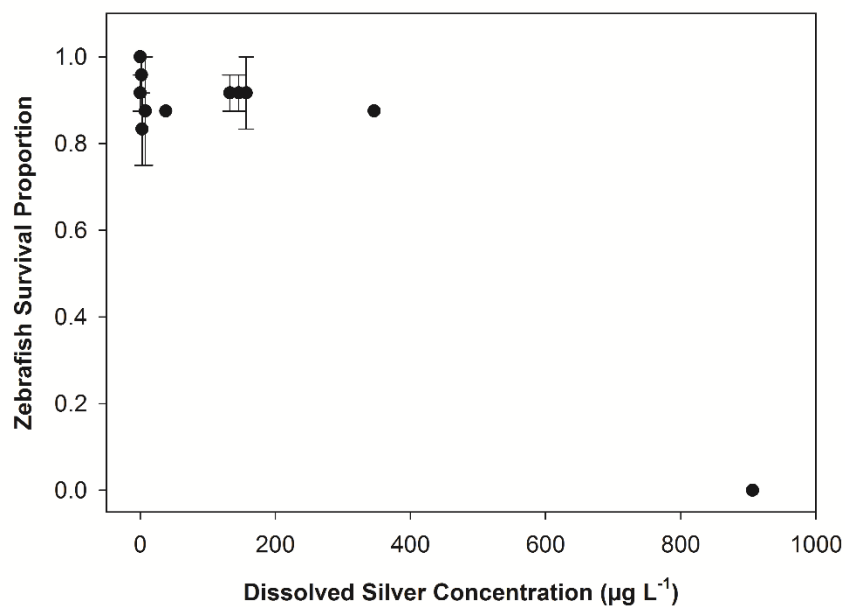
**Figure S5-11.** Concentration-response relationship between the dissolved Ag concentration in each exposure nanocosm and bacterial survival.



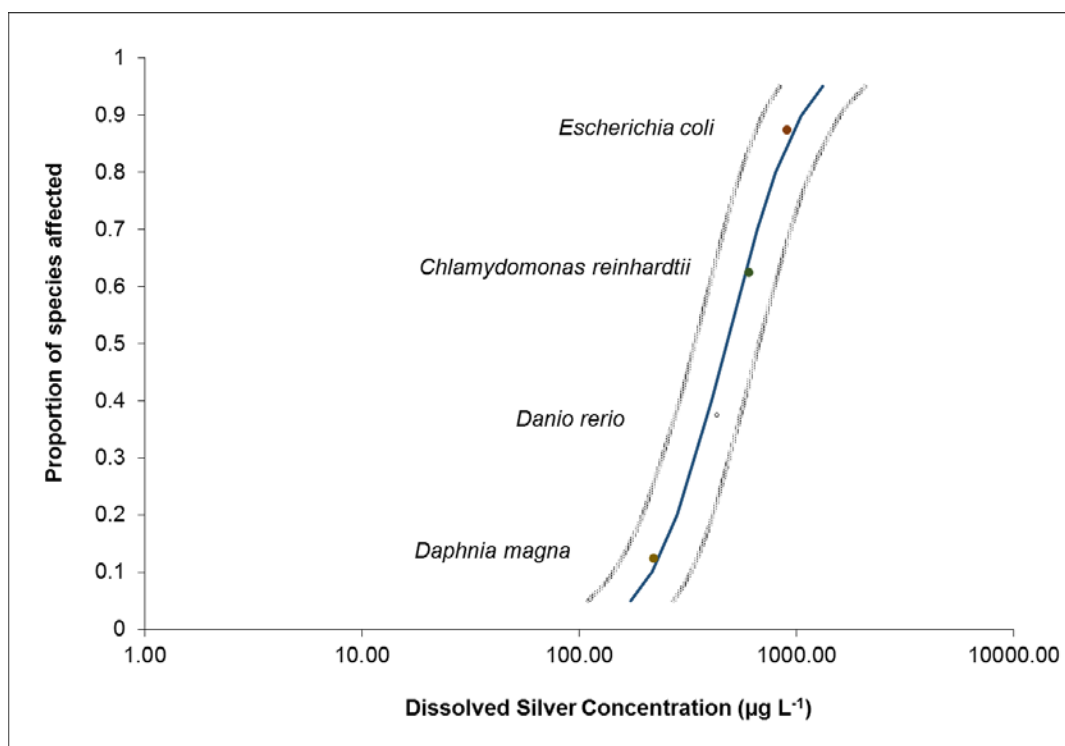
**Figure S5-12.** Concentration-response relationship between *D. magna* survival and the dissolved Ag concentration in each exposure nanocosm.



**Figure S5-13.** Concentration-response relationship between zebrafish survival and the dissolved Ag concentration in each exposure nanocosm.



**Figure S5-14.** Species sensitivity distributions (SSDs) of organisms in nanocosm using the mean  $LC_{50}$  value calculated from Table 2 and the dissolved Ag concentration in the exposure vessels.



## **Chapter 6. Evaluation of Cu and CuO nanoparticle environmental impacts using laboratory small scale microcosms**

*Fan Wu<sup>1</sup>, Lindsay Denluck<sup>2</sup>, Bryan J. Harper<sup>2</sup>, Stacey L. Harper<sup>1,2,3\*</sup>*

<sup>1</sup>School of Chemical, Biological and Environmental Engineering, Oregon State University, Corvallis, OR, United States; <sup>2</sup>Department of Environmental and Molecular Toxicology, Oregon State University, Corvallis, OR, United States; <sup>3</sup>Oregon Nanoscience and Microtechnologies Institute, Eugene, Oregon, United States

Submittal expected June 2017



## 6.1 Introduction

Copper based nanoparticles (NPs) are widely used in industrial and commercial products as sensors (49%), catalysts (20%), surfactants (6%), antimicrobials (4%), and for other purposes (21%) (Ebrahimnia-Bajestan, Niazmand et al. 2011; Bondarenko, Juganson et al. 2013; Xiao, Vijver et al. 2015). The high production volume and increasing use of copper based NPs make their ecological risk a concern. The aquatic environment is particularly at risk to engineered nanomaterials as is it a natural sink for pollutants and a natural vehicle for pollutant migration, including those copper based NPs entering wastewater streams following industrial and commercial use (Nowack and Bucheli 2007; Scown, Van Aerle et al. 2010; Keller and Lazareva 2013). Currently, their toxicity to individual species is demonstrated to multiple target organisms (Bondarenko, Juganson et al. 2013). Some have concluded that ionic Cu released from copper based NPs is the main mechanism of toxicity to a variety of aquatic organisms and can cause profound negative ecological effects (Griffitt et al., 2007; Hua et al., 2014; Misra et al., 2014; Buffet, Richard et al. 2013). Others have found and have even suggested synergism exists when both ions and nanoparticles are present (Lopes et al., 2016). It is still unclear whether copper based NM toxicity is driven primarily by ionic or particulate effects, or a combination of the two.

Commonly used copper based NPs are composed of metallic copper or copper oxide (Cu and CuO NPs), however, their environmental toxicity can vary dramatically. For instance, the reported LC<sub>50</sub> values for Cu NPs in developing zebrafish range from 0.22 – 24 mg L<sup>-1</sup> (Bai et al., 2010; Chen et al., 2011; Griffitt et al., 2007; Hua et al., 2014; Kovrižnych et al., 2013; Song et al., 2015), while CuO NPs are significantly less toxic, with values reported between 64 – 840 mg

L<sup>-1</sup> (Ganesan et al., 2016; Heinlaan et al., 2016; Kovřížnych et al., 2013; Lin et al., 2011).

Metallic Cu and CuO are insoluble in aqueous solutions at neutral pH, yet Cu ion release is commonly detected from copper-based nanomaterials (Al-Bairuty et al., 2016; Kent and Vikesland, 2016; Lin et al., 2015). The dissolution of metallic Cu can generate reactive oxygen species (Olszowka et al., 1992), while the dissolution of CuO is unclear. In addition, Cu NPs can form a thin oxidized surface layer while aged in the ambient environment and transform the surface reactivity of the particle. Aged Cu NPs can have unique surface chemistry from the formation of multiple oxide phases and altered adsorption properties (Mudunkotuwa, Pettibone et al. 2012). Additionally, Cu NPs and CuO NPs may have different aggregation tendencies even if primary particle size is held constant due to the difference in their surface reactivity. Moreover, any alteration to the available surface of the NP can alter its ability to release toxic Cu ions (Bian, Mudunkotuwa et al. 2011). It is therefore possible that Cu NPs and CuO NPs can elicit different toxicities to aquatic organisms.

Environmentally relevant nanomaterial ecotoxicity assessments are essential to evaluate the risks of engineered NMs, but are difficult to conduct due to the intense consumption of resources they require (time-consuming, labor-intensive, expensive, etc.). Thus, there remains a large gap in our understanding of ecological impacts of NMs, and single species toxicity testing lacks environmental relevance making it difficult to truly define the ecotoxicity of NMs (Bernhardt, Colman et al. 2010). Alternatively, large scale mesocosms are environmentally relevant, but prohibitive in cost, time, and resources and require massive amounts of material, space, and animals. Rapid alternative testing strategies are necessary to close this data gap and prioritize NMs for more intensive investigation.

To test and compare the ecotoxicological impacts of Cu NPs and CuO NPs, we employed our previously successful nanocosm assay in which four species (bacteria, algae, crustacean, and fish) in a small-scale microcosm environment are used to rapidly evaluate fate and toxicity of NMs (Wu, Harper et al. 2017). Previously, we found that increased community complexity can mitigate the toxicity of dissolvable NMs when compared to individual species exposures due to environmental resistance. Here, we hypothesize that Cu NPs and CuO NPs can elicit differential toxicity to nanocosms due to the alteration in dissolved Cu and organismal uptake. We use copper chloride as an ionic control to determine the relative contribution of Cu ions to uptake and toxicity.

## **6.2 Materials and Methods**

### *6.2.1 Nanoparticle characterization*

CuO NPs and CuCl<sub>2</sub> were purchased from Sigma Aldrich (St. Louis, MO, USA), and Cu NPs were purchased from Aelfa Aesar (Ward Hill, MA, USA). Both Cu and CuO NPs are <50 nm, where Cu NPs contain 2 nm oxidized layers. Hydrodynamic diameter (HDD) and zeta potential (ZP) were measured by dynamic light scattering using a Malvern Zetasizer (Nano ZS, Malvern Instruments, Worcestershire, UK) every 24 hours up to 120 hours at 10 mg L<sup>-1</sup>. HDD and ZP were measured in exposure media, hereafter referred to as nanocosm media (NCM). Two experimental replicates were prepared and each measurement was taken in triplicate.

### 6.2.2 Exposure setup and toxicity evaluation

The detailed culture information for *C. reinhardtii*, *E. coli*, *D. magna* and embryonic zebrafish (*D. rerio*) and setup procedures can be found in Wu et al. (Wu, Harper et al. 2017). Triplicate nanocosm flasks were prepared for Cu NP and CuO NP exposures at concentrations at 0, 0.1, 1, 5 or 10 mg Cu L<sup>-1</sup>. CuCl<sub>2</sub> was used as an ionic comparison, and the concentrations were determined based on the measured higher dissolved Cu concentrations from NP exposures at 1 (0.47 mg Cu L<sup>-1</sup>), 5 (1.97 mg Cu L<sup>-1</sup>), and 10 mg L<sup>-1</sup> (2.69 mg Cu L<sup>-1</sup>).

Algal and bacterial viability were measured as proportion of live:dead every 24 hours during the experiment. 200 µL of sample from each exposure flask with 0.2 µL SYTOX green dead cell stain (Life Technologies, Grand Island, NY) were incubated in the dark for 15-20 minutes prior to being analyzed via flow cytometry. *D. magna* mortality was recorded daily. At the end of the 120 hour experimental period, live daphnids were removed from the experimental flasks and imaged using an Olympus SC100 high-resolution digital color camera (Olympus Corporation, Center Valley, PA). Zebrafish embryo hatching rate and mortality were monitored daily. At the end of the five-day exposure, zebrafish embryos were examined under a dissecting microscope for malformations (body axis, brain, heart, eyes, fins, jaw, trunk, and somite), physiological abnormalities (pigmentation, impaired circulation, pericardial edema, and yolk sac edema), and the presence of a touch response. Zebrafish developmental stage at our experimental temperature was corrected using equation 6.1:

$$H_T = \left( \frac{h}{0.055T - 0.57} \right) \quad (\text{equation 6.1})$$

where  $H_T$  represents the hours of development at temperature  $T$ , and  $h$  represents the hours of development to reach that stage at 28.5 °C (Kimmel, Ballard et al. 1995).

### *6.2.3 Dissolution and organism uptake measurements*

Abiotic Cu NP and CuO NP dissolution in the NCM was measured by collecting 0.5 mL of a 10 mg L<sup>-1</sup> suspension at 0 hours and repeated at 24, 72, and 120 hours. Biotic dissolution was measured at the end of 120-hour period by gently agitating the nanocosms prior to sampling to resuspend any settled NPs, then collecting a 0.5 ml sample from each replicate nanocosm flask and centrifuging at 8,000×g for 10 minutes through 3kDa membrane centrifugation tubes. After centrifugation, 0.45 ml of the filtered media was transferred to a polystyrene tube and stored at -4 °C until sample digestion.

Cu uptake by organisms was measured following toxicological observations at the end of the experiment. Dead daphnids and zebrafish were removed and were not evaluated. Individual daphnids and zebrafish were rinsed three times with Milli-Q water to remove loosely attached algae, bacteria, and NPs. Unhatched zebrafish were dissected to remove the chorionic membrane. Chorionic membranes, zebrafish embryos, and daphnids were stored at -4 °C in polystyrene tubes until acid digestion was performed to prepare the samples for inductively coupled plasma optical emission spectrometry (ICP-OES) analysis of Cu content. Samples were thawed and digested in teflon tubes at 200 °C with 3 ml 70% trace-metal grade nitric acid.(Kim, Truong et al. 2013) The acid was evaporated and the process repeated a total of three times. Trace-metal grade nitric acid (0.3 ml) was added to each teflon tube while the tube was still hot, followed by 4.7 ml Milli-Q

water, bringing the final sample volume to 5 ml with a final concentration of 3% nitric acid. Copper ICP standards were purchased from RICCA Chemical Company (Arlington, TX). All samples were measured in triplicate. *D. magna* mean dry mass was obtained from the mean weight of 6 groups of daphnids (each group containing 10 daphnids). Zebrafish dry mass was estimated based on work by Hachicho et al. 2015, using the normalized development at the experimental temperature of 20.5 °C (Hachicho, Reithel et al. 2015).

#### 6.2.4 Statistics

Dissolved Cu concentration released from Cu NPs and CuO NPs in NCM and dissolved Cu in nanocosms at 120 hours were compared using one way ANOVA. The abiotic dissolution of Cu NPs and CuO NPs was compared using one way ANCOVA. The dissolution rate ( $k$ ) and maximum dissolved Cu ( $[Cu_{diss}]_{max}$ ) was calculated by fitting a first order reaction (equation 6.2):

$$[Cu_{diss}] = [Cu_{diss}]_{max} [1 - e^{-kt}] \quad (\text{equation 6.2})$$

Algal and bacterial growth rates were modelled using a three parameter logistic model (equation 6.3):

$$M = \frac{k}{(1 + (\frac{k}{M_0 - 1})) \times e^{-rt}} \quad (\text{equation 6.3})$$

where  $r$  is the specific growth rate ( $h^{-1}$ ),  $t$  is the time (hour),  $k$  represents the maximum capacity of cells,  $M_0$  is the initial cell counts at  $t = 0$ , and  $M$  represents the cell count at  $t = t$ . (Paine, Marthews

et al. 2012) Algal and bacterial survival was corrected using equation 6.4 to compensate for possible differences in the surviving proportion of organisms occurring post-treatment:

$$\text{Corrected survival \%} = \left( \frac{n_{Cb} \times n_{Ta}}{n_{Ca} \times n_{Tb}} \right) \times 100 \quad (\text{equation 6.4})$$

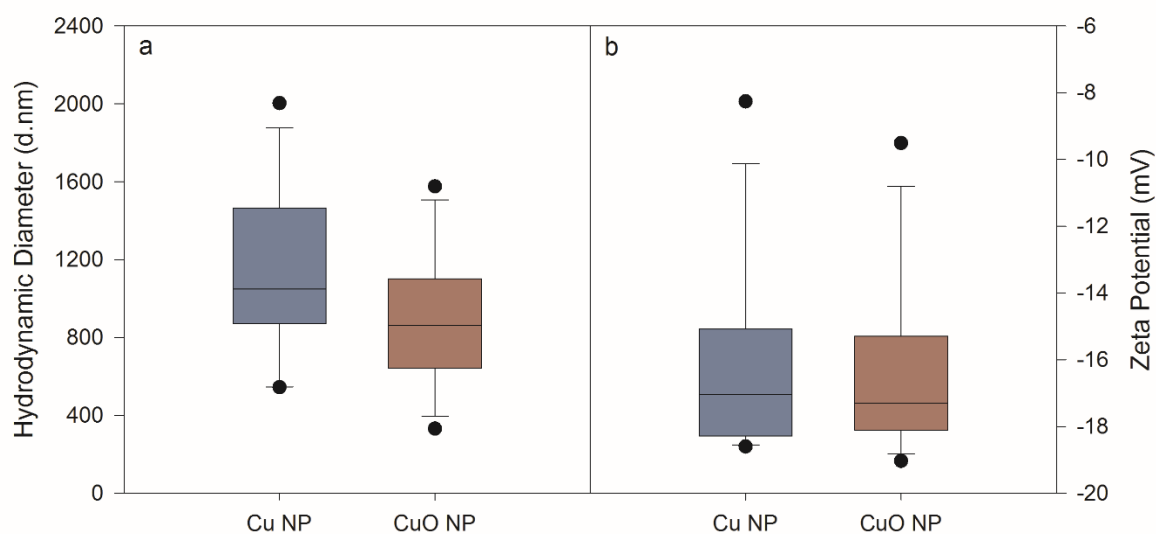
where  $n_C$  is the survival proportion (live cell/total cell) in the control group,  $n_T$  is the survival proportion in the treatment group, and a and b designate after and before treatment, respectively. (Henderson and Tilton 1955) SigmaPlot version 13.0 (Systat Software, San Jose, CA, USA) was used to perform statistical analyses. The corrected algal and bacterial cell mortality in the presence of NPs was compared to control responses using a Kruskal-Wallis rank sum test followed by a Tukey post-hoc test. The growth rates of algae and bacteria were calculated in SAS 9.3 (SAS Institute, Cary NC) using a sigmoid growth model (Gauss-Newton method). (Nyholm and Källqvist 1989) *D. magna* survival among the control and treatments was compared using a two-way ANOVA with a Tukey post-hoc test. Developmental abnormalities in zebrafish were compared between treatments and the corresponding controls using a Fisher's exact test. All differences were considered statistically significant at  $p \leq 0.05$  for all analyses.

## 6.3 Results

### 6.3.1 NP characterization

HDD and ZP of Cu NPs and CuO NPs were characterized in NCM at  $10 \text{ mg L}^{-1}$  over 120 hours (Figure S6-1). Figure 6-1 represents the HDD and ZP throughout 120 hour period based on the peak HDD measured. Both NPs had significant agglomeration from their primary particle size though size and ZP did not change over time and was not significantly different between

particles. The average HDD of Cu NPs was  $1137.1 \pm 123.8$  nm, and their corresponding ZP was  $-16.1 \pm 0.84$  mV. CuO NPs had an average HDD of  $900.4 \pm 100.9$  nm with an average ZP of  $-16.5 \pm 0.76$ .



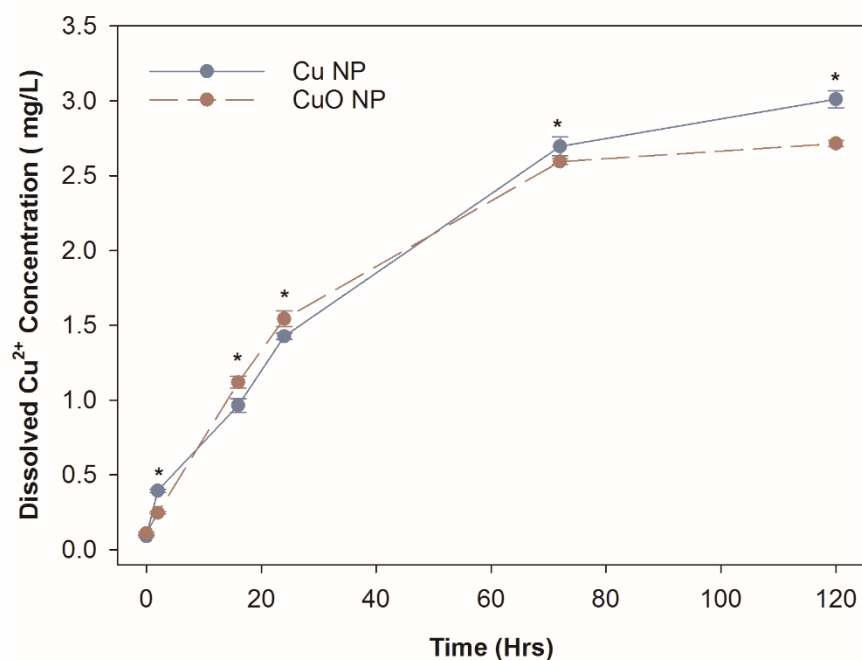
**Figure 6-1.** Hydrodynamic diameter (a) and zeta potential (b) of Cu and CuO NP measured in nanocosm media at  $10 \text{ mg L}^{-1}$  averaged over five days.

### 6.3.2 Dissolved Cu measured in abiotic and biotic environment

The abiotic dissolution of Cu and CuO NPs were measured over 120 hours (Figure 6-2). No difference was seen between the two trends when compared via one-way ANCOVA, though differences were statistically different when comparing individual time points between particles. CuO NPs showed significantly higher dissolved Cu concentration than Cu NPs at 16 and 24 hours, and Cu NPs had higher dissolution than CuO NPs at 2, 72, and 120 hours. To obtain the

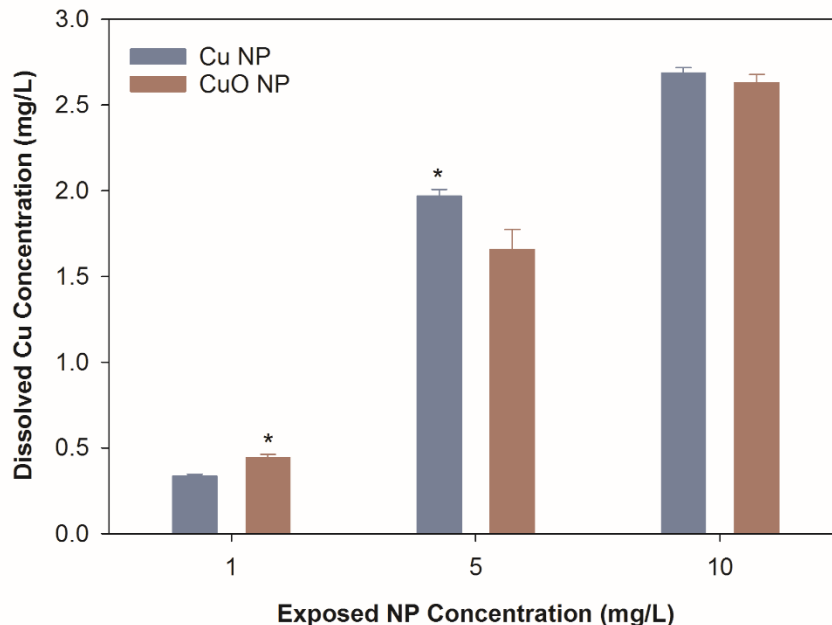


dissolution rates and maximum dissolved Cu, a first order exponential model was used to fit the measured Cu concentrations. The dissolution rates and predicted maximum dissolved Cu released when they reach a plateau are shown in Table S6-1. The dissolution rate suggests that CuO NPs released ions more rapidly than Cu NPs. However, the final dissolved Cu concentration was predicted to be much higher in the Cu NPs group than CuO NP when reaching plateau (14.3% higher).



**Figure 6-2.** Abiotic Cu NP and CuO NP dissolution were measured in nanocosm media at  $10 \text{ mg L}^{-1}$ . \* indicates significantly different between Cu and CuO NPs at each time point. Error bar represents standard error of three sample replicates.

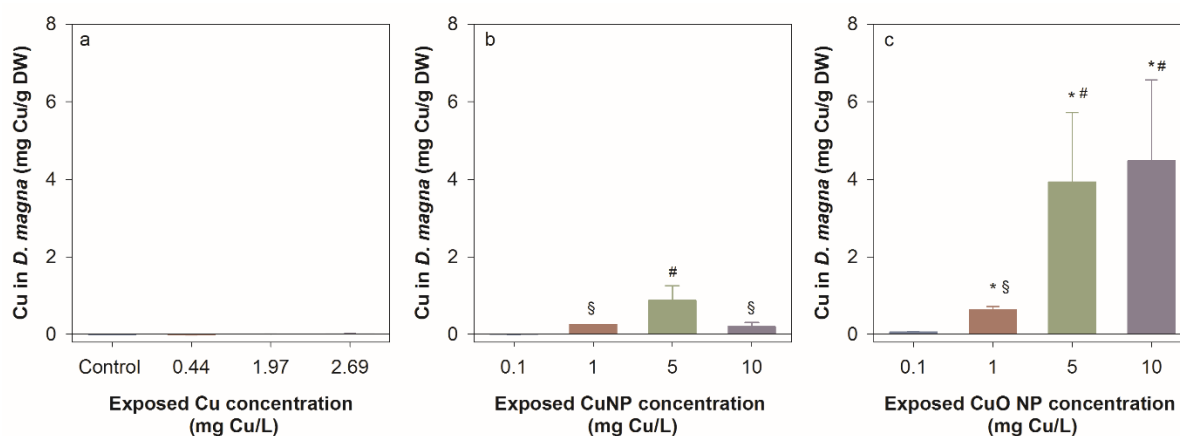
The final dissolved Cu concentration measured in each exposed nanocosm (biotic) is shown in Figure 6-3. At 1 mg Cu/L, CuO NP exposures had more detectable dissolved Cu than Cu NP exposures. However, at 5 mg Cu/L, Cu NP exposures had higher dissolved Cu. There was no difference in detected dissolved Cu between Cu NP and CuO NP exposures at 10 mg Cu/L. In addition, the dissolved Cu concentrations in abiotic environment measured at 10 mg Cu/L was significantly decreased for Cu and CuO NPs compared to those in the abiotic environment at 120 hour (Figure 6-2). For CuCl<sub>2</sub> exposures, the measured total Cu concentrations decreased by 11.4% and 10.3% than the initial Cu exposed (1.97 mg L<sup>-1</sup> and 2.69 mg L<sup>-1</sup>) in the biotic nanocosm environment after 120 hour.



**Figure 6-3.** Dissolved Cu measured from Cu NPs and CuO NP at 1, 5, and 10 mg L<sup>-1</sup> at 120 hours. \* indicates significant difference between Cu NPs and CuO NPs at the same concentration. Error bar represents standard error of three sample replicates.

### 6.3.3 Cu uptake in *D. magna* and zebrafish

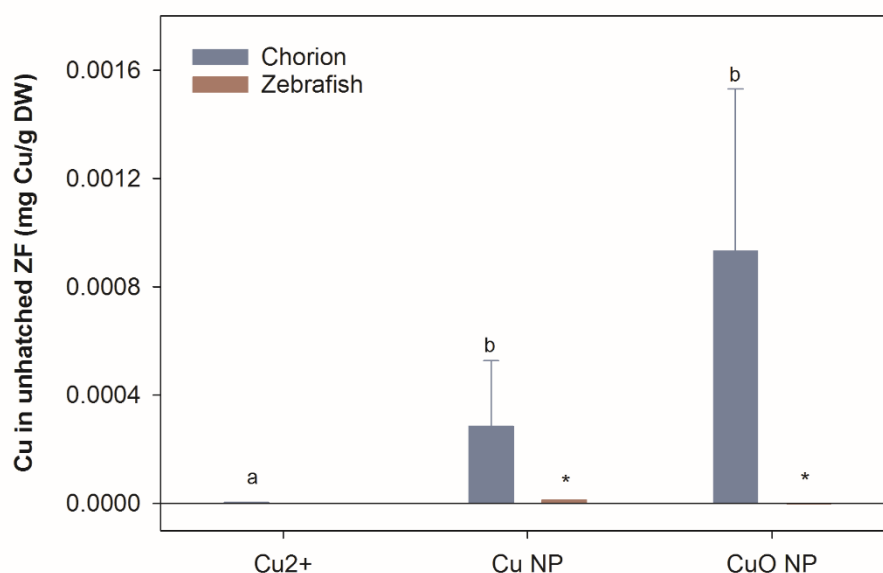
There was no measurable Cu uptake in *D. magna* from CuCl<sub>2</sub> exposures (Figure 6-4a). In comparison, both Cu NP and CuO NP exposure resulted in significant Cu uptake in *D. magna* at 1, 5, and 10 mg Cu/L. This indicates that NPs contributed for the Cu accumulation in *D. magna*. Daphnids exposed to CuO NPs had higher overall Cu uptake than those exposed to Cu NPs at 1, 5, and 10 mg Cu/L.



**Figure 6-4.** Cu uptake in *D. magna* from a) ionic Cu, b) CuO NP, and c) CuO NP at multiple exposure concentration. Error bar represents standard error of three sample replicates. Symbol \$ and # indicate significant difference among exposure concentrations, and \* represents significant difference among type of Cu exposures.

To determine the uptake of Cu in zebrafish, unhatched fish chorions were manually removed and separated from zebrafish for analyzing the Cu content. Large amounts of Cu were

measured in zebrafish chorions relative to zebrafish bodies in both Cu and CuO NP exposures, but not with CuCl<sub>2</sub> exposure (Figure 6-5). In addition, both NPs elicited much higher Cu content in the collected chorions, and CuO NP exposure caused significantly more chorionic accumulation than Cu NP exposure.

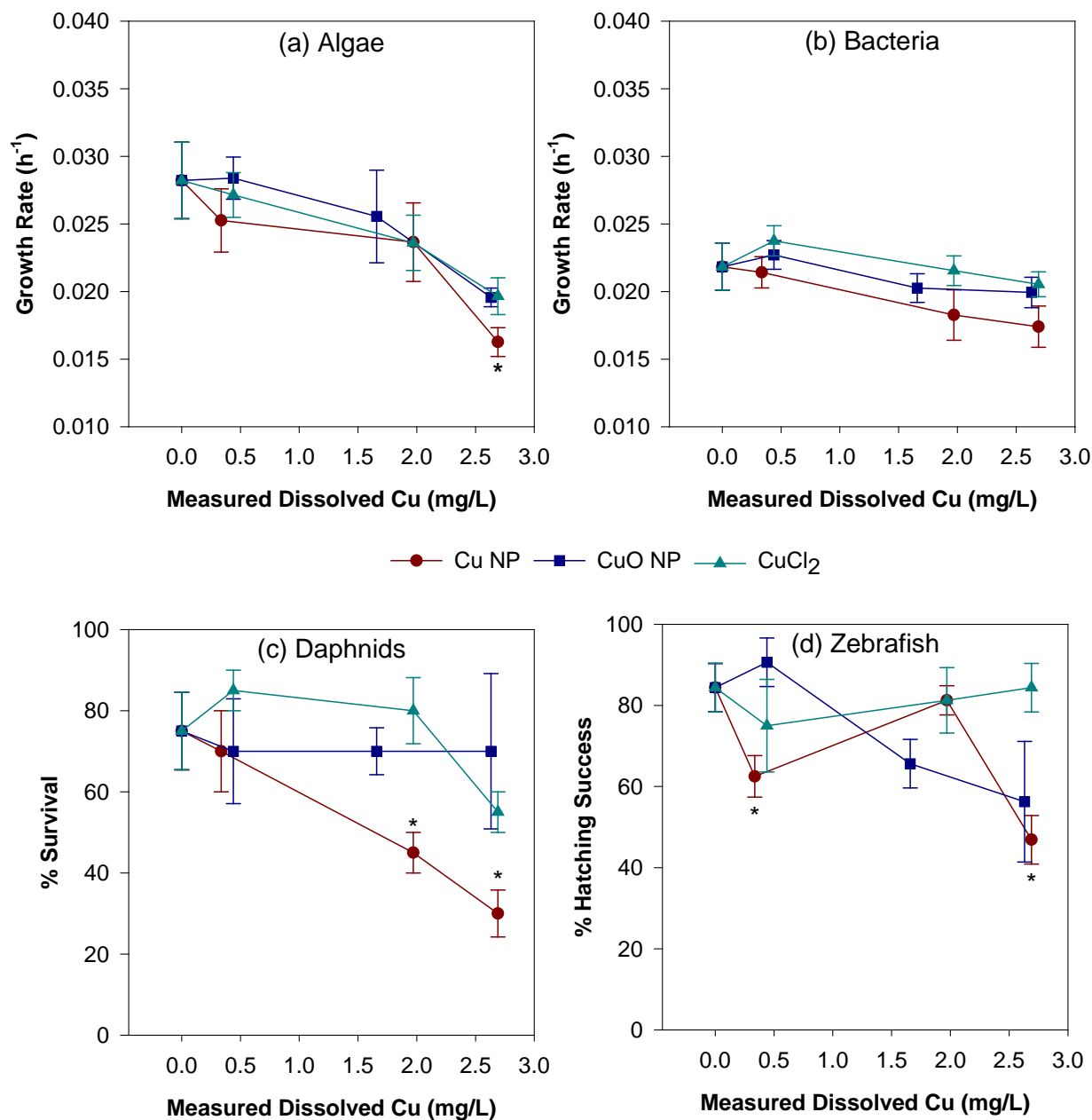


**Figure 6-5.** Cu uptake in manually dethatched chorions (from delay hatched zebrafish) and hatched zebrafish from CuNP, CuO NP, and ionic Cu at 10 mg L<sup>-1</sup>. Error bar represents standard error of three sample replicates. Letters indicate significant difference among exposure concentration, and \* indicates difference between measured Cu in chorion and ZF body.

#### 6.3.4 Toxicity results

Cu NPs elicited significant toxicity to algae, *D. magna*, and zebrafish as measured by the most sensitive observed endpoint. CuO NP and CuCl<sub>2</sub> exposure caused no difference from control. Algae growth rates were significantly decreased with Cu NP exposure at the highest concentration (Figure 6-6a), while bacterial growth rates were not affected by any type of Cu

exposure (Figure 6-6b). Cu NP exposure was the only scenario to cause significant *D. magna* mortality (Figure 6-6c), which occurred at 1.97 mg dissolved Cu/L and 2.69 mg dissolved Cu/L, which is equivalent to 5 and 10 mg Cu/L Cu NP exposure, respectively. CuO NPs and CuCl<sub>2</sub> exposure did not cause mortality that was significantly different from controls. CuO NPs and CuCl<sub>2</sub> did not significantly inhibit zebrafish hatching, while Cu NPs did at 1 and 10 mg Cu/L (Figure 6-6d).



**Figure 6-6.** Toxicity endpoint in each tested organism using the measured dissolved Cu from each exposure type. \* indicates significant difference from corresponding controls (0 mg Cu/L).

## 6.4 Discussion

Our goal was to test and compare the ecotoxicological impacts of Cu NPs and CuO NPs using the nanocosm assay to rapidly evaluate fate and toxicity of NMs in a community environment. We hypothesized that Cu NPs and CuO NPs can elicit differential toxicity to nanocosms due to alterations in dissolved Cu and organismal uptake based on type of NP and used copper chloride as an ionic control to determine the relative contribution of Cu ions. We found that Cu NPs elicit significant toxicity to our nanocosm community and that toxicity is likely due to a particle-specific effect, since the same effects were not observed with dissolved Cu controls.

Abiotic behavior of the two NPs was very similar, with no significant differences in measured HDD or ZP over time and no difference in dissolution trends. Both NPs had significant agglomeration from their primary particle size and formed large agglomerates in solution. This was expected as NPs tend to agglomerate in electrolyte solutions (Badawy, Luxton et al. 2010). In the abiotic environment, the dissolved Cu concentration from Cu NPs was higher than what was found from CuO NPs at 120 hours. The dissolution of Cu based NPs can vary dramatically, depending on the temperature, pH, and ionic strength of the exposure media (Conway, Adeleye et al. 2015). Although there was a significant difference in the dissolution rates and dissolved Cu predicted at equilibrium, the difference (11% higher in Cu NP exposures) was lower than we were expected. This minor difference was likely due to the similar surfaces of the NPs, since the Cu NPs we used here had a 2 nm CuO shell.

The presence of organisms affected the dissolved Cu concentrations in the nanocosm. This could be due to active uptake of dissolved Cu species by the organisms. In addition, Cu and CuO NPs could be coated by extracellular organic species generated by the organisms or associate with microorganisms to decrease the available reactive surface, both of which inhibit dissolution. Phytoplankton-derived soluble extracellular polymeric substances can improve the stability of copper based NPs and influence their dissolution, depending on the pH of the water and  $\text{Cl}^-$  (Adeleye, Conway et al. 2014).

Because of similar dissolution and agglomeration, we expected organism responses to be similar between Cu NPs and CuO NPs due to the dependence of nanomaterial biological interactions on measured parameters. However, NPs elicited different biotic responses in three of the four organisms in our nanocosm. Uptake measurements in both *D.magna* and zebrafish revealed a significant increase in Cu content when exposed to CuO NPs and Cu NPs but not  $\text{CuCl}_2$ . CuO NP uptake appears to be strongly concentration dependent; the same trend is not seen with Cu NPs. In *D. magna*, this is likely due to their filter feeding behavior which could cause accumulation of NPs from the exposure environment. Adam et al. have demonstrated that *D. magna* could accumulate Cu NPs following waterborne exposure (Adam, Leroux et al. 2014). It could also be attributed to trophic transfer from preying on algae and bacteria. We previously demonstrated that CuO NPs can be transferred through the food chain, and accumulate in *D. magna* though preying on NP contaminated algae (Chapter 3). In zebrafish, we found large amounts of Cu and CuO NPs associated with the unhatched fish chorion, but not in the body of the fish, suggesting that the chorion prevented the uptake of Cu and CuO NPs into the zebrafish directly. In addition, it provides strong evidence that the delayed hatching was caused by



blockage of chorion pore by NPs and interference with the hatching enzyme ZHE1 (Lin, Zhao et al. 2013; Muller, Lin et al. 2015). Higher Cu uptake in organisms with CuO NP exposures lead us to hypothesize that the higher Cu content in CuO NP exposed organisms is caused by a higher affinity of CuO NPs to organic ligands than Cu NPs.

The toxicity of all three exposed Cu sources was largely mitigated in the nanocosm compared to the LC<sub>50</sub> values from individual exposures obtained from the literature. For example, ionic Cu exposure were listed as extremely toxic, with mean LC<sub>50</sub>s of 0.024, 0.07, and 0.28 mg Cu/L for crustaceans, algae, and fish species, respectively (Bondarenko, Juganson et al. 2013). In our study, we did not observe significantly higher mortality until 2.69 mg Cu/L exposure to *D. magna*. The lower toxicity observed in the nanocosm exposure is likely due to the presence of organic matter, species interactions, and organismal sinks. Organic matter can affect the toxicity and bioavailability of Cu metals to organisms by complexing metal ions (Kim, Ma et al. 1999). This can mitigate the toxicity by reducing the exposure of freely available ions to the organisms present (Lin, Taylor et al. 2015). We have previously demonstrated that the nanocosm exhibits environmental resistance to contaminants due to species interactions and organism sinks (validated in Chapter 4). The resilience of the community can lead to mitigated toxicity due to the distribution of the exposed Cu to multiple species and lower bioavailable Cu.

Overall, significant higher toxicity was observed with Cu NP exposures. Cu NPs significantly inhibited algal growth rate, *D. magna* survival, and zebrafish hatching while exposure to equivalent concentrations of CuCl<sub>2</sub> and CuO NPs did not. This indicates that Cu NPs themselves elicited particle-specific toxicity to the tested organisms, or a combination effect

from ionic Cu and Cu NPs (Muller, Lin et al. 2015). In addition, metal NPs can cause toxicity by generating reactive oxygen species (ROS) to organisms (Carlson, Hussain et al. 2008; Karlsson, Cronholm et al. 2008). It has been demonstrated that Cu dissolution produces hydrogen peroxide and ROS as a byproduct of the process (Olszowka, Manning et al. 1992). In comparison, the dissolution of CuO NPs does not generate ROS, though intracellular ROS have been detected in other studies (Gunawan, Teoh et al. 2011). The difference in ROS production between both particles likely contributed a large proportion to the different toxicities we observed.

## 6.5 Conclusion

This work addresses the importance of investigating the environmental impacts of NPs in a more environmentally realistic test condition and provided much-needed knowledge about the potential ecological impacts of Cu based NPs. We demonstrated that Cu and CuO NPs have different uptake behavior in organisms and hypothesized that this was due to differences in attachment affinity. Both NPs had higher uptake in *D. magna* and zebrafish than equivalent ionic exposures, and Cu NPs elicited particle specific toxicity to test organisms. Moreover, we identified that Cu NPs can elicit specific adverse impacts to organism communities. This assay can generate large datasets for screening environmental impacts of nanomaterials and inform nanomaterial design and risk management. This proposed testing framework is an effective addition to existing testing paradigms to meet current and future needs of the nanoscience community for rapid evaluations of effects.

## 6.6 Reference

- Adam, N., F. Leroux, et al. (2014). "The uptake of ZnO and CuO nanoparticles in the water-flea *Daphnia magna* under acute exposure scenarios." Environmental Pollution **194**: 130-137.
- Adeleye, A. S., J. R. Conway, et al. (2014). "Influence of extracellular polymeric substances on the long-term fate, dissolution, and speciation of copper-based nanoparticles." Environmental science & technology **48**(21): 12561-12568.
- Badawy, A. M. E., T. P. Luxton, et al. (2010). "Impact of environmental conditions (pH, ionic strength, and electrolyte type) on the surface charge and aggregation of silver nanoparticles suspensions." Environmental science & technology **44**(4): 1260-1266.
- Bernhardt, E. S., B. P. Colman, et al. (2010). "An ecological perspective on nanomaterial impacts in the environment." Journal of Environmental Quality **39**(6): 1954-1965.
- Bian, S.-W., I. A. Mudunkotuwa, et al. (2011). "Aggregation and dissolution of 4 nm ZnO nanoparticles in aqueous environments: influence of pH, ionic strength, size, and adsorption of humic acid." Langmuir **27**(10): 6059-6068.
- Bondarenko, O., K. Juganson, et al. (2013). "Toxicity of Ag, CuO and ZnO nanoparticles to selected environmentally relevant test organisms and mammalian cells in vitro: a critical review." Archives of toxicology **87**(7): 1181-1200.
- Buffet, P.-E., M. Richard, et al. (2013). "A mesocosm study of fate and effects of CuO nanoparticles on endobenthic species (*Scrobicularia plana*, *Hediste diversicolor*)." Environmental science & technology **47**(3): 1620-1628.
- Carlson, C., S. M. Hussain, et al. (2008). "Unique cellular interaction of silver nanoparticles: size-dependent generation of reactive oxygen species." The journal of physical chemistry B **112**(43): 13608-13619.
- Conway, J. R., A. S. Adeleye, et al. (2015). "Aggregation, dissolution, and transformation of copper nanoparticles in natural waters." Environmental science & technology **49**(5): 2749-2756.
- Ebrahimnia-Bajestan, E., H. Niazmand, et al. (2011). "Numerical investigation of effective parameters in convective heat transfer of nanofluids flowing under a laminar flow regime." International journal of heat and mass transfer **54**(19): 4376-4388.
- Gunawan, C., W. Y. Teoh, et al. (2011). "Cytotoxic origin of copper (II) oxide nanoparticles: comparative studies with micron-sized particles, leachate, and metal salts." ACS nano **5**(9): 7214-7225.

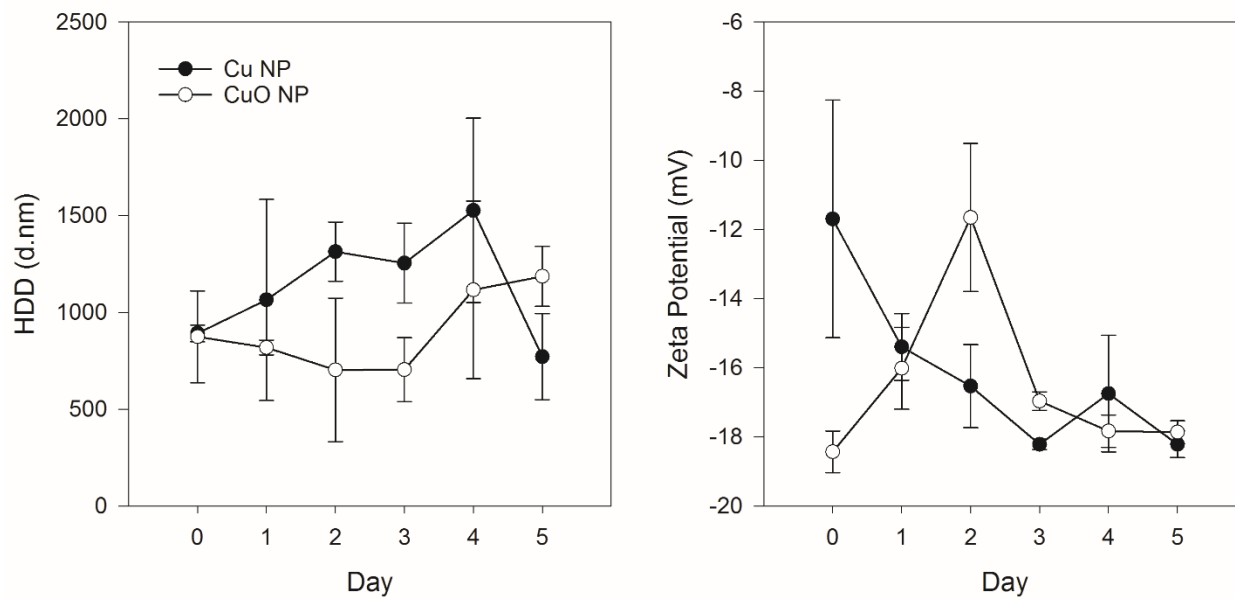
- Hachicho, N., S. Reithel, et al. (2015). "Body mass parameters, lipid profiles and protein contents of zebrafish embryos and effects of 2, 4-dinitrophenol exposure." PloS one **10**(8): e0134755.
- Henderson, C. F. and E. W. Tilton (1955). "Tests with acaricides against the brown wheat mite." Journal of Economic Entomology **48**(2): 157-161.
- Karlsson, H. L., P. Cronholm, et al. (2008). "Copper oxide nanoparticles are highly toxic: a comparison between metal oxide nanoparticles and carbon nanotubes." Chemical research in toxicology **21**(9): 1726-1732.
- Keller, A. A. and A. Lazareva (2013). "Predicted releases of engineered nanomaterials: from global to regional to local." Environmental Science & Technology Letters **1**(1): 65-70.
- Kim, K.-T., L. Truong, et al. (2013). "Silver nanoparticle toxicity in the embryonic zebrafish is governed by particle dispersion and ionic environment." Nanotechnology **24**(11): 115101.
- Kim, S. D., H. Ma, et al. (1999). "Influence of dissolved organic matter on the toxicity of copper to *Ceriodaphnia dubia*: effect of complexation kinetics." Environmental Toxicology and Chemistry **18**(11): 2433-2437.
- Kimmel, C. B., W. W. Ballard, et al. (1995). "Stages of embryonic development of the zebrafish." Developmental dynamics **203**(3): 253-310.
- Lin, S., A. A. Taylor, et al. (2015). "Understanding the transformation, speciation, and hazard potential of copper particles in a model septic tank system using zebrafish to monitor the effluent." ACS nano **9**(2): 2038.
- Lin, S., Y. Zhao, et al. (2013). "Zebrafish high-throughput screening to study the impact of dissolvable metal oxide nanoparticles on the hatching enzyme, ZHE1." Small **9**(9-10): 1776-1785.
- Mudunkotuwa, I. A., J. M. Pettibone, et al. (2012). "Environmental implications of nanoparticle aging in the processing and fate of copper-based nanomaterials." Environmental science & technology **46**(13): 7001-7010.
- Muller, E. B., S. Lin, et al. (2015). "Quantitative adverse outcome pathway analysis of hatching in zebrafish with CuO nanoparticles." Environmental science & technology **49**(19): 11817-11824.
- Nowack, B. and T. D. Bucheli (2007). "Occurrence, behavior and effects of nanoparticles in the environment." Environmental Pollution **150**(1): 5-22.

- Nyholm, N. and T. Källqvist (1989). "Methods for growth inhibition toxicity tests with freshwater algae." Environmental Toxicology and Chemistry **8**(8): 689-703.
- Olszowka, S., M. Manning, et al. (1992). "Copper dissolution and hydrogen peroxide formation in aqueous media." Corrosion **48**(5): 411-418.
- Paine, C., T. R. Marthens, et al. (2012). "How to fit nonlinear plant growth models and calculate growth rates: an update for ecologists." Methods in Ecology and Evolution **3**(2): 245-256.
- Scown, T., R. Van Aerle, et al. (2010). "Review: do engineered nanoparticles pose a significant threat to the aquatic environment?" Critical reviews in toxicology **40**(7): 653-670.
- Wu, F., B. J. Harper, et al. (2017). "Differential dissolution and toxicity of surface functionalized silver nanoparticles in small-scale microcosms: impacts of community complexity." Environmental Science: Nano.
- Xiao, Y., M. G. Vijver, et al. (2015). "Toxicity and accumulation of Cu and ZnO nanoparticles in *Daphnia magna*." Environmental science & technology **49**(7): 4657-4664.

## 6.7 Appendix

**Table S6-1.** The dissolution rates and predicted maximum dissolved Cu released in the exposure media by fitting the measured data using a first order reaction.

Function	Cu NP	CuO NP
$[Cu_{diss}]_{max}$ (mg Cu/L)	$3.20 \pm 0.185$	$2.80 \pm 0.073$
$k$ ( $hr^{-1}$ )	$0.0246 \pm 0.0036$	$0.0334 \pm 0.0025$



**Figure S6-1.** Hydrodynamic diameter (a) and zeta potential (b) of Cu and CuO NP measured in nanocosm media at  $10 \text{ mg L}^{-1}$  over 120 hours.

## **Chapter 7. Monoalkyl tin cluster films: High-resolution patterning materials with low environmental impact under simulated natural conditions**

*Fan Wu<sup>1</sup>, Sumit Saha<sup>2</sup>, Jennie M. Amador<sup>2</sup>, Bryan J. Harper<sup>3</sup>, David Marsh<sup>4</sup>, Douglas A. Keszler<sup>2</sup>, Bettye L.S. Maddux<sup>1,2</sup>, Stacey L. Harper<sup>1, 3</sup>*

*School of Chemical, Biological and Environmental Engineering<sup>1</sup>, Department of Chemistry<sup>2</sup>, Department of Environmental and Molecular Toxicology<sup>3</sup>, Oregon State University; Alfred University<sup>4</sup>*

Submittal Expected June 2017

## 7.1 Abstract

For more than 50 years, the semiconductor industry has relied on polymer resist chemistries to produce ever decreasing feature sizes, which supports the quest for smaller transistors and higher performance integrated circuits. Recently, monoalkyl oxo-hydroxo tin clusters have emerged as a new class of metal-oxide resist to support the semiconductor industry transition to Extreme ultraviolet lithography (EUV) lithography. Under EUV exposure, these tin-based clusters exhibit higher performance and wider process windows than conventional polymer materials. While the environmental toxicity of simple, monomeric dialkyltin and trialkyltin compounds is well documented, the response of living organisms to monoalkyltin clusters is unknown. Here, we explore the toxicity of  $(n\text{-C}_4\text{H}_9\text{Sn})_{12}\text{O}_{14}(\text{OH})_8$  clusters in algae *Chlamydomonas reinhardtii* and crustaceans *Daphnia magna* at exposure concentrations ranging from 0 to 250 mg/L. The clusters have no effect on *C. reinhardtii* growth rate irrespective of cluster concentration, whereas very high cluster concentrations ( $\geq 100$  mg/L) increase *D. magna* immobilization and mortality significantly. To simulate an end-of-life disposal and leachate contamination,  $(n\text{-C}_4\text{H}_9\text{Sn})_{12}\text{O}_{14}(\text{OH})_8$  coated wafers were incubated in water at pH 5.6 and 7.0, each at 20 and 37 °C for 14 and 90 days to investigate leaching rates and subsequent toxicity of the leachates. While small quantities of tin (1.1 – 3.4% of deposited mass) leached from the wafers, it was insufficient to elicit a toxic response, regardless of pH, incubation time, or temperature. The low toxicity of the tin-based thin films shows they can be an environmentally friendly addition to the materials sets useful for semiconductor manufacturing.



## 7.2 Introduction

Organotin compounds have found widespread industrial, commercial, and agricultural uses since the 1980s (Horiguchi 2017), with approximately 30,000 tons of organotin generated annually (Davies and Smith 1980). Trialkyltins are well-known for their powerful toxic action on the central nervous system, and they have been described as “*perhaps the most acutely toxic chemicals to aquatic organisms ever deliberately introduced to water*” (Maguire 1987). They alter fat storage in the freshwater crustacean *D. magna*, impact feeding at  $EC_{50} = 3 \mu\text{g/L}$ , and decrease body length and offspring size at solution concentrations near  $1 \mu\text{g/L}$  (Jordão, Garreta et al. 2016). Dialkyltins exhibit lower toxicity than trialkyltins, but they still can be highly toxic to aquatic organisms. Tributyltin chloride  $(\text{C}_4\text{H}_9)_3\text{SnCl}$ , for example, exhibits a 24-hour  $LC_{50} = 0.95 \mu\text{g/L}$  to *D. magna*, while dibutyltin diacetate  $(\text{C}_4\text{H}_9)_2\text{Sn}(\text{CH}_3\text{COO})_2$ , with a corresponding  $LC_{50} = 0.17 \text{ mg/L}$ , is much less toxic (Kungolos, Hadjispyrou et al. 2004). In addition, dibutyltin and dioctyltin can induce thymus atrophy and their effect on the immune system (Seinen and Willems 1976; Arakawa, Yamazaki et al. 1980; Arakawa 1998). Research evaluated the toxicity of organotin compounds to algae species *Ankistrodemus falcatus* indicates trialkyltin compounds are the most toxic, followed by dialkyl, inorganic, and monoalkyltin species (Wong, Chau et al. 1982). This study is consistent with the general trend in organotin toxicity based on alkyl substitution:  $\text{RSnX}_3$  (monoalkyltin) <  $\text{R}_2\text{SnX}_2$  (dialkyltin) <  $\text{R}_4\text{Sn}$  (tetraalkyltin) <<  $\text{R}_3\text{SnX}$  (trialkyltin) (Kerk, Der et al. 1954; Van der Kerk and Luijten 1956; Winship 1987). In addition, for the same degree of alkyl substitution, the longer chain carbon groups with higher solubility in octanol were more toxic to the algae, as demonstrated by minimum inhibition concentrations:  $\text{Bu}_3\text{Sn}$ :  $0.02 \text{ mg/L}$ ;  $\text{Bu}_2\text{Sn}$ :  $6.8 \text{ mg/L}$ ;  $\text{BuSn}$ :  $25 \text{ mg/L}$ .

The severe toxicity of trialkyl- and dialkyl-tin compounds inevitably raises environmental concerns about new applications and eventual disposal of new alkyltin systems. While simple, molecular monoalkyltin compounds are much less toxic than their di- and tri-alkyltin analogues (Stoner, Barnes et al. 1955), no environmental studies of monoalkyltin compounds in condensed-cluster and thin-film forms have been reported. Grenville and co-workers have recently introduced new monoalkyltin-based oxo-hydroxo clusters and films to support the introduction of EUV lithography in the semiconductor industry (Grenville, Anderson et al. 2015). This work is based on the high EUV absorption cross section of tin and the associated radiolytic efficiency of Sn-C bond scission (Cardineau, Del Re et al. 2014), which together enable transformational patterning performance for production of features at single-digit-nm resolution. These clusters and films are now being distributed to all major semiconductor manufacturers. The Registration, Evaluation, Authorization and Restriction of Chemicals (REACH) regulation dictates chemicals and nanoparticles sold in the European market in volumes greater than one ton per year must be characterized for potential impact on aquatic ecosystems (2006). Herein, we report the first toxicity assessment of a representative nanocluster, i.e.,  $n\text{-C}_4\text{H}_9\text{Sn})_{12}\text{O}_{14}(\text{OH})_8$ , and the leachate of thin films deposited therefrom. The results show the tin clusters to be environmentally benign materials suitable for large-scale use in the semiconductor industry.

## 7.3 Materials and Methods

### 7.3.1 Synthesis of $[(\text{BuSn})_{12}\text{O}_{14}(\text{OH})_6][\text{OH}]_2$ .

$[(\text{BuSn})_{12}\text{O}_{14}(\text{OH})_6][\text{OH}]_2$  was prepared based on slightly modified literature procedures (Eychenne-Baron, Ribot et al. 1998).  $\text{BuSnOOH}$  (20.0 g) and p-toluene sulfonic acid ( $\text{TsOH}$ ) monohydrate (5.77 g) were suspended in toluene and refluxed with a Dean-Stark trap for 48 h. After centrifugation to remove solids, the supernatant was removed under reduced pressure to yield solid  $[(\text{BuSn})_{12}\text{O}_{14}(\text{OH})_6][\text{OTs}]_2$ , which was washed with acetonitrile and allowed to dry in an open container (45% yield). A 20 wt% suspension of  $[(\text{BuSn})_{12}\text{O}_{14}(\text{OH})_6][\text{OTs}]_2$  was created by mixing 2.00 g of  $[(\text{BuSn})_{12}\text{O}_{14}(\text{OH})_6][\text{OTs}]_2$  with 8.00 g isopropanol. Separately a 65-wt% solution of tetramethylammonium hydroxide (TMAH) was prepared by mixing 1.69 g TMAH solution (1 M aqueous concentration) with isopropanol to get a total mass of 2.3 g. With vigorous stirring, the TMAH solution was added all at once to the suspension of  $[(\text{BuSn})_{12}\text{O}_{14}(\text{OH})_6][\text{OTs}]_2$ . After stirring for 30 minutes, the suspension was more homogenous but still remained slightly turbid, and without filtering was placed in a vial in the freezer ( $-20^\circ\text{C}$ ). After 2-3 days, needle shaped crystals of  $[(\text{BuSn})_{12}\text{O}_{14}(\text{OH})_6][\text{OH}]_2$  had formed and were isolated and washed with acetonitrile (28% yield). The structure is shown in Figure S7-1.

### 7.3.2 Film preparation

N-type Si (100) wafers were sourced from Sumco Oregon Corporation;  $\text{SiO}_2/\text{Si}$  substrates with 100 nm of thermally grown  $\text{SiO}_2$  on silicon (100) were obtained from Silicon Valley Microelectronics, Inc. Prior to thin film deposition, all substrates were cleaned thoroughly in a bath of deionized water by sonication. Following this rinse, the surfaces were treated with low-energy  $\text{O}_2$  plasma, creating a clean, hydrophilic surface. Films were spun on 100 nm

thermally grown SiO<sub>2</sub>/Si from 0.04M conc. of [(BuSn)<sub>12</sub>O<sub>14</sub>(OH)<sub>6</sub>][OH]<sub>2</sub> cluster in 2-heptanone. Films were deposited by spin coating the precursor at 3000 rpm for 30s. Film thickness was measured via ellipsometry and modeled using the Cauchy equation over the wavelengths 400-1000nm. Film thickness of these films are ~16 nm.

### 7.3.3 Toxicity testing

(BuSn)<sub>12</sub>(OH)<sub>6</sub> nano-cluster stock solution was prepared at 500 mg L<sup>-1</sup> in ultrapure water (18.2 MΩ·cm at 25 °C) and ultra-sonicated for 1, 6, 16, and 31 minutes at maximum intensity using a VCX 750 Vibra-Cell sonicator (Sonics & Materials Inc., Newtown, CT). The smallest hydrodynamic diameter (HDD) and PDI value were determined at after 1 minutes of sonication (Figure S7-2). Freshly prepared stock solutions were sonicated for 1 minute prior to exposing organisms. TAP media were used for algae exposure media (Gorman and Levine 1965), and *D. magna* exposure media were adapted from the EPA hard water recipe consist of sodium bicarbonate (192 mg L<sup>-1</sup>), calcium sulfate dihydrate (120 mg L<sup>-1</sup>), magnesium sulfate (120 mg L<sup>-1</sup>), potassium chloride (6 mg L<sup>-1</sup>). In algae exposures, the initial algae population density was fixed at 10<sup>4</sup> cells/mL with a final volume of 5 mL in a 15 mL glass vial, and the exposure concentrations of (BuSn)<sub>12</sub>(OH)<sub>6</sub> nano-cluster were 0, 15.6, 31.3, 62.5, 125, 250 mg L<sup>-1</sup>. Stock solution were vortexed every time before exposure to ensure the particles were well-suspended. The vials were placed on shaker table at 120 rpm during the experimental period. Algal viability was measured using SYTOX™ Green Dead Cell Stain (Life Technologies, Grand Island, NY) in conjunction with flow cytometry at 3, 20, 28, 48 and 72 hours. Algae growth rates

were modeled using first order exponential growth model. For *D. magna* acute toxicity testing, (BuSn)<sub>12</sub>(OH)<sub>6</sub> crystals was exposed to 5 neonates (<24 hours) with 10 ml daphnia culture media in a 50 ml plastic beaker with the final concentrations of 50, 100, 125, 150, 175, 200, 225, 250 mg L<sup>-1</sup>. Mortality and immobilization were recorded at 24 and 48 hours. Each treatment was conducted in triplicate. All organisms and experiments were maintained and conducted at 20.5 ± 0.5 °C with a 16:8-h light:dark photoperiod under 1690 ± 246 lux light intensity provided by full-spectrum fluorescent grow lights.

#### 7.3.4 Leachate collection

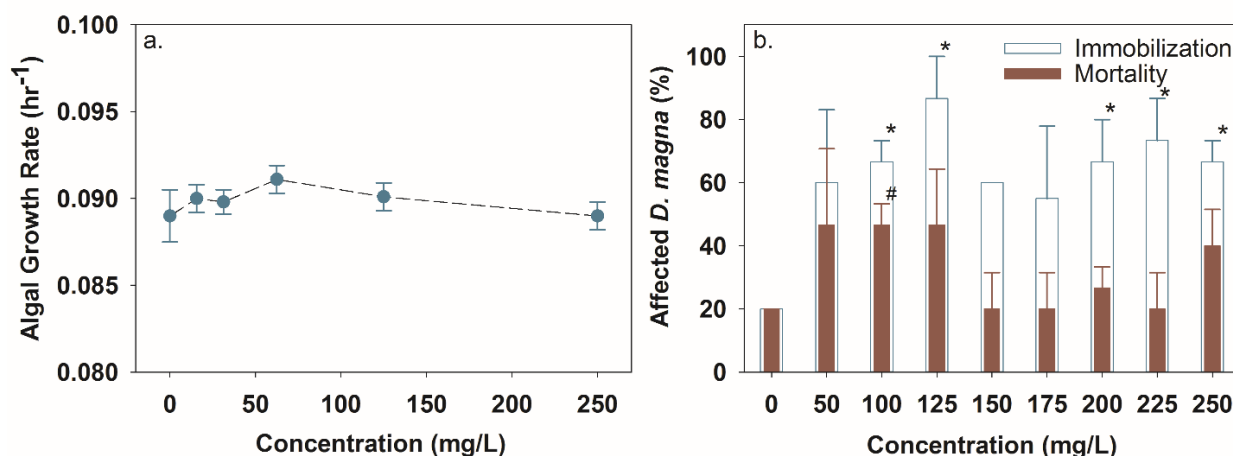
Ultrapure water with 10 mM of HEPES buffer was prepared and the pH was adjusted with 0.5 M NaOH to 5.6 and 7, respectively. Thin films were each placed in 50 ml of four incubation scenarios (a. Temp = 20°C, pH = 7; b. Temp = 20°C, pH = 5.6; c. Temp = 37°C, pH = 7; d. Temp = 37°C, pH = 5.6) (Figure S7-3). Triplicate incubations were prepared for 14 and 90 days of toxicity evaluations and tin leaching kinetics. For toxicity evaluation, collected leachate was first adjusted back to pH 7.0 with 0.5M NaOH solution. 100 times concentrated algae (TAP media) and *D. magna* exposure media (EPA hard water) were diluted using each collected leachate to provide essential nutrients prior to toxicity testing. The toxicity of each collected leachate was evaluated by exposing algae for 72 hour growth evaluation and *D. magna* for 48 hour mortality and immobilization testing. To evaluate tin leaching kinetics, 5 ml of sample from each incubating beaker was taken at day 1, 7, 14, 60, and 90. Water samples were digested with 69% trace grade nitric acid at 200°C prior to ICP-MS analysis.

## 7.4 Results and Discussion

### 7.4.1 Toxicity of $(\text{BuSn})_{12}(\text{OH})_6$ clusters

We investigated the ecotoxicity of the organotin clusters using freshwater algae and plankton. In accordance with OECD standards, we assessed the impact of  $(\text{BuSn})_{12}(\text{OH})_6$  clusters on 72 hours growth inhibition to *C. reinhardtii* and 48 hours immobilization and mortality to *D. magna* using pure clusters at exposure concentrations from 50 to 250 mg L<sup>-1</sup>. Figure 7-1 shows that the organotin clusters had no impact on algal growth rates up to 250 mg L<sup>-1</sup>, whereas *D. magna* immobilization and mortality were significantly increased at high concentrations ( $\geq 100$  mg L<sup>-1</sup>). This is likely due to the high sensitivity of *D. magna* from their unique filter feeding behavior in which they take up suspended particles in the water column. The estimated EC<sub>50</sub> (including both immobilization and mortality) of  $(\text{BuSn})_{12}(\text{OH})_6$  crystals to *D. magna* was  $45.9 \pm 24.4$  mg L<sup>-1</sup>. Large variance in the EC<sub>50</sub> values was likely due to the extreme hydrophobicity of  $(\text{BuSn})_{12}(\text{OH})_6$  clusters and the agglomerates that can form at high concentrations, but which can lead to non-homogeneous bioavailability to target organisms (Hotze, Phenrat et al. 2010). Agglomerate size of the clusters, measured as hydrodynamic diameter (HDD), was lowest after 1 minute of ultra-sonication, but significantly increased over time. This is likely due to the low stability of clusters in water. With more energy input to the suspension, enhanced Brownian motion could boost the collision frequency of clusters and significantly increase the agglomeration behavior of the clusters in solution. Based on the Environmental Protection Agency's Ecotoxicity Categories for Terrestrial and Aquatic Organisms,  $(\text{BuSn})_{12}(\text{OH})_6$  cluster

toxicity would be considered *slightly toxic* to *D. magna* but *practically nontoxic* category for *C. reinhardtii*.



**Figure 7-1.** Toxicity of (BuSn)<sub>12</sub>(OH)<sub>6</sub> clusters measured as *C. reinhardtii* growth rates (a) and *D. magna* immobilization and mortality (b). Error bars represent standard error of three sample replicates. Asterisk (\*) indicates significantly different immobilization and octothorp (#) shows significantly different mortality compared to control.

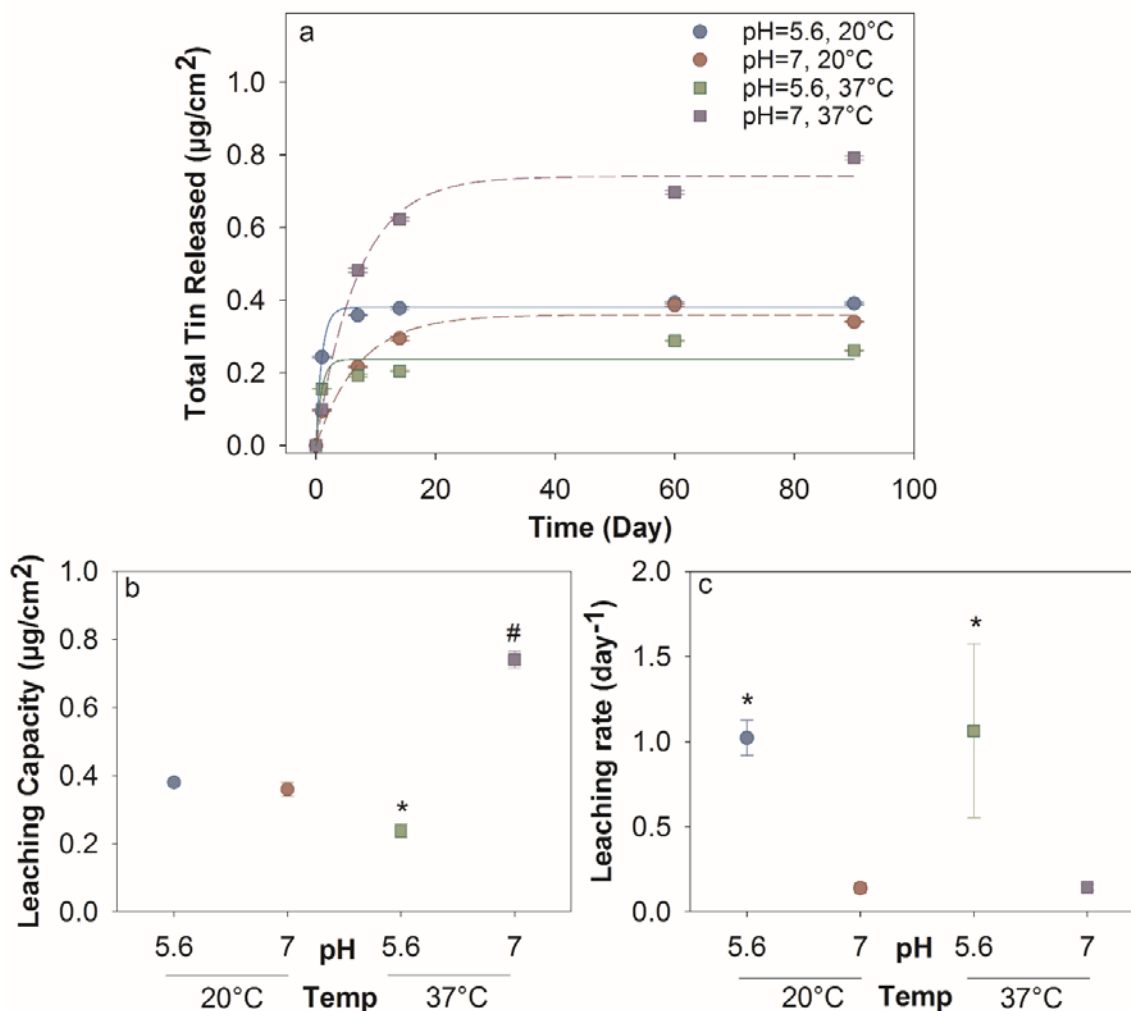
#### 7.4.2 Leachate characterization

A well-designed landfill should have a long residence time (years) for the leachate (LaGrega, Buckingham et al. 2010), but can range from weeks to months depending on the location of the site and its seasonal hydrological dynamics (Mangimbulude, van Breukelen et al. 2009). In addition, pH of landfill leachate can also vary dramatically both spatially and temporally (Christensen, Kjeldsen et al. 2001). Initially, leachate tends to have low pH due to high concentrations of degradable organic compounds and heavy metals, and can be as low as

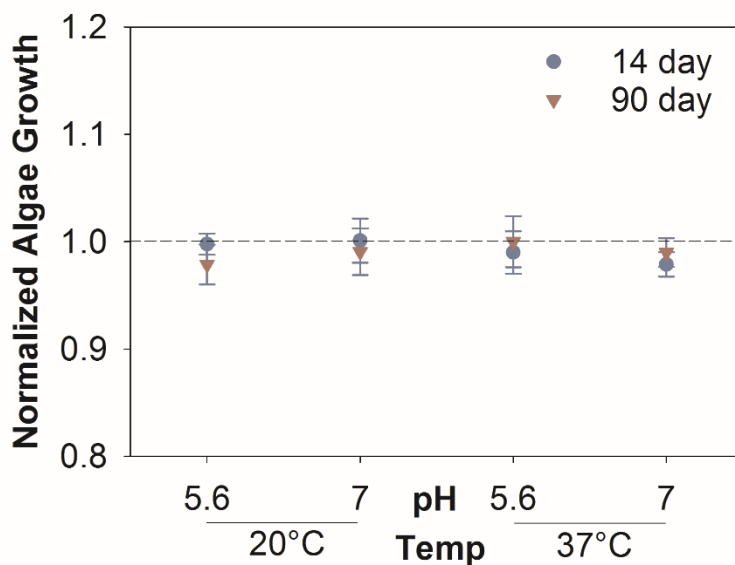
pH 5 in some extreme situations (Renou, Givaudan et al. 2008). Over time, the landfill enters the methanogenic phase, which can produce  $\text{CH}_4$  and thus increase pH. To investigate end-of-life effects of our wafers, we simulated short-term (14 day) and long-term (90 day) leaching scenarios in water with varied pH (5.6, 7.0) and temperature (20, 37°C) to evaluate the stability of the surface coatings and to investigate potential changes in toxicity when leached.

We quantified the leached tin concentration at 1, 7, 14, 30, 60, and 90 days. Significantly more tin leached from the coated wafers compared to control wafers in all four incubation scenarios (Figure S7-4). Tin leaching kinetics was described by a first-order kinetic model (Figure 7-2a). Tin leaching capacity was the highest in the incubation scenario at 37°C, pH = 7 at  $0.74 \mu\text{g}/\text{cm}^2$ , and was lowest at 37°C and pH = 5.6 at  $0.24 \mu\text{g}/\text{cm}^2$  (Figure 7-2b). All four incubation scenarios had relatively rapid tin release from day 0 to day 14; however, the modeled rate suggests that pH is responsible for accelerating tin leaching (Figure 7-2c). After 14 days, tin leaching trends reached a plateau. Overall, the total tin leached from the wafers would be considered to be low. The total mass applied per area ( $1 \text{ cm}^2$ ) of thin film was 23.74 mg of tin, suggesting only 1.1% - 3.4 % of tin released from wafers after 90 days, depending on the incubation scenarios. Thus, it will require a considerable amount of thin films to be disposed in the environment to cause adverse impacts to aquatic species. For instance, it will require at least  $6.2 \text{ m}^2$  of coated wafer incubated in 1 L of water to reach the  $\text{EC}_{50}$  for *D. magna*. Importantly, the tin leaching kinetics show that the released tin concentration reached plateau within the first month, suggesting that longer landfill residence time would have further minimized impact on the continuous tin release.

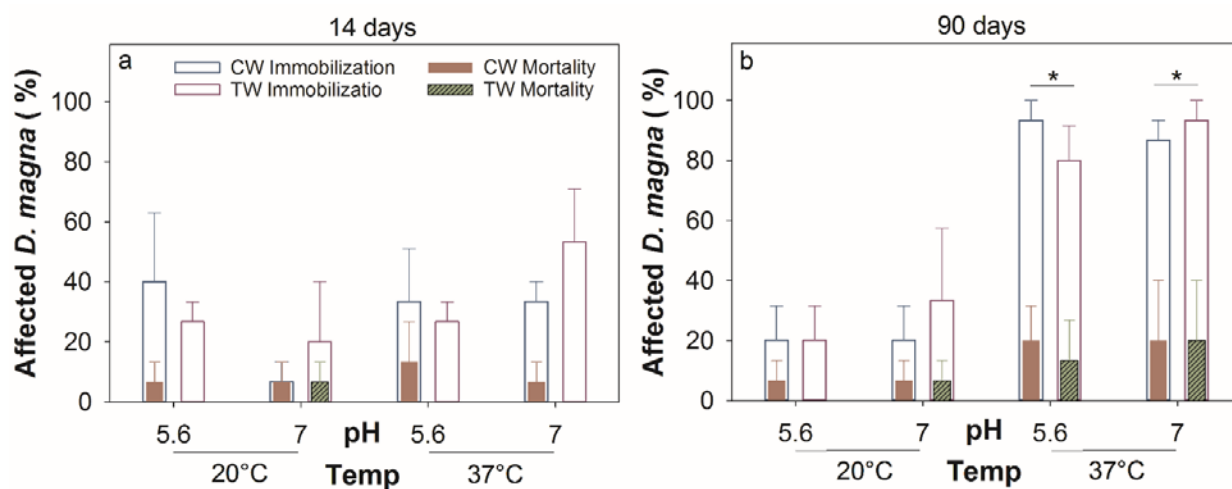




**Figure 7-2.** Releasing kinetic of tin coated wafers (a), modeled leaching capacity over 90 days (b), and the leaching rate of tin from wafers (c) under four different environmental scenarios. Error bars represent standard error of modeled values. Asterisk (\*) indicates significantly higher immobilization and octothorp (#) indicates significantly higher mortality compared to control.



**Figure 7-3.** The ratio of algal growth rates after exposing to control and tin wafer leachate under each incubation scenario. The dash line is the reference line of ratio=1. Error bars represent standard deviation of three replicates of normalized ratios.



**Figure 7-4.** *D. magna* 48-hour immobilization and mortality after exposed to simulated leachate after 14 (a) and 90 (b) days. (CW: Control wafer; TW: Tin wafer). Asterisks (\*) indicate significant difference in algae growth rate between 14 and 90 days incubation with the same type wafer. Error bars represent standard deviation of three replicates.

### 7.4.3 Toxicity of leachate

We evaluated the leachate toxicity in both algae (*C. reinhardtii*) and crustacean (*D. magna*). Algae growth rates in tin leachate were normalized based on each corresponding algae growth rates in control wafer leachate. The normalized ratio provide comparison on the toxicity of collected leachate between control wafers and the tin-coated wafers under the same incubation conditions. A ratio is less than 1 suggests that coated wafers can elicit toxicity to algae through releasing tin compound. However, there was no significant difference in normalized algae growth regardless of the timeframe, pH or temperature. *D. magna* mortality and immobilization after exposure to each collected leachate are shown in Figure 7-4. In Figure 7-4b, significantly higher immobilization was observed with both control and tin coated wafer leachate under 37°C; however, there was no significant difference in *D. magna* mortality and immobilization between the control wafer and tin wafer leachates in any of the incubation conditions.

We observed no significant difference in toxicity between control and tin-coated wafers leachates, and the overall low toxicity was expected since the quantified tin concentrations were substantially lower compared to the concentrations eliciting responses to the nano-clusters alone (Figure 7-1). Toxicity observed from both control (Si 100) and tin coated wafer leachates collected at high temperature indicates that some unknown chemical species was slowly leached out from the original silicon wafers. Further analysis will be performed to identify the toxicity agent.

Environmental degradation has the capacity to further reduce any potential adverse impact of these tin wafers to the environment. The main factors limiting the persistence of  $\text{Bu}_3\text{Sn}$

in aquatic ecosystems and sediments are photolysis and biological degradation. Reported half-life ( $T_{1/2}$ ) of the organotin compounds (butyltins) in water for photolytic decomposition in sunlight is about 89 days (Luijten 1972), and may be as short as 18 days (Slesinger and Dressler 1978), or a week in water exposed to sunlight with microbial degradation (Maguire, Carey et al. 1983; Seligman, Grovhoug et al. 1989). The results of our ecotoxicology and leachate studies provide convincing evidence that our organotin leachate has low toxicity and presents a low hazard to freshwater aquatic organisms. Our  $(\text{BuSn})_{12}(\text{OH})_6$  thin films would be more environmentally friendly than currently used organotin compounds for applications in the semiconductor field.

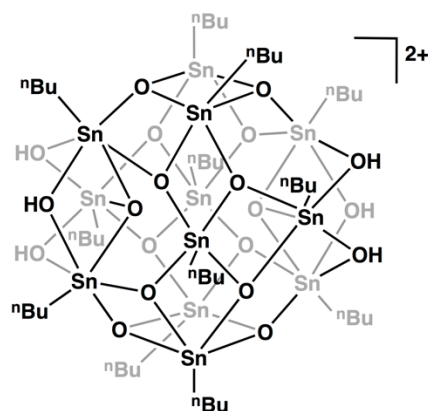
## 7.5 Reference

- European Parliament (2006). Directive of the European Parliament and of the Council. 67/548/EEC. European Union, Official Journal of the European Union. **2006/121/EC**
- Arakawa, Y. (1998). Recent studies on the mode of biological action of di- and trialkyltin compounds. Chemistry of Tin, Springer: 388-428.
- Arakawa, Y., N. Yamazaki, et al. (1980). "Effects of organotin compounds on the immune functions: Atrophy of thymus by di-n-butyltin dichloride." Journal of toxicological sciences **5**(3): 258.
- Cardineau, B., R. Del Re, et al. (2014). "Photolithographic properties of tin-oxo clusters using extreme ultraviolet light (13.5 nm)." Microelectronic Engineering **127**: 44-50.
- Christensen, T. H., P. Kjeldsen, et al. (2001). "Biogeochemistry of landfill leachate plumes." Applied geochemistry **16**(7): 659-718.
- Davies, A. G. and P. J. Smith (1980). "Recent advances in organotin chemistry." Advances in inorganic chemistry and radiochemistry **23**: 1-77.
- Eychenne-Baron, C., F. Ribot, et al. (1998). "New synthesis of the nanobuilding block  $\{(\text{BuSn})_{12}\text{O}_{14}(\text{OH})_6\}^{2+}$  and exchange properties of  $\{(\text{BuSn})_{12}\text{O}_{14}(\text{OH})_6\}(\text{O}_3\text{SC}_6\text{H}_4\text{CH}_3)_2$ ." Journal of organometallic chemistry **567**(1): 137-142.
- Gorman, D. S. and R. Levine (1965). "Cytochrome f and plastocyanin: their sequence in the photosynthetic electron transport chain of *Chlamydomonas reinhardtii*." Proceedings of the National Academy of Sciences **54**(6): 1665-1669.
- Grenville, A., J. T. Anderson, et al. (2015). Integrated fab process for metal oxide EUV photoresist. SPIE Advanced Lithography, International Society for Optics and Photonics.
- Horiguchi, T. (2017). Contamination by Organotins and Its Population-Level Effects Involved by Imposex in Prosobranch Gastropods. Biological Effects by Organotins, Springer: 73-99.
- Hotze, E. M., T. Phenrat, et al. (2010). "Nanoparticle aggregation: challenges to understanding transport and reactivity in the environment." Journal of environmental quality **39**(6): 1909-1924.
- Jordão, R., E. Garreta, et al. (2016). "Compounds altering fat storage in *Daphnia magna*." Science of the Total Environment **545**: 127-136.

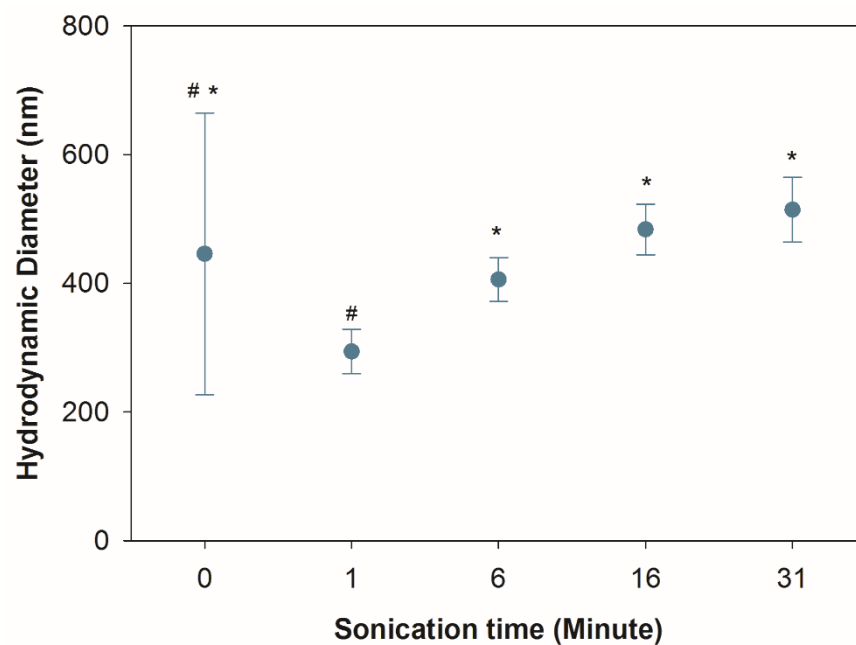
- Kerk, V., G. Der, et al. (1954). "Investigations on organo-tin compounds. III. The biocidal properties of organo-tin compounds." Journal of Applied Chemistry **4**(6): 314-319.
- Kungolos, A., S. Hadjispyrou, et al. (2004). "Toxic properties of metals and organotin compounds and their interactions on *Daphnia magna* and *Vibrio fischeri*." Water, Air and Soil Pollution: Focus **4**(4-5): 101-110.
- LaGrega, M. D., P. L. Buckingham, et al. (2010). Hazardous waste management, Waveland Press.
- Luijten, J. (1972). "Applications and biological effects of organotin compounds." Organotin compounds **3**: 931-974.
- Maguire, R. J. (1987). "Environmental aspects of tributyltin." Applied Organometallic Chemistry **1**(6): 475-498.
- Maguire, R. J., J. H. Carey, et al. (1983). "Degradation of the tri-n-butyltin species in water." Journal of Agricultural and Food Chemistry **31**(5): 1060-1065.
- Mangimbulude, J. C., B. M. van Breukelen, et al. (2009). "Seasonal dynamics in leachate hydrochemistry and natural attenuation in surface run-off water from a tropical landfill." Waste Management **29**(2): 829-838.
- Renou, S., J. Givaudan, et al. (2008). "Landfill leachate treatment: review and opportunity." Journal of hazardous materials **150**(3): 468-493.
- Seinen, W. and M. I. Willems (1976). "Toxicity of organotin compounds. I. Atrophy of thymus and thymus-dependent lymphoid tissue in rats fed di-n-octyltin dichloride." Toxicology and applied pharmacology **35**(1): 63-75.
- Seligman, P. F., J. G. Grovhoug, et al. (1989). "Distribution and fate of tributyltin in the United States marine environment." Applied Organometallic Chemistry **3**(1): 31-47.
- Slesinger, A. and I. Dressler (1978). The environmental chemistry of three organotin chemicals. Report of the Organotin Workshop. Good, M.(Ed.). University of New Orleans, New Orleans, LA.
- Stoner, H., J. Barnes, et al. (1955). "Studies on the toxicity of alkyl tin compounds." British journal of pharmacology and chemotherapy **10**(1): 16-25.
- Van der Kerk, G. and J. G. A. Luijten (1956). "Investigations on organo-tin compounds. V The preparation and antifungal properties of unsymmetrical tri-n- alkyltin acetates." Journal of Applied Chemistry **6**(2): 56-60.

- Winship, K. (1987). "Toxicity of tin and its compounds." Adverse drug reactions and acute poisoning reviews **7**(1): 19-38.
- Wong, P., Y. Chau, et al. (1982). "Structure-toxicity relationship of tin compounds on algae." Canadian Journal of Fisheries and Aquatic Sciences **39**(3): 483-488.

## 7.6 Appendix

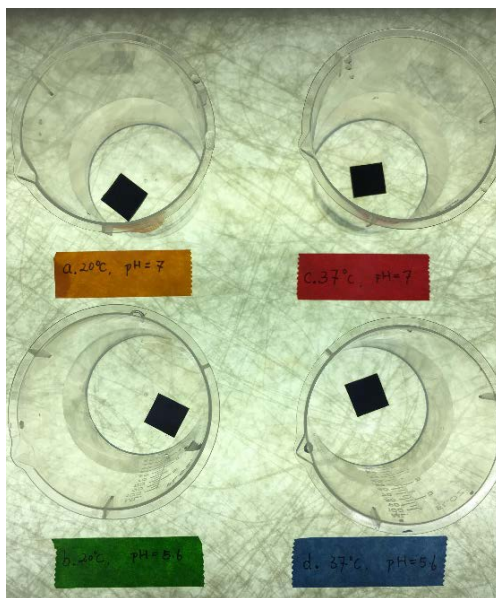


**Figure S7-1.** Chemical Structure of  $[(\text{BuSn})_{12}\text{O}_{14}(\text{OH})_6][\text{OH}]_2$ .

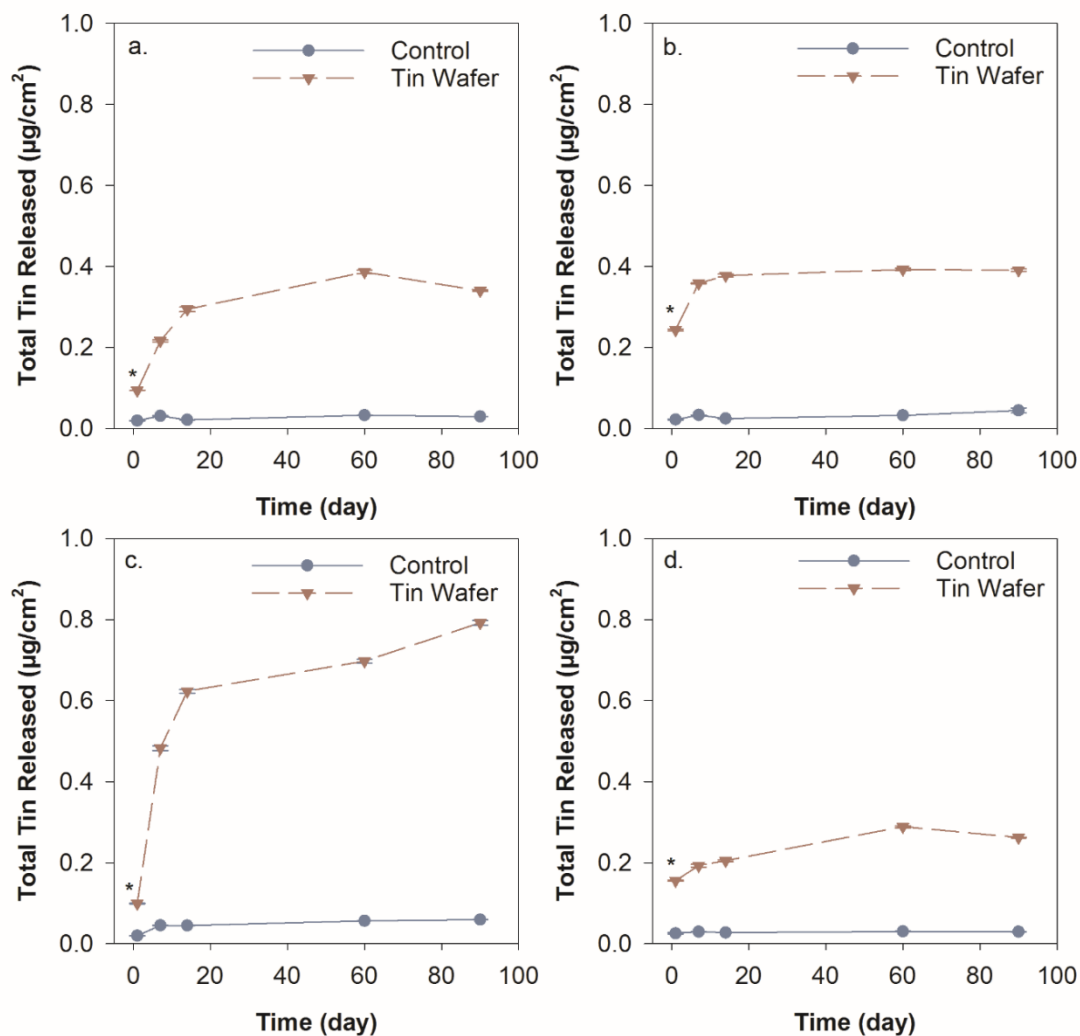


**Figure S7-2.** Sonication time versus the corresponding particle HDDs. Error bars represent standard error of three HDD measurements. Symbols (\*) and (#) indicate significant difference in HDD among differing sonication time.

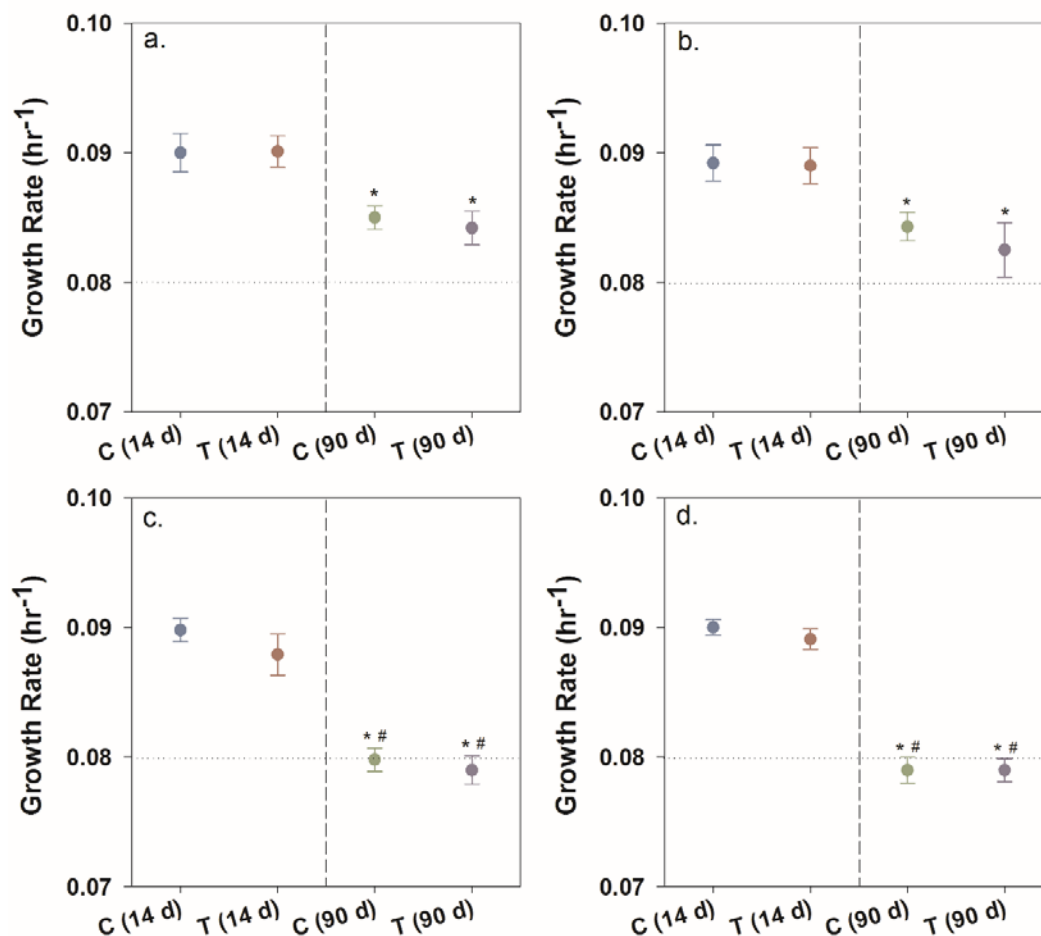




**Figure S7-3.** Four different incubation scenarios with control wafers and tin-coated wafers (a. 20°C, pH = 7, b. 20°C, pH = 5.6, c. 37°C, pH = 7, and d. 37°C, pH = 5.6).



**Figure S7-4.** Total tin (mass) leached from control and tin-coated wafers through four different incubation conditions (a. Temp = 20°C, pH = 7; b. Temp = 20°C, pH = 5.6; c. Temp = 37°C, pH = 7; d. Temp = 37°C, pH = 5.6). Error bars represent standard error of three technical replicates. Asterisks (\*) represents significantly different tin concentration compare to control starting at the time point including the following time points.



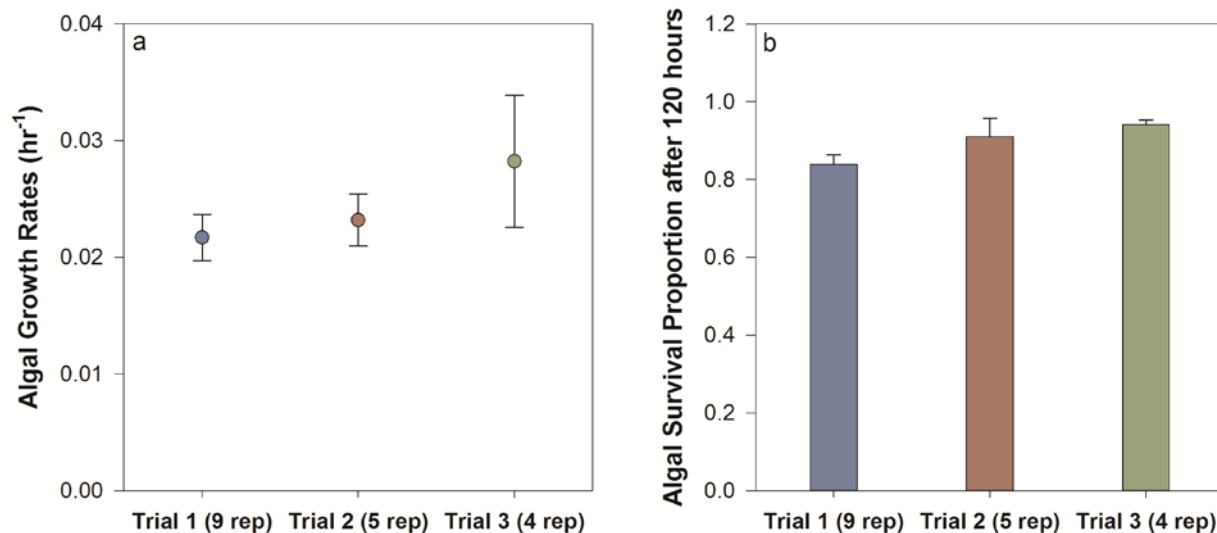
**Figure S7-5.** Algae growth rate with the exposure of simulated leachate under varying scenarios: a. Temp = 20°C, pH = 7; b. Temp = 20°C, pH = 5.6; c. Temp = 37°C, pH = 7; d. Temp = 37°C, pH = 5.6. Asterisks (\*) indicate significant difference in algae growth rate between 14 and 90 days incubation with the same type wafer. Octothorps (#) suggest significant difference in algae growth rate between 20 and 37 °C (same pH) with the same type of wafer.

## Chapter 8. Validation and Summary

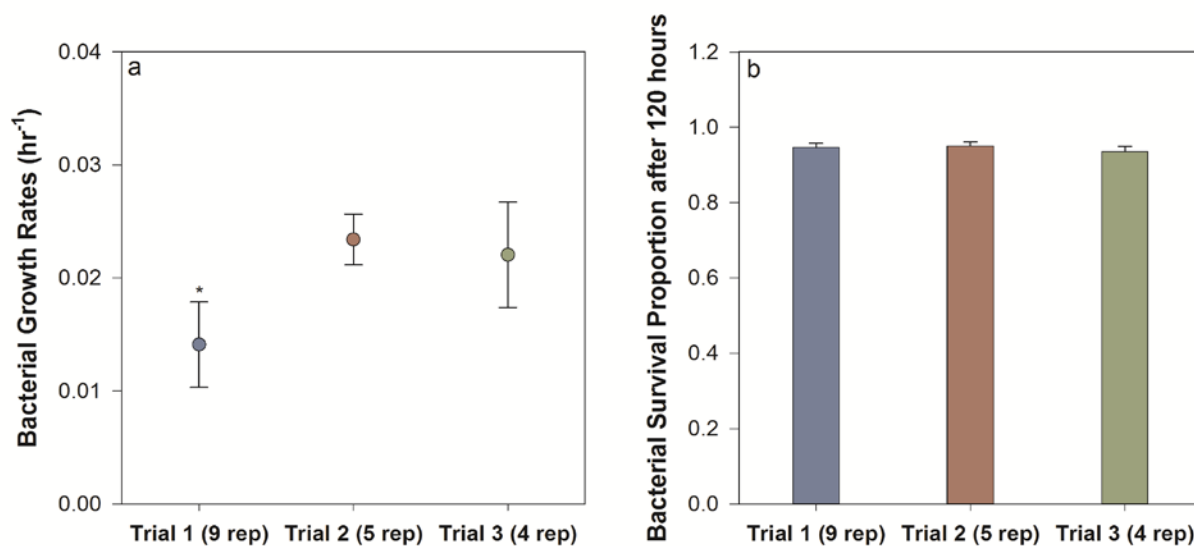
### 8.1 Nanocosm Validation

#### *8.1.1 Comparison of control species for standardization*

The control organism growth, survival, and zebrafish hatching success across studies from Chapter 4 to 6 were compared to determine the consistency of the nanocosm assay. Control nanocosms were compiled from Chapter 4 (trial 1), Chapter 5 (trial 2), and Chapter 6 (trial 3). Due to the difference in specific hypotheses tested, there were nine, five, and four control replicates included in trial 1, 2 and 3, respectively. There are no significant differences in algal growth rates or algal survival over the different exposure trials (Figure 8-1). Figure 8-2 shows the comparison of bacterial growth rates and bacterial survival after 120 hours. Trial 1 had significantly lower bacterial growth rate compared to other two trials. However, there was no significant difference in bacterial survival among different controls.

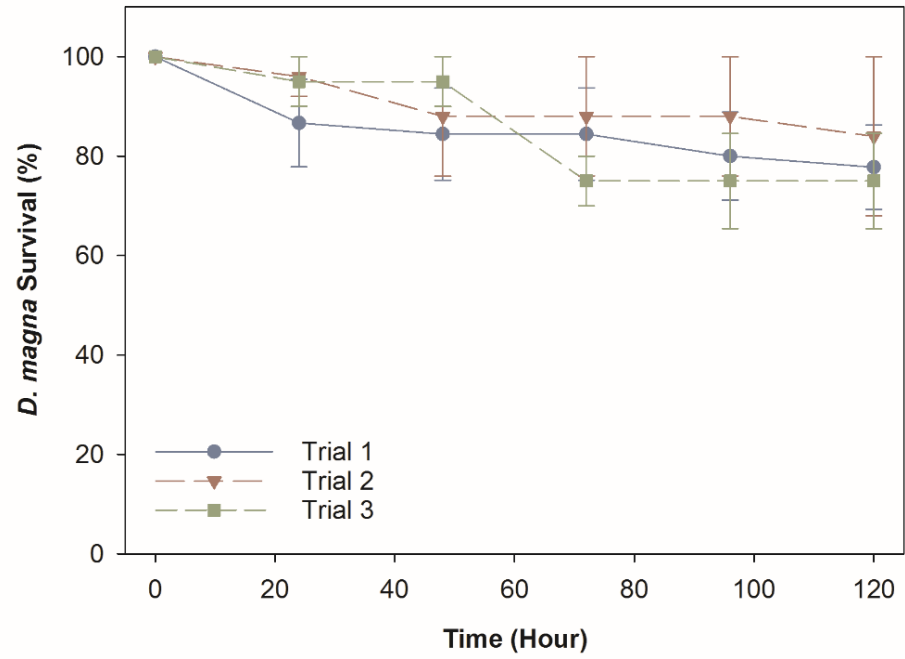


**Figure 8-1.** Combined algal growth rates (a) and 120-hour algal survival probability (b) from different trials of experiments with multiple replicates. Error bar represents standard error of sample replicates.

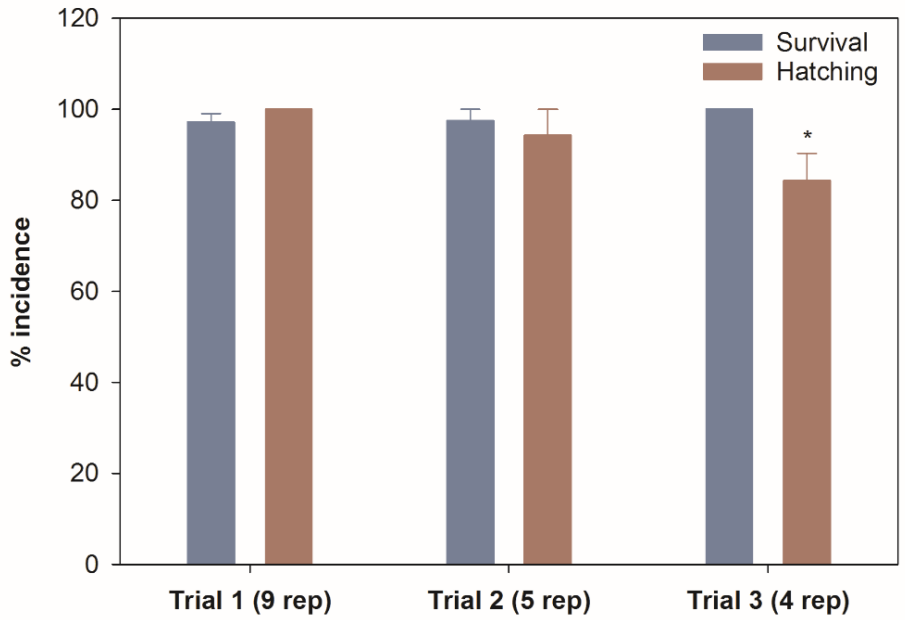


**Figure 8-2.** Combined bacterial growth rates (a) and 120-hour bacterial survival probability (b) from different trials of experiments with multiple replicates. Error bar represents standard error of sample replicates. \* indicates significant difference in bacterial growth rates.

Figure 8-3 shows *D. magna* survival rates in different trials of experiments. There was no significant difference among exposure trials. The mean *D. magna* survival is at 80%. Using four control replicates as an example, 75% survival rate will elicit significant higher mortality compared to 100% survival rate. Thus, to consider the success of control nanocosm, it requires no more than one out of five *D. magna* mortality from each sample replicate. Figure 8-4 combines the zebrafish survival and hatching rate of controls from different trials. No significant difference was found in zebrafish survival among controls. However, there was a significant lower zebrafish hatching rate in trial 3, with 84% hatching rate compared to 100% and 94% in trial 1 and 2, respectively. In trial 3, two replicates had two out of eight embryos that had delayed hatching. The significantly lower hatching rate is likely due to the smaller sample size compared to other control trials. For quality control, we recommend to use seven out of eight fish for both survival and hatching rate to be consider a successful control for future reference.



**Figure 8-3.** Combined *D. magna* survival rate from different trials of experiments with multiple replicates. Error bar represents standard error of sample replicates.



**Figure 8-4.** 120-hour zebrafish survival (blue bars) and hatching rate (red bars) from different trials of experiments with multiple replicates. Error bar represents standard error of sample replicates. \* indicates significant difference in hatching rates among three experimental trials.

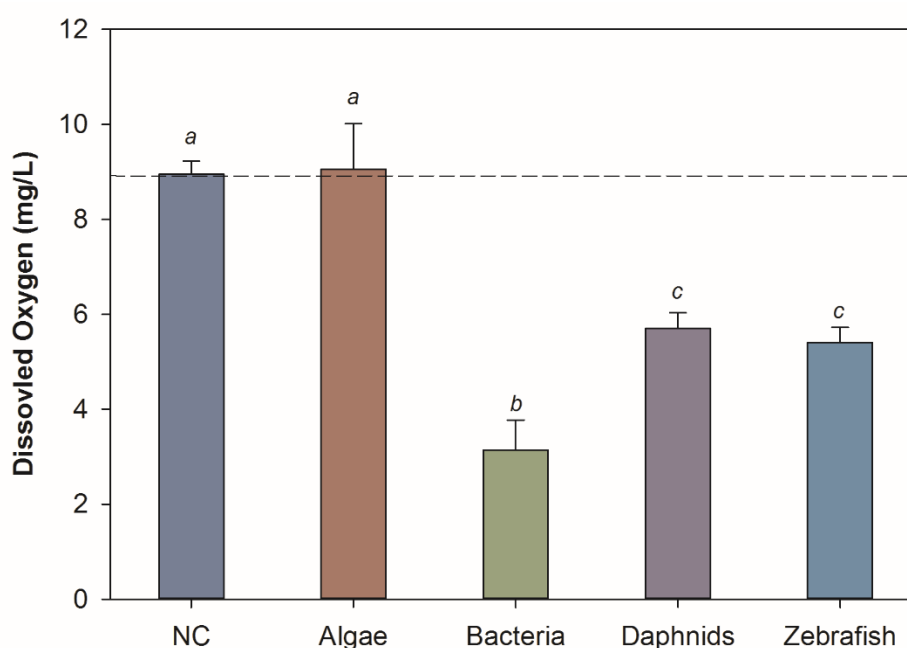
Overall, there was above 80% survivability in all organisms after 120 hours. The high survival rate and consistency throughout different trials of experiments indicates that the nanocosm assay is repeatable in our laboratory. To further validate and improve repeatability, inter-laboratory testing is required and will be moving forward as next stage.

#### 8.1.2 Dissolved Oxygen

A dissolved oxygen meter with a micro-oxygen electrode (Lazar Research Laboratories, Inc., Los Angeles, CA) was used to measure the dissolved oxygen in nanocosm and each individual species. Individual species was prepared in the same nanocosm media and with the same quantity of organisms but separately. The dissolved oxygen was measured in the nanocosm and each individual species at 120 hour of the experiment (48 hours for *D. magna*) and is presented in Figure 8-5. Nanocosm controls have demonstrated that the dissolved oxygen reached saturation measured at 120 hours. Thus, the dissolved oxygen is not the limiting factor for organismal growth in nanocosm controls. The high dissolved oxygen is due to production of oxygen through algae photosynthesis. Although other species can utilize oxygen in nanocosm, the small volume and the shallow depth of the exposure environment, helps the oxygen exchange readily. In ecology, production/respiration represents the relationship between gross production and total community respiration, and  $P/R = 1$  indicates a steady-state community results. Future study will be continuing measuring the P/R ratio in the nanocosm. In



addition, the light: dark cycle dissolved oxygen content in a nanocosm will be further analyzed to better understand the ecosystem respiration.


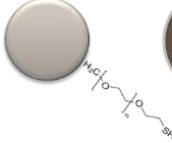
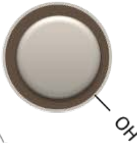





**Figure 8-5.** Dissolved oxygen measured in each species and NC community after 120 hours (Dissolved oxygen measured in *D. magna* were measured at 48 hour). Dashed line is the saturation dissolved oxygen at 21 °C. Lowercase letters indicate significant difference of measured dissolved oxygen among exposure scenarios. Error bars represent standard error of two experimental trials, each trial includes three sample replicates ( $n = 6$  measures).

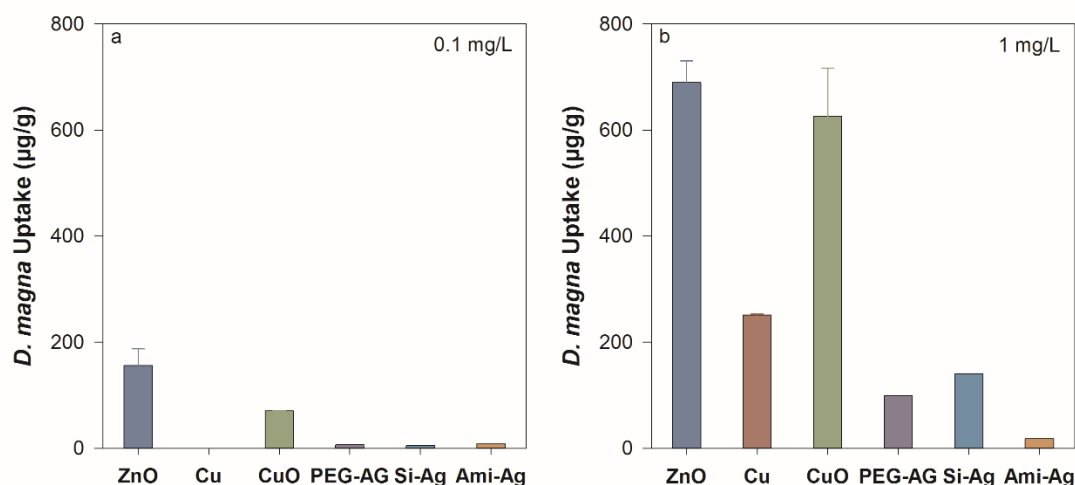
## 8.2 Summary of the fate and toxicity of tested NPs

The toxicity, uptake, and dissolved fraction of all evaluated NPs using nanocosm assay were presented in Figure 8-6. ZnO, Ag, Cu, and CuO NPs showed different uptake in organisms (Figure 8-7). In *D. magna*, the highest uptake in *D. magna* was shown in ZnO NP and CuO NP under the same exposure concentration. ZnO NP uptake was demonstrated to mainly due to the high dissolved Zn released from ZnO NPs. High CuO NP accumulation in *D. magna* was

attributed to the high attachment affinity of CuO NPs on *D. magna* and their food source, algae and bacteria. *D. magna* had much higher uptake than zebrafish due to their filter feeding behavior, and serve as primary consumer in the nanocosm. The zebrafish chorion is likely to prevent NP uptake in zebrafish, but zebrafish mouth gaping after hatching could take up potential NPs in the exposure media. Therefore, zebrafish showed low uptake to all types of NPs.

	ZnO (<50 nm)	PEG-Ag (73 nm)	Si-Ag (95 nm)	Ami-Si-Ag (88 nm)	Cu (<50 nm)	CuO (<50 nm)
						
<b>Toxicity</b>	Moderate	High	High	Moderate	Moderate	Low
<b>Uptake</b>	High	Low	Low	Low	Moderate	High
<b>Dissolved Fraction</b>	High (55%)	Low (16%)	Low (15%)	Low (5%)	Moderate (27%)	Moderate (26%)

**Figure 8-6.** Summary of the toxicity, uptake, and dissolved fraction of all evaluated NPs using nanocosm assay.



**Figure 8-7.** *D. magna* uptake in different types of NP exposures at 0.1 (a) and 1 (b) mg L<sup>-1</sup>. Error bars represent standard errors of three sample replicates. *D. magna* uptake measured with three AgNP exposures did not include error bars due to the small sample sizes.

In the abiotic nanocosm environment, the dissolution profiles of all NPs were similar to their known solubility ( $\text{ZnO} > \text{Cu} \approx \text{CuO} > \text{Ag}$ ). ZnO NPs had the highest dissolution rate, followed by Cu and CuO NPs. Ag NPs had the lowest dissolution rates in nanocosm media over 120-hour exposure period, primary due to the surface coating which likely prevented the dissolution of Ag NPs. However, AgNP had significantly higher dissolved Ag released in biotic environment compared to abiotic scenario. In nanocosm biotic exposure scenario, the final dissolved metal species follows the trend  $\text{ZnO} > \text{Ag} > \text{Cu} \approx \text{CuO}$ . Organisms can impact the final dissolved metal fraction in the nanocosm. They can actively take up small NPs and dissolved metal species. In addition, the exudates generated by organisms can impact the dissolution of NPs by coating NPs. Ag NPs was influenced by organisms the most, with significantly higher dissolved fraction in biotic than abiotic environment.

The toxicity of all tested NPs follow the order of  $\text{Ag} > \text{ZnO} > \text{Cu} > \text{CuO}$ . All tested NPs showed dissolved metal species contributed to the toxicity observed. This is due to the difference in metal toxicity to the tested organisms. In addition, it also implies that different mechanisms were dominating the toxicity of modeled NPs. In Ag NP exposures, surface functional groups dictated the release of Ag species, therefore, elicited different toxicity to test organisms. ZnO NPs had high dissolved Zn concentration, which attributed for the observed toxicity. Although ZnO NPs had higher percentage of released ions (~80%), all three AgNPs showed higher toxicity than ZnO NPs due to the extreme toxic nature of ionic Ag. However, between Cu and CuO NPs, there was significantly difference in toxicity to nanocosms. With Cu NP eliciting higher toxicity and uptake than ionic Cu control, it suggests that Cu NP can elicit specific toxicity to tested organisms, likely due to their higher surface reactivity, and potential ability to generate high levels of reactive oxygen species. In addition, dissolved organic carbon (DOC) have proven to impact the toxicity of metal ions, and NPs to organisms (Aiken, Hsu-Kim et al. 2011; Wang, Li et al. 2011). Given the high DOC can be generated in the nanocosm, future experiment will consider measuring the DOC over time in nanocosm and investigate their contribution in nanoparticle toxicity.

### 8.3 Nanocosm modeling

Geitner and colleagues introduced nanoparticle surface affinity as a predictor of trophic transfer (Geitner, Marinakos et al. 2016). In chapter 3, we have also demonstrated that CuO NPs was agglomerated with algal cells and transferred to *D. magna* (Figure 8-6). Here, the Geitner concepts were used to model nanoparticle fate and distribution in nanocosm with some

adaptations. In this adapted model, once NPs are introduced to a nanocosm, nanoparticles and organism surfaces could directly interact immediately. Meanwhile, soluble NPs start to dissolve and release ions, modeled as pseudo-first order reaction in the media. Once initial attachment and dissolution occurs, nanomaterials transit through the food web as a function of feeding, predation, and depuration rates. For the adapted model, NP concentrations are considered in the water column (n), algae (A), bacteria (E), *Daphnia* (D), and zebrafish (F) compartments. The flow of nanoparticles into and out of each compartment was defined by a set of equations and models that can describe species interactions and the distribution of NPs.

$$\frac{dn}{dt} = S - \sum \alpha \beta B_i n - K_d \quad (\text{Equation 8.1})$$

where n is the number concentration of free nanoparticles, S is the total concentration of nanoparticles exposed to the system initially,  $\alpha$  is the attachment probability to organism surface,  $\beta$  represents the collision frequency between the nanoparticle and background particulates and background organisms, B indicates the concentration of background particles or collectors (in this case represents each organism in the nanocosm), and  $K_d$  is the dissolution rate of NPs.

a. Algae:

$$\frac{dA}{dt} = \alpha_{An} \beta_{An} B_A n - k_{fDA} B_D A - k_{fFA} B_F A \quad (\text{Equation 8.2})$$

A is the number concentration of nanoparticles in the system attached to algae,  $\alpha_{An}$  is the attachment probability to algae surface,  $\beta_{An}$  is the collision rate between nanoparticles and surface of algae,  $k_{fDA}$  is the feeding rate of *D. magna* on algae, and  $k_{fFA}$  is the feeding rate of zebrafish on algae.

b. Bacteria (*E. coli*):

$$\frac{dE}{dt} = \alpha_{En}\beta_{En}B_E n - k_{fDE}B_DE - k_{fFE}B_FE \quad (\text{Equation 8.3})$$

E is the number concentration of nanoparticles in the system attached to bacteria,  $\alpha_{En}$  is the attachment probability to bacteria surface,  $\beta_{En}$  is the collision rate between nanoparticles and collecting surface of bacteria,  $k_{fDE}$  is the feeding rate of *D. magna* on bacteria,  $k_{fFE}$  is the feeding rate of zebrafish on bacteria.

Since the predation from zebrafish did not significantly impact the growth rates of algae and bacteria [as shown in chapter 5 (Figure 5-4) and the low uptake of NP in zebrafish throughout the dissertation], equation 8.2 and 8.3 can be simplified as equation 8.4 and 8.5, respectively.

$$\frac{dA}{dt} = \alpha_{An}\beta_{An}B_A n - k_{fDA}B_DA \quad (\text{Equation 8.4})$$

$$\frac{dE}{dt} = \alpha_{En}\beta_{En}B_E n - k_{fDE}B_DE \quad (\text{Equation 8.5})$$

c. *Daphnia magna*:

$$\frac{dD}{dt} = \alpha_{Dn}\beta_{Dn}B_D n - k_{fFD}B_FD \quad (\text{Equation 8.6})$$

$$\frac{dP_D}{dt} = k_{fDA}\beta_D + k_{fDE}\beta_D - k_{dD}P_D - k_{fFD}\beta_F P_D \quad (\text{Equation 8.7})$$

D is the number concentration of nanoparticles in the system attached to *Daphnia*,  $\alpha_{Dn}$  is the attachment probability to *Daphnia* surface,  $\beta_{Dn}$  is the collision rate between nanoparticles and collecting surface of *Daphnia*,  $k_{fDA}$  is the feeding rate of *Daphnia* on algae,  $k_{fDE}$  is the feeding rate of *Daphnia* on bacteria,  $k_{fFD}$  is the feeding rate of fish on *Daphnia*,  $k_d$  is the depuration rate of *D. magna*, and  $P_D$  is the number concentration of nanoparticles in *Daphnia* due to ingestion.

Since zebrafish were not preying on *D. magna* in our nanocosm assay, equation 8.5 and 8.6 can be simplified as:

$$\frac{dD}{dt} = \alpha_{Dn}\beta_{Dn}B_Dn \quad (\text{Equation 8.8})$$

$$\frac{dP_D}{dt} = k_{fDA}\beta_D + k_{fDE}\beta_D - k_{dD}P_D \quad (\text{Equation 8.9})$$

d. Zebrafish:

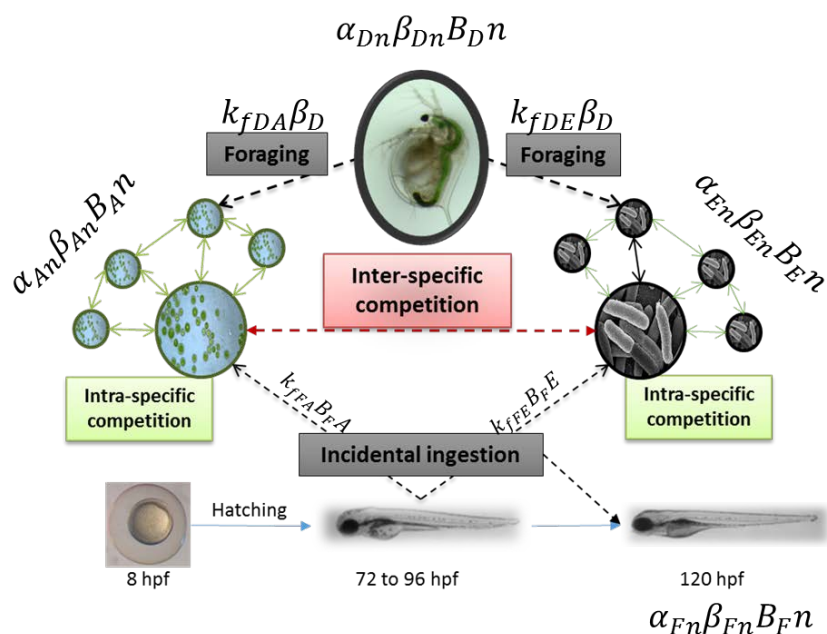
$$\frac{dF}{dt} = \alpha_{Fn}\beta_{Fn}B_Fn \quad (\text{Equation 8.10})$$

$$\frac{dF}{dt} = k_{fDA}\beta_D - k_{dF}P_F \quad (\text{Equation 8.11})$$

F is the number concentration of nanoparticles in the system attached to zebrafish,  $\alpha_{Fn}$  is the attachment probability to zebrafish surface,  $\beta_{Fn}$  is the collision rate between nanoparticles and collecting surface of zebrafish,  $k_{fFD}$  is the feeding rate of zebrafish on *Daphnia*,  $k_{dF}$  is the depuration rate of zebrafish, and  $P_F$  is the number concentration of nanoparticles in zebrafish due to ingestion. However, since zebrafish predation was minimized in the nanocosm experiment, the zebrafish uptake is considered only as a having a strong surface attachment. After hatching, zebrafish mouth gapping can result in incidental uptake of the nanoparticles. However, modeling incidental uptake is difficult and usually inaccurate. Thus, we considered the predation of zebrafish and depuration to be negligible (equation 8.11).

The combination of equation 8.1, 8.4, 8.5, 8.8, 8.9, 8.10 can then be used to describe the species interaction and nanoparticle transport in a nanocosm system. The functions and organism interactions illustration is presented in Figure 8-7. However, there are still critical assumptions

associated with this model. First, the model assumes organism population and NP in the community remains equilibrium at the time of each measurement. Second, although the released ions and the depuration from organisms can be taken up by organisms and transfer through food web, in this model, we assume the depuration will be removed from the current system, such as to the sediment. However, to account for the released ion contribution, perform ionic exposure controls can solve the problem. Third, although the dissolution will impact the surface and the size of NPs, the particle size is assumed to remain consistent as the measured aggregated size (abiotic) in this model; the dissolution is only depending on the particle counts in the exposure environment. Future work will incorporate the experimental data to the developed models, and test the fitting probability of the model for validation and improvement.



**Figure 8-8.** The potential interactions of the four species in the nanocosm assay including the distribution of NP under exposures.



## 8.4 Cost-benefit analysis

Detailed cost-benefit analysis of performing nanocosm assay were summarized in multiple aspects (Table 8-1). By comparing to the standardized ASTM freshwater microcosm, the nanocosm assay is much easier to start up and less labor-intensive to perform. In addition, the low materials requirements and rapid assessment means nanocosm assay can be easily adapted by most of laboratories under standard laboratory conditions.

**Table 8-1.** Cost benefit analysis comparing nanocosm assay to ASTM microcosm assay.

	Nanocosm assay	ASTM microcosm
<b>Volume</b>	<b>0.015 L</b>	<b>2 L</b>
<b>Time</b>	<b>5 days</b>	<b>60 days</b>
<b>Species required</b>	<b>4</b>	<b>15</b>
<b>Organism cost (Startup)</b>	<b>\$400</b>	<b>\$2,000</b>
<b>Organism Maintenance cost</b>	<b>\$100/month</b>	<b>\$400/month</b>
<b>Labor required</b>	<b>1 ~ 2 persons</b>	<b>5 ~ 8 persons</b>
<b>Instrumentation (Startup)</b>	<b>Flow cytometer (replicable with hemocytometer), shaker, pH meter, Microscope, DO meter</b>	<b>Shaker, DO meter, pH meter, Microscope, Nitrate photometer, Spectrophotometer</b>
<b>Instrumentation (Est. cost)</b>	<b>\$ 20,000 – 70,000</b>	<b>\$30,000</b>
<b>Infrastructure (space needed)</b>	<b>Culture (4 m<sup>2</sup>) Experiment (2 m<sup>2</sup>)</b>	<b>Culture (12 m<sup>2</sup>) Experiment (10 m<sup>2</sup>)</b>
<b>Flask cost</b>	<b>\$2</b>	<b>\$20</b>
<b>Est. cost per sample</b>	<b>\$10</b>	<b>\$200</b>
<b>NP mass (1 mg/L)</b>	<b>0.015 mg material</b>	<b>2 mg material</b>
<b>Cost (Ag NP)</b>	<b>\$3</b>	<b>\$400</b>

## 8.5 The advantages and disadvantages of the approaches

In Chapter 3, we highlighted the importance of testing NP ecotoxicity in multi-species communities including multiple routes of exposure. Understanding the role of the trophic route is essential in ecotoxicology because organisms living in contaminated ecosystems are likely to feed on contaminated food. The ingestion of contaminants through food sources can affect organisms differently than just direct exposure to the environment. This study identified the differential chronic toxicity of direct exposure and indirect exposure to CuO NPs. This chronic approach can provide us information on how NPs transport and bioaccumulate through trophic chains, and the long-term impact of NPs to aquatic organisms. However, this approach is hard to be widely implemented to assess all suites of nanomaterials since it is quite time-consuming and labor-intensive. This study highlighted the importance of testing ecological impact of NPs under ecological relevant exposure scenarios, and urgency for a rapid and cost-effective assay for replacement.

From Chapter 4 to Chapter 6, we developed and validated a rapid, standardized, small-scale microcosm assay which has high repeatability and incorporates trophic interactions to systematically evaluating NP ecotoxicity and ecological interactions. A series of metal and metal oxide NPs were assessed to validate the assay, meanwhile, identify the most sensitive species in the system.

In Chapter 4, we compared the responses of individual organisms to ZnO NPs exposures and within a community. ZnO microparticles and ZnCl<sub>2</sub> were used to compare the effect of the size and the dissolved Zn impact to individual and community exposure scenarios. The study

further validates the nanocosm assay by showing environmental resilience to Zn exposures. The organismal responses were mitigated in the nanocosm community due to interspecies interactions and biological sinks present. Additionally, ZnO NPs elicited high toxicity to aquatic organisms due to the high solubility and dissolution rate.

In Chapter 5, we investigated the impact of three different surface functionalized Ag NPs on communities with increasing complexity. Three same size AgNPs (primary particle size: 70 nm) with PEG, Si, and Ami-Si surfaces were assessed to compare how NP surfaces affect AgNP dissolution, in terms affecting organismal uptake and toxicity. In addition, higher community complexity decreased the toxicity of AgNPs to organism. The significance of this work is two-fold. First, this study demonstrated that surface coatings can influence NP behavior in aquatic environments and toxicity to organisms. Second, this study further validated our nanocosm assay and enhanced our knowledge on the species interactions within the system.

In Chapter 6, we explored the environmental fate and toxicity of Cu and CuO NPs using the nanocosm assay. Cu and CuO NPs were compared due to the potential difference in agglomeration status, surface chemistry, and dissolution behavior. CuO NPs had higher potential to be attached and associated with organisms in the nanocosm, but higher toxicity was elicited by Cu NPs, likely due to their higher surface reactivity, and potential ability to generate high level of reactive oxygen species.

Across these studies, there are several advantages of the nanocosm assay that can be recognized in general.

- First, the nanocosm assay can identify the most sensitive species within target species and non-target species in the same exposure system, the corresponding toxicity of

each organism in the nanocosm can be assessed simultaneously with consideration of the interactions among organisms. Although mesocosm studies are environmentally realistic due to their higher environmental complexity, this approach is a rapid (120 hours), cost-effective (approximately \$10 for each nanocosm), not labor intensive, and generates small amount of wastes compared to other micro- and mesocosms. Moreover, the nanocosm approach overcomes the disadvantage when the testing materials are quite limited. Take ASTM standard freshwater microcosm as an example, 2 liters in volume requires 134 times more materials to reach the same exposure concentration as the nanocosm, which will be hundreds time more expensive and generates more wastes than the nanocosm assay.

- Second, the nanocosm assay has controlled water parameters that will allow standardizing and further comparison among laboratories. Since the water parameters (pH, dissolved organic carbon content, water hardness, and ionic strength) can impact the stability and the fate of the NPs, our assay has the potential to serve as a standardized method and have controlled environmental factors to enable high repeatability. Both biotic and abiotic characterization can be tightly controlled using the nanocosm approach.

- Third, nanocosm assays are easy to handle for different types of exposure scenarios due to their small size. For instance, it can be gently agitated to resuspend nanoparticles from the sediment.

Despite these advantages, the nanocosm assay still has some limitations. The nanocosm assay is a short-term acute evaluation approach, it serves as a screening assay for NPs toxicity, and does not reflect the long-term environmental impacts of NPs. In addition, the species used in

the nanocosm are representative through a broad spectrum across trophic levels, but may not co-exist in a nature ecosystem. Even so, the approach is a novel and easily implementable method that allows for rapidly and cost-effectively assessing nanoparticle ecotoxicity.

In Chapter 7, we performed an end-of-life toxicity evaluation on monoalkyltin coated thin film wafers. An end-of-life disposal and landfill leachate contamination was simulated and leachate was incubated in water with varied pH and temperature to investigate the leaching rate and subsequent toxicity of those leachates. The low toxicity of synthesized tin films and the tin clusters can be environmentally benign materials suitable for large-scale use in the semiconductor industry. This approach evaluated the leaching rate of monoalkyltin from the thin films and the corresponding toxicity under varied pH and temperature. Due to the time-consuming nature of this approach and the diversity of natural environment, it is hard to be widely implemented on large variety nano-based products. However, end-of-life evaluation is important and realistic for understanding the environmental impact of nano-based products, this approach should be considered for some largely applied nano-based products which can leach to the environment.

## **8.6 Summary**

In conclusion, we utilized three different approaches in this dissertation to evaluate metal based NP environmental impacts. Importantly, we developed a rapid and cost-effective multi-species nanocosm assay, including a mathematic model to describe the nanoparticle fate in a simulated small scale community, and identified the key parameters of metal and metal oxide

nanomaterials that affect the toxicity. Dissolved metal ions contribute a large fraction of toxicity to the environment. However, NPs can also elicit particle-specific uptake and toxicity depending on the particle type, and surface functionality can dramatically modify NP fate and toxicity. The nanocosm approach is a rapid, cost-effective assay to evaluate the environmental impacts of nanomaterials. The nanocosm assay can enhance our ability to rapidly screen the toxicity of nanomaterials and understand their impacts at the community level, which will be beneficial to risk assessment and the manufacture of safer nanomaterials. The comprehensive understanding gained throughout this dissertation provides the basis for nanomaterial environmental impact evaluation and risk management for sustainable nanotechnology development.

Future studies will focus on inter-laboratory studies to continuously test more nanomaterials, validate the assay, and optimize the mathematic models to improve the nanocosm assay. In addition, continuously generating larger data sets use the nanocosm assay can establish platforms to test, integrate, and analyze data in multiple systems to yield targeted structure-activity relationships that inform nanomaterial design and risk management. This testing framework has the potential to shift existing testing paradigms and meet current and future needs regarding rapid evaluation for the nanoscience community.

## Chapter 9. Bibliography

- Adams, L. K., D. Y. Lyon, et al. (2006). "Comparative eco-toxicity of nanoscale TiO<sub>2</sub>, SiO<sub>2</sub>, and ZnO water suspensions." Water research **40**(19): 3527-3532.
- Aiken, G. R., H. Hsu-Kim, et al. (2011). Influence of dissolved organic matter on the environmental fate of metals, nanoparticles, and colloids, American Chemical Society.
- Aruoja, V., H.-C. Dubourguier, et al. (2009). "Toxicity of nanoparticles of CuO, ZnO and TiO<sub>2</sub> to microalgae *Pseudokirchneriella subcapitata*." Science of the Total Environment **407**(4): 1461-1468.
- Bian, S.-W., I. A. Mudunkotuwa, et al. (2011). "Aggregation and dissolution of 4 nm ZnO nanoparticles in aqueous environments: influence of pH, ionic strength, size, and adsorption of humic acid." Langmuir **27**(10): 6059-6068.
- Blaser, S. A., M. Scheringer, et al. (2008). "Estimation of cumulative aquatic exposure and risk due to silver: contribution of nano-functionalized plastics and textiles." Science of the total environment **390**(2): 396-409.
- Blinova, I., A. Ivask, et al. (2010). "Ecotoxicity of nanoparticles of CuO and ZnO in natural water." Environmental Pollution **158**(1): 41-47.
- Bondarenko, O., K. Juganson, et al. (2013). "Toxicity of Ag, CuO and ZnO nanoparticles to selected environmentally relevant test organisms and mammalian cells in vitro: a critical review." Archives of toxicology **87**(7): 1181-1200.
- Bone, A. J., C. W. Matson, et al. (2015). "Silver nanoparticle toxicity to Atlantic killifish (*Fundulus heteroclitus*) and *Caenorhabditis elegans*: A comparison of mesocosm, microcosm, and conventional laboratory studies." Environmental Toxicology and Chemistry **34**(2): 275-282.
- Bonventre, J. A., J. B. Pryor, et al. (2014). "The impact of aminated surface ligands and silica shells on the stability, uptake, and toxicity of engineered silver nanoparticles." Journal of Nanoparticle Research **16**(12): 2761.
- Bour, A., F. Mouchet, et al. (2015). "Environmentally relevant approaches to assess nanoparticles ecotoxicity: A review." Journal of hazardous materials **283**: 764-777.
- Bradford, A., R. D. Handy, et al. (2009). "Impact of silver nanoparticle contamination on the genetic diversity of natural bacterial assemblages in estuarine sediments." Environmental science & technology **43**(12): 4530-4536.

- Brayner, R., R. Ferrari-Iliou, et al. (2006). "Toxicological impact studies based on *Escherichia coli* bacteria in ultrafine ZnO nanoparticles colloidal medium." Nano Letters **6**(4): 866-870.
- Buffet, P.-E., J.-F. Pan, et al. (2013). "Biochemical and behavioural responses of the endobenthic bivalve *Scrobicularia plana* to silver nanoparticles in seawater and microalgal food." Ecotoxicology and environmental safety **89**: 117-124.
- Carnes, C. L. and K. J. Klabunde (2003). "The catalytic methanol synthesis over nanoparticle metal oxide catalysts." Journal of Molecular Catalysis A: Chemical **194**(1): 227-236.
- Casals, E., E. Gonzalez, et al. (2012). "Reactivity of inorganic nanoparticles in biological environments: insights into nanotoxicity mechanisms." Journal of Physics D: Applied Physics **45**(44): 443001.
- Chen, L., L. Zhou, et al. (2012). "Toxicological effects of nanometer titanium dioxide (nano-TiO<sub>2</sub>) on *Chlamydomonas reinhardtii*." Ecotoxicology and environmental safety **84**: 155-162.
- Colman, B. P., C. L. Arnaout, et al. (2013). "Low Concentrations of Silver Nanoparticles in Biosolids Cause Adverse Ecosystem Responses under Realistic Field Scenario." PloS one **8**(2): e57189.
- Colman, B. P., B. Espinasse, et al. (2014). "Emerging contaminant or an old toxin in disguise? Silver nanoparticle impacts on ecosystems." Environmental science & technology **48**(9): 5229-5236.
- Colman, B. P., S.-Y. Wang, et al. (2012). "Antimicrobial effects of commercial silver nanoparticles are attenuated in natural streamwater and sediment." Ecotoxicology **21**(7): 1867-1877.
- Consumer Products Inventory (2012). "Consumer products inventory Project on Emerging Nanotechnologies, a project of the Woodrow Wilson International Center for Scholars. ." from <http://www.nanotechproject.org>.
- Doiron, K., E. Pelletier, et al. (2012). "Impact of polymer-coated silver nanoparticles on marine microbial communities: a microcosm study." Aquatic toxicology **124**: 22-27.
- Eatemadi, A., H. Daraee, et al. (2014). "Carbon nanotubes: properties, synthesis, purification, and medical applications." Nanoscale Res Lett **9**(1): 393.



- Ebrahimnia-Bajestan, E., H. Niazmand, et al. (2011). "Numerical investigation of effective parameters in convective heat transfer of nanofluids flowing under a laminar flow regime." International journal of heat and mass transfer **54**(19): 4376-4388.
- European Parliament (2010). "Brussels, 6.10. 2010, COM (2010) 546 final. Communication from the Commission to the European Parliament, the Council, the European Economic and Social Committee and Committee of the Regions." Europe 2020 Flagship Initiative Innovation Union.
- Fouqueray, M., P. Noury, et al. (2013). "Exposure of juvenile Danio rerio to aged TiO<sub>2</sub> nanomaterial from sunscreen." Environmental Science and Pollution Research **20**(5): 3340-3350.
- Franklin, N. M., N. J. Rogers, et al. (2007). "Comparative toxicity of nanoparticulate ZnO, bulk ZnO, and ZnCl<sub>2</sub> to a freshwater microalga (*Pseudokirchneriella subcapitata*): the importance of particle solubility." Environmental science & technology **41**(24): 8484-8490.
- Geitner, N. K., S. M. Marinakos, et al. (2016). "Nanoparticle Surface Affinity as a Predictor of Trophic Transfer." Environmental science & technology **50**(13): 6663-6669.
- Gottschalk, F., T. Sonderer, et al. (2009). "Modeled environmental concentrations of engineered nanomaterials (TiO<sub>2</sub>, ZnO, Ag, CNT, fullerenes) for different regions." Environmental science & technology **43**(24): 9216-9222.
- Harper, S., C. Usenko, et al. (2008). "In vivo biodistribution and toxicity depends on nanomaterial composition, size, surface functionalisation and route of exposure." Journal of Experimental Nanoscience **3**(3): 195-206.
- Harper, S. L., J. L. Carriere, et al. (2011). "Systematic evaluation of nanomaterial toxicity: utility of standardized materials and rapid assays." ACS nano **5**(6): 4688-4697.
- Heinlaan, M., A. Ivask, et al. (2008). "Toxicity of nanosized and bulk ZnO, CuO and TiO<sub>2</sub> to bacteria *Vibrio fischeri* and crustaceans *Daphnia magna* and *Thamnocephalus platyurus*." Chemosphere **71**(7): 1308-1316.
- Hotze, E. M., T. Phenrat, et al. (2010). "Nanoparticle aggregation: challenges to understanding transport and reactivity in the environment." Journal of environmental quality **39**(6): 1909-1924.
- Huang, Z., X. Zheng, et al. (2008). "Toxicological effect of ZnO nanoparticles based on bacteria." Langmuir **24**(8): 4140-4144.

- Jackson, B. P., D. Bugge, et al. (2012). "Bioavailability, toxicity, and bioaccumulation of quantum dot nanoparticles to the amphipod *Leptocheirus plumulosus*." Environmental science & technology **46**(10): 5550-5556.
- Jiang, C., B. T. Castellon, et al. (2017). "Relative Contributions of Copper Oxide Nanoparticles and Dissolved Copper to Cu Uptake Kinetics of Gulf Killifish (*Fundulus grandis*) Embryos."
- Jin, R. (2015). "Atomically precise metal nanoclusters: Stable sizes and optical properties." Nanoscale **7**(5): 1549-1565.
- Kahru, A. and H.-C. Dubourguier (2010). "From ecotoxicology to nanoecotoxicology." Toxicology **269**(2): 105-119.
- Kulacki, K. J., B. J. Cardinale, et al. (2012). "How do stream organisms respond to, and influence, the concentration of titanium dioxide nanoparticles? A mesocosm study with algae and herbivores." Environmental Toxicology and Chemistry **31**(10): 2414-2422.
- Levard, C., E. M. Hotze, et al. (2012). "Environmental transformations of silver nanoparticles: impact on stability and toxicity." Environmental science & technology **46**(13): 6900-6914.
- Levy, J. L., J. L. Stauber, et al. (2009). "The effect of bacteria on the sensitivity of microalgae to copper in laboratory bioassays." Chemosphere **74**(9): 1266-1274.
- Li, Y., J. Liang, et al. (2008). "CuO particles and plates: synthesis and gas-sensor application." Materials Research Bulletin **43**(8): 2380-2385.
- Lowry, G. V., B. P. Espinasse, et al. (2012). "Long-term transformation and fate of manufactured Ag nanoparticles in a simulated large scale freshwater emergent wetland." Environmental science & technology **46**(13): 7027-7036.
- Maurer-Jones, M. A., I. L. Gunsolus, et al. (2013). "Toxicity of engineered nanoparticles in the environment." Analytical chemistry **85**(6): 3036.
- McTeer, J., A. P. Dean, et al. (2014). "Bioaccumulation of silver nanoparticles into *Daphnia magna* from a freshwater algal diet and the impact of phosphate availability." Nanotoxicology **8**(3): 305-316.
- Mitrano, D. M., S. Motellier, et al. (2015). "Review of nanomaterial aging and transformations through the life cycle of nano-enhanced products." Environment international **77**: 132-147.

- Mueller, N. C. and B. Nowack (2008). "Exposure modeling of engineered nanoparticles in the environment." Environmental science & technology **42**(12): 4447-4453.
- Navarro, E., F. Piccapietra, et al. (2008). "Toxicity of silver nanoparticles to *Chlamydomonas reinhardtii*." Environmental science & technology **42**(23): 8959-8964.
- Nel, A., T. Xia, et al. (2006). "Toxic potential of materials at the nanolevel." science **311**(5761): 622-627.
- Pakrashi, S., S. Dalai, et al. (2012). "A temporal study on fate of Al<sub>2</sub>O<sub>3</sub> nanoparticles in a fresh water microcosm at environmentally relevant low concentrations." Ecotoxicology and environmental safety **84**: 70-77.
- Perreault, F., A. Oukarroum, et al. (2012). "Polymer coating of copper oxide nanoparticles increases nanoparticles uptake and toxicity in the green alga *Chlamydomonas reinhardtii*." Chemosphere **87**(11): 1388-1394.
- Piccinno, F., F. Gottschalk, et al. (2012). "Industrial production quantities and uses of ten engineered nanomaterials in Europe and the world." Journal of Nanoparticle Research **14**(9): 1109.
- Ramsden, C. S., T. J. Smith, et al. (2009). "Dietary exposure to titanium dioxide nanoparticles in rainbow trout, (*Oncorhynchus mykiss*): no effect on growth, but subtle biochemical disturbances in the brain." Ecotoxicology **18**(7): 939-951.
- Saikia, J., M. Yazdimamaghani, et al. (2016). "Differential Protein Adsorption and Cellular Uptake of Silica Nanoparticles Based on Size and Porosity." ACS Applied Materials & Interfaces **8**(50): 34820-34832.
- Sondi, I. and B. Salopek-Sondi (2004). "Silver nanoparticles as antimicrobial agent: a case study on *E. coli* as a model for Gram-negative bacteria." Journal of colloid and interface science **275**(1): 177-182.
- Sun, T. Y., F. Gottschalk, et al. (2014). "Comprehensive probabilistic modelling of environmental emissions of engineered nanomaterials." Environmental Pollution **185**: 69-76.
- Tiede, K., M. Hassellöv, et al. (2009). "Considerations for environmental fate and ecotoxicity testing to support environmental risk assessments for engineered nanoparticles." Journal of Chromatography A **1216**(3): 503-509.
- Von der Kammer, F., P. L. Ferguson, et al. (2012). "Analysis of engineered nanomaterials in complex matrices (environment and biota): general considerations and conceptual case studies." Environmental Toxicology and Chemistry **31**(1): 32-49.

- Wang, Z., J. Li, et al. (2011). "Toxicity and internalization of CuO nanoparticles to prokaryotic alga *Microcystis aeruginosa* as affected by dissolved organic matter." Environmental science & technology **45**(14): 6032-6040.
- Wong, S. W., P. T. Leung, et al. (2010). "Toxicities of nano zinc oxide to five marine organisms: influences of aggregate size and ion solubility." Analytical and bioanalytical chemistry **396**(2): 609-618.
- Xiong, D., T. Fang, et al. (2011). "Effects of nano-scale TiO<sub>2</sub>, ZnO and their bulk counterparts on zebrafish: Acute toxicity, oxidative stress and oxidative damage." Science of the total environment **409**(8): 1444-1452.
- Zhang, L., Y. Jiang, et al. (2007). "Investigation into the antibacterial behaviour of suspensions of ZnO nanoparticles (ZnO nanofluids)." Journal of Nanoparticle Research **9**(3): 479-489.
- Zhao, C.-M. and W.-X. Wang (2010). "Biokinetic uptake and efflux of silver nanoparticles in *Daphnia magna*." Environmental science & technology **44**(19): 7699-7704.
- Zhu, X., Y. Chang, et al. (2010). "Toxicity and bioaccumulation of TiO<sub>2</sub> nanoparticle aggregates in *Daphnia magna*." Chemosphere **78**(3): 209-215.